

The symmetry approach to quark and lepton masses and mixing

Gui-Jun Ding^a*, José W.F. Valle^b†

^a*Department of Modern Physics, University of Science and Technology of China,
Hefei, Anhui 230026, China*

^b*AHEP Group, Instituto de Física Corpuscular - CSIC/Universitat de València, Parque Científico
C/Catedrático José Beltrán, 2, E-46980 Paterna (València) - SPAIN*

Abstract

The Standard Model lacks an organizing principle to describe quark and lepton “flavours”. We review the impact of neutrino oscillation experiments, which show that leptons mix very differently from quarks, placing a major challenge, but also providing a key input to the flavour puzzle. We briefly sketch the seesaw and “scotogenic” approaches to neutrino mass, the latter including also WIMP dark matter. We discuss the limitations of popular neutrino mixing patterns and examine the possibility that they arise from symmetry, giving a bottom-up approach to residual flavour and CP symmetries. We show how family and/or CP symmetries can generate novel viable and predictive mixing patterns. We review the model-independent ways to predict lepton mixing and test both mixing predictions as well as mass sum rules. We also discuss UV-complete flavour theories in four and more space-time dimensions, and their predictions. Benchmarks given include an A_4 scotogenic construction with trimaximal mixing pattern TM2. Higher-dimensional completions are also reviewed, such as 5-D warped flavordynamics. We present a T' warped flavordynamics theory with TM1 mixing pattern, detectable neutrinoless double beta decay rates and providing a very good fit of flavour observables, including quarks. We also review how 6-D orbifolds offer a way to determine the structure of the 4-D family symmetry from the symmetries between the extra-D branes. We describe a scotogenic A_4 orbifold predicting the “golden” quark-lepton mass relation, large neutrino mass with normal ordering, higher atmospheric octant, restricted reactor angle, and an excellent global flavour fit, including quark observables. Finally, we discuss promising recent progress in tackling the flavor issue through the use of modular symmetries.

Keywords: Fermion mixing, CP violation, generalized CP, flavor and modular symmetry, orbifolds, warped-flavordynamics.

*E-mail: dinggj@ustc.edu.cn

†E-mail: valle@ific.uv.es

Contents

1	Introduction	4
1.1	Quark masses and mixing	6
1.2	Lepton masses and mixing	7
1.3	Neutrino oscillation recap	9
1.4	Neutrinoless double beta decay	12
2	Origin of neutrino masses and flavour puzzle	16
2.1	Effective neutrino masses	16
2.2	The seesaw paradigm	16
2.3	Dark matter as the source of neutrino mass	18
2.4	Missing partner seesaw and dark matter: the scoto-seesaw	18
2.5	The low-scale inverse and linear seesaw mechanisms	19
2.6	Dark inverse and linear seesaw mechanisms	20
2.7	Neutrinos and the flavour puzzle	21
3	Lepton mixing patterns	24
3.1	Tri-bimaximal mixing (TBM)	24
3.2	Generalizations of tri-bimaximal mixing	25
3.3	Golden ratio mixing pattern	26
3.4	Bi-maximal mixing pattern	27
4	Flavour and CP symmetries from the bottom-up	29
4.1	Residual symmetries of leptons	29
4.2	Reconstructing lepton mixing from remnant CP symmetry	33
4.3	Residual symmetries of quarks	36
5	Viable lepton mixing patterns	39
5.1	Revamped TBM mixing	39
5.1.1	Case a: G_1 flavour and X_1, X_4 CP symmetries	41
5.1.2	Case b: G_2 flavour and X_2, X_4 CP symmetries	43
5.2	Revamped Golden-Ratio mixing scheme	44
5.3	Bi-large mixing	46
5.3.1	Bi-large mixing from abelian family symmetry	47
5.3.2	Confronting bi-large mixing with oscillation data	51
6	Lepton mixing from flavour and CP symmetry	54
6.1	Lepton mixing from flavour symmetry alone	54
6.1.1	Fully preserved residual symmetry $G_\nu = K_4$	56
6.1.2	Partially preserved residual symmetry $G_\nu = Z_2$	57

6.2	Combining flavour and CP symmetry	59
6.2.1	Mathematical consistency	60
6.2.2	Implications of residual flavour and CP symmetries	63
6.3	Predictive scenarios with CP symmetry	64
6.3.1	$\mathcal{G}_l = Z_n$ ($n \geq 3$), $\mathcal{G}_\nu = Z_2 \times CP$	65
6.3.2	$\mathcal{G}_l = Z_2 \times CP$, $\mathcal{G}_\nu = Z_2 \times CP'$	72
6.4	Quark and lepton mixing from a common flavour group	75
6.5	Geometrical CP violation	79
7	Testing flavor and CP symmetries	81
7.1	Testing mixing predictions	81
7.2	Testing mass sum rules	84
7.3	Flavor symmetry toolkit	88
8	Benchmark UV-complete models in 4-D	89
8.1	A_4 family symmetry in a scotogenic model	89
8.1.1	Charged lepton masses	90
8.1.2	Dark fermion masses	91
8.1.3	Scotogenic neutrino masses	92
8.2	A benchmark model with both flavour and CP symmetries	95
8.2.1	Flavon superpotential	96
8.2.2	The charged lepton sector	97
8.2.3	The neutrino sector	98
9	Family symmetry in 5-D models with a warped extra dimension	102
9.1	Warped flavourdynamics with the T' family group	102
9.1.1	Lepton masses and mixing	103
9.1.2	Quark masses and CKM matrix	107
9.2	Global flavour fit	108
10	Family symmetry from 6-D orbifolds	111
10.1	General preliminaries	111
10.2	Scotogenic orbifold	113
10.3	Symmetry breaking and fermion masses	115
10.3.1	Quark and lepton masses	116
10.3.2	Scotogenic neutrino masses	117
10.4	Global fit of flavour observables	118
10.4.1	Preliminaries	118
10.4.2	Fit procedure	119
10.5	Flavour predictions of the scotogenic orbifold model	119

10.5.1 Golden quark-lepton mass relation	119
10.5.2 Neutrino oscillation predictions	120
10.5.3 Neutrinoless double beta decay predictions	121
11 Recent progress: modular symmetry	123
11.1 The modular group	123
11.2 Modular invariance	125
11.3 Generalized CP in modular symmetry	126
11.4 Modular symmetry from top-down	127
11.5 Quark-lepton mass relations from modular symmetry	127
11.6 Modular versus traditional flavor symmetry	128
12 Summary and outlook	129
A The A_4 group	133
B The S_4 group	135
C The dihedral group	138
D Diagonalization of a 2×2 complex symmetric matrix	141

1 Introduction

Elucidating the spontaneous mechanism of symmetry breaking [1] within the Standard Model (SM) [2–5], i.e. the existence of a physical Higgs boson [6–8], has so far been the main accomplished goal of the successful LHC programme. This was achieved, at least partially, with the discovery of a scalar particle with properties closely resembling those of the SM Higgs, by the ATLAS [9] and CMS [10] experiments at CERN. More is expected from future studies, for example, at the upcoming FCC facility [11, 12] and other complementary lepton accelerators [13–17].

Another major milestone in elementary particle physics has been the discovery of neutrino oscillations in solar and atmospheric neutrino experiments [18, 19]. These were followed by reactor- and accelerator-based studies, e.g. [20–23] which, altogether, imply nonzero neutrino masses, as well as large mixing angles in the lepton sector [24, 25]¹. This comes as a surprise, when compared with the pattern seen in the Cabibbo-Kobayashi-Maskawa matrix describing quark mixing and CP violation [28]. It also means that, even after the discovery of the Higgs boson, the architecture of particle physics is still quite far from “complete”.

The origin of neutrino masses is one of the deepest secrets of modern particle physics [29]. The most general neutrino mass generation template is given by the $SU(3)_c \otimes SU(2)_L \otimes U(1)_Y$ gauge theory framework characterizing the SM [30–32]. In this review we will be mainly concerned with bottom-up

¹There is a fairly good agreement with the other determinations, by the Bari group [26] and NuFit [27].

approaches, for which this is the most appropriate choice. However the seesaw can also be discussed in terms of left-right theories and $SO(10)$ [33–38].

Following the gauge principle that underlies the SM construction, neutrinos should also get mass through spontaneous symmetry breaking (SSB). Small neutrino masses would be understood dynamically through new vacuum expectation values (VEVs). A specially interesting case is that of spontaneous violation of lepton number [32, 39]. Besides the high-scale seesaw, we stress that one can also have dynamical generation of neutrino masses at low scales [40–42].

Within the SM picture three of the fundamental interactions of nature (electromagnetic, weak and strong) all have a gauge description. It would be very appealing if these could also have a common origin at very high energies [34, 43–47], though no hard evidence for this beautiful idea has ever been found. Despite their potential in providing an all-encompassing unified description including also gravity [48–50], superstring theories have so-far also failed to provide a phenomenologically convincing roadmap.

Another major drawback of the SM construction is that it fails to explain family replication, fermion mass hierarchies and mixing pattern. The discovery of oscillations has only exacerbated this fact. The disparity observed in the pattern of quark and lepton mixing parameters appears to us unlikely to be the result of pure chance. As a result, we will not examine the possibility of neutrino mixing anarchy [51, 52]. Although viable, we find this hypothesis theoretically unsatisfactory. Instead, our main common thread in this review will be the symmetry approach to the “flavour problem”.

Here we will be mainly concerned with explaining the detailed pattern of the weak interactions of quarks and leptons within family-symmetry extended theories based on the $SU(3)_c \otimes SU(2)_L \otimes U(1)_Y$ gauge group, with special emphasis on the case of leptons. Early attempts to understand the lepton mixing pattern starting from the quark sector have now become obsolete, since the discovery of neutrino oscillations. A fully successful flavour theory should explain not only the observed large mixing angles in the lepton sector but also the CKM mixing pattern governing quark mixing and CP violation. Likewise, it should also account for the pattern of quark and lepton masses. In this review we will illustrate how this may, at least partially, be achieved either within 4-dimensional renormalizable gauge field theories [53–69] or in the context of theories with extra spacetime dimensions [70–84]. To set up notation for the following chapters here we start with some preliminaries on the gauge-theoretic description of quark and lepton mixing, followed by a very brief critique of the SM drawbacks.

We should stress that there are already several excellent reviews on the discrete flavor symmetry approach to address the SM flavor puzzle [85–93]. Apart from providing an update to these, the present review will focus on how the residual flavor and CP symmetries can constrain the fermion mixing angles and CP violation phases independently of the details of a specific implementation. We discuss in detail both theory and phenomenological predictions. In addition, we discuss several other topics and predictive benchmark flavor model examples, both in four dimensions and extra dimensions. The latter include warped 5D flavordynamics as well as orbifold-based scenarios, which are reviewed here for the first time. We discuss extensively the predictions of a broad class of symmetry-based theories of flavor. Finally, we also give a brief discussion of theories based on modular symmetries and how these may help with the

vacuum alignment problem.

1.1 Quark masses and mixing

We recall that in a gauge field theory like the Standard Model all the fermion masses arise from spontaneous symmetry breaking. The most general quark Yukawa interactions with the Higgs doublet H allowed by symmetry are given by [94–96],

$$\mathcal{L}_{\text{Yuk}}^q = -(y_D)_{ij} \overline{D_R^i} H^\dagger Q_L^j - (y_U)_{ij} \overline{U_R^i} \tilde{H}^\dagger Q_L^j + \text{h.c.}, \quad (1.1)$$

where $\tilde{H} = i\tau_2 H^*$ and $Q_L^i = (U_L^i, D_L^i)^T$. The Yukawa matrices y_D and y_U are arbitrary complex matrices in flavour space. Upon electroweak symmetry breaking, the Higgs vacuum expectation value (VEV) $\langle H \rangle = (0, v/\sqrt{2})^T$ with $v \simeq 246\text{GeV}$ gives us the quark mass terms

$$\mathcal{L}_{\text{mass}}^q = -\overline{U}_R m_U U_L - \overline{D}_R m_D D_L + \text{h.c.}, \quad (1.2)$$

where $U_L \equiv (u_L, c_L, t_L)^T$, $D_L \equiv (d_L, s_L, b_L)^T$, $U_R \equiv (u_R, c_R, t_R)^T$ and $D_R \equiv (d_R, s_R, b_R)^T$ denote the three generations of left and right-handed up- and down-type quark fields, respectively. The mass matrices are determined by the Yukawa couplings and the Higgs VEV as follows

$$m_U = \frac{v}{\sqrt{2}} y_U, \quad m_D = \frac{v}{\sqrt{2}} y_D. \quad (1.3)$$

Gauge invariance does not constrain the flavour structure of the Yukawa couplings y_D and y_U and therefore m_U and m_D are arbitrary complex matrices. These matrices can be brought into diagonal form by separate unitary transformations on the left and right fermions, i.e.

$$W_u^\dagger m_U V_u = \text{diag}(m_u, m_c, m_t), \quad W_d^\dagger m_D V_d = \text{diag}(m_d, m_s, m_b), \quad (1.4)$$

which implies

$$V_u^\dagger m_U^\dagger m_U V_u = \text{diag}(m_u^2, m_c^2, m_t^2), \quad (1.5)$$

$$V_d^\dagger m_D^\dagger m_D V_d = \text{diag}(m_d^2, m_s^2, m_b^2). \quad (1.6)$$

By performing such unitary transformations $U_L \rightarrow V_u U_L$, $D_L \rightarrow V_d D_L$, $U_R \rightarrow W_u U_R$ and $D_R \rightarrow W_d D_R$ one can go to the physical mass eigenstates. The resulting flavour-changing quark charged current weak interaction reads

$$\mathcal{L}_{CC}^q = \frac{g}{\sqrt{2}} \overline{U}_L \gamma^\mu V_{CKM} D_L W_\mu^+ + \text{h.c.}, \quad (1.7)$$

where $V_{CKM} \equiv V_u^\dagger V_d$ is the Cabibbo-Kobayshi-Maskawa (CKM) mixing matrix [97, 98]. In what follows we adopt the standard form for the CKM matrix describing quark mixing, i.e.

$$V_{CKM} = \begin{pmatrix} c_{12}^q c_{13}^q & s_{12}^q c_{13}^q & s_{13}^q e^{-i\delta^q} \\ -s_{12}^q c_{23}^q - c_{12}^q s_{13}^q s_{23}^q e^{i\delta^q} & c_{12}^q c_{23}^q - s_{12}^q s_{13}^q s_{23}^q e^{i\delta^q} & c_{13}^q s_{23}^q \\ s_{12}^q s_{23}^q - c_{12}^q s_{13}^q c_{23}^q e^{i\delta^q} & -c_{12}^q s_{23}^q - s_{12}^q s_{13}^q c_{23}^q e^{i\delta^q} & c_{13}^q c_{23}^q \end{pmatrix}, \quad (1.8)$$

with $c_{ij}^q \equiv \cos \theta_{ij}^q$, $s_{ij}^q \equiv \sin \theta_{ij}^q$. This parameterization is the one adopted by the Review of Particle Physics of the Particle Data Group (PDG) [28], and supplements the original proposal in Ref. [30] by specifying a convenient factor ordering. Notice that only one physical phase remains after the allowed quark phase redefinitions. The CKM-phase-parameter δ_q is expressed in a neat and rephasing-invariant way as [99],

$$\delta^q = \phi_{13}^q - \phi_{12}^q - \phi_{23}^q, \quad (1.9)$$

in terms of the fundamental ϕ_{ij}^q phases. These are the relative phases between up- and down-type diagonalization matrices. From Ref. [28] we extract the following allowed ranges [100, 101] for the CKM parameters,

$$V_{CKM} = \begin{pmatrix} 0.97431 \pm 0.00012 & 0.22514 \pm 0.00055 & (0.00365 \pm 0.00010)e^{i(-66.8 \pm 2.0)^\circ} \\ (-0.22500 \pm 0.00054)e^{i(0.0351 \pm 0.0010)^\circ} & (0.97344 \pm 0.00012)e^{i(-0.001880 \pm 0.000052)^\circ} & 0.04241 \pm 0.00065 \\ (0.00869 \pm 0.00014)e^{i(-22.23 \pm 0.63)^\circ} & (-0.04124 \pm 0.00056)e^{i(1.056 \pm 0.032)^\circ} & 0.999112 \pm 0.000024 \end{pmatrix}. \quad (1.10)$$

1.2 Lepton masses and mixing

It is a characteristic feature of the Standard Model that spontaneous gauge symmetry breaking leaves neutrinos as massless fermions. However, the discovery of neutrino oscillations [18, 19] implies non-zero neutrino masses and neutrino mixing. One can introduce three right-handed neutrino fields ν_R^i for $i = 1, 2, 3$ as full $SU(3)_c \otimes SU(2)_L \otimes U(1)_Y$ singlets. In analogy with the quark sector the neutrino and charged lepton masses are described by the Yukawa interactions,

$$\mathcal{L}_{\text{Yuk}}^l = -(y_l)_{ij} \bar{l}_R^i H^\dagger L_L^j - (y_\nu)_{ij} \bar{\nu}_R^i \tilde{H}^\dagger L_L^j + \text{h.c.}, \quad (1.11)$$

where $L_L^i = (\nu_L^i, l_L^i)^T$ are the lepton doublet fields. In this case neutrinos would be Dirac particles. This requires the *ad hoc* imposition of lepton number symmetry to forbid the right-handed Majorana mass term $M_{ij} \overline{\nu_R^i} (\nu_R^j)^c$ allowed by SM gauge invariance. Moreover, the Yukawa coupling y_ν should be of order 10^{-11} in order to accommodate the neutrino masses below the eV scale.

Under the assumption of lepton number conservation one gets, after electroweak symmetry breaking, the following charged lepton and neutrino mass terms,

$$\mathcal{L}_{\text{mass}}^l = -\bar{l}_R m_l l_L - \bar{\nu}_R m_\nu \nu_L + \text{h.c.}. \quad (1.12)$$

However, without *a priori* assumptions, gauge theories suggest that neutrinos are Majorana particles [30]². However, this important issue of the nature of neutrinos must be settled by experiment. A prime example is to search for neutrinoless double beta decay [106–109]. A positive detection would imply, by the black-box theorem, the Majorana nature of at least one of the neutrinos [110].

Majorana neutrino masses can be effectively described by the non-renormalizable Weinberg operator $(y_\nu)_{ij} \left(\overline{(L_L^i)^c} i\tau_2 H \right) \left(H^T i\tau_2 L_L^j \right) / (2\Lambda)$ [29]. As a result the charged lepton and neutrino mass terms take of the following form

$$\mathcal{L}_{\text{mass}}^l = -\bar{l}_R m_l l_L - \frac{1}{2} \overline{\nu_L^c} m_\nu \nu_L + \text{h.c.}, \quad (1.13)$$

where $m_\nu = y_\nu v^2 / (2\Lambda)$. The smallness of neutrino mass may be ascribed to the large new physics scale Λ . There are also attractive low-scale realizations of the seesaw mechanism, as we comment below. Both charged lepton and neutrino mass matrices are diagonalized through unitary transformations as follows

$$U_l^\dagger m_l^\dagger m_l U_l = \text{diag} (m_e^2, m_\mu^2, m_\tau^2), \quad (1.14)$$

and

$$\begin{aligned} U_\nu^T m_\nu U_\nu &= \text{diag} (m_1, m_2, m_3), & \text{for Majorana neutrinos,} \\ U_\nu^\dagger m_\nu^\dagger m_\nu U_\nu &= \text{diag} (m_1^2, m_2^2, m_3^2), & \text{for Dirac neutrinos.} \end{aligned} \quad (1.15)$$

where the light neutrino masses $m_{1,2,3}$ are real and non-negative. The nonzero mass squared differences measured in neutrino oscillation experiments imply a non-degenerate mass spectrum $m_1 \neq m_2 \neq m_3$. As a consequence, we can express the lepton mass matrices in terms of U_l , U_ν and the mass eigenvalues as

$$m_l^\dagger m_l = U_l \text{diag} (m_e^2, m_\mu^2, m_\tau^2) U_l^\dagger, \quad (1.16)$$

$$m_\nu = U_\nu^* \text{diag} (m_1, m_2, m_3) U_\nu^\dagger, \quad \text{for Majorana neutrinos,} \quad (1.17)$$

$$m_\nu^\dagger m_\nu = U_\nu \text{diag} (m_1^2, m_2^2, m_3^2) U_\nu^\dagger, \quad \text{for Dirac neutrinos.} \quad (1.18)$$

Transforming to the charged lepton and neutrino mass eigenstates, one obtains the leptonic charged-current weak interaction as [30]

$$\mathcal{L}_{CC}^l = \frac{g}{\sqrt{2}} \bar{l}_L \gamma^\mu U_l^\dagger U_\nu \nu_L W_\mu^- + \text{h.c.}, \quad (1.19)$$

where the combination $U_l^\dagger U_\nu$ defines the lepton mixing matrix, i.e.

$$U = U_l^\dagger U_\nu. \quad (1.20)$$

²Note that the most general description of neutrinos is in terms of two-component spinors, Dirac fermions being just a particular case of Majorana [102]. Although the two-component approach is universal and often more insightful, in this review we will adopt the more familiar four-component formalism used in most textbooks, for example [103–105], in which Majorana and Dirac neutrinos appear as separate “cases”.

Like the CKM matrix describing quark mixing, the lepton mixing matrix U arises from the mismatch between the diagonalizations of charged leptons and neutrinos. Assuming unitarity, the matrix U is characterized by three angles and three physical CP phases [30],

$$U = \begin{pmatrix} c_{12}^{\ell} c_{13}^{\ell} & s_{12}^{\ell} c_{13}^{\ell} e^{-i\phi_{12}} & s_{13}^{\ell} e^{-i\phi_{13}} \\ -s_{12}^{\ell} c_{23}^{\ell} e^{i\phi_{12}} - c_{12}^{\ell} s_{13}^{\ell} s_{23}^{\ell} e^{-i(\phi_{23}-\phi_{13})} & c_{12}^{\ell} c_{23}^{\ell} - s_{12}^{\ell} s_{13}^{\ell} s_{23}^{\ell} e^{-i(\phi_{23}+\phi_{12}-\phi_{13})} & c_{13}^{\ell} s_{23}^{\ell} e^{-i\phi_{23}} \\ s_{12}^{\ell} s_{23}^{\ell} e^{i(\phi_{23}+\phi_{12})} - c_{12}^{\ell} s_{13}^{\ell} c_{23}^{\ell} e^{i\phi_{13}} & -c_{12}^{\ell} s_{23}^{\ell} e^{i\phi_{23}} - s_{12}^{\ell} s_{13}^{\ell} c_{23}^{\ell} e^{-i(\phi_{12}-\phi_{13})} & c_{13}^{\ell} c_{23}^{\ell} \end{pmatrix}, \quad (1.21)$$

with the abbreviation $c_{ij}^{\ell} \equiv \cos \theta_{ij}^{\ell}$ and $s_{ij}^{\ell} \equiv \sin \theta_{ij}^{\ell}$. The above universal symmetrical presentation for the matrix U in Eq. (1.21) is very convenient both for the description of quark as well as lepton mixing [30]. Notice that there is an important difference between leptons and quarks concerning CP violation, namely, all three CP phases in Eq. (1.21) are physical parameters. One of them is the lepton analogue of the CKM phase in Eq. (1.9), also called *Dirac phase*.

$$\delta^{\ell} = \phi_{13} - \phi_{12} - \phi_{23}. \quad (1.22)$$

The others are the so-called *Majorana phases*, which can not be eliminated by field redefinitions [30] if neutrinos are Majorana particles. Only the Dirac phase affects conventional neutrino oscillation probabilities, while the Majorana phases can only affect lepton number violating processes [111, 112]. Note that in what follows we will also use the notation δ_{CP} for the lepton Dirac CP phase δ^{ℓ} . It will be an experimental challenge to obtain robust information on their magnitudes.

Current neutrino oscillation data restrict the elements of the lepton mixing matrix. One finds, at 3σ , the following ranges [24, 25]

$$U^{\text{NO}} = \begin{pmatrix} 0.7838 \rightarrow 0.8442 & 0.5133 \rightarrow 0.6004 & (-0.1568 \rightarrow 0.1489) + i(-0.1182 \rightarrow 0.1520) \\ (-0.4831 \rightarrow -0.2394) + i(-0.0749 \rightarrow 0.0963) & (0.4635 \rightarrow 0.6749) + i(-0.0521 \rightarrow 0.0668) & 0.6499 \rightarrow 0.7719 \\ (0.3068 \rightarrow 0.5391) + i(-0.0643 \rightarrow 0.0933) & (-0.6897 \rightarrow -0.4821) + i(-0.0446 \rightarrow 0.0644) & 0.6161 \rightarrow 0.7434 \end{pmatrix} \quad (1.23)$$

for the case of normal neutrino mass-ordering. On the other hand, for inverted-ordered neutrino masses one has [24, 25],

$$U^{\text{IO}} = \begin{pmatrix} 0.7835 \rightarrow 0.8440 & 0.5133 \rightarrow 0.6005 & (-0.1423 \rightarrow 0.1490) + i(0.0191 \rightarrow 0.1553) \\ (-0.4806 \rightarrow -0.2682) + i(0.0114 \rightarrow 0.0990) & (0.4546 \rightarrow 0.6395) + i(0.0074 \rightarrow 0.0695) & 0.6493 \rightarrow 0.7711 \\ (0.3102 \rightarrow 0.5133) + i(0.0094 \rightarrow 0.0947) & (-0.6956 \rightarrow -0.5248) + i(0.0057 \rightarrow 0.0654) & 0.6171 \rightarrow 0.7436 \end{pmatrix} \quad (1.24)$$

Current determinations of the mass-ordering and the atmospheric octant are not yet fully robust. On the other hand we still struggle with a very poor determination of the magnitude of the Dirac CP phase (see below).

1.3 Neutrino oscillation recap

We now give a ‘‘drone view’’ of the current status of neutrino oscillation parameters. The basic discovery made in solar and atmospheric studies was soon followed by reactor and accelerator-based experiments that have not only provided independent confirmation, but also improved parameter determination. Current experimental data mainly converge towards a consistent global picture – the three-neutrino paradigm – in which the oscillation parameters are determined as shown in figure 1.

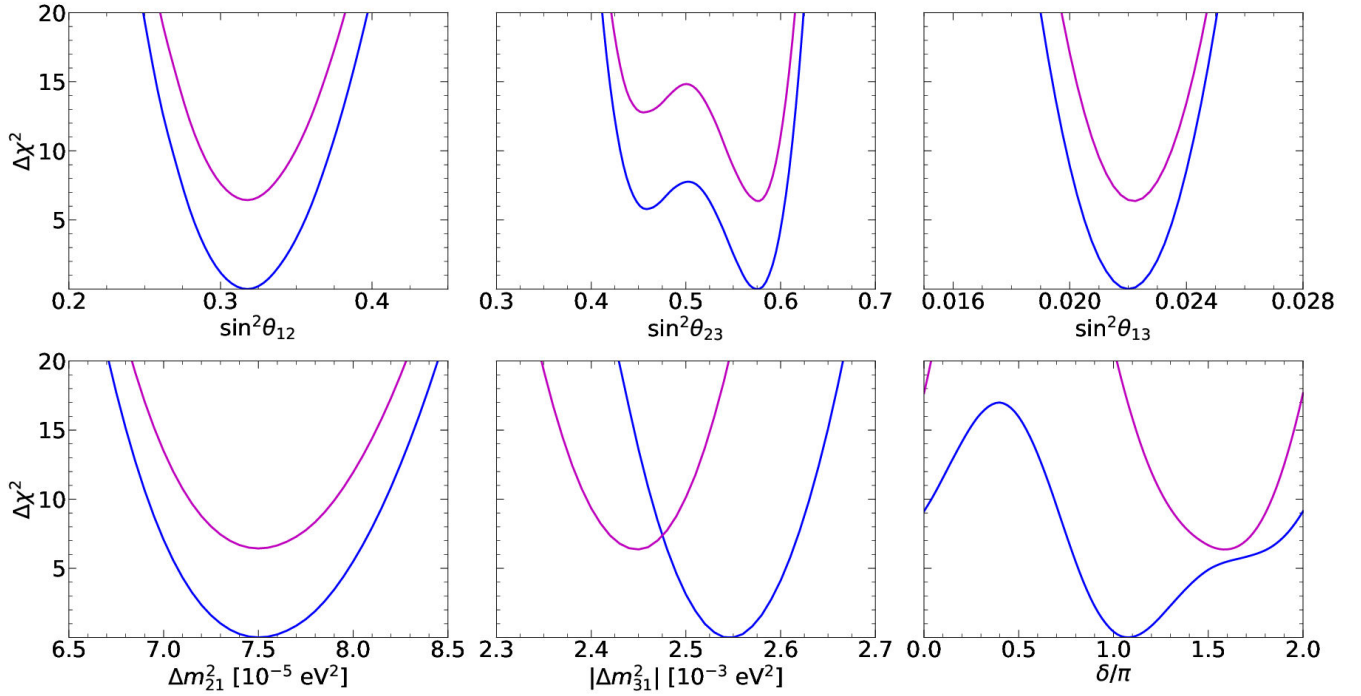


Figure 1: Current summary of neutrino oscillation parameters, where $\delta \equiv \delta_{CP}$. From [24, 25].

The top-three panels show that two mixing angles are fairly large, at odds with the corresponding mixing angles observed in the quark sector. In fact, it is the smallest lepton mixing angle, θ_{13} , that lies intriguingly close in magnitude to the largest of the quark mixing angles, i.e. the Cabibbo angle. Currently we have no explanation for this fact.

The global oscillation parameter determinations can also be shown as the “matrix” in figure 2. Besides the individual oscillation parameter determinations, given by the “diagonal” entries, the “off-diagonal” entries of figure 2 show all pairwise parameter correlations³, very useful for model-builders. Indeed, any flavour model leads to predictions for various entries of the above triangular matrix. The zenodo website in [25] will be used extensively in this review in order to examine the allowed parameter regions in different theoretical setups.

At this point one should stress that, although the overall picture provided by the “three-neutrino paradigm” is mostly robust, there are still loose ends. As already mentioned, the determination of the neutrino spectrum and the octant of the atmospheric angle is not fully robust yet, while the precise value of the leptonic CP phase also remains an open challenge. A robust CP determination will be a key objective of the Deep Underground Neutrino Experiment (DUNE) [113]. The experiment will have two detector systems placed along Fermilab’s Long Baseline Neutrino Facility (LBNF) beam. One of them will be near the beam source, while a much larger one will be placed underground 1300 km away at the Sanford Underground Research Laboratory in South Dakota, in the same mine where Ray Davis

³Numerical tables for the relevant χ^2 profiles can be downloaded from Ref. [25], including all pairwise correlations. These tables can be used to test various neutrino mixing patterns predicted by different flavour theories, such as those in Refs. [53–56, 59–84].

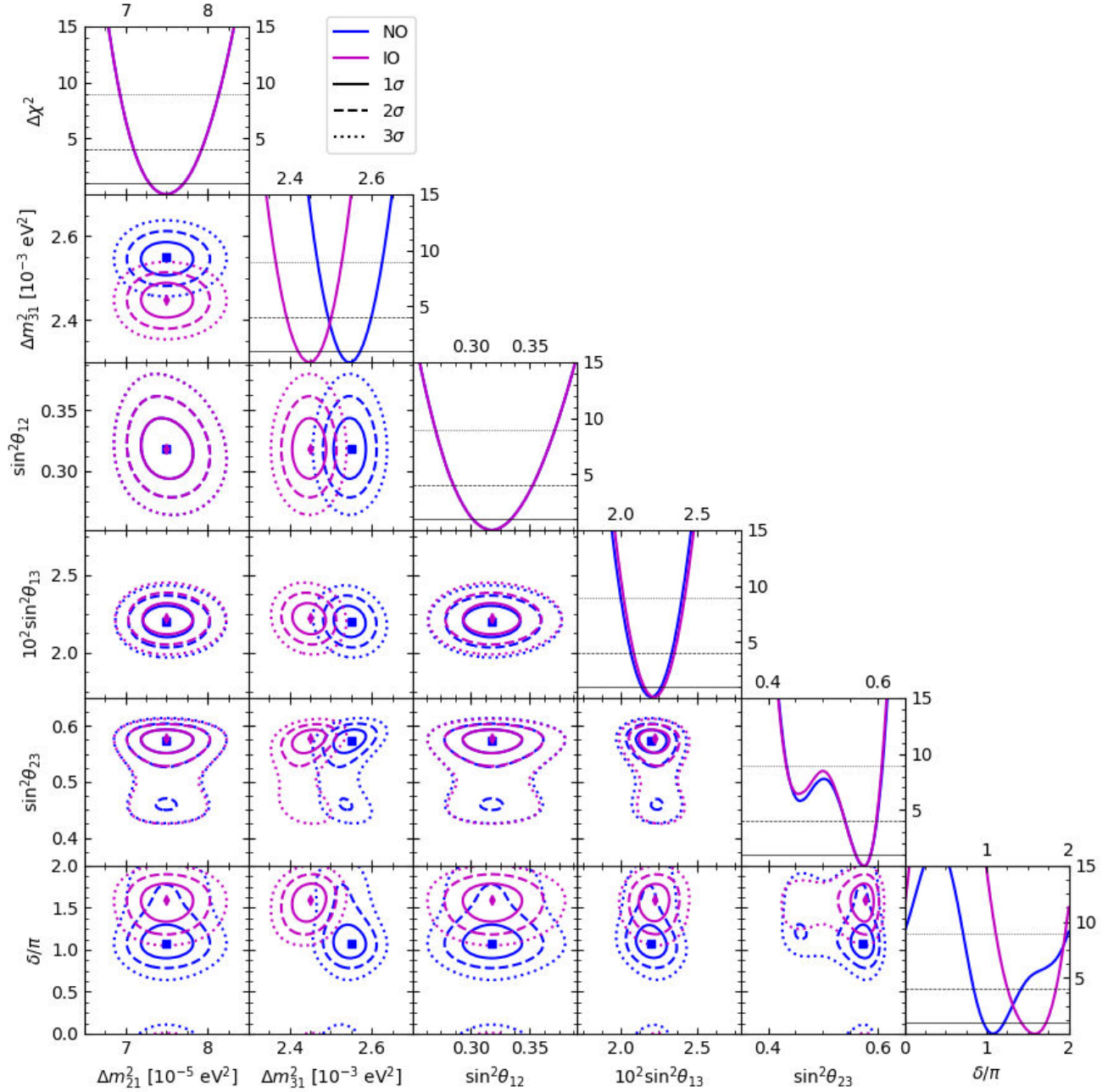


Figure 2: Neutrino oscillation parameters pair-correlations. As before $\delta \equiv \delta_{CP}$. From [24, 25].

pioneered neutrino oscillation studies in the sixties. Further improvements are expected at the ambitious T2HK proposal in Japan [114]. Reaching a precise CP phase determination will be a challenge for the coming years. Likewise, underpinning the mass ordering [115]. Octant resolution may be harder, if the preferred θ_{23} value lies close to maximality. See for example Refs. [116, 117] for details and related references. Altogether, octant discrimination, underpinning the mass-ordering and performing a precise CP determination constitute the target of the next generation of oscillation searches [118].

Last, but not least, we mention that there are also some experimental anomalies in neutrino physics

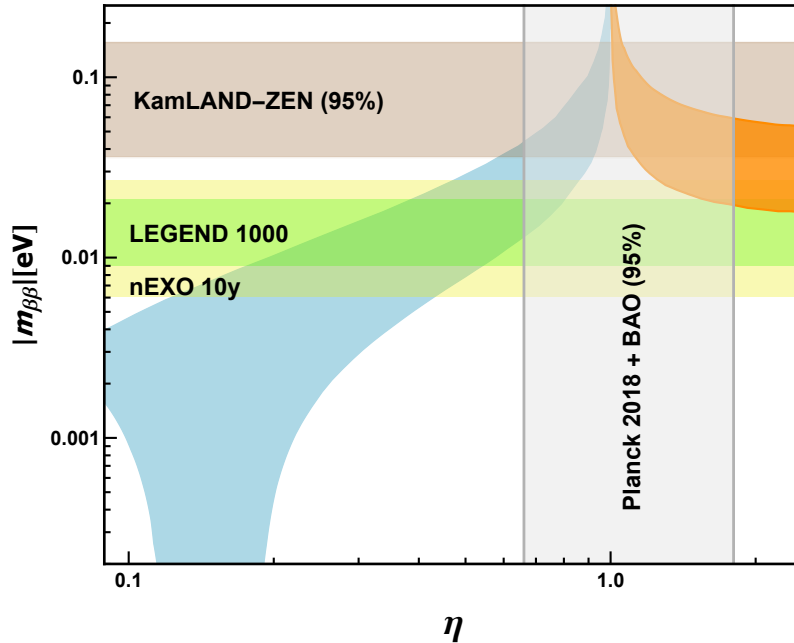


Figure 3: The $0\nu\beta\beta$ decay amplitude in a generic three-neutrino scheme versus the degeneracy parameter η . The curved bands are the normal and inverted ordering branches allowed by neutrino oscillations respectively [124]. The current experimental bound $|m_{\beta\beta}| < (36 - 156)$ meV at 90% confidence level (C.L.) from KamLAND-Zen [125] and the future sensitivity ranges $|m_{\beta\beta}| < (9.0 - 21)$ meV from LEGEND-1000 [126] and $|m_{\beta\beta}| < (6.1 - 27)$ meV from nEXO [127] are indicated by light brown, light yellow and light green horizontal bands respectively. The vertical grey band is excluded by the 95% C.L. limit $\Sigma_i m_i < 0.120$ eV from Planck [128, 129].

that challenge the simple picture provided by the “three-neutrino paradigm” suggesting, perhaps, a four-neutrino oscillation scenario [119]. They will not be discussed in this review, the interested readers can see Refs. [120–123].

1.4 Neutrinoless double beta decay

Neutrinoless double-beta decay (or $0\nu\beta\beta$ for short) is the prime lepton number violating process [106–109]. Given that neutrinos are observed to be massive fermions, and expected to be Majorana-type [30], it follows that $0\nu\beta\beta$ decay should take place, as a consequence of neutrino exchange. In this case, the effective mass parameter characterizing the amplitude is given as

$$|m_{\beta\beta}| = \left| \sum_{j=1}^3 U_{ej}^2 m_j \right| = \left| c_{12}^{\ell 2} c_{13}^{\ell 2} m_1 + s_{12}^{\ell 2} c_{13}^{\ell 2} m_2 e^{-2i\phi_{12}} + s_{13}^{\ell 2} m_3 e^{-2i\phi_{13}} \right|. \quad (1.25)$$

Here we note that, in contrast with the parametrization adopted by the PDG, the symmetrical form of the lepton mixing matrix provides a conceptually transparent description of $0\nu\beta\beta$ in which, as it should, only Majorana phases appear [99]. Altogether, the original symmetrical form of the lepton mixing matrix, Eq. (1.21), provides an insightful description both for the Dirac phase, Eq. (1.22), as well as the Majorana phases, Eq. (1.25).

An important point to notice from Eq. (1.25) is that, thanks to the Majorana phases, the $0\nu\beta\beta$ amplitude can vanish due to possible destructive interference among the three individual neutrino amplitudes. This is clearly seen in the blue branch of figure 3, taken from Ref. [124], which shows the $0\nu\beta\beta$ decay amplitude versus the degeneracy parameter η . When $\eta \rightarrow 1$ neutrino masses become degenerate, and the two bands correspond to the two possible mass orderings. The most favorable case for $0\nu\beta\beta$ decay detectability happens when neutrinos are nearly degenerate, as predicted in some UV-complete flavour theories [53–55]. The $\eta \equiv 1$ case corresponds to the idealized limit where neutrinos would be strictly degenerate. In order to generate oscillations neutrino masses must deviate from exact degeneracy. This can happen in two ways, corresponding to the two curved branches seen in the figure. The normal-ordered (NO) neutrino region is indicated in the left (blue) band, while inverted ordering (IO) gives the upper-right (orange) branch. One sees that, thanks to the presence of the Majorana phases [30], the $0\nu\beta\beta$ amplitude can vanish for normal ordering (but not for inverted). The horizontal band denotes the current KamLAND-Zen limit [125], while the vertical one is excluded [124] by cosmological observations [128,129] e.g. by the Planck collaboration. Altogether, one sees current data strongly disfavour nearly degenerate neutrinos.

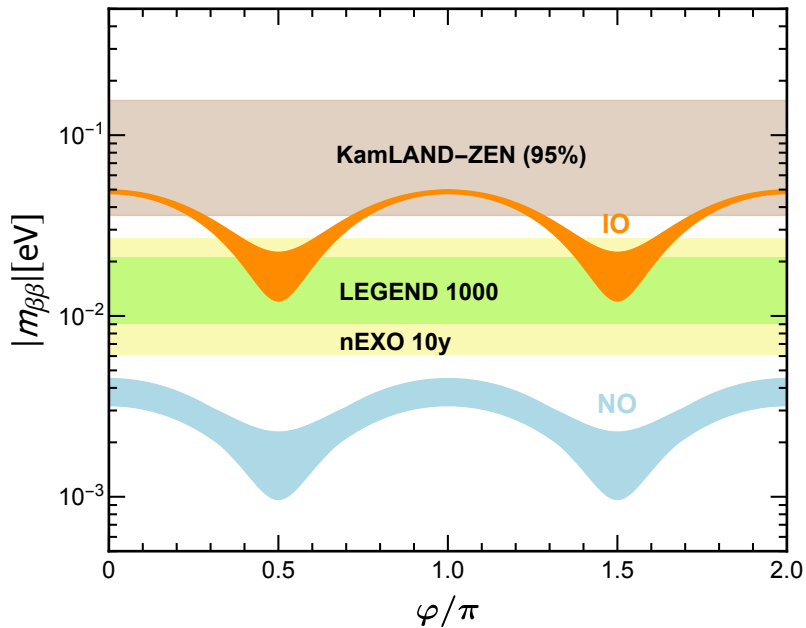


Figure 4: $0\nu\beta\beta$ decay amplitude when one neutrino is massless. The light-blue and light-orange bands are the current 3σ C.L. regions for normal and inverted mass-ordering. The current bound from KamLAND-ZEN [125] and projected sensitivities of LEGEND 1000 [126] and nEXO [127] are indicated.

Another interesting situation happens if one (or two) of the three neutrinos is massless or nearly so, as in the “missing partner” seesaw mechanism [30] and other “incomplete-multiplet” schemes ⁴. The minimal viable tree-level type-I seesaw has only two right-handed neutrinos [131–133]. In such a scheme no cancellation is possible, even for normal-ordering [134–138]. The resulting regions are the two periodic

⁴A massless neutrino may also arise from the presence of anti-symmetric Yukawa couplings, see e.g. [130].

bands seen in figure 4, which are expressed in terms of the only free parameter available, namely, the relative neutrino Majorana phase φ ⁵. The colored horizontal bands show current experimental limits of KamLAND-ZEN and the expected sensitivities of LEGEND 1000 and nEXO, where the width of the bands reflects nuclear matrix element uncertainties [108, 109]. Notice in this case the existence of a predicted theoretical lower bound on $|m_{\beta\beta}|$. Taking into account the sensitivities expected at upcoming $0\nu\beta\beta$ experiments, one sees that this lower bound for NO lies below detectability in the foreseeable future.

In contrast, inverse mass-ordering provides a lower bound that lies higher than the one generically expected for the IO three-massive-neutrino case. This implies a guaranteed discovery in the next round of experiments [139, 140]. In fact, for this case, the recent KamLAND-Zen limit [125] already probes the Majorana phase, as seen by the magenta band in figure 4. In short, for the one-massless-neutrino case there is a chance, perhaps, that one could be able to extract the value of the relevant Majorana phase from experiment.

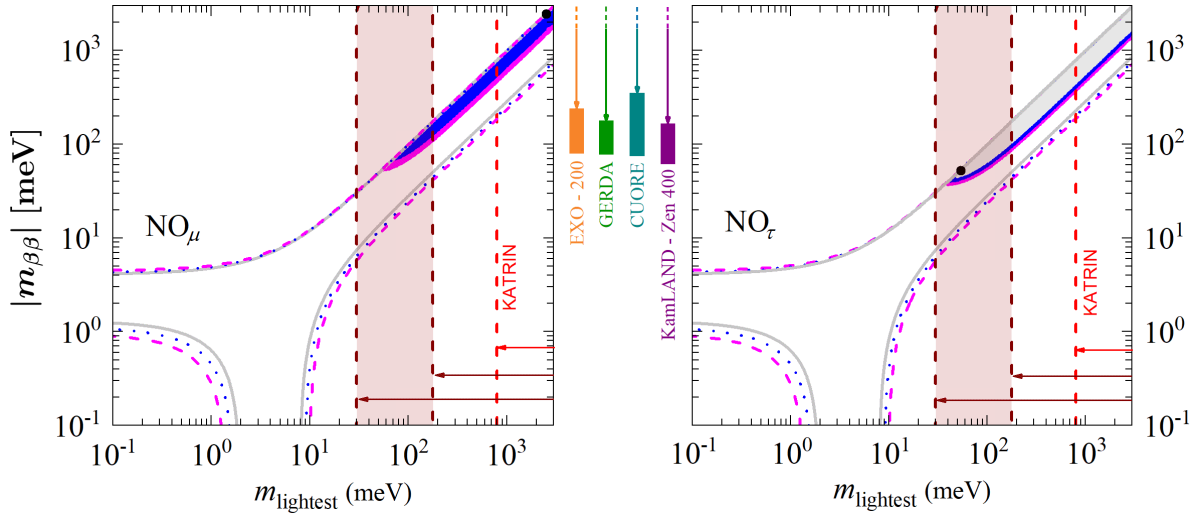


Figure 5: The solid (dotted) [dashed] lines delimit the 1σ (2σ) [3σ] $|m_{\beta\beta}|$ regions allowed by oscillations. Predictions of two normal-ordered \mathcal{Z}_8 schemes are given [148]. Vertical bars in mid-panels indicate current 95%CL $|m_{\beta\beta}|$ upper bounds from KamLAND-Zen 400 [149], GERDA [150], CUORE [151] and EXO-200 [152].

We now turn to the general three-massive-neutrino case. Although there is no guaranteed minimum value for $|m_{\beta\beta}|$ in this case, there can still be a lower-bound, even for normal mass-ordering, provided the cancellation of the amplitudes is prevented by the structure of the leptonic weak interaction vertex [66, 68, 69, 141–144]. This can happen as a result of the imposition of a family symmetry to account for the mixing pattern seen in oscillations. As an example, figure 5 shows the predictions of a \mathcal{Z}_8 family symmetry scheme. The hollow solid (dotted) [dashed] lines delimit the 1σ (2σ) [3σ] $|m_{\beta\beta}|$ regions allowed in the general three-neutrino case. The sub-regions shown in gray, blue and magenta, respectively, are the flavour-model predictions. The black dots correspond to best-fits. The vertical shaded band indicates the current sensitivity of cosmological data [128]. The vertical dashed red line corresponds to the KATRIN

⁵For vanishing lightest neutrino mass the relevant Majorana phase is $\varphi = \phi_{12} - \phi_{13}$ for NO and $\varphi = \phi_{12}$ for IO.

tritium beta decay [145] upper limit $m_\beta < 0.8$ eV (90% CL) [146,147]. The heights of the bars shown in the mid-part of figure 5 reflect the uncertainties in the nuclear matrix elements relevant for the computation of the decay rates. The flavour predictions for $|m_{\beta\beta}|$ illustrate our point. For example, one sees how the preferred flavour-predicted point in the right panel sits right inside the cosmologically interesting band, and close to the current $0\nu\beta\beta$ limits, as indicated in between the panels. Similar predictions for $0\nu\beta\beta$ amplitudes occur in other family symmetry models, some of which will be discussed in this review, see for instance discussions given in Chapters 8 and 10.

In short, oscillations have left an important imprint upon neutrinoless double beta decay studies. The results of the negative searches conducted so-far imply that we must consider both the possibilities of Dirac or Majorana neutrinos, as we do in this review. Nonetheless, there is a reasonable chance that, perhaps, $0\nu\beta\beta$ could be seen in the coming round of experiments. This would constitute a major breakthrough. Indeed, a positive $0\nu\beta\beta$ decay detection would imply, as a consequence of the black box theorem, that at least one of the neutrinos has Majorana nature [110]. The argument is illustrated in figure 6. Note that the black-box argument holds irrespective of the underlying physics responsible for generating the process [153, 154].

In some cases, as we saw in figure 4, the discovery of $0\nu\beta\beta$ decay might allow us to underpin also the value of the relevant Majorana phase. Note however that, although a positive $0\nu\beta\beta$ discovery would imply that at least one of the neutrinos is a Majorana particle, a negative result would not imply that neutrinos are Dirac-type, as the amplitude can be suppressed even for Majorana-type neutrinos, due to the effect of the Majorana phases. It has been argued that if a null $0\nu\beta\beta$ decay signal was accompanied by a positive $0\nu 4\beta$ quadruple beta decay signal [155, 156], then at least one neutrino should be a Dirac particle [157].

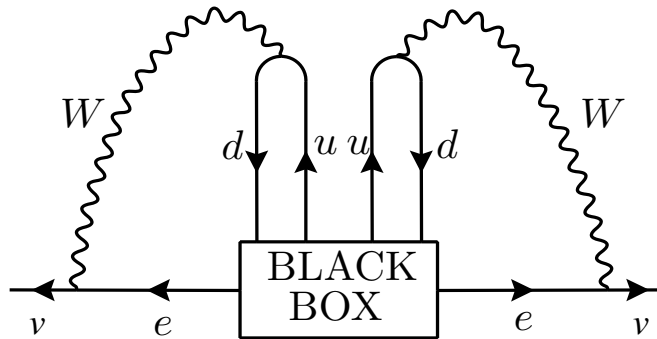


Figure 6: The observation of $0\nu\beta\beta$ decay implies that at least one neutrino is a Majorana fermion [110].

2 Origin of neutrino masses and flavour puzzle

Despite its amazing success in describing three out of the four known fundamental forces of nature, there are many drawbacks and open issues in the Standard Model. Altogether, they imply that the theory of particle physics needs a completion beyond its current form. Here we start with one of the most important issues, i.e. the lack of neutrino masses.

2.1 Effective neutrino masses

Although the Standard Model lacks neutrino masses, these can arise effectively from a unique dimension-five operator characterizing lepton number non-conservation [29], as illustrated in figure 7. In this case neutrinos are Majorana fermions, as generally expected in gauge theories. Indeed, on general grounds it was argued in [30], within the $SU(3)_c \otimes SU(2)_L \otimes U(1)_Y$ setup, that neutrinos are expected to be Majorana fermions.

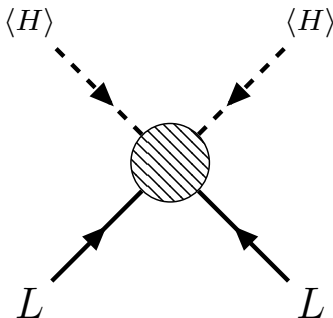


Figure 7: Majorana neutrino mass generation from the dimension-five operator.

However, neutrinos could also be Dirac fermions, this is currently an open experimental question. Dirac neutrinos can indeed emerge in the presence of extra symmetries, that could be discrete or continuous, global or local. For example, the imposition of $U(1)_{B-L}$ symmetry, where B and L are baryon and lepton numbers respectively, would forbid the Majorana mass terms of the right-handed neutrinos [158–161]. Alternatively, as mentioned below, the Dirac nature of neutrinos could result from the presence of an underlying Peccei-Quinn symmetry [162, 163] or be associated with dark matter stability [164–171]. Small Dirac-type neutrino masses as in Eq. (1.11), could arise from effective dimension-five [172–175] as well as dimension-six operators [176, 177], that have by now been classified.

2.2 The seesaw paradigm

An attractive ultraviolet completion of the dimension-five operator is provided by the seesaw mechanism. It is specially interesting, as it gives a simple *dynamical* understanding of small neutrino masses by minimizing the Higgs potential, as well as the possibility of having a stable electroweak vacuum [178–183].

It has become usual to distinguish three main seesaw varieties, namely type-I [30–35], type-II [30–32, 36–38] and type-III [184], illustrated in figure 8. These generate neutrino masses at tree level from the mediation of new heavy singlet fermion (ν_R), triplet scalar (Δ) and triplet fermion (Σ_R), respectively. In the simplest seesaw neutrinos acquire masses through the exchange of heavy scalars, called type-I in [30] and today called type-II. Such seesaw realization allows one to reconstruct the parameters characterizing the neutrino sector from various experiments [185], in particular those from high energy colliders [186,187]. Moreover, the type-II seesaw opens the really tantalizing possibility of probing the absolute neutrino mass and mass ordering in collider experiments [188].

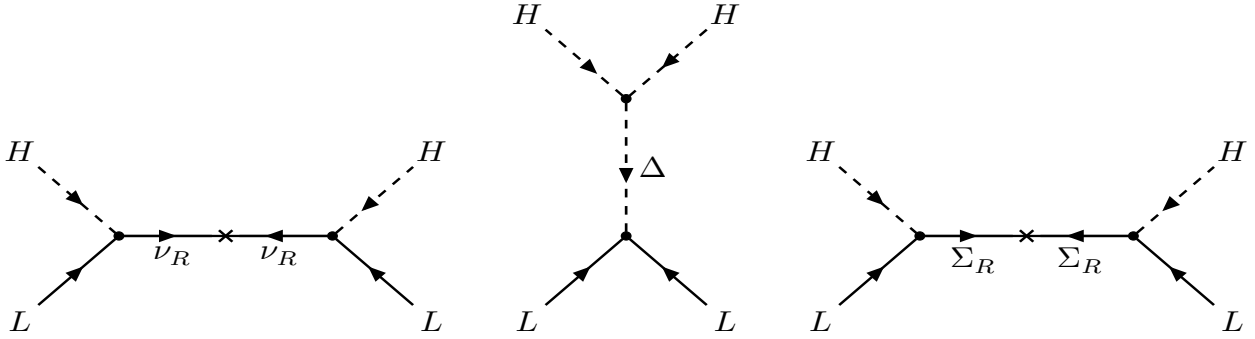


Figure 8: Feynman diagrams for the conventional seesaw types, where the mediators ν_R and Σ_R are SM singlet and triplet fermions respectively, while Δ is a SM triplet scalar.

Here we focus on the type-I seesaw mechanism, where neutrinos acquire masses through the exchange of heavy gauge-singlet fermions, as illustrated in the left panel of figure 8. Seesaw mediators were originally thought to lie at a high mass scale, associated to SO(10) unification or left-right symmetry. The associated physics has been covered in several textbooks [102–105] and reviews [189]. Note that, following Ref. [30], here we do not assume left-right symmetry in the seesaw mechanism, but simply the minimal well-tested $SU(3)_c \otimes SU(2)_L \otimes U(1)_Y$ gauge structure. Notice that this seesaw description of neutrino mass generation can be made fully dynamical in the presence of a singlet vacuum expectation value (VEV) driving the spontaneous violation of lepton number symmetry. The theory is then accompanied by a Nambu-Goldstone boson, dubbed Majoron [32,39].

Notice that the most general realization of the seesaw mechanism leads most naturally to Majorana neutrinos. However, in the presence of adequate extra symmetries, Dirac neutrinos can emerge from the seesaw [190]. Indeed, there may be good reasons for neutrinos to be Dirac-type. For example, the Dirac nature of neutrinos could also be associated to the existence of an underlying Peccei-Quinn symmetry [162,163]. Moreover, it could signal the stability of dark matter [164–171]. Finally, there are interesting scenarios where the Dirac nature of neutrinos is associated with a family symmetry [191,192].

2.3 Dark matter as the source of neutrino mass

It is well-known that about 85% of the matter in the universe is “dark” in the sense that it does not appear to interact with the electromagnetic field and is, as a consequence, very hard to detect. It is not our purpose to provide a comprehensive discussion of the observational aspects of cosmological dark matter; for a review see Ref. [193]. The first point we note is that the existence of such cosmological Dark matter is totally unaccounted for within the Standard Model. A very interesting possibility is that dark matter is made up of a novel weakly interacting massive particle, dubbed WIMP, typically present in the case of supersymmetric theories with conserved R-parity [194].

Underpinning the mechanism yielding small neutrino masses and/or dark matter is of paramount importance in particle physics, as it may select which new physics to expect as the next step. This is a very broad subject which we will not try to review. Rather, in this review we just comment on the issue of particle dark matter candidates, and how they may be simply related to the mechanism of neutrino mass generation. We focus on the very interesting possibility that the dark matter sector mediates neutrino mass generation, as postulated within the scotogenic picture [195–201]. An interesting twist is to imagine the existence of a universal “hidden” dark matter sector that *seeds* neutrino mass generation, which proceeds *a la seesaw*, as in the dark inverse seesaw [202] mechanism. Alternatively, one can envisage a dark linear seesaw mechanism [203, 204].

Both dark inverse and dark linear seesaw realizations will be described below. In either case dark matter will be WIMP-like. Instead of being related to supersymmetry, WIMP dark matter in these models is closely related to neutrino physics, either as mediator or as seed of neutrino mass generation. Flavored scotogenic dark matter may also be implemented [205], providing an attractive way to reconcile low-scale radiative neutrino mass generation with dark matter, while addressing the flavour problem at the same time, see Sec. 2.7.

Last, but not least, we mention that particle physics theories where neutrino masses arise from the spontaneous breaking of a continuous global lepton number symmetry have a natural dark matter candidate [206, 207], namely the associated Nambu-Goldstone boson, dubbed majoron [32, 39]. Indeed, the majoron is likely to pick up a mass from gravitational instanton effects, that explicitly violate global symmetries [208]. The majoron necessarily decays to neutrinos, with an amplitude proportional to their tiny mass, which typically gives it cosmologically long lifetimes [32]. The associated restrictions on the decaying warm dark matter picture coming from the CMB [209] as well as mono-energetic photon emission in astrophysics have been examined in detail [210]. Using N-body simulations it has also been shown that the warm majoron dark matter model provides a viable alternative to the Λ CDM scenario, with predictions that can differ substantially on small scales [211].

2.4 Missing partner seesaw and dark matter: the scoto-seesaw

In contrast to a left-right symmetric SO(10)-based seesaw mechanism, where the number of “left” and “right” neutrinos must match as a consequence of gauge invariance, in the most general SM-based seesaw mechanism [30] one can have any number (m) of “right-handed” neutrino mediators, since they are gauge

singlets. Theories with $m < 3$ in the classification of [30] could simplify substantially the form of the lepton mixing matrix ⁶.

Such “missing partner” seesaw schemes with less “right” than “left” neutrinos, imply that some of the active “left” neutrinos remain massless [30, 131, 132]. The (3,2) choice corresponds to the minimal viable type-I seesaw, in which there are only two mass parameters corresponding to the experimentally measured solar and atmospheric splittings. The lightest neutrino is massless, leading to the $0\nu\beta\beta$ prediction discussed in Sec. 1.4.

On the other hand, the minimal (3,1) seesaw leads to the same $0\nu\beta\beta$ prediction as (3,2), but has only one neutrino mass parameter [30]. Although such setup is not consistent with current neutrino data, as it lacks solar neutrino oscillations, the later may arise from a completion in which the degeneracy between the lowest-mass neutrinos is lifted by some other mechanism, for example, as a result of radiative corrections.

Indeed, the (3,1) setup offers a template to reconcile the seesaw paradigm and the WIMP dark matter paradigm within a minimal hybrid construction called “scoto-seesaw” mechanism. Such simplest (3,1) “scoto-seesaw” scheme provides a comprehensive theory of neutrino mass generation as well as WIMP dark matter, in which the relative magnitudes of solar and atmospheric oscillation lengths are explained due to a loop factor [136, 137].

2.5 The low-scale inverse and linear seesaw mechanisms

As a final example, one may consider having more “right-” than “left-handed” neutrinos in the seesaw mechanism, for example, two isosinglets for each “active” isodoublet family. This can be implemented with explicit [213] as well as spontaneous violation of lepton number [40]. In the lepton-number-conserving limit one finds that the three light neutrinos remain massless, as in the Standard Model [214–216]. In contrast to the Standard Model, however, lepton flavour and lepton CP symmetries can be substantially violated ⁷. This shows that flavour and CP violation can exist in the leptonic weak interaction despite the masslessness of neutrinos, implying that such processes need not be suppressed by the small neutrino masses, and hence can have large rates [214–216, 222, 223] ⁸. Such “(3,6)” setup [30], where the 3 doublet neutrinos are accompanied by 6 heavy singlet neutral leptons, provides the template for building genuine “low-scale” realizations of the seesaw mechanism in which lepton number is restored at low values of the lepton number violation scale. The models are natural in *t’Hooft* sense, leading to small, symmetry-protected neutrino masses. Realizations of such genuine “low-scale” seesaw mechanisms include the inverse [40, 213] as well as the linear seesaw [229–231]. Last, but not least, we notice that a dynamical realization of the seesaw mechanism involving the spontaneous violation of lepton number symmetry can improve the consistency properties of the electroweak vacuum [178–183].

If realized at low-scale, the type-I seesaw mechanism may also lead to signals at high-energy colliders. Already back in the LEP days, it was suggested that the neutrino mass mediators could be produced

⁶For an early example, with lepton number symmetry conservation, see [212].

⁷General discussions of leptonic flavour and CP violation are given in [217–221].

⁸For generic references on lepton flavour violation and seesaw schemes see, for example [224–228].

at high energy colliders [232–237]. This proposal was indeed taken up by subsequent experiments, for example the ATLAS and CMS experiments at the LHC [238–240] as well as future proposals [12, 241–243]. These have also taken into account the possibility of having displaced vertices [244–246]⁹ coming from the fact that the couplings responsible for the mediator decays can be neutrino-mass-suppressed.

2.6 Dark inverse and linear seesaw mechanisms

The symmetry protection provided by the above schemes can be upgraded into a “double protection”, by having the seed of lepton number violation to arise radiatively. Indeed, a very interesting possibility has been suggested, namely the dark inverse [202] and also the dark linear seesaw mechanism [203, 204]. In the former case there is a universal gauge-singlet or “hidden” dark matter sector that *seeds* neutrino mass generation, which proceeds *a la seesaw*. The same idea can be used to promote the linear seesaw mechanism into a mechanism sourced by a dark sector. The latter is not unique, interesting examples were given in [203] and [204].

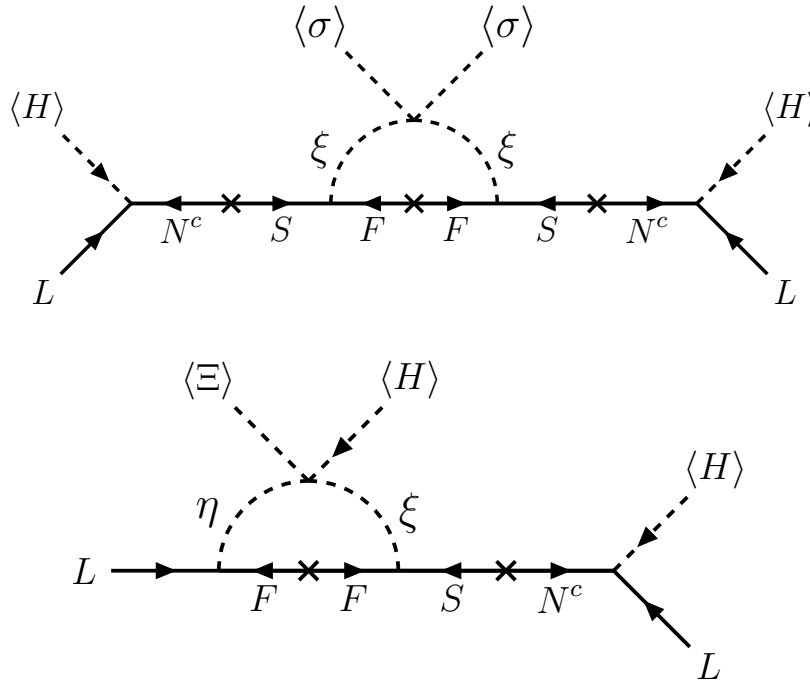


Figure 9: Feynman diagrams for “dark” inverse seesaw (upper panel) [202], and the “dark” linear seesaw mechanism (lower one) [203]. For another realization of the linear seesaw see [204].

The dark inverse seesaw is illustrated in the upper panel of figure 9. The lepton number violation loop that “seeds” neutrino mass is mediated by the “dark” gauge singlet fermion F and dark singlet scalar ξ [202]. This provides an elegant way to reconcile the seesaw and dark matter paradigms, providing an interesting dynamical seesaw theory where dark matter and neutrino mass generation are closely

⁹Other neutrino mass mediator searches can also lead to displaced vertices [247–249].

inter-connected. Scenarios have also been proposed where a dark sector seeds neutrino mass generation radiatively within the linear seesaw mechanism [203, 204], as illustrated in the lower panel. Neutrino masses are also calculable, since tree-level contributions are forbidden by symmetry. By having the seesaw realized at low-scale [40, 213], as indicated in figure 9, in either case one has charged lepton flavour violating processes e.g. $\mu \rightarrow e\gamma$ with accessible rates [202]. We stress that these can be large, despite the tiny neutrino masses. Interesting dark-matter and collider physics implications have also been discussed.

2.7 Neutrinos and the flavour puzzle

We now turn to the issue of understanding the pattern of the weak interactions of quarks and leptons from first principles. Such “flavour problem” constitutes a major challenge in modern particle physics. Why three families of quarks and leptons? How to explain their mass hierarchies e.g. why, though otherwise so similar, the muon is about 200 times heavier than the electron? Why is the top quark mass so large compared with the masses of the other fermions? On the other hand, we also face the question of explaining why do the fermion mixing matrices follow the peculiar pattern observed? In particular, why do leptons mix so differently from the way quarks do? All of these shortcomings pose a real challenge on unified descriptions of nature.

As it stands, the Standard Model of particle physics lacks an organizing principle in terms of which to understand the flavour problem. Hence it can not be a complete theory of nature. Although the Standard Model suffers from many other drawbacks, in this review we focus mainly on explaining the fermion mixing pattern and CP violation, though we also discuss some ideas to account for the fermion mass hierarchies. A “flavour completion” of the SM would have potentially important tests in the laboratory. Moreover, a deep understanding of the flavour problem and CP violation may prove crucial in understanding the baryon asymmetry of the universe [250, 251].

In this review we cover some recent attempts to account for the pattern of neutrino mixing indicated by oscillation experiments. Our key ingredient in formulating a theory of flavour is the imposition of an extra symmetry G_f relating the families. The leading Lagrangian for the lepton masses should be invariant under both the SM gauge symmetry as well as the flavour symmetry, and it can be generally written as

$$\mathcal{L}_m^l = -[y_l(\Phi_l)]_{ij} \bar{l}_R^i H^\dagger L_L^j - \frac{1}{2\Lambda} [y_\nu(\Phi_\nu)]_{ij} \overline{(L_L^i)^c} i\sigma_2 H H^T i\sigma_2 L_L^j + \text{h.c.}, \quad (2.1)$$

where $\sigma_2 = \begin{pmatrix} 0 & -i \\ i & 0 \end{pmatrix}$ is Pauli’s conjugation matrix, $y(\Phi)$ generically denotes the Yukawa couplings, which are determined as functions of the flavons, and the neutrino masses are described by the Weinberg operator [29]. Here Φ_l and Φ_ν denote the flavon fields with vacuum expectation values that break G_f down to the residual subgroups G_l and G_ν in the charged lepton and neutrino sectors respectively. In concrete models the higher-order terms can lead to subleading corrections. As a result, the mismatch of the residual symmetries G_l and G_ν allows one to make model-independent symmetry predictions for the lepton mixing matrix $U = U_l^\dagger U_\nu$, as illustrated in figure 10.

Within the bottom-up approach one may consider remnant flavour symmetries and/or remnant CP

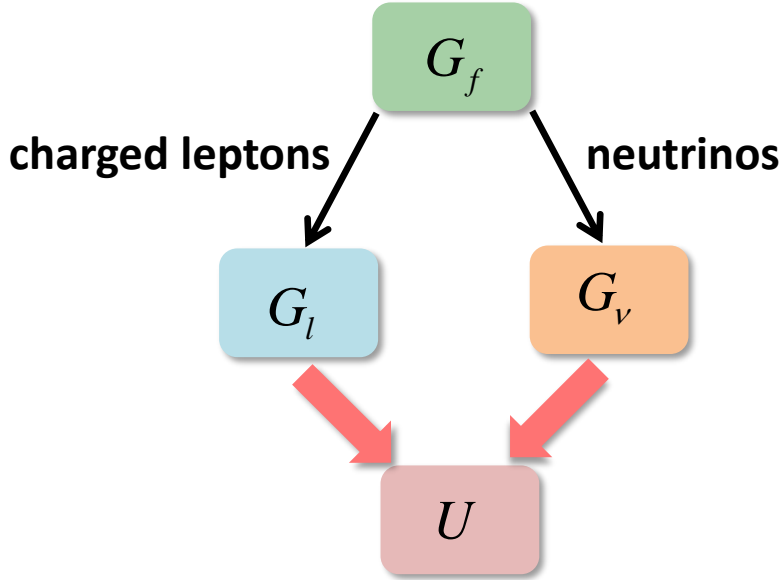


Figure 10: Predicting lepton flavour mixing from the flavour group G_f breaking to different subgroups.

symmetries, such as generalizations of the $\mu - \tau$ reflection symmetry [252–258], as a way to restrict the lepton mass matrices, irrespective of the details of the underlying flavour symmetry. This can be used in turn to constrain the lepton flavour mixing parameters, such as mixing angles [259–263] and especially the CP phases [264–268]. In what follows we call this approach “residual symmetry method” [269–272]. We notice that such $\mu - \tau$ reflection symmetry can emerge within UV-complete theories, e.g. [54, 264]. Indeed, one may seek to constrain the flavour mixing parameters within a complete flavour theory. Attaining a satisfactory theory that explains both quark and lepton sectors together remains an open challenge [273, 274], especially within a quark-lepton unified framework [34, 43–47, 275]. This difficulty [85–93] follows mainly due to the disparity between quark and lepton mixing angles. A possible idea is that lepton mixing angles are large with respect to quark mixing angles because neutrino masses are degenerate in the family symmetry limit [54]. However, nearly degenerate neutrinos are now strongly disfavored by cosmological restrictions [124].

There have been many efforts to approach the flavour problem in the quark sector in terms of an underlying family symmetry, either within a bottom-up or top-down approach [276–286]. For example, the Cabibbo mixing angle can be described by a flavour symmetry [263, 270, 278, 281, 287]. Similarly, quark mixing angles and CP violation may also be accounted for in the framework of generalized CP symmetries [282–286].

Turning now to mass predictions, we note that some quark-lepton relations may emerge naturally from the imposition of family symmetries, even in the absence of a genuine unification group. A prime example is the “golden” formula,

$$\frac{m_\tau}{\sqrt{m_\mu m_e}} \approx \frac{m_b}{\sqrt{m_s m_d}}, \quad (2.2)$$

relating charged-lepton and down-type quark masses. This successful relation may constitute, perhaps, part of any complete theory of flavour. The golden formula could be associated to an underlying Peccei-Quinn symmetry [287]. Alternatively, it could arise within UV-complete family-symmetry-based theories such as [288–290] or [65, 66]. Finally, we note that distinct variants of the golden formula can arise from modular symmetries [291].

We stress that the golden-type relations involve mass ratios, stable under renormalization-group evolution, and allow us to relate quarks and leptons without invoking a genuine unified gauge group such as SU(5) or SO(10). More ambitious approaches to the flavour problem have been proposed within extra spacetime dimensions. For example, 5-D warped schemes were proposed in which mass hierarchies are accounted for by adequate choices of the bulk mass parameters, while quark and lepton mixing angles are restricted by the imposition of a flavour symmetry [70–84]. Predictions for neutrino mixing, CP violation and $0\nu\beta\beta$ decay, as well as a good global fit of flavour observables emerge in warped flavordynamics [78, 79].

On the other hand, 6-dimensional orbifold compactification has been suggested as a promising way to determine the structure of the family symmetry in four dimensions. In this approach the 4-dimensional flavour group emerges from the symmetries between the branes in extra dimensions [292, 293]. Interesting flavour and CP predictions have been obtained from 6-dimensional orbifold compactification schemes, including neutrino oscillation and $0\nu\beta\beta$ decay predictions, as well as a successful global description of the flavour observables [143, 144, 294, 295].

3 Lepton mixing patterns

The most striking implications of the oscillation experiments is that leptons mix quite differently from quarks. Here we consider the interpretation of the oscillation results in terms of phenomenological neutrino mixing patterns. Several of these were suggested, largely motivated by the desire to shed light on the neutrino oscillation parameters. The most salient features of the oscillation phenomenon are captured by the so-called tri-bimaximal (TBM) mixing pattern [296–298]. However there are other interesting mixing patterns, some of which we survey below ¹⁰.

3.1 Tri-bimaximal mixing (TBM)

The Tri-bimaximal lepton mixing pattern embodies bi-maximal mixing of atmospheric neutrinos, tri-maximal solar mixing, no reactor mixing and hence no CP violation. It has been taken very seriously until the Daya Bay collaboration [21,303,304] provided a robust measurement of the angle θ_{13} in 2012. The latest and most precise measurement of Daya Bay gives $\sin^2 2\theta_{13} = 0.0851 \pm 0.0024$ [305,306]. Nevertheless, the TBM pattern still remains as an interesting first step towards a full description of neutrino mixing. Its mixing matrix is given by

$$U_{TBM} = \begin{pmatrix} \sqrt{\frac{2}{3}} & \frac{1}{\sqrt{3}} & 0 \\ -\frac{1}{\sqrt{6}} & \frac{1}{\sqrt{3}} & \frac{1}{\sqrt{2}} \\ -\frac{1}{\sqrt{6}} & \frac{1}{\sqrt{3}} & -\frac{1}{\sqrt{2}} \end{pmatrix}, \quad (3.1)$$

which gives

$$\theta_{23} = 45^\circ, \quad \theta_{12} = \arctan \frac{1}{\sqrt{2}} \simeq 35.26^\circ, \quad \theta_{13} = 0^\circ. \quad (3.2)$$

Under the assumption of Majorana neutrinos, the most general form of the associated neutrino mass matrix in the charged lepton diagonal basis is

$$\begin{aligned} m_\nu^{TBM} &= U_{TBM} \text{diag}(m_1, m_2, m_3) U_{TBM}^T \\ &= \frac{1}{6} \begin{pmatrix} 4m_1 + 2m_2 & -2m_1 + 2m_2 & -2m_1 + 2m_2 \\ -2m_1 + 2m_2 & m_1 + 2m_2 + 3m_3 & m_1 + 2m_2 - 3m_3 \\ -2m_1 + 2m_2 & m_1 + 2m_2 - 3m_3 & m_1 + 2m_2 + 3m_3 \end{pmatrix}. \end{aligned} \quad (3.3)$$

It is easy to check that the above neutrino mass matrix is invariant under the following residual flavour transformations

$$G_1^{TBM} = \frac{1}{3} \begin{pmatrix} 1 & -2 & -2 \\ -2 & -2 & 1 \\ -2 & 1 & -2 \end{pmatrix}, \quad G_2^{TBM} = \frac{1}{3} \begin{pmatrix} -1 & 2 & 2 \\ 2 & -1 & 2 \\ 2 & 2 & -1 \end{pmatrix}, \quad G_3^{TBM} = - \begin{pmatrix} 1 & 0 & 0 \\ 0 & 0 & 1 \\ 0 & 1 & 0 \end{pmatrix}, \quad (3.4)$$

¹⁰Note that, within a UV-complete theory framework, there can be radiative corrections to the TBM predictions [299–302]. This issue lies beyond the scope of the model-independent approach followed here.

up to an overall sign. In other words, the neutrino mass matrix m_ν^{TBM} fulfills

$$(G_i^{TBM})^T m_\nu^{TBM} G_i^{TBM} = m_\nu^{TBM}. \quad (3.5)$$

The symmetry transformation G_3^{TBM} exchanges the second and third columns as well as the second and third rows of the neutrino mass matrix, it is the well-known $\mu - \tau$ permutation symmetry [307–311], and it enforces maximal θ_{23} and vanishing θ_{13} . This symmetry emerges in some UV-complete theories, e.g. [54].

The second transformation G_2^{TBM} requires that the sum of the entries in each row of the light neutrino mass matrix should be equal to that of the corresponding column, the so-called magic symmetry [255, 312]. The invariance under G_2^{TBM} determines one column of the lepton mixing matrix to be $(1, 1, 1)^T / \sqrt{3}$. The residual symmetry transformation G_e of the charged lepton mass matrix is a generic diagonal phase matrix in the flavour basis¹¹. The simplest choice for G_e which can distinguish the three charged leptons is

$$G_e^{TBM} = \begin{pmatrix} 1 & 0 & 0 \\ 0 & \omega^2 & 0 \\ 0 & 0 & \omega \end{pmatrix} \quad (3.6)$$

where ω is the cubic root of one, i.e. $\omega = e^{2\pi i/3}$.

The group generated by G_1^{TBM} , G_2^{TBM} , G_3^{TBM} and G_e^{TBM} turns out to be S_4 group. Consequently, the minimal flavour symmetry group capable of yielding the tri-bimaximal mixing is S_4 [269, 270]. However, in the absence of symmetry breaking by flavons in the $\mathbf{1}'$ and $\mathbf{1}''$ representations the A_4 flavor symmetry can also give rise to the tri-bimaximal mixing pattern [53, 54, 59, 70, 313–315].

3.2 Generalizations of tri-bimaximal mixing

Soon after the tri-bimaximal mixing ansatz was proposed, possible deviations were considered. A simple generalization is obtained by assuming that just one given row or column of the lepton mixing matrix takes the same form as for tri-bimaximal [252]. If the first column of the tri-bimaximal mixing is retained, this is known as the TM1 mixing pattern [316–318], and the associated mixing matrix can be parameterized as

$$U_{TM1} = \frac{1}{\sqrt{6}} \begin{pmatrix} 2 & \sqrt{2} \cos \theta & \sqrt{2} e^{-i\delta} \sin \theta \\ -1 & \sqrt{2} \cos \theta - \sqrt{3} e^{i\delta} \sin \theta & \sqrt{3} \cos \theta + \sqrt{2} e^{-i\delta} \sin \theta \\ -1 & \sqrt{2} \cos \theta + \sqrt{3} e^{i\delta} \sin \theta & -\sqrt{3} \cos \theta + \sqrt{2} e^{-i\delta} \sin \theta \end{pmatrix}. \quad (3.7)$$

The predictions for the lepton mixing angles and leptonic Jarlskog invariant are expressed in terms of just two free parameters δ and θ as

$$\sin^2 \theta_{13} = \frac{1}{3} \sin^2 \theta, \quad \sin^2 \theta_{12} = \frac{1 + \cos 2\theta}{5 + \cos 2\theta},$$

¹¹If G_e is a non-abelian subgroup, the charged lepton mass spectrum would be completely or partially degenerate. Thus G_e should be a cyclic group Z_n with the index $n \geq 3$ or a product of cyclic groups such as $Z_2 \times Z_2$ in order to distinguish among the generations.

$$\sin^2 \theta_{23} = \frac{1}{2} + \frac{\sqrt{6} \cos \delta \sin 2\theta}{5 + \cos 2\theta}, \quad J_{CP} = \frac{1}{6\sqrt{6}} \sin \delta \sin 2\theta. \quad (3.8)$$

One finds that the lepton mixing angles and Dirac CP phases are correlated as follows

$$3 \cos^2 \theta_{12} \cos^2 \theta_{13} = 2, \quad \tan 2\theta_{23} \cos \delta^\ell = \frac{5 \sin^2 \theta_{13} - 1}{2 \sin \theta_{13} \sqrt{2 - 6 \sin^2 \theta_{13}}}. \quad (3.9)$$

We notice that this TM1 pattern emerges as a prediction of the UV-complete models proposed in Refs. [64, 79, 319, 320].

On the other hand, by retaining the second column of the tri-bimaximal mixing matrix one obtains the TM2 [316–318] pattern, a particular case of trimaximal mixing [252, 321–323], given as

$$U_{TM2} = \frac{1}{\sqrt{6}} \begin{pmatrix} 2 \cos \theta & \sqrt{2} & 2e^{-i\delta} \sin \theta \\ -\cos \theta - \sqrt{3} e^{i\delta} \sin \theta & \sqrt{2} & \sqrt{3} \cos \theta - e^{-i\delta} \sin \theta \\ -\cos \theta + \sqrt{3} e^{i\delta} \sin \theta & \sqrt{2} & -\sqrt{3} \cos \theta - e^{-i\delta} \sin \theta \end{pmatrix}. \quad (3.10)$$

All the lepton mixing parameters depend on just two free parameters δ and θ ,

$$\begin{aligned} \sin^2 \theta_{13} &= \frac{2}{3} \sin^2 \theta, & \sin^2 \theta_{12} &= \frac{1}{2 + \cos 2\theta}, \\ \sin^2 \theta_{23} &= \frac{1}{2} - \frac{\sqrt{3} \cos \delta \sin 2\theta}{2(2 + \cos 2\theta)}, & J_{CP} &= \frac{1}{6\sqrt{3}} \sin \delta \sin 2\theta, \end{aligned} \quad (3.11)$$

which implies the following correlations

$$3 \sin^2 \theta_{12} \cos^2 \theta_{13} = 1, \quad \tan 2\theta_{23} \cos \delta^\ell = \frac{\cos 2\theta_{13}}{\sin \theta_{13} \sqrt{2 - 3 \sin^2 \theta_{13}}}. \quad (3.12)$$

Here we note also that this TM2 neutrino mixing pattern emerges within the UV-complete models described in Refs. [61, 62, 78, 205, 323–325].

3.3 Golden ratio mixing pattern

Within the standard golden ratio (GR) mixing pattern¹², the lepton mixing angles are given by $\theta_{23} = 45^\circ$, $\theta_{13} = 0^\circ$ and $\cot \theta_{12} = \phi_g$, where $\phi_g = (1 + \sqrt{5})/2$ is the golden ratio [328, 329]. The lepton mixing matrix is of the form

$$U_{GR} = \begin{pmatrix} c_{12} & s_{12} & 0 \\ -\frac{s_{12}}{\sqrt{2}} & \frac{c_{12}}{\sqrt{2}} & \frac{1}{\sqrt{2}} \\ -\frac{s_{12}}{\sqrt{2}} & \frac{c_{12}}{\sqrt{2}} & -\frac{1}{\sqrt{2}} \end{pmatrix} \equiv \frac{1}{\sqrt{2\sqrt{5}\phi_g}} \begin{pmatrix} \sqrt{2}\phi_g & \sqrt{2} & 0 \\ -1 & \phi_g & \sqrt{\sqrt{5}\phi_g} \\ -1 & \phi_g & -\sqrt{\sqrt{5}\phi_g} \end{pmatrix}. \quad (3.13)$$

¹²Another proposal for the golden ratio mixing has the solar mixing angle given as $\cos \theta_{12} = \phi_g/2$ [326, 327].

In this case, the neutrino mass matrix is given by

$$m_\nu^{GR} = \frac{m_1}{2\sqrt{5}} \begin{pmatrix} 2\phi_g & -\sqrt{2} & -\sqrt{2} \\ -\sqrt{2} & -1/\phi_g & -1/\phi_g \\ -\sqrt{2} & -1/\phi_g & -1/\phi_g \end{pmatrix} + \frac{m_2}{2\sqrt{5}} \begin{pmatrix} 2/\phi_g & \sqrt{2} & \sqrt{2} \\ \sqrt{2} & \phi_g & \phi_g \\ \sqrt{2} & \phi_g & \phi_g \end{pmatrix} + \frac{m_3}{2} \begin{pmatrix} 0 & 0 & 0 \\ 0 & 1 & -1 \\ 0 & -1 & 1 \end{pmatrix}. \quad (3.14)$$

The residual flavour symmetry transformations of m_ν^{GR} take the form

$$G_1^{GR} = \frac{1}{\sqrt{5}} \begin{pmatrix} 1 & -\sqrt{2} & -\sqrt{2} \\ -\sqrt{2} & -\phi_g & 1/\phi_g \\ -\sqrt{2} & 1/\phi_g & -\phi_g \end{pmatrix}, \quad G_2^{GR} = \frac{1}{\sqrt{5}} \begin{pmatrix} -1 & \sqrt{2} & \sqrt{2} \\ \sqrt{2} & -1/\phi_g & \phi_g \\ \sqrt{2} & \phi_g & -1/\phi_g \end{pmatrix},$$

$$G_3^{GR} = - \begin{pmatrix} 1 & 0 & 0 \\ 0 & 0 & 1 \\ 0 & 1 & 0 \end{pmatrix}. \quad (3.15)$$

The minimal flavour symmetry that can produce the golden ratio mixing pattern is the A_5 group [330–332]. Accordingly, a finite Z_5 subgroup is preserved by the charged lepton mass term with

$$G_e = \begin{pmatrix} 1 & 0 & 0 \\ 0 & e^{2\pi i/5} & 0 \\ 0 & 0 & e^{-2\pi i/5} \end{pmatrix}. \quad (3.16)$$

In order to be phenomenologically viable, the golden-ratio pattern would certainly require a revamping, along the lines considered in section 5.

3.4 Bi-maximal mixing pattern

For the bi-maximal mixing, both solar angle and atmospheric mixing angles are maximal $\theta_{12} = \theta_{23} = 45^\circ$ while the reactor angle is vanishing [333]. In the basis where the charged lepton mass matrix is diagonal, the corresponding neutrino mass matrix is given by

$$m_\nu^{BM} = \frac{1}{4} \begin{pmatrix} 2(m_1 + m_2) & \sqrt{2}(m_2 - m_1) & \sqrt{2}(m_2 - m_1) \\ \sqrt{2}(m_2 - m_1) & m_1 + m_2 + 2m_3 & m_1 + m_2 - 2m_3 \\ \sqrt{2}(m_2 - m_1) & m_1 + m_2 - 2m_3 & m_1 + m_2 + 2m_3 \end{pmatrix}. \quad (3.17)$$

The residual flavour symmetry transformations of the above neutrino mass matrix are

$$G_1^{BM} = \frac{1}{2} \begin{pmatrix} 0 & -\sqrt{2} & -\sqrt{2} \\ -\sqrt{2} & -1 & 1 \\ -\sqrt{2} & 1 & -1 \end{pmatrix}, \quad G_2^{BM} = \frac{1}{2} \begin{pmatrix} 0 & \sqrt{2} & \sqrt{2} \\ \sqrt{2} & -1 & 1 \\ \sqrt{2} & 1 & -1 \end{pmatrix}, \quad G_3^{BM} = - \begin{pmatrix} 1 & 0 & 0 \\ 0 & 0 & 1 \\ 0 & 1 & 0 \end{pmatrix}. \quad (3.18)$$

We can choose the residual flavour symmetry of the charged lepton mass matrix to be a Z_4 subgroup with

$$G_e^{BM} = \begin{pmatrix} 1 & 0 & 0 \\ 0 & i & 0 \\ 0 & 0 & -i \end{pmatrix}. \quad (3.19)$$

The group generated by G_1^{BM} , G_2^{BM} , G_3^{BM} and G_e^{BM} is also the S_4 group [334, 335]. Therefore the S_4 flavour symmetry can also be used to produce the bimaximal mixing.

Note, however, that the solar angle θ_{12} and reactor angle θ_{13} would have to undergo very large corrections in order to be compatible with current neutrino oscillation data [24, 25], making this pattern very problematic. As a result, Bi-maximal mixing should be discarded or generalized in a radical way. One of its possible radical generalizations is the Bi-large mixing pattern discussed in section 5.3.

Besides the tri-bimaximal, golden ratio and bi-maximal mixing patterns, there are other constant mixing patterns compatible with experimental data with nonzero θ_{13} [259, 336–338]. They could be derived from the breaking of large flavor symmetry groups such as $\Delta(96)$, $\Delta(384)$ etc. No sizable corrections are necessary for these mixing patterns, however the required vacuum configuration and symmetry breaking are more complicated.

As shown above, the neutrino mass matrices corresponding to the simple tri-bimaximal, golden ratio and bi-maximal mixing patterns obey certain residual flavour symmetries. In the following section, we will show that the neutrino and charged lepton mass matrices generally can have both residual flavour and residual CP symmetries, and also that a residual flavour symmetry can be generated by a residual CP symmetry. In particular, residual symmetries can provide a method to revamp all mixing patterns discussed above. Indeed, in the next section we will show how to revamp them in a systematic manner by using the residual symmetry method. The generalized patterns are not only phenomenologically viable, but also predictive, since the form of the resulting lepton mixing matrices can be restricted.

4 Flavour and CP symmetries from the bottom-up

In this section, we will examine quark and lepton mass matrices that have both remnant flavour and CP symmetry. Remnant flavour symmetries can be generated by performing two remnant CP transformations in succession, with explicit forms of the remnant CP symmetry derived from the experimentally measured mixing matrix. On the other hand, the fermion mixing matrices can be constructed from the postulated residual CP transformations of the quark and lepton mass matrices. In the following, we present the remnant flavour and CP symmetries of the quark and lepton mass matrices, their parametrization and the master formula to construct the mixing matrix from the remnant CP symmetry.

4.1 Residual symmetries of leptons

In the absence of a fundamental theory of flavour we study the effect of possible remnant symmetries G_ν and G_l of the neutrino and charged lepton mass terms. Their existence may provide a model-independent approach towards underpinning the ultimate nature of the underlying theory. Let us now focus on this point.

The lepton masses terms are given in Eq. (1.12) and Eq. (1.13) for Dirac and Majorana neutrinos respectively. Since in the SM the only physical mixing matrix relates to left-handed fermions, we are concerned with the hermitian mass matrix $m_l^\dagger m_l$ connecting left-handed charged leptons on both sides. Under generic unitary transformations of the left-handed lepton fields l_L and ν_L ,

$$l_L \rightarrow G_l l_L, \quad \nu_L \rightarrow G_\nu \nu_L, \quad (4.1)$$

where both G_l and G_ν are three-dimensional unitary matrices, the charged lepton and neutrino mass matrices transform as

$$m_l^\dagger m_l \rightarrow G_l^\dagger m_l^\dagger m_l G_l, \quad (4.2)$$

$$m_\nu \rightarrow G_\nu^T m_\nu G_\nu, \quad \text{for Majorana neutrinos,} \quad (4.3)$$

$$m_\nu^\dagger m_\nu \rightarrow G_\nu^\dagger m_\nu^\dagger m_\nu G_\nu, \quad \text{for Dirac neutrinos.} \quad (4.4)$$

In order for the symmetry to hold, the mass matrices must satisfy

$$G_l^\dagger m_l^\dagger m_l G_l = m_l^\dagger m_l, \quad (4.5)$$

$$G_\nu^T m_\nu G_\nu = m_\nu, \quad \text{for Majorana neutrinos,} \quad (4.6)$$

$$G_\nu^\dagger m_\nu^\dagger m_\nu G_\nu = m_\nu^\dagger m_\nu, \quad \text{for Dirac neutrinos.} \quad (4.7)$$

Applying these invariance conditions to Eqs. (1.16, 1.17, 1.18) and assuming no mass eigenvalue vanishes we obtain

$$U_l^\dagger G_l U_l = \text{diag} (e^{i\alpha_e}, e^{i\alpha_\mu}, e^{i\alpha_\tau}), \quad (4.8)$$

$$U_\nu^\dagger G_\nu U_\nu = \text{diag}(\pm 1, \pm 1, \pm 1), \quad \text{for Majorana neutrinos,} \quad (4.9)$$

$$U_\nu^\dagger G_\nu U_\nu = \text{diag}(e^{i\alpha_{\nu e}}, e^{i\alpha_{\nu\mu}}, e^{i\alpha_{\nu\tau}}), \quad \text{for Dirac neutrinos,} \quad (4.10)$$

where $\alpha_{e,\mu,\tau}$ and $\alpha_{\nu e,\nu\mu,\nu\tau}$, are arbitrary real parameters. It follows that the residual flavour symmetry transformations G_l and G_ν are of the following form [263, 265]:

$$G_l = U_l \text{diag}(e^{i\alpha_e}, e^{i\alpha_\mu}, e^{i\alpha_\tau}) U_l^\dagger, \quad (4.11)$$

$$G_\nu = U_\nu \text{diag}(\pm 1, \pm 1, \pm 1) U_\nu^\dagger, \quad \text{for Majorana neutrinos,} \quad (4.12)$$

$$G_\nu = U_\nu \text{diag}(e^{i\alpha_{\nu e}}, e^{i\alpha_{\nu\mu}}, e^{i\alpha_{\nu\tau}}) U_\nu^\dagger, \quad \text{for Dirac neutrinos.} \quad (4.13)$$

One sees that the charged lepton mass term generically admits a $U(1) \times U(1) \times U(1)$ remnant flavour symmetry. For the neutrino mass matrix the remnant flavour symmetry depends on the nature of neutrinos. For the case of Dirac neutrinos it is also $U(1) \times U(1) \times U(1)$ [263]. For Majorana neutrinos, the eight possible choices of G_ν in Eq. (4.12) correspond to $Z_2 \times Z_2 \times Z_2$. Notice that G_ν and $-G_\nu$ should be identified as the same residual flavour symmetry transformation, since the minus sign can be absorbed as a neutrino field redefinition. Indeed, they both lead to the same constraint on the neutrino mass matrix. We are therefore left with four possible solutions for G_ν , which can be chosen as [269–272],

$$G_i = U_\nu d_i U_\nu^\dagger, \quad i = 1, 2, 3, 4, \quad (4.14)$$

where the d_i are given as

$$\begin{aligned} d_1 &= \text{diag}(1, -1, -1), & d_2 &= \text{diag}(-1, 1, -1), \\ d_3 &= \text{diag}(-1, -1, 1), & d_4 &= \text{diag}(1, 1, 1). \end{aligned} \quad (4.15)$$

One sees that G_4 is simply the trivial identity matrix, and we can further check that

$$G_i^2 = 1, \quad G_i G_j = G_j G_i = G_k \quad \text{with } i \neq j \neq k \neq 4. \quad (4.16)$$

It follows that the residual flavour symmetry of the Majorana neutrino mass matrix is a Klein group isomorphic to $Z_2 \times Z_2$. In the flavour basis where the charged lepton mass matrix m_l is diagonal, U_l would be trivial, so that the lepton mixing comes just from the neutrino sector, i.e. $U = U_\nu$. Hence the residual symmetries of the neutrino and charged lepton mass matrices are determined in terms of the mixing angles and CP violation phases contained in the mixing matrix.

An important observation is that, besides the above residual flavour symmetry, the lepton mass matrices can have residual CP (or charge conjugation parity) symmetry. The CP transformation properties of the left-handed neutrino and charged lepton fields are given by

$$l_L(x) \xrightarrow{CP} i X_l \gamma^0 C \bar{l}_L^T(\mathcal{P}x), \quad \nu_L(x) \xrightarrow{CP} i X_\nu \gamma^0 C \bar{\nu}_L^T(\mathcal{P}x), \quad (4.17)$$

where $\mathcal{P}x = (t, -\vec{x})$, C is the charge-conjugation matrix [94–96], X_l and X_ν are 3×3 unitary matrices acting in family space. Notice that the matrices X_l and X_ν generalize the conventional CP transformation prescription. As a result, they are referred to in the literature as generalized CP transformations [264, 339–344].

Requiring that X_l and X_ν are symmetries of the lepton mass terms in Eqs. (1.12, 1.13) implies that the lepton mass matrices m_l and m_ν should satisfy [265, 345]

$$X_l^\dagger m_l^\dagger m_l X_l = \left(m_l^\dagger m_l\right)^* , \quad (4.18)$$

$$X_\nu^T m_\nu X_\nu = m_\nu^* , \quad \text{for Majorana neutrinos} , \quad (4.19)$$

$$X_\nu^\dagger m_\nu^\dagger m_\nu X_\nu = \left(m_\nu^\dagger m_\nu\right)^* , \quad \text{for Dirac neutrinos} . \quad (4.20)$$

Plugging Eqs. (1.16, 1.17, 1.18) into the above invariance conditions, one sees that the unitary transformations U_l and U_ν must be subject to the following conditions

$$U_l^\dagger X_l U_l^* = \text{diag} \left(e^{i\beta_e}, e^{i\beta_\mu}, e^{i\beta_\tau} \right) , \quad (4.21)$$

$$U_\nu^\dagger X_\nu U_\nu^* = \text{diag} (\pm 1, \pm 1, \pm 1) , \quad \text{for Majorana neutrinos} , \quad (4.22)$$

$$U_\nu^\dagger X_\nu U_\nu^* = \text{diag} \left(e^{i\beta_{\nu e}}, e^{i\beta_{\nu\mu}}, e^{i\beta_{\nu\tau}} \right) , \quad \text{for Dirac neutrinos} , \quad (4.23)$$

where $\beta_{e,\mu,\tau}$ and $\beta_{\nu e,\nu\mu,\nu\tau}$ are real free parameters. Hence the residual CP transformations X_l and X_ν should be of the form [263–268]

$$X_l = U_l \text{diag} \left(e^{i\beta_e}, e^{i\beta_\mu}, e^{i\beta_\tau} \right) U_l^T , \quad (4.24)$$

$$X_\nu = U_\nu \text{diag} (\pm 1, \pm 1, \pm 1) U_\nu^T , \quad \text{for Majorana neutrinos} , \quad (4.25)$$

$$X_\nu = U_\nu \text{diag} \left(e^{i\beta_{\nu e}}, e^{i\beta_{\nu\mu}}, e^{i\beta_{\nu\tau}} \right) U_\nu^T , \quad \text{for Dirac neutrinos} . \quad (4.26)$$

Clearly, both X_l and X_ν are unitary and symmetric matrices [264, 265]

$$X_l = X_l^T , \quad X_\nu = X_\nu^T , \quad X_l X_l^\dagger = X_\nu X_\nu^\dagger = 1 . \quad (4.27)$$

From the expressions of remnant flavor symmetry in Eqs. (4.11, 4.12, 4.13) and remnant CP transformations in Eqs. (4.24, 4.25, 4.26), one can check that the residual flavour and CP symmetries satisfy the following restricted consistency conditions

$$\begin{aligned} X_l G_l^* X_l^{-1} &= G_l^{-1} , \\ X_\nu G_\nu^* X_\nu^{-1} &= G_\nu , \quad \text{for Majorana neutrinos} , \\ X_\nu G_\nu^* X_\nu^{-1} &= G_\nu^{-1} , \quad \text{for Dirac neutrinos} . \end{aligned} \quad (4.28)$$

If we successively perform two CP transformations on the left-handed charged lepton fields, characterized

by $X_l = U_l \text{diag}(e^{i\beta_e}, e^{i\beta_\mu}, e^{i\beta_\tau}) U_l^T$ and $X_l' = U_l \text{diag}(e^{i\beta_e'}, e^{i\beta_\mu'}, e^{i\beta_\tau'}) U_l^T$ we obtain ¹³

$$l_L(x) \xrightarrow{CP} iX_l \gamma^0 C \bar{l}_L^T(\mathcal{P}x) \xrightarrow{CP} X_l X_l'^* l_L(x), \quad (4.29)$$

with

$$X_l X_l'^* = U_l \text{diag}(e^{i(\beta_e - \beta_e')}, e^{i(\beta_\mu - \beta_\mu')}, e^{i(\beta_\tau - \beta_\tau')}) U_l^\dagger. \quad (4.30)$$

Moreover, from the invariance condition of $m_l^\dagger m_l$ under the residual CP symmetry, Eq. (4.18), it is easy to show that

$$X_l'^T X_l^\dagger m_l^\dagger m_l X_l X_l'^* = m_l^\dagger m_l. \quad (4.31)$$

This means that performing two CP transformations in succession is equivalent to a flavour symmetry transformation $X_l X_l'^* \equiv G_l$ [265]. The same conclusion also holds true for neutrinos if they are Dirac particles.

For the case of Majorana neutrinos, there are eight possibilities for X_ν . In this case one should take X_ν and $-X_\nu$ as the same CP transformation, since the minus sign can be absorbed into the neutrino fields since the mass term involves a product of two neutrino fields. As a result only four of them are relevant. Without loss of generality they can be chosen to be [265–267]

$$X_i = U_\nu d_i U_\nu^T, \quad i = 1, 2, 3, 4, \quad (4.32)$$

with d_i given in Eq. (4.15). The remaining four can be obtained from the above by multiplying an overall -1 factor. It is straightforward to check that the neutrino mass matrix m_ν satisfies

$$X_j^\dagger X_i^T m_\nu X_i X_j^* = m_\nu. \quad (4.33)$$

As a result, remnant flavour symmetries can be generated by remnant CP symmetries as well. Explicitly, we have the following relations [265]:

$$\begin{aligned} X_2 X_3^* &= X_3 X_2^* = X_4 X_1^* = X_1 X_4^* = G_1, \\ X_1 X_3^* &= X_3 X_1^* = X_4 X_2^* = X_2 X_4^* = G_2, \\ X_1 X_2^* &= X_2 X_1^* = X_4 X_3^* = X_3 X_4^* = G_3, \\ X_1 X_1^* &= X_2 X_2^* = X_3 X_3^* = X_4 X_4^* = G_4 = 1. \end{aligned} \quad (4.34)$$

As a result, once we impose a set of generalized CP transformations, there is always an associated flavour symmetry. Furthermore, Eq. (4.34) implies that any residual CP transformation can be expressed in terms of the remaining ones as follows [265],

$$X_i = X_j X_m^* X_n, \quad i \neq j \neq m \neq n. \quad (4.35)$$

¹³Notice that an overall minus sign is dropped in the last step, as it can be absorbed into the lepton field.

In other words, only three of the four remnant CP transformations are independent. In the flavour basis where m_l is diagonal, the residual CP transformation X_l is an arbitrary diagonal phase matrix, while $X_\nu = U \text{diag}(\pm 1, \pm 1, \pm 1) U^T$. Hence the remnant CP symmetry can be constructed from the neutrino mixing matrix, and its explicit form can be determined more precisely with the improved measurement of the mixing angles and CP phases [24, 25].

Here we have so far assumed that the three light neutrino masses are non-vanishing. If the lightest neutrino is massless one can analyze the residual symmetry of the neutrino mass matrix in the same way. This interesting situation occurs generically in the “missing partner” seesaw mechanism [30] in which there are less “right” than “left”-handed neutrinos¹⁴ (a massless neutrino also emerges in theories where anti-symmetric Yukawa couplings are involved in generating neutrino mass [130]). Note that an incomplete fermion multiplet structure¹⁵ can also be interesting in cosmology [134–138].

With one neutrino massless one has $m_1 = 0$ for normal ordered (NO) neutrino mass spectrum, and $m_3 = 0$ for the inverted ordered (IO) spectrum. If neutrinos have Dirac nature, one finds that the residual CP transformation X_ν would still be given by Eq. (4.26). On the other hand, if neutrinos are Majorana particles, one must use Eq. (4.25) replacing the diagonal entry “ ± 1 ” in the position (11) for NO and (33) for IO with an arbitrary phase factor [348], i.e.

$$X_\nu = \begin{cases} U_\nu \text{diag}(e^{i\beta}, \pm 1, \pm 1) U_\nu^T, & \text{for NO,} \\ U_\nu \text{diag}(\pm 1, \pm 1, e^{i\beta}) U_\nu^T, & \text{for IO,} \end{cases} \quad (4.36)$$

where β is real. Similarly the residual flavour symmetry G_ν becomes [265, 348]

$$G_\nu = \begin{cases} U_\nu \text{diag}(e^{i\alpha}, \pm 1, \pm 1) U_\nu^\dagger, & \text{for NO,} \\ U_\nu \text{diag}(\pm 1, \pm 1, e^{i\alpha}) U_\nu^\dagger, & \text{for IO,} \end{cases} \quad (4.37)$$

with real α . Hence the generalized CP and residual flavour symmetry groups have the structure $U(1) \times Z_2$ (instead of $Z_2 \times Z_2$) modulo a possible overall factor -1 in this case. On the other hand, this kind of residual symmetry can enforce a massless Majorana neutrino. The breaking of finite discrete groups into this form of G_ν in the neutrino sector was analyzed in [349–351], where the angle α was a rational multiple of π .

4.2 Reconstructing lepton mixing from remnant CP symmetry

As shown in above, residual CP symmetries can be derived from the mixing matrix, and conversely, the lepton mixing matrix can be constructed from the remnant CP symmetries in the neutrino and the charged lepton sectors. In concrete models, we can start from a set of CP transformations $\mathcal{X}_{\mathcal{CP}}$ respected by the Lagrangian at some high energy scale. Subsequently $\mathcal{X}_{\mathcal{CP}}$ is spontaneously broken by some scalar fields into different remnant symmetries in the neutrino and the charged lepton sectors. The misalignment

¹⁴The present neutrino data allows the possibility that the lightest neutrino is massless, consequently at least two right-handed neutrinos are necessary in type-I seesaw [131–133].

¹⁵For a discussion of seesaw leptogenesis with two and three right-handed neutrinos see [346, 347].

between the two remnant symmetries is responsible for the mismatch of the rotations which diagonalize the neutrino and charged lepton matrices, leading to the lepton mixing matrix. We now present the general parametrization for the remnant CP symmetries of the neutrino and charged lepton sector, and the corresponding restrictions on the unitary transformations U_ν and U_l .

We start from the simplest nontrivial case in which a single remnant CP transformation X_R is preserved by the neutrino mass matrix. As shown in section 4.1, X_R should be a symmetric unitary matrix, otherwise the light neutrino masses would be degenerate. Thus X_R can be parameterized as follows [265]:

$$X_R = e^{i\kappa_1} v_1 v_1^T + e^{i\kappa_2} v_2 v_2^T + e^{i\kappa_3} v_3 v_3^T, \quad (4.38)$$

where the phases κ_1 , κ_2 and κ_3 can be taken in the range of 0 and 2π without loss of generality, v_1 , v_2 and v_3 are mutually orthogonal vectors with

$$\begin{aligned} v_1 &= \begin{pmatrix} \cos \varphi \\ \sin \varphi \cos \phi \\ \sin \varphi \sin \phi \end{pmatrix}, & v_2 &= \begin{pmatrix} \sin \varphi \cos \rho \\ -\sin \phi \sin \rho - \cos \varphi \cos \phi \cos \rho \\ \cos \phi \sin \rho - \cos \varphi \sin \phi \cos \rho \end{pmatrix}, \\ v_3 &= \begin{pmatrix} \sin \varphi \sin \rho \\ \sin \phi \cos \rho - \cos \varphi \cos \phi \sin \rho \\ -\cos \phi \cos \rho - \cos \varphi \sin \phi \sin \rho \end{pmatrix}. \end{aligned} \quad (4.39)$$

Invariance of the neutrino mass matrix under X_R implies that U_ν should be subject to the constraint in Eq. (4.22) and Eq. (4.23) for Majorana and Dirac neutrinos. As a consequence, U_ν is fixed to be [265]

$$U_\nu = (v_1, v_2, v_3) \text{diag}(e^{i\frac{\kappa_1}{2}}, e^{i\frac{\kappa_2}{2}}, e^{i\frac{\kappa_3}{2}}) O_3(\theta_1, \theta_2, \theta_3) Q_\nu, \quad (4.40)$$

where O_3 is a generic real orthogonal matrix,

$$O_3(\theta_1, \theta_2, \theta_3) = \begin{pmatrix} 1 & 0 & 0 \\ 0 & \cos \theta_1 & \sin \theta_1 \\ 0 & -\sin \theta_1 & \cos \theta_1 \end{pmatrix} \begin{pmatrix} \cos \theta_2 & 0 & \sin \theta_2 \\ 0 & 1 & 0 \\ -\sin \theta_2 & 0 & \cos \theta_2 \end{pmatrix} \begin{pmatrix} \cos \theta_3 & \sin \theta_3 & 0 \\ -\sin \theta_3 & \cos \theta_3 & 0 \\ 0 & 0 & 1 \end{pmatrix}, \quad (4.41)$$

where the rotation angles $\theta_{1,2,3}$ are free. The matrix Q_ν is diagonal, and its entries are ± 1 and $\pm i$ which encode the CP parity of the neutrinos, while it is unphysical for Dirac neutrinos.

If two remnant CP transformations X_{R1} and X_{R2} out of the original CP symmetry are preserved in the neutrino sector, they can generally be written as [265]

$$\begin{aligned} X_{R1} &= e^{i\kappa_1} v_1 v_1^T + e^{i\kappa_2} v_2 v_2^T + e^{i\kappa_3} v_3 v_3^T, \\ X_{R2} &= e^{i\kappa_1} v_1 v_1^T - e^{i\kappa_2} v_2 v_2^T - e^{i\kappa_3} v_3 v_3^T, \end{aligned} \quad (4.42)$$

for Majorana neutrinos¹⁶. A remnant flavour transformation G_R can be obtained from X_{R1} and X_{R2} as

$$G_R = X_{R1}X_{R2}^* = X_{R2}X_{R1}^* = 2v_1v_1^T - 1, \quad (4.43)$$

which satisfies $G_R^2 = 1$. Hence a remnant Z_2 flavor symmetry generated by G_R is induced and it fixes one column of U_ν to be v_1 . Besides the parameters characterizing the remnant CP symmetry, U_ν is determined just by a free rotation angle θ [265],

$$U_\nu = (v_1, v_2, v_3) \text{diag}(e^{i\frac{\kappa_1}{2}}, e^{i\frac{\kappa_2}{2}}, e^{i\frac{\kappa_3}{2}}) R_{23}(\theta) P_\nu Q_\nu, \quad (4.44)$$

where $R_{23}(\theta)$ denotes a rotation matrix through an angle θ in the (23)-plane with $0 \leq \theta < \pi$,

$$R_{23}(\theta) = \begin{pmatrix} 1 & 0 & 0 \\ 0 & \cos \theta & \sin \theta \\ 0 & -\sin \theta & \cos \theta \end{pmatrix}. \quad (4.45)$$

Since the remnant symmetry can not constrain the ordering of the light neutrino mass eigenvalues, U_ν is determined up to independent column permutations, and consequently P_ν is a generic permutation matrix which can take six possible forms 1, P_{12} , P_{13} , P_{23} , $P_{23}P_{12}$, $P_{23}P_{13}$ with

$$P_{12} = \begin{pmatrix} 0 & 1 & 0 \\ 1 & 0 & 0 \\ 0 & 0 & 1 \end{pmatrix}, \quad P_{13} = \begin{pmatrix} 0 & 0 & 1 \\ 0 & 1 & 0 \\ 1 & 0 & 0 \end{pmatrix}, \quad P_{23} = \begin{pmatrix} 1 & 0 & 0 \\ 0 & 0 & 1 \\ 0 & 1 & 0 \end{pmatrix}. \quad (4.46)$$

We see that the unitary transformations U_ν for the two permutations P_ν and $P_{23}P_\nu$ are related by the redefinitions $\theta \rightarrow \theta - \pi/2$ and $Q_\nu \rightarrow P_\nu^T \text{diag}(1, 1, -1) P_\nu Q_\nu$. Hence only three inequivalent permutations of the columns are relevant in this case. In other words, the fixed vector $(\cos \varphi, \sin \varphi \cos \phi, \sin \varphi \sin \phi)^T$ can be the first column, the second column or the third column of the matrix U_ν .

For the case of Majorana neutrinos, we consider the scenario that all independent remnant CP transformations are preserved by the neutrino mass matrix. The remnant CP transformations can be parameterized as [267]

$$\begin{aligned} X_{R1} &= e^{i\kappa_1} v_1 v_1^T + e^{i\kappa_2} v_2 v_2^T + e^{i\kappa_3} v_3 v_3^T, \\ X_{R2} &= e^{i\lambda_1} v_1 v_1^T + e^{i\lambda_2} w_2 w_2^T + e^{i\lambda_3} w_3 w_3^T, \\ X_{R3} &= e^{i\lambda_1} v_1 v_1^T - e^{i\lambda_2} w_2 w_2^T - e^{i\lambda_3} w_3 w_3^T, \\ X_{R4} &= e^{i\kappa_1} v_1 v_1^T - e^{i\kappa_2} v_2 v_2^T - e^{i\kappa_3} v_3 v_3^T, \end{aligned} \quad (4.47)$$

¹⁶For Dirac neutrinos, the neutrino mixing matrix U_ν would be completely fixed up to column permutations, if the order of the remnant flavour transformation $G_R = X_{R1}X_{R2}^* = X_{R2}X_{R1}^*$ is greater than or equal to three, so as to distinguish the three families.

where v_1 , w_2 and w_3 also form another set of real orthonormal vectors with

$$w_2 = \cos \xi v_2 - \sin \xi v_3, \quad w_3 = \sin \xi v_2 + \cos \xi v_3, \quad (4.48)$$

and the phases $e^{i\lambda_1}$, $e^{i\lambda_2}$ and $e^{i\lambda_3}$ are given by

$$e^{i\lambda_1} = -e^{i\kappa_1}, \quad e^{i\lambda_2} = -\frac{e^{i\kappa_2} \cos^2 \xi + e^{i\kappa_3} \sin^2 \xi}{|e^{i\kappa_2} \cos^2 \xi + e^{i\kappa_3} \sin^2 \xi|}, \quad e^{i\lambda_3} = \frac{e^{i\kappa_2} \sin^2 \xi + e^{i\kappa_3} \cos^2 \xi}{|e^{i\kappa_2} \sin^2 \xi + e^{i\kappa_3} \cos^2 \xi|}. \quad (4.49)$$

A remnant Klein four flavour symmetry $K_4 \equiv \{1, G_{R1}, G_{R2}, G_{R3}\}$ can be generated by performing two CP transformations, and the three nontrivial residual flavour symmetry transformations G_{Ri} for $i = 1, 2, 3$ can be expressed as

$$\begin{aligned} G_{R1} &= X_{R1} X_{R4}^* = v_1 v_1^T - v_2 v_2^T - v_3 v_3^T, \\ G_{R2} &= X_{R1} X_{R3}^* = -v_1 v_1^T - c_{22} v_2 v_2^T - c_{33} v_3 v_3^T - c_{23} v_2 v_3^T - c_{32} v_3 v_2^T, \\ G_{R3} &= X_{R1} X_{R2}^* = -v_1 v_1^T + c_{22} v_2 v_2^T + c_{33} v_3 v_3^T + c_{23} v_2 v_3^T + c_{32} v_3 v_2^T, \end{aligned} \quad (4.50)$$

with

$$c_{22} = -c_{33} = -\frac{\cos 2\xi}{|e^{i\kappa_2} \cos^2 \xi + e^{i\kappa_3} \sin^2 \xi|}, \quad c_{23} = c_{32}^* = \frac{\cos\left(\frac{\kappa_2 - \kappa_3}{2}\right) e^{i\frac{\kappa_2 - \kappa_3}{2}} \sin 2\xi}{|e^{i\kappa_2} \cos^2 \xi + e^{i\kappa_3} \sin^2 \xi|}. \quad (4.51)$$

In this case, the neutrino mixing matrix U_ν is completely determined by the remnant CP transformations without additional free parameters [267],

$$U_\nu = (v_1, v_2, v_3) \text{diag}(e^{i\frac{\kappa_1}{2}}, e^{i\frac{\kappa_2}{2}}, e^{i\frac{\kappa_3}{2}}) R_{23}(\chi) P_\nu Q_\nu, \quad (4.52)$$

where the angle χ fulfills

$$\tan 2\chi = \cos\left(\frac{\kappa_2 - \kappa_3}{2}\right) \tan 2\xi. \quad (4.53)$$

Notice that the lepton mixing angles and the three CP violating phases are completely fixed by the remnant CP symmetry in this case. Moreover, note that the master *formulae* of Eqs. (4.40, 4.44, 4.52) for U_ν hold irrespective of how the remnant CP symmetry is dynamically realized.

4.3 Residual symmetries of quarks

In this section, we turn to the residual flavour and CP symmetries of the quark mass matrices. The Lagrangian for the quark masses is given in Eq. (1.2). One can easily check that the hermitian combinations $m_U^\dagger m_U$ and $m_D^\dagger m_D$ are invariant under the following unitary transformations [263],

$$U_L \rightarrow G_u U_L, \quad D_L \rightarrow G_d D_L, \quad (4.54)$$

with

$$G_u = V_u \text{diag}(e^{i\alpha_u}, e^{i\alpha_c}, e^{i\alpha_t}) V_u^\dagger, \quad G_d = V_d \text{diag}(e^{i\alpha_d}, e^{i\alpha_s}, e^{i\alpha_b}) V_d^\dagger, \quad (4.55)$$

where α_q ($q = u, d, c, s, t, b$) are arbitrary phase parameters. Hence the following equalities are satisfied,

$$G_u^\dagger m_U^\dagger m_U G_u = m_U^\dagger m_U, \quad G_d^\dagger m_D^\dagger m_D G_d = m_D^\dagger m_D. \quad (4.56)$$

In other words, both the up-quark mass matrix m_U and down-quark mass matrix m_D have a residual $U(1) \times U(1) \times U(1)$ flavour symmetry [263]. Notice that the same conclusion holds true for any Dirac fermion mass matrix, hence it also applies for the charged lepton mass term.

Let us now turn to the discussion of residual CP symmetries of the quark mass term. Assuming the left-handed quarks U_L and D_L transform as

$$U_L(x) \xrightarrow{CP} iX_u \gamma^0 C \bar{U}_L^T(\mathcal{P}x), \quad D_L(x) \xrightarrow{CP} iX_d \gamma^0 C \bar{D}_L^T(\mathcal{P}x), \quad (4.57)$$

this is a symmetry of the quark mass matrices m_U and m_D if and only if $m_U^\dagger m_U$ and $m_D^\dagger m_D$ fulfill the conditions

$$X_u^\dagger m_U^\dagger m_U X_u = (m_U^\dagger m_U)^*, \quad X_d^\dagger m_D^\dagger m_D X_d = (m_D^\dagger m_D)^*. \quad (4.58)$$

Similarly to the charged lepton sector, one can show that X_u and X_d must take the following form

$$X_u = V_u \text{diag} \left(e^{i\beta_u}, e^{i\beta_c}, e^{i\beta_t} \right) V_u^T, \quad X_d = V_d \text{diag} \left(e^{i\beta_d}, e^{i\beta_s}, e^{i\beta_b} \right) V_d^T, \quad (4.59)$$

where β_q ($q = u, d, c, s, t, b$) are real. It is easy to see that both X_u and X_d are unitary symmetric matrices, and that residual flavour symmetries G_u and G_d will be generated by X_u and X_d , respectively. In the basis where the up-quark mass matrix is diagonal, V_u is diagonal, so that V_d coincides with the CKM matrix, $V_d = V_{CKM}$. As a result, the explicit form of the remnant flavour symmetries G_u , G_d and the remnant CP symmetries X_u , X_d can be fixed in terms of the measured values of the CKM matrix elements [28]. As in section 4.2 for lepton sector, the quark mixing matrix can also be fixed by the remnant CP symmetry.

So far we have shown that lepton and quark mass terms generically admit residual flavour and CP symmetries. These are associated to the charged current flavour mixing matrix. One may ask about the origin of these residual symmetries. It is well known that the spontaneous breaking of the $SU(3)_c \otimes SU(2)_L \otimes U(1)_Y$ gauge symmetry preserves the $U(1)$ gauge symmetry associated to electromagnetism. Likewise, one may conjecture that at some high energy scale the true underlying theory has a flavour and CP symmetry which is subsequently broken down to the residual symmetry or a subgroup of it. This gives a further motivation for introducing flavour and CP symmetries, i.e. to explain flavour mixing and CP violation in a model-independent manner. We also saw that the residual flavour symmetry of the charged leptons and quarks should be contained in $U(1) \times U(1) \times U(1)$. The same holds for neutrinos if they are Dirac particles. In contrast, the residual flavour symmetry of the neutrino sector should be a subgroup of $Z_2 \times Z_2 \times Z_2$ if they are Majorana fermions.

In a pioneering work [276], Froggatt and Nielsen originally took the $G_f = U(1)$ flavor symmetry in order to explain the quark mass ratios and the CKM mixing angles, which are expressed as powers of small G_f breaking parameters. This is the so-called FN mechanism. Concerning the lepton sector,

broken flavor symmetries based on non-abelian discrete groups were found to reproduce certain interesting mixing patterns, such as TBM as a first order approximation [53, 54, 70, 313]. Continuous Lie groups $U(2)$ [277, 352–354], $SO(3)$ [287, 355, 356] and $SU(3)$ [293, 357–359] as flavor symmetries were also studied to address the flavor puzzles. Typically, they must be strongly broken.

Besides the use of full-fledged flavor symmetries, there are more phenomenological approaches to the flavor puzzle involving, e.g., the use of texture zeros in the fermion mass matrices [360–363]. Alternatively the assumption of lepton mixing “anarchy” [51, 52]. In the present review, we shall focus on the approach of discrete flavor symmetry as well as generalized CP symmetry.

5 Viable lepton mixing patterns

The “constant” lepton mixing patterns discussed in section 3, such as the tri-bimaximal, golden ratio and bi-maximal mixing, characterized by numerical predictions for the mixing angles and phase, are all ruled out by neutrino oscillation data [24, 25], especially by the precise measurement of the “reactor angle” θ_{13} [305, 306]. They all need to be “revamped” in order to be compatible with experimental data and to enable meaningful theoretical predictions for CP violation.

In this section we assume that neutrinos are Majorana particles and show how the imposition of residual flavour and CP symmetries [257, 258, 265, 364–366] can be used to produce systematic generalizations of the patterns discussed in the section 3. Indeed, imposing the residual symmetries G_i in Sec. 4 fixes the i -th column of the mixing matrix. In this way one can obtain generalized patterns which can be not only viable, but also predictive, in which the mixing matrix is described by just a few parameters. This model-independent approach of predicting new mixing patterns holds irrespective of how the relevant mass matrices arise from first principles. We now describe some examples.

5.1 Revamped TBM mixing

Working in the charged lepton diagonal basis, we start our discussion with the “complex TBM” matrix (cTBM) [367], which is given by

$$U_{cTBM} = \begin{pmatrix} \sqrt{\frac{2}{3}} & \frac{e^{-i\rho}}{\sqrt{3}} & 0 \\ -\frac{e^{i\rho}}{\sqrt{6}} & \frac{1}{\sqrt{3}} & \frac{e^{-i\sigma}}{\sqrt{2}} \\ \frac{e^{i(\rho+\sigma)}}{\sqrt{6}} & -\frac{e^{i\sigma}}{\sqrt{3}} & \frac{1}{\sqrt{2}} \end{pmatrix}. \quad (5.1)$$

This cTBM mixing matrix predicts the same mixing angles as the usual real TBM pattern in Eq. (3.2), though the Majorana phases are non-vanishing. Within the symmetrical parametrization of the lepton mixing matrix in Eqs. (1.21) and (1.22) they are given by

$$\phi_{12} = \rho, \quad \phi_{23} = \sigma. \quad (5.2)$$

The TBM matrix in Eq. (3.1) corresponds to zero Majorana phases $\rho = \sigma = 0$ and hence we call it real TBM¹⁷. From Eq. (4.32), we know the four CP symmetry matrices $X_{1,2,3,4}$ associated with the cTBM mixing pattern are

$$X_i = U_{cTBM} d_i U_{cTBM}^T, \quad (5.3)$$

¹⁷The minus sign of the third row is absorbed into the charged leptons.

where $d_{1,2,3,4}$ are diagonal matrices with entries ± 1 given in Eq. (4.15). Thus the above four CP symmetries are given in matrix form as

$$\begin{aligned}
X_1 &= \frac{1}{6} \begin{pmatrix} 4 - 2e^{-2i\rho} & -2e^{-i\rho} - 2e^{i\rho} & 2e^{i(\rho+\sigma)} + 2e^{-i(\rho-\sigma)} \\ -2e^{-i\rho} - 2e^{i\rho} & -2 + e^{2i\rho} - 3e^{-2i\sigma} & -3e^{-i\sigma} - e^{i(2\rho+\sigma)} + 2e^{i\sigma} \\ 2e^{i(\rho+\sigma)} + 2e^{-i(\rho-\sigma)} & -3e^{-i\sigma} - e^{i(2\rho+\sigma)} + 2e^{i\sigma} & -3 + e^{2i(\rho+\sigma)} - 2e^{2i\sigma} \end{pmatrix}, \\
X_2 &= \frac{1}{6} \begin{pmatrix} -4 + 2e^{-2i\rho} & 2e^{-i\rho} + 2e^{i\rho} & -2e^{i(\rho+\sigma)} - 2e^{-i(\rho-\sigma)} \\ 2e^{-i\rho} + 2e^{i\rho} & 2 - e^{2i\rho} - 3e^{-2i\sigma} & -3e^{-i\sigma} + e^{i(2\rho+\sigma)} - 2e^{i\sigma} \\ -2e^{i(\rho+\sigma)} - 2e^{-i(\rho-\sigma)} & -3e^{-i\sigma} + e^{i(2\rho+\sigma)} - 2e^{i\sigma} & -3 - e^{2i(\rho+\sigma)} + 2e^{2i\sigma} \end{pmatrix}, \\
X_3 &= \frac{1}{6} \begin{pmatrix} -4 - 2e^{-2i\rho} & -2e^{-i\rho} + 2e^{i\rho} & -2e^{i(\rho+\sigma)} + 2e^{-i(\rho-\sigma)} \\ -2e^{-i\rho} + 2e^{i\rho} & -2 - e^{2i\rho} + 3e^{-2i\sigma} & 3e^{-i\sigma} + e^{i(2\rho+\sigma)} + 2e^{i\sigma} \\ -2e^{i(\rho+\sigma)} + 2e^{-i(\rho-\sigma)} & 3e^{-i\sigma} + e^{i(2\rho+\sigma)} + 2e^{i\sigma} & 3 - e^{2i(\rho+\sigma)} - 2e^{2i\sigma} \end{pmatrix}, \\
X_4 &= \frac{1}{6} \begin{pmatrix} 4 + 2e^{-2i\rho} & 2e^{-i\rho} - 2e^{i\rho} & 2e^{i(\rho+\sigma)} - 2e^{-i(\rho-\sigma)} \\ 2e^{-i\rho} - 2e^{i\rho} & 2 + e^{2i\rho} + 3e^{-2i\sigma} & 3e^{-i\sigma} - e^{i(2\rho+\sigma)} - 2e^{i\sigma} \\ 2e^{i(\rho+\sigma)} - 2e^{-i(\rho-\sigma)} & 3e^{-i\sigma} - e^{i(2\rho+\sigma)} - 2e^{i\sigma} & 3 + e^{2i(\rho+\sigma)} + 2e^{2i\sigma} \end{pmatrix}. \tag{5.4}
\end{aligned}$$

The CP symmetries corresponding to the ‘‘standard’’ real TBM matrix of Eq. (3.1) are obtained simply by taking the limit of $\rho, \sigma \rightarrow 0$ in Eq. (5.4). These CP symmetries are therefore given by

$$\begin{aligned}
X_1 &= \frac{1}{3} \begin{pmatrix} 1 & -2 & 2 \\ -2 & -2 & -1 \\ 2 & -1 & -2 \end{pmatrix}, & X_2 &= \frac{1}{3} \begin{pmatrix} -1 & 2 & -2 \\ 2 & -1 & -2 \\ -2 & -2 & -1 \end{pmatrix}, \\
X_3 &= \begin{pmatrix} -1 & 0 & 0 \\ 0 & 0 & 1 \\ 0 & 1 & 0 \end{pmatrix}, & X_4 &= \begin{pmatrix} 1 & 0 & 0 \\ 0 & 1 & 0 \\ 0 & 0 & 1 \end{pmatrix}. \tag{5.5}
\end{aligned}$$

As shown in Eq. (4.34), the residual flavour symmetry can be generated by the CP transformations,

$$\begin{aligned}
G_1 &= X_2 X_3^* = X_3 X_2^* = X_4 X_1^* = X_1 X_4^*, & G_2 &= X_1 X_3^* = X_3 X_1^* = X_4 X_2^* = X_2 X_4^*, \\
G_3 &= X_1 X_2^* = X_2 X_1^* = X_4 X_3^* = X_3 X_4^*, & G_4 &= X_1 X_1^* = X_2 X_2^* = X_3 X_3^* = X_4 X_4^*. \tag{5.6}
\end{aligned}$$

It is our goal here to obtain generalized but restricted forms for the mixing matrices starting from the ‘‘original’’ ones by exploiting residual flavour and CP symmetries. Notice that only three of the four CP and flavour symmetries are really independent [265, 267]. If any three of the four CP symmetries in Eq. (5.4) are imposed simultaneously, the neutrino mixing matrix would be the cTBM matrix in Eq. (5.1) with $\theta_{13} = 0$. Therefore, we will impose only two or only one of these CP symmetries, so that realistic mixing patterns with non-vanishing θ_{13} and CP violation are obtained.

5.1.1 Case a: G_1 flavour and X_1, X_4 CP symmetries

The requirement that the CP transformations X_1 and X_4 are symmetries of the neutrino mass matrix m_ν implies that the G_1 flavour symmetry is preserved and m_ν satisfies

$$X_1^T m_\nu X_1 = m_\nu^*, \quad X_4^T m_\nu X_4 = m_\nu^*. \quad (5.7)$$

Consequently the light neutrino mass matrix is of the following form

$$m'_\nu = U_{cTBM}^T m_\nu U_{cTBM} = \begin{pmatrix} m_1 & 0 & 0 \\ 0 & m_2 & \delta m \\ 0 & \delta m & m_3 \end{pmatrix}, \quad (5.8)$$

where the parameters m_1, m_2, m_3 and δm are real. The mass matrix m'_ν can be diagonalized by a real orthogonal matrix $R_{23}(\theta)$ given by

$$R_{23}(\theta) = \begin{pmatrix} 1 & 0 & 0 \\ 0 & \cos \theta & \sin \theta \\ 0 & -\sin \theta & \cos \theta \end{pmatrix} \quad \text{with} \quad \tan 2\theta = \frac{2\delta m}{m_3 - m_2}. \quad (5.9)$$

As a result, in this case the lepton mixing matrix is given as

$$\begin{aligned} U &= U_{cTBM} R_{23} Q_\nu \\ &= \frac{1}{\sqrt{6}} \begin{pmatrix} 2 & \sqrt{2}e^{-i\rho} \cos \theta & \sqrt{2}e^{-i\rho} \sin \theta \\ -e^{i\rho} & \sqrt{2} \cos \theta - \sqrt{3}e^{-i\sigma} \sin \theta & \sqrt{2} \sin \theta + \sqrt{3}e^{-i\sigma} \cos \theta \\ e^{i(\rho+\sigma)} & -\sqrt{3} \sin \theta - \sqrt{2}e^{i\sigma} \cos \theta & \sqrt{3} \cos \theta - \sqrt{2}e^{i\sigma} \sin \theta \end{pmatrix} Q_\nu, \end{aligned} \quad (5.10)$$

where $Q_\nu = \text{diag}(e^{ik_1\pi/2}, e^{ik_2\pi/2}, e^{ik_3\pi/2})$ is a diagonal unitary matrix with $k_{1,2,3} = 0, 1, 2, 3$. The entries ± 1 and $\pm i$ encode the CP parities of the neutrino states and render the neutrino mass eigenvalues non-negative. From Eq. (5.10) one can then extract the expressions of lepton mixing angles and CP violating phases as follows,

$$\begin{aligned} \sin^2 \theta_{13} &= \frac{\sin^2 \theta}{3}, \quad \sin^2 \theta_{12} = \frac{\cos^2 \theta}{\cos^2 \theta + 2}, \quad \sin^2 \theta_{23} = \frac{1}{2} + \frac{\sqrt{6} \sin 2\theta \cos \sigma}{2 \cos^2 \theta + 4}, \\ \sin \delta^\ell &= -\frac{\text{sign}(\sin 2\theta)(\cos^2 \theta + 2) \sin \sigma}{\sqrt{(\cos^2 \theta + 2)^2 - 6 \sin^2 2\theta \cos^2 \sigma}}, \quad \tan \delta^\ell = \frac{2 + \cos^2 \theta}{2 - 5 \cos^2 \theta} \tan \sigma, \\ \phi_{12} &= \rho + \frac{(k_1 - k_2)\pi}{2}, \quad \phi_{13} = \rho + \frac{(k_1 - k_3)\pi}{2}. \end{aligned} \quad (5.11)$$

Notice that in the symmetric parametrization the CP violating phase characterizing neutrino oscillations is given by the invariant combination $\delta^\ell = \phi_{13} - \phi_{12} - \phi_{23}$ [99], see Eq. (1.22). We see that the first column of the lepton mixing matrix in Eq. (5.10) is $(2, -e^{i\rho}, e^{i(\rho+\sigma)})^T/\sqrt{6}$ which is in common with that of the cTBM mixing pattern. This arises from the preserved G_1 symmetry. Eliminating the parameters

θ and σ in Eq. (5.11), we see that the lepton mixing angles and CP phases are correlated with each other according to

$$\cos^2 \theta_{12} \cos^2 \theta_{13} = \frac{2}{3}, \quad \tan 2\theta_{23} \cos \delta^\ell = \frac{5 \sin^2 \theta_{13} - 1}{2 \sin \theta_{13} \sqrt{2 - 6 \sin^2 \theta_{13}}}. \quad (5.12)$$

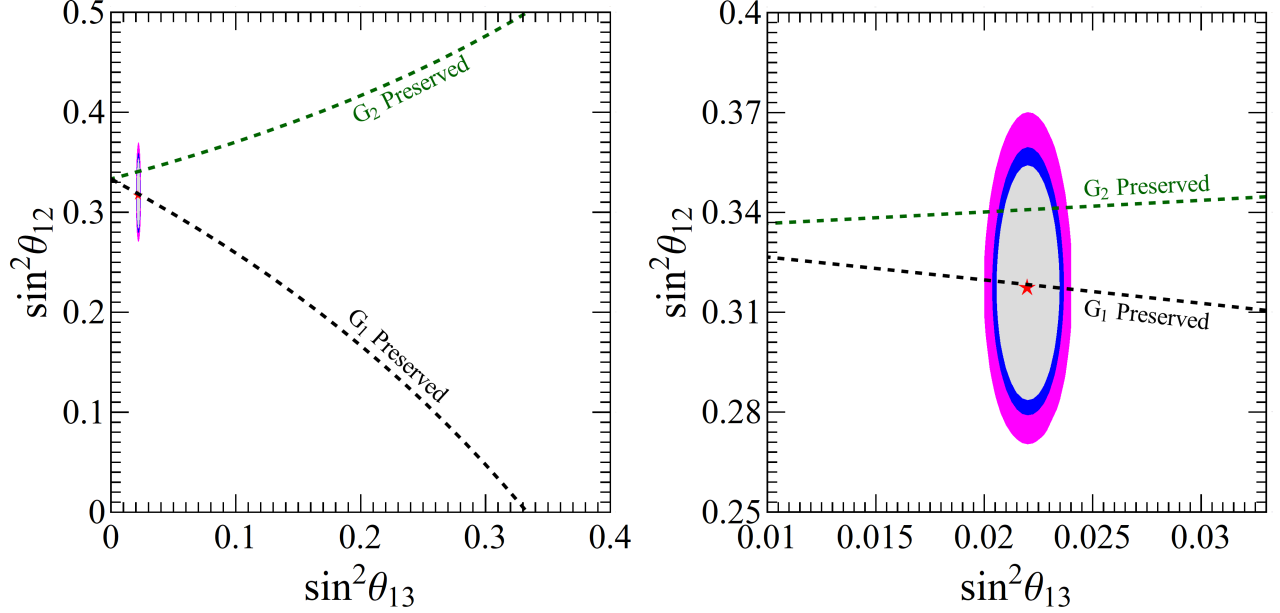


Figure 11: Predicted correlation between $\sin^2 \theta_{12}$ and $\sin^2 \theta_{13}$ in the revamped TBM scheme. The black-dashed line corresponds to the case where G_1 is preserved by the neutrino sector (Eq. (5.12), left), while the green-dashed one refers to the case where G_2 is preserved (Eq. (5.18), left). The right panel is a zoom of the left one. The global fit regions correspond to 90%, 95% and 99% confidence levels [24, 25].

The first equation in Eq. (5.12) relates the solar and the reactor angles while, for given values of the latter, the second equation correlates the CP phase δ^ℓ and the atmospheric angle. These correlations can be used to test the mixing matrix of Eq. (5.10) at current and future oscillation experiments. Notice that these correlations are a generic feature of mass matrices which preserve the G_1 symmetry. These are displayed in figure 11 and figure 12. In the limit of $\rho, \sigma \rightarrow 0$, we see that the mixing angles θ_{12} and θ_{13} remain the same, while the Dirac CP phase vanishes $\sin \delta^\ell \rightarrow 0$, so that CP would be conserved in neutrino oscillations. Notice that both Majorana phases [111] become some integer multiples of $\pi/2$ and therefore they correspond to just CP signs [368, 369].

When the two CP symmetries X_2 and X_3 are imposed, the neutrino mass matrix preserves the flavour symmetry $G_1 = X_2 X_3^* = X_3 X_2^*$ as well. The resulting predictions for lepton mixing parameters are obtained from Eq. (5.11) by redefining $\rho \rightarrow \rho + \pi/2$ and $\sigma \rightarrow \sigma - \pi/2$.

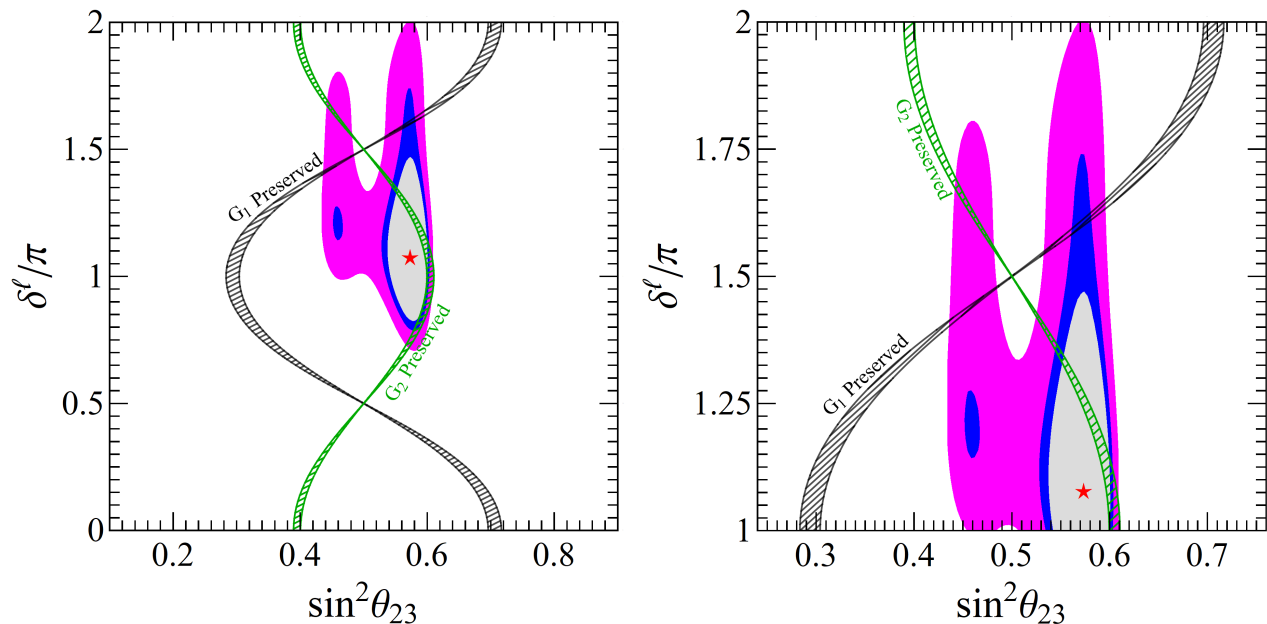


Figure 12: Predicted correlation between δ^ℓ and $\sin^2 \theta_{23}$ in the revamped TBM scheme. The black region corresponds to the case where G_1 is preserved by the neutrino sector, as given by Eq. (5.12), right. The green region corresponds to the case where G_2 is preserved, as given by Eq. (5.18), right. The right panel is a zoom of the left one. The global fit regions correspond to 90%, 95% and 99% confidence levels [24,25].

5.1.2 Case b: G_2 flavour and X_2, X_4 CP symmetries

The combination of X_2 and X_4 leads to the conservation of $G_2 = X_2 X_4^* = X_4 X_2^*$ flavour symmetry. The invariance of neutrino mass matrix under the action of X_2 and X_4 requires

$$X_2^T m_\nu X_2 = m_\nu^*, \quad X_4^T m_\nu X_4 = m_\nu^*, \quad (5.13)$$

from which we can determine the neutrino mass matrix to be of the following form

$$m'_\nu = U_{cTBM}^T m_\nu U_{cTBM} = \begin{pmatrix} m_1 & 0 & \delta m \\ 0 & m_2 & 0 \\ \delta m & 0 & m_3 \end{pmatrix}, \quad (5.14)$$

where $m_{1,2,3}$ and δm are generic real parameters. The matrix m'_ν can be diagonalized by a rotation matrix $R_{13}(\theta)$ in the (13)-plane,

$$R_{13}(\theta) = \begin{pmatrix} \cos \theta & 0 & \sin \theta \\ 0 & 1 & 0 \\ -\sin \theta & 0 & \cos \theta \end{pmatrix} \quad \text{with} \quad \tan 2\theta = \frac{2 \delta m}{m_3 - m_1}. \quad (5.15)$$

Consequently the residual CP symmetries X_2 and X_4 fix the lepton mixing matrix to be

$$\begin{aligned}
U &= U_{cTBM} R_{13}(\theta) Q_\nu \\
&= \frac{1}{\sqrt{6}} \begin{pmatrix} 2 \cos \theta & \sqrt{2} e^{-i\rho} & 2 \sin \theta \\ -e^{i\rho} \cos \theta - \sqrt{3} e^{-i\sigma} \sin \theta & \sqrt{2} & -e^{i\rho} \sin \theta + \sqrt{3} e^{-i\sigma} \cos \theta \\ e^{i(\rho+\sigma)} \cos \theta - \sqrt{3} \sin \theta & -\sqrt{2} e^{i\sigma} & e^{i(\rho+\sigma)} \sin \theta + \sqrt{3} \cos \theta \end{pmatrix} Q_\nu. \quad (5.16)
\end{aligned}$$

Note that the second column of the mixing matrix is $(e^{-i\rho}, 1, -e^{i\sigma})^T / \sqrt{3}$ which matches with that of the cTBM mixing pattern. We can extract the mixing angles and the predicted CP violation phases from Eq. (5.16) in the usual way, leading to

$$\begin{aligned}
\sin^2 \theta_{13} &= \frac{2 \sin^2 \theta}{3}, \quad \sin^2 \theta_{12} = \frac{1}{2 \cos^2 \theta + 1}, \quad \sin^2 \theta_{23} = \frac{1}{2} - \frac{\sqrt{3} \sin 2\theta \cos(\rho + \sigma)}{4 \cos^2 \theta + 2}, \\
\sin \delta^\ell &= -\frac{\text{sign}(\sin 2\theta)(2 \cos^2 \theta + 1) \sin(\rho + \sigma)}{\sqrt{(2 \cos^2 \theta + 1)^2 - 3 \cos^2(\rho + \sigma) \sin^2 2\theta}}, \quad \tan \delta^\ell = \frac{(2 \cos^2 \theta + 1) \tan(\rho + \sigma)}{1 - 4 \cos^2 \theta}, \\
\phi_{12} &= \rho + \frac{(k_1 - k_2)\pi}{2}, \quad \phi_{13} = \frac{(k_1 - k_3)\pi}{2}. \quad (5.17)
\end{aligned}$$

The mixing parameters are again correlated with each other, as follows

$$\sin^2 \theta_{12} \cos^2 \theta_{13} = \frac{1}{3}, \quad \tan 2\theta_{23} \cos \delta^\ell = \frac{\cos 2\theta_{13}}{\sin \theta_{13} \sqrt{2 - 3 \sin^2 \theta_{13}}}. \quad (5.18)$$

These correlations lead to predictions for the oscillations parameters, given in figures 11 and 12.

For the case that the CP symmetries X_1 and X_3 are preserved, the flavour symmetry $G_2 = X_1 X_3^* = X_3 X_1^*$ would be preserved as well¹⁸. The resulting predictions for lepton mixing matrix and mixing parameters can be obtained from Eqs. (5.16, 5.17) by redefining $\rho \rightarrow \rho + \pi/2$, $\sigma \rightarrow \sigma - \pi$.

Finally, if a single CP symmetry is preserved by the neutrino mass matrix, the lepton mixing matrix is determined up to a three dimensional orthogonal matrix. The resulting lepton flavour mixing predictions can be analyzed in a similar fashion [365]. The simple TBM mixing matrix can also be revamped by exploiting the generalized CP symmetries of the charged lepton mass matrix [370].

5.2 Revamped Golden-Ratio mixing scheme

In a way analogous to what we did for the TBM mixing matrix, we can also revamp the Golden-Ratio (GR) mixing pattern. We start from the complex GR mixing matrix, in the charged lepton diagonal basis,

$$U_{cGR} = \frac{1}{\sqrt{2\sqrt{5}\phi_g}} \begin{pmatrix} \sqrt{2}\phi_g & \sqrt{2}e^{-i\rho} & 0 \\ -e^{i\rho} & \phi_g & \sqrt{\sqrt{5}\phi_g}e^{-i\sigma} \\ -e^{i(\rho+\sigma)} & \phi_g e^{i\sigma} & -\sqrt{\sqrt{5}\phi_g} \end{pmatrix}, \quad (5.19)$$

¹⁸The imposition of G_3 is uninteresting here, as it leads to $\theta_{13} = 0$.

which reduces to the real GR mixing matrix of Eq. (3.13) in the limit of $\rho = \sigma = 0$. The four CP symmetry matrices $X_i = U_{cGR} d_i U_{cGR}^T$ associated with the cGR mixing pattern are of the following form,

$$\begin{aligned}
X_1 &= \frac{1}{\sqrt{5}} \begin{pmatrix} 1 + \frac{2i \sin \rho}{\phi_g} e^{-i\rho} & -\sqrt{2} \cos \rho & -\sqrt{2} e^{i\sigma} \cos \rho \\ -\sqrt{2} \cos \rho & -\frac{1+\sqrt{5}e^{-2i\sigma}}{2} + \frac{i \sin \rho}{\phi_g} e^{i\rho} & -\frac{e^{i\sigma} + \sqrt{5}e^{-i\sigma}}{2} + \frac{i \sin \rho}{\phi_g} e^{i(\rho+\sigma)} \\ -\sqrt{2} e^{i\sigma} \cos \rho & -\frac{e^{i\sigma} + \sqrt{5}e^{-i\sigma}}{2} + \frac{i \sin \rho}{\phi_g} e^{i(\rho+\sigma)} & -\frac{e^{2i\sigma} + \sqrt{5}}{2} + \frac{i \sin \rho}{\phi_g} e^{i(\rho+2\sigma)} \end{pmatrix}, \\
X_2 &= \frac{1}{\sqrt{5}} \begin{pmatrix} -1 - \frac{2i \sin \rho}{\phi_g} e^{-i\rho} & \sqrt{2} \cos \rho & \sqrt{2} e^{i\sigma} \cos \rho \\ \sqrt{2} \cos \rho & \frac{1-\sqrt{5}e^{-2i\sigma}}{2} - \frac{i \sin \rho}{\phi_g} e^{i\rho} & \frac{e^{i\sigma} + \sqrt{5}e^{-i\sigma}}{2} - \frac{i \sin \rho}{\phi_g} e^{i(\rho+\sigma)} \\ \sqrt{2} e^{i\sigma} \cos \rho & \frac{e^{i\sigma} + \sqrt{5}e^{-i\sigma}}{2} - \frac{i \sin \rho}{\phi_g} e^{i(\rho+\sigma)} & \frac{e^{2i\sigma} - \sqrt{5}}{2} - \frac{i \sin \rho}{\phi_g} e^{i(\rho+2\sigma)} \end{pmatrix}, \\
X_3 &= \frac{1}{\sqrt{5}} \begin{pmatrix} -1 - \frac{2 \cos \rho}{\phi_g} e^{-i\rho} & \sqrt{2} i \sin \rho & \sqrt{2} i e^{i\sigma} \sin \rho \\ \sqrt{2} i \sin \rho & -\frac{1+\sqrt{5}e^{-2i\sigma}}{2} - \frac{\cos \rho}{\phi_g} e^{i\rho} & -\frac{e^{i\sigma} + \sqrt{5}e^{-i\sigma}}{2} - \frac{\cos \rho}{\phi_g} e^{i(\rho+\sigma)} \\ \sqrt{2} i e^{i\sigma} \sin \rho & -\frac{e^{i\sigma} + \sqrt{5}e^{-i\sigma}}{2} - \frac{\cos \rho}{\phi_g} e^{i(\rho+\sigma)} & -\frac{e^{2i\sigma} + \sqrt{5}}{2} - \frac{\cos \rho}{\phi_g} e^{i(\rho+2\sigma)} \end{pmatrix}, \\
X_4 &= \frac{1}{\sqrt{5}} \begin{pmatrix} 1 + \frac{2 \cos \rho}{\phi_g} e^{-i\rho} & -\sqrt{2} i \sin \rho & -\sqrt{2} i e^{i\sigma} \sin \rho \\ -\sqrt{2} i \sin \rho & \frac{1+\sqrt{5}e^{-2i\sigma}}{2} + \frac{\cos \rho}{\phi_g} e^{i\rho} & \frac{e^{i\sigma} - \sqrt{5}e^{-i\sigma}}{2} + \frac{\cos \rho}{\phi_g} e^{i(\rho+\sigma)} \\ -\sqrt{2} i e^{i\sigma} \sin \rho & \frac{e^{i\sigma} - \sqrt{5}e^{-i\sigma}}{2} + \frac{\cos \rho}{\phi_g} e^{i(\rho+\sigma)} & \frac{e^{2i\sigma} + \sqrt{5}}{2} + \frac{\cos \rho}{\phi_g} e^{i(\rho+2\sigma)} \end{pmatrix}. \tag{5.20}
\end{aligned}$$

Taking the limit of $\rho, \sigma \rightarrow 0$, we obtain

$$\begin{aligned}
X_1 &= \frac{1}{\sqrt{5}} \begin{pmatrix} 1 & -\sqrt{2} & -\sqrt{2} \\ -\sqrt{2} & -\phi_g & 1/\phi_g \\ -\sqrt{2} & 1/\phi_g & -\phi_g \end{pmatrix}, \quad X_2 = \frac{1}{\sqrt{5}} \begin{pmatrix} -1 & \sqrt{2} & \sqrt{2} \\ \sqrt{2} & -1/\phi_g & \phi_g \\ \sqrt{2} & \phi_g & -1/\phi_g \end{pmatrix}, \\
X_3 &= - \begin{pmatrix} 1 & 0 & 0 \\ 0 & 0 & 1 \\ 0 & 1 & 0 \end{pmatrix}, \quad X_4 = \begin{pmatrix} 1 & 0 & 0 \\ 0 & 1 & 0 \\ 0 & 0 & 1 \end{pmatrix}. \tag{5.21}
\end{aligned}$$

The relations between residual flavour and CP symmetries in Eq. (5.6) are fulfilled. If all the four remnant CP transformations in Eq. (5.20) are preserved by the neutrino mass matrix, the complex GR mixing pattern with vanishing θ_{13} would be produced.

Similarly to section 5.1, we consider the scenario of partially preserved remnant CP symmetries. If the CP symmetries X_1, X_4 or X_2, X_3 are preserved in the neutrino sector, the remnant flavour symmetry $G_1 = X_1 X_4^* = X_4 X_1^* = X_2 X_3^* = X_3 X_2^*$ would be conserved as well. As a consequence, the first column of the lepton mixing matrix would be determined to be $(\sqrt{2}\phi_g, -e^{i\rho}, -e^{i(\rho+\sigma)})^T / \sqrt{2\sqrt{5}\phi_g}$, the same as in the cGR mixing. It follows that the relation $\cos^2 \theta_{12} \cos^2 \theta_{13} = \frac{\phi_g}{\sqrt{5}}$ is fulfilled. Using the 3σ allowed range $2.000 \times 10^{-2} \leq \sin^2 \theta_{13} \leq 2.405 \times 10^{-2}$ [24, 25], we find the solar mixing angle must lie in the region $0.2586 \leq \sin^2 \theta_{12} \leq 0.2616$ which doesn't overlap with the experimental 3σ range of θ_{12} [24, 25].

The phenomenologically viable case is found when the CP symmetries X_2, X_4 or X_1, X_3 are preserved by the neutrino mass matrix. The mixing parameters for the latter CP transformation can be obtained from those of the former by redefining $\rho \rightarrow \rho + \pi/2, \sigma \rightarrow \sigma - \pi$. Without loss of generality, we shall focus on preserved CP transformations X_2, X_4 which leads to conservation of the flavour symmetry generated

by the $G_2 = X_2 X_4^* = X_4 X_2^*$ transformation¹⁹. The lepton mixing matrix is found to be

$$U = U_{cGR} R_{13}(\theta) Q_\nu$$

$$= \frac{1}{\sqrt{2\sqrt{5}\phi_g}} \begin{pmatrix} \sqrt{2}\phi_g \cos \theta & \sqrt{2}e^{-i\rho} & \sqrt{2}\phi_g \sin \theta \\ -e^{i\rho} \cos \theta - 5^{1/4}e^{-i\sigma} \sqrt{\phi_g} \sin \theta & \phi_g & -e^{i\rho} \sin \theta + 5^{1/4}e^{-i\sigma} \sqrt{\phi_g} \cos \theta \\ -e^{i(\rho+\sigma)} \cos \theta + 5^{1/4} \sqrt{\phi_g} \sin \theta & e^{i\sigma} \phi_g & -e^{i(\rho+\sigma)} \sin \theta - 5^{1/4} \sqrt{\phi_g} \cos \theta \end{pmatrix} Q_\nu. \quad (5.22)$$

The mixing angles and CP violating phases read as

$$\sin^2 \theta_{13} = \frac{\phi_g \sin^2 \theta}{\sqrt{5}}, \quad \sin^2 \theta_{12} = \frac{1}{1 + \phi_g^2 \cos^2 \theta}, \quad \sin^2 \theta_{23} = \frac{1}{2} - \frac{\sqrt{\sqrt{5}\phi_g \sin 2\theta \cos(\rho + \sigma)}}{2\phi_g^2 \cos^2 \theta + 2},$$

$$\sin \delta^\ell = -\frac{\text{sign}(\sin 2\theta)(\phi_g^2 \cos^2 \theta + 1) \sin(\rho + \sigma)}{\sqrt{(\phi_g^2 \cos^2 \theta + 1)^2 - \sqrt{5}\phi_g \sin^2 2\theta \cos^2(\rho + \sigma)}},$$

$$\tan \delta^\ell = -\frac{(\phi_g^2 \cos^2 \theta + 1) \tan(\rho + \sigma)}{\cos 2\theta + \phi_g^2 \cos^2 \theta}, \quad \phi_{12} = \rho + \frac{(k_1 - k_2)\pi}{2}, \quad \phi_{13} = \frac{(k_1 - k_3)\pi}{2}. \quad (5.23)$$

As a consequence, we can derive the following exact relations among the mixing parameters

$$\sin^2 \theta_{12} \cos^2 \theta_{13} = \frac{1}{\sqrt{5}\phi_g}, \quad \tan 2\theta_{23} \cos \delta^\ell = \frac{\phi_g^2 \cot^2 \theta_{13} - 2}{2\sqrt{\phi_g^2 \cot^2 \theta_{13} - 1}}. \quad (5.24)$$

For the best fit value $\sin^2 \theta_{13} = 2.200 \times 10^{-2}$ [24, 25], we find the solar mixing angle $\sin^2 \theta_{12} = 0.2826$ which is within the 3σ range. The correlations of Eq. (5.24) are displayed in figure 13.

5.3 Bi-large mixing

It is unlikely that any revamping procedure can make the bi-maximal mixing pattern of section 3.4 consistent with the oscillation data, since the measured value of the solar angle θ_{12} deviates too much from the maximal value [24, 25]. The bi-large pattern is phenomenologically motivated by the fact that the smallest lepton mixing angle θ_{13} is similar in magnitude to the largest of the elements of the quark mixing matrix, the Cabibbo angle. It suggests that the latter may act as the universal seed for quark and lepton mixings [371–375]. Bi-large neutrino mixing implies that the lepton and quark sectors may be related with each other, a possible new strategy in the quest for quark-lepton symmetry and unification.

Within the simplest bi-large mixing hypothesis, the solar and atmospheric mixing angles are expressed as [371],

$$\sin \theta_{13} = \lambda, \quad \sin \theta_{12} = s\lambda, \quad \sin \theta_{23} = a\lambda, \quad (5.25)$$

where the small parameter λ is the reactor angle, s and a are free parameters of order one. Using the best fit values of the mixing angles [24, 25], one finds $\lambda \simeq 0.148$, $s \simeq 3.802$ and $a \simeq 5.108$ for normal neutrino mass ordering. Since the bi-large approach describes the structure of the lepton mixing matrix in terms of θ_{13} as input, no revamping is needed.

¹⁹Notice again that imposing G_3 is uninteresting here, as it leads to $\theta_{13} = 0$.

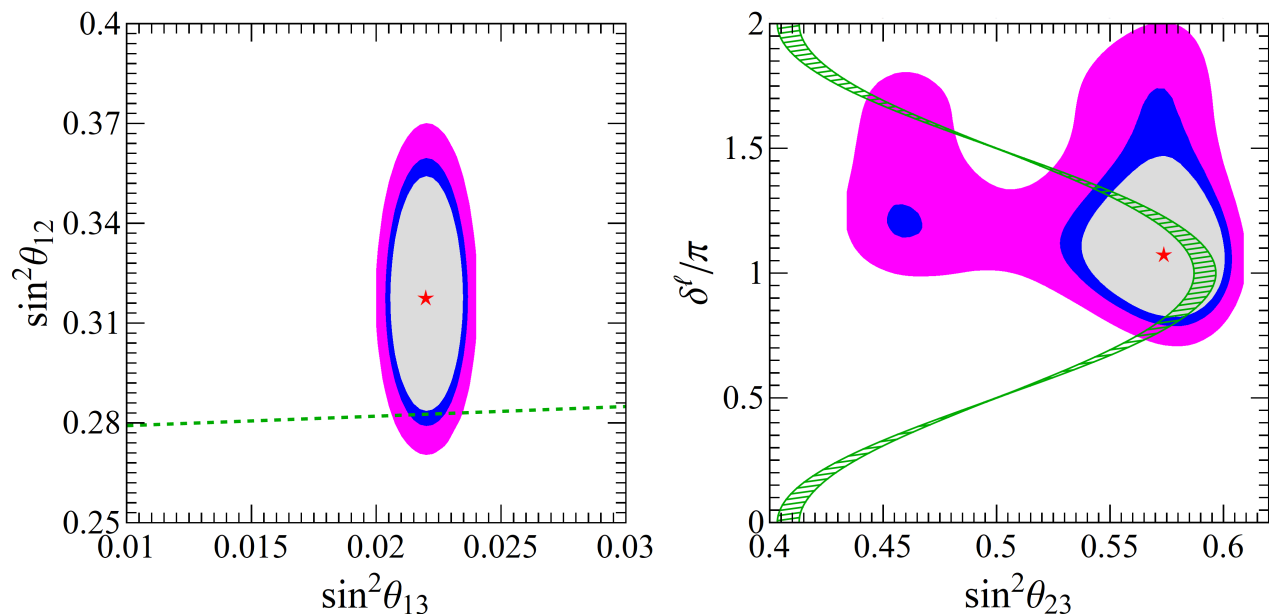


Figure 13: Predicted oscillation parameter correlations in the revamped GR scheme. The “generic” global-fit allowed regions corresponding to 90%, 95% and 99% confidence level are displayed [24, 25].

5.3.1 Bi-large mixing from abelian family symmetry

As shown above, the bi-large mixing ansatz assumes that the three lepton mixing angles are of the same order of magnitude, to first approximation,

$$\text{BL}_1 : \quad \sin \theta_{12} \sim \lambda_c, \quad \sin \theta_{13} \sim \lambda_c, \quad \sin \theta_{23} \sim \lambda_c, \quad (5.26)$$

where $\lambda_c \simeq 0.23$ is the Cabibbo angle [28], and the notation “ \sim ” implies that the above relations contain unknown factors of order one. The freedom in these factors can be used to obtain an adequate description of neutrino mixing. Although global analyses of neutrino oscillation data show preference for the second octant of the atmospheric mixing angle θ_{23} [24, 25], the significance is not yet overwhelming. For θ_{23} in the preferred higher octant, it has been proposed [372] that the bi-large mixing ansatz could be

$$\text{BL}_2 : \quad \sin \theta_{12} \sim \lambda_c, \quad \sin \theta_{13} \sim \lambda_c, \quad \sin \theta_{23} \sim 1 - \lambda_c. \quad (5.27)$$

Here we will show how the above variants of the bi-large mixing patterns can be achieved in a Froggatt-Nielsen-type scenario [276] with an Abelian flavour symmetry. Assuming the presence of two Higgs doublets $H_{u,d}$, and that neutrino masses are described by an effective Weinberg operator we generalize the well-known $U(1)$ flavour symmetry to a larger $U(1) \times Z_m \times Z_n \subset U(1) \times U(1)' \times U(1)''$ family symmetry. In order to break the $U(1)$, Z_m and Z_n flavour groups we assume three flavons Θ_1 , Θ_2 and Θ_3 with horizontal charges $\Theta_1 : (-1, 0, 0)$, $\Theta_2 : (0, -1, 0)$, $\Theta_3 : (0, 0, -1)$, respectively, and their VEVs $\langle \Theta_{1,2,3} \rangle / \Lambda$ scaled by the cutoff Λ are of order λ_c . We assume the horizontal charges of $H_{u,d}$ to be zero.

Fermion masses are then described by the following effective Yukawa couplings [372],

$$\begin{aligned}
\mathcal{W} = & (y_u)_{ij} Q_i U_j^c H_u \left(\frac{\Theta_1}{\Lambda} \right)^{F(Q_i)+F(U_j^c)} \left(\frac{\Theta_2}{\Lambda} \right)^{[Z_m(Q_i)+Z_m(U_j^c)]} \left(\frac{\Theta_3}{\Lambda} \right)^{[Z_n(Q_i)+Z_n(U_j^c)]} \\
& + (y_d)_{ij} Q_i D_j^c H_d \left(\frac{\Theta_1}{\Lambda} \right)^{F(Q_i)+F(D_j^c)} \left(\frac{\Theta_2}{\Lambda} \right)^{[Z_m(Q_i)+Z_m(D_j^c)]} \left(\frac{\Theta_3}{\Lambda} \right)^{[Z_n(Q_i)+Z_n(D_j^c)]} \\
& + (y_e)_{ij} L_i E_j^c H_d \left(\frac{\Theta_1}{\Lambda} \right)^{F(L_i)+F(E_j^c)} \left(\frac{\Theta_2}{\Lambda} \right)^{[Z_m(L_i)+Z_m(E_j^c)]} \left(\frac{\Theta_3}{\Lambda} \right)^{[Z_n(L_i)+Z_n(E_j^c)]} \\
& + (y_\nu)_{ij} \frac{1}{\Lambda} L_i L_j H_u H_u \left(\frac{\Theta_1}{\Lambda} \right)^{F(L_i)+F(L_j)} \left(\frac{\Theta_2}{\Lambda} \right)^{[Z_m(L_i)+Z_m(L_j)]} \left(\frac{\Theta_3}{\Lambda} \right)^{[Z_n(L_i)+Z_n(L_j)]}, \quad (5.28)
\end{aligned}$$

where $F(\psi)$ denotes the $U(1)$ charge of the field ψ , $Z_{m,n}(\psi)$ stand for the $Z_{m,n}$ charge of ψ , and the brackets [...] around the exponents denote that we are modding out by m (n) according to the Z_m (Z_n) addition rule, i.e., $[Z_m(Q_i) + Z_m(U_j^c)] = Z_m(Q_i) + Z_m(U_j^c) \pmod{m}$. Hence fermion mass matrices are expressed in terms of the horizontal charges as follows,

$$\begin{aligned}
(M_u)_{ij} &= (y_u)_{ij} \lambda_c^{F(Q_i)+F(U_j^c)+[Z_m(Q_i)+Z_m(U_j^c)]+[Z_n(Q_i)+Z_n(U_j^c)]} v_u, \\
(M_d)_{ij} &= (y_d)_{ij} \lambda_c^{F(Q_i)+F(D_j^c)+[Z_m(Q_i)+Z_m(D_j^c)]+[Z_n(Q_i)+Z_n(D_j^c)]} v_d, \\
(M_e)_{ij} &= (y_e)_{ij} \lambda_c^{F(L_i)+F(E_j^c)+[Z_m(L_i)+Z_m(E_j^c)]+[Z_n(L_i)+Z_n(E_j^c)]} v_d, \\
(M_\nu)_{ij} &= (y_\nu)_{ij} \lambda_c^{F(L_i)+F(L_j)+[Z_m(L_i)+Z_m(L_j)]+[Z_n(L_i)+Z_n(L_j)]} \frac{v_u^2}{\Lambda}. \quad (5.29)
\end{aligned}$$

If all the horizontal charges are positive, the hierarchical structure of the mass matrices allows a simple order-of-magnitude estimate of the various mass ratios and mixing angles. For instance, the entries of the CKM matrix are estimated to be,

$$(V_{CKM})_{ij} \sim \lambda_c^{F_{\text{eff}}(Q_i)-F_{\text{eff}}(Q_j)\pm\alpha m\pm\beta n}, \quad (5.30)$$

where $F_{\text{eff}}(\psi) = F(\psi) + Z_m(\psi) + Z_n(\psi)$, and $\alpha, \beta = 0, 1$ depends on the charge assignment under Z_m and Z_n . Likewise for the lepton sector, one obtains

$$\sin \theta_{ij} \sim \lambda_c^{F_{\text{eff}}(L_i)-F_{\text{eff}}(L_j)\pm\alpha m\pm\beta n}. \quad (5.31)$$

Notice that the mixing angles can be enhanced or suppressed by $\lambda^{\pm m \pm n}$ relative to the scaling predictions obtained with the continuous $U(1) \times U(1)' \times U(1)''$ family symmetry. Moreover, $U(1) \times Z_m \times Z_n$ reduces to $U(1) \times Z_m$ if $n = 1$, and to the usual $U(1)$ if $m = n = 1$.

- Model for BL_1 mixing

The family symmetry group is $U(1) \times Z_3 \times Z_4$, and we assign the lepton fields to transform under the

flavour symmetry as follows [372],

$$\begin{aligned} L_1 &: (4, 1, 3), & L_2 &: (3, 2, 2), & L_3 &: (1, 1, 1), \\ E_1^c &: (3, 2, 2), & E_2^c &: (1, 2, 2), & E_3^c &: (0, 0, 0). \end{aligned} \quad (5.32)$$

One can then read out the pattern of charged lepton and neutrino mass matrices,

$$M_e \sim \begin{pmatrix} \lambda_c^8 & \lambda_c^6 & \lambda_c^8 \\ \lambda_c^7 & \lambda_c^5 & \lambda_c^7 \\ \lambda_c^7 & \lambda_c^5 & \lambda_c^3 \end{pmatrix} v_d, \quad M_\nu \sim \begin{pmatrix} \lambda_c^{12} & \lambda_c^8 & \lambda_c^7 \\ \lambda_c^8 & \lambda_c^7 & \lambda_c^7 \\ \lambda_c^7 & \lambda_c^7 & \lambda_c^6 \end{pmatrix} \frac{v_u^2}{\Lambda}. \quad (5.33)$$

These give rise to the following mass ratios and lepton mixing angles,

$$\begin{aligned} \frac{m_e}{m_\mu} &\sim \lambda_c^3, & \frac{m_\mu}{m_\tau} &\sim \lambda_c^2, \\ m_1 &\sim \lambda_c^8 \frac{v_u^2}{\Lambda}, & m_2 &\sim \lambda_c^7 \frac{v_u^2}{\Lambda}, & m_3 &\sim \lambda_c^6 \frac{v_u^2}{\Lambda}, \\ \sin \theta_{12} &\sim \lambda_c, & \sin \theta_{13} &\sim \lambda_c, & \sin \theta_{23} &\sim \lambda_c. \end{aligned} \quad (5.34)$$

This way we obtain the BL₁ mixing pattern. A simple numerical analysis with different seed procedures for the order-one Yukawa coefficients, leads to the θ_{23} distributions given in figure 14. One sees that $\sin^2 \theta_{23} < 1/2$ (first octant) is preferred in this case.

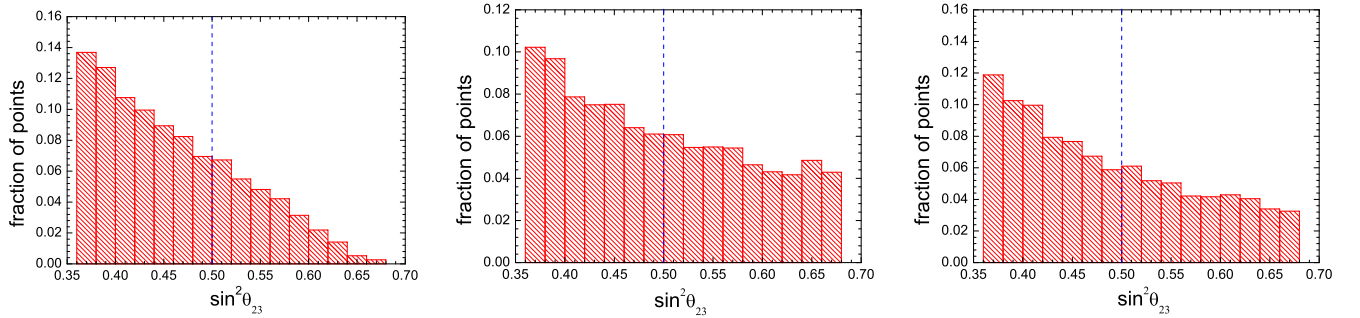


Figure 14: Distributions of the atmospheric neutrino mixing angle θ_{23} in the BL₁ model. The left, middle and right panels are obtained with flat, exponential and Gaussian seed procedures. From [372].

We now extend the model to the quark sector along the lines of $SU(5)$ unification. Each family of standard quarks and leptons is embedded in $SU(5)$ multiplets $\mathbf{10} = (Q, U^c, E^c)$ and $\bar{\mathbf{5}} = (D^c, L)$. The fields within a single $SU(5)$ multiplet transform in the same way under the family symmetry. Therefore the lepton assignment in Eq. (5.32) implies that the quark charges under the flavour group $U(1) \times Z_3 \times Z_4$ should be

$$Q_1 : (3, 2, 2), \quad Q_2 : (1, 2, 2), \quad Q_3 : (0, 0, 0),$$

$$\begin{aligned}
U_1^c &: (3, 2, 2), & U_2^c &: (1, 2, 2), & U_3^c &: (0, 0, 0), \\
D_1^c &: (4, 1, 3), & D_2^c &: (3, 2, 2), & D_3^c &: (1, 1, 1).
\end{aligned} \tag{5.35}$$

Consequently, the up-type and down-type quark mass matrices are given as

$$M_u \sim \begin{pmatrix} \lambda_c^7 & \lambda_c^5 & \lambda_c^7 \\ \lambda_c^5 & \lambda_c^3 & \lambda_c^5 \\ \lambda_c^7 & \lambda_c^5 & 1 \end{pmatrix} v_u, \quad M_d \sim \begin{pmatrix} \lambda_c^8 & \lambda_c^7 & \lambda_c^7 \\ \lambda_c^6 & \lambda_c^5 & \lambda_c^5 \\ \lambda_c^8 & \lambda_c^7 & \lambda_c^3 \end{pmatrix} v_d, \tag{5.36}$$

The resulting quark masses and CKM mixing matrix are determined to follow the pattern

$$\begin{aligned}
m_u &\sim \lambda_c^7 v_u, & m_c &\sim \lambda_c^3 v_u, & m_t &\sim v_u, \\
m_d &\sim \lambda_c^8 v_d, & m_s &\sim \lambda_c^5 v_d, & m_b &\sim \lambda_c^3 v_d, \\
|V_{us}| &\sim \lambda_c^2, & |V_{cb}| &\sim \lambda_c^2, & |V_{ub}| &\sim \lambda_c^4,
\end{aligned} \tag{5.37}$$

which are in agreement with experimental data except $|V_{us}|$, for which an accidental enhancement of $\mathcal{O}(\lambda^{-1})$ amongst the free order-one coefficients is needed so as to reproduce the correct Cabibbo angle.

- Model for BL_2 mixing

Here the flavour symmetry is $U(1) \times Z_2$, and the charge assignments for the quarks and leptons are taken as [372]

$$\begin{aligned}
D_1^c, L_1 &: (3, 0), & D_2^c, L_2 &: (3, 1), & D_3^c, L_3 &: (2, 0), \\
Q_1, U_1^c, E_1^c &: (4, 0), & Q_2, U_2^c, E_2^c &: (2, 1), & Q_3, U_3^c, E_3^c &: (0, 1).
\end{aligned} \tag{5.38}$$

Consequently the neutrino and charged lepton mass matrices take the following form

$$M_e \sim \begin{pmatrix} \lambda_c^7 & \lambda_c^6 & \lambda_c^4 \\ \lambda_c^8 & \lambda_c^5 & \lambda_c^3 \\ \lambda_c^6 & \lambda_c^5 & \lambda_c^3 \end{pmatrix} v_d, \quad M_\nu \sim \begin{pmatrix} \lambda_c^6 & \lambda_c^7 & \lambda_c^5 \\ \lambda_c^7 & \lambda_c^6 & \lambda_c^6 \\ \lambda_c^5 & \lambda_c^6 & \lambda_c^4 \end{pmatrix} \frac{v_u^2}{\Lambda}. \tag{5.39}$$

The charged lepton mass matrix M_e has a ‘‘lopsided’’ structure, and can give the correct order-of-magnitude for the charged lepton masses and a large 2-3 mixing. Combining neutrino and charged lepton diagonalization matrices, the resulting BL_2 lepton mixing pattern is determined as,

$$\sin \theta_{12} \sim \lambda_c, \quad \sin \theta_{13} \sim \lambda_c, \quad \sin \theta_{23} \sim 1. \tag{5.40}$$

Using the master formula of Eq. (5.29) we can easily read off the quark mass matrices as

$$M_u \sim \begin{pmatrix} \lambda_c^8 & \lambda_c^7 & \lambda_c^5 \\ \lambda_c^7 & \lambda_c^4 & \lambda_c^2 \\ \lambda_c^5 & \lambda_c^2 & 1 \end{pmatrix} v_u, \quad M_d \sim \begin{pmatrix} \lambda_c^7 & \lambda_c^8 & \lambda_c^6 \\ \lambda_c^6 & \lambda_c^5 & \lambda_c^5 \\ \lambda_c^4 & \lambda_c^3 & \lambda_c^3 \end{pmatrix} v_d. \quad (5.41)$$

This leads to the following pattern of CKM matrix elements and quark mass ratios,

$$\begin{aligned} |V_{us}| &\sim \lambda_c, & |V_{cb}| &\sim \lambda_c^2, & |V_{ub}| &\sim \lambda_c^3, \\ \frac{m_u}{m_c} &\sim \lambda_c^4, & \frac{m_c}{m_t} &\sim \lambda_c^4, & \frac{m_d}{m_s} &\sim \lambda_c^2, & \frac{m_s}{m_b} &\sim \lambda_c^2, & \frac{m_b}{m_t} &\sim \lambda_c^3, \end{aligned} \quad (5.42)$$

in very good qualitative agreement with observed values.

5.3.2 Confronting bi-large mixing with oscillation data

We now make the bi-large mixing ansatz more predictive. We assume a CP conserving neutrino diagonalization matrix U_ν , with its three angles related to the Cabibbo angle in a simple manner, and a CKM-like charged lepton diagonalization. Under these assumptions we illustrate the predictive power of bi-large mixing [374].

- Constraining bi-large mixing: pattern I

Here the neutrino mixing angles are assumed to be related to the Cabibbo angle as follows [374]

$$\sin \theta_{13} = \lambda_c, \quad \sin \theta_{12} = 2\lambda_c, \quad \sin \theta_{23} = 1 - \lambda_c. \quad (5.43)$$

The Dirac CP phase is taken as $\delta_{CP}^\nu = \pi$ with vanishing Majorana phases. The resulting neutrino diagonalization matrix is given by

$$U_\nu \simeq \begin{pmatrix} 1 - \frac{5\lambda_c^2}{2} & 2\lambda_c & -\lambda_c \\ \lambda_c - 2\sqrt{2}\lambda_c^{3/2} & \sqrt{2}\lambda_c - \frac{\lambda_c^{3/2}}{2\sqrt{2}} & 1 - \lambda_c - \frac{\lambda_c^2}{2} \\ 2\lambda_c + \sqrt{2}\lambda_c^{3/2} & -1 + \lambda_c & \sqrt{2}\lambda_c - \frac{\lambda_c^{3/2}}{2\sqrt{2}} \end{pmatrix}. \quad (5.44)$$

Motivated by $SO(10)$, we take a CKM-type charged lepton diagonalization matrix

$$U_l = R_{23}(\theta_{23}^{CKM}) \Phi R_{12}(\theta_{12}^{CKM}) \Phi^\dagger \simeq \begin{pmatrix} 1 - \frac{\lambda_c^2}{2} & \lambda_c e^{-i\phi} & 0 \\ -\lambda_c e^{i\phi} & 1 - \frac{\lambda_c^2}{2} & A\lambda_c^2 \\ A\lambda_c^3 e^{i\phi} & -A\lambda_c^2 & 1 \end{pmatrix}, \quad (5.45)$$

where $\sin \theta_{12}^{CKM} = \lambda_c$, $\sin \theta_{23}^{CKM} = A\lambda_c^2$, $\lambda_c = 0.22453 \pm 0.00044$ and $A = 0.836 \pm 0.015$ are the Wolfenstein parameters [28], and $\Phi = \text{diag}(e^{-i\phi/2}, e^{i\phi/2}, 1)$ where ϕ is a free phase parameter. One sees that the lepton mixing matrix $U = U_l^\dagger U_\nu$ only depends on a single free phase parameter ϕ , which can in general

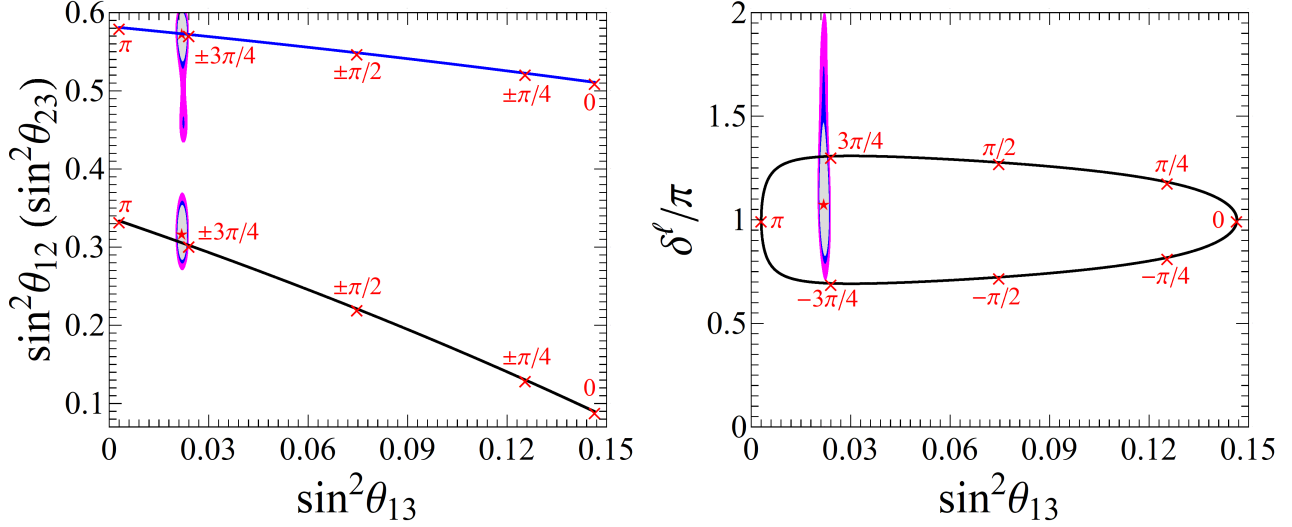


Figure 15: Predicting the solar and atmospheric mixing parameters $\sin^2 \theta_{12}$ (lower, black line) and $\sin^2 \theta_{23}$ (upper, blue line) versus $\sin^2 \theta_{13}$ in the first kind of constrained bi-large mixing scheme. The right panel shows δ^ℓ versus $\sin^2 \theta_{13}$. The allowed 90%, 95% and 99% CL regions of the global oscillation fit are displayed [24, 25]. The crosses correspond to $\phi = 0, \pi, \pm\pi/4, \pm\pi/2, \pm 3\pi/4$.

take values between $-\pi$ and π . The leptonic mixing angles and Jarlskog invariant are found to be

$$\begin{aligned}
\sin^2 \theta_{13} &\simeq 4\lambda_c^2(1 - \lambda_c) \cos^2 \frac{\phi}{2}, \\
\sin^2 \theta_{12} &\simeq 2\lambda_c^2(2 - 2\sqrt{2\lambda_c} \cos \phi + \lambda_c), \\
\sin^2 \theta_{23} &\simeq (1 - \lambda_c)^2 - 2\sqrt{2}A\lambda_c^{\frac{5}{2}} - 2\lambda_c^3(1 + 2 \cos \phi), \\
J_{CP} &\simeq -2(\sqrt{2} + \sqrt{\lambda}) \lambda_c^{5/2} \sin \phi.
\end{aligned} \tag{5.46}$$

We show these correlations in figure 15. They show how the precise measurement of the reactor angle can be promoted to sharp predictions for solar and atmospheric mixing angles. Similarly, the Dirac CP phase is also predicted, up to a two-fold degeneracy.

- Constraining bi-large mixing: pattern II

In this case the bi-large ansatz for the neutrino mixing angles is [374]

$$\sin \theta_{13}^\nu = \lambda_c, \quad \sin \theta_{12}^\nu = 2\lambda_c, \quad \sin \theta_{23}^\nu = 3\lambda_c, \tag{5.47}$$

with $\delta_{CP}^\nu = \pi$ and vanishing Majorana phases. Motivated by $SU(5)$ unification, we take the charged-lepton diagonalization matrix to be of the form

$$U_l = \Phi^\dagger R_{12}^T(\theta_{12}^{CKM}) \Phi R_{23}^T(\theta_{23}^{CKM}) \simeq \begin{pmatrix} 1 - \frac{1}{2}\lambda_c^2 & -\lambda_c e^{i\phi} & A\lambda_c^3 e^{i\phi} \\ \lambda_c e^{-i\phi} & 1 - \frac{1}{2}\lambda_c^2 & -A\lambda_c^2 \\ 0 & A\lambda_c^2 & 1 \end{pmatrix}. \tag{5.48}$$

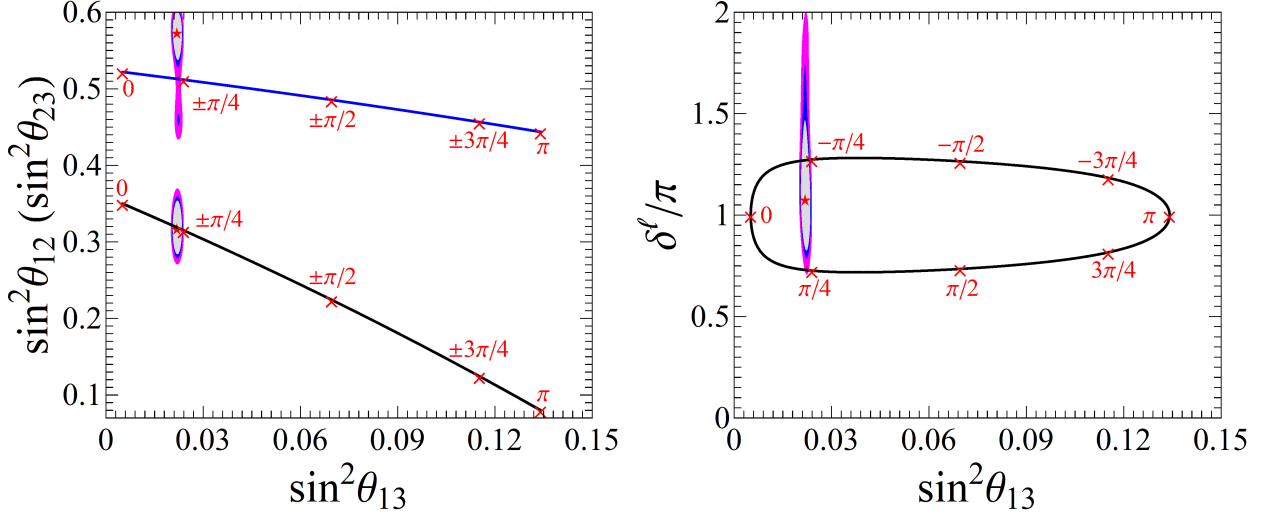


Figure 16: Predicting the solar and atmospheric mixing angles and Dirac phase in the second constrained bi-large mixing scheme. We adopt the same convention as in figure 15.

Taking into account both charged and neutral diagonalizations we can extract the following results for the lepton mixing angles and leptonic Jarlskog invariant,

$$\begin{aligned}
\sin^2 \theta_{13} &\simeq \lambda_c^2 - 6\lambda_c^3 \cos \phi + 8\lambda_c^4, \\
\sin^2 \theta_{12} &\simeq \lambda_c^2(5 + 4 \cos \phi) - 2\lambda_c^4(8 + 13 \cos \phi), \\
\sin^2 \theta_{23} &\simeq 9\lambda_c^2 + 6\lambda_c^3(A + \cos \phi) - \lambda_c^4(8 - 2A \cos \phi - A^2), \\
J_{CP} &\simeq -[3 + (16 + A)\lambda_c] \lambda_c^3 \sin \phi.
\end{aligned} \tag{5.49}$$

The resulting correlations between mixing parameters are displayed in figure 16. As before, requiring $\sin^2 \theta_{13}$ in the 3σ range [24, 25], we find that the other oscillation parameters θ_{12} , θ_{23} and δ_{CP} vary in the following regions

$$\begin{aligned}
0.02000 \leq \sin^2 \theta_{13} \leq 0.02405, & \quad 0.314824 \leq \sin^2 \theta_{12} \leq 0.322459, \\
0.511755 \leq \sin^2 \theta_{23} \leq 0.513969, & \quad 1.26643 \leq \delta_{CP}/\pi \leq 1.27402.
\end{aligned} \tag{5.50}$$

6 Lepton mixing from flavour and CP symmetry

Symmetries have been widely used to address the family puzzle. Early attempts employed a $U(1)$ flavour symmetry [276], spontaneously broken by the vacuum expectation value of a singlet scalar field. This would qualitatively account for the small quark mass ratios, as well as mixing angles. With the discovery of neutrino oscillations the idea of flavour symmetry was substantially extended, with many symmetry groups and breaking patterns studied. It has been found that finite discrete flavour groups [376] are particularly suitable to reproduce the large lepton mixing angles and provide non-trivial predictions. The basic theory is assumed to be invariant under a flavour group G_f , but G_f is spontaneously broken into different subgroups G_ν and G_l in the neutrino and charged lepton sectors respectively. This is achieved by the VEVs of a set of scalar fields, and the misalignment between neutrino and charged lepton mass matrices arises from the non-trivial breaking pattern of the flavour symmetry.

Neutrino model building using non-abelian discrete flavor symmetries has been surveyed in a number of dedicated reviews [85–93]. A prime non-abelian discrete flavour symmetry is A_4 [53, 54, 70, 313] which, under some circumstances, leads to the celebrated tri-bimaximal mixing pattern. Although no longer compatible with the experimental measurement of the reactor angle $\theta_{13} \simeq 8.5^\circ$ [21, 22, 303, 305, 306, 377], the simplest A_4 symmetry can, as we saw, be revamped so as to produce viable and predictive patterns of neutrino mixing.

All in all, the idea that lepton mixing emerges from the mismatch of the embedding of the two residual subgroups G_ν and G_l into of the flavour group G_f is still viable, interesting and predictive. In particular, if combining flavour symmetry with the generalized CP symmetry, one can not only accommodate lepton mixing angles but also predict leptonic CP violating phases in terms of few free parameters. In what follows, we shall review the possible schemes of predicting lepton mixing from residual symmetry, emphasizing the role of generalized CP symmetry. The results only depend on the assumed symmetry breaking pattern and are independent of the details of the residual symmetry and the particle content of the flavor symmetry breaking sector, or possible additional symmetries of the theory.

6.1 Lepton mixing from flavour symmetry alone

Within a top-down approach, one imposes a certain flavour symmetry group G_f at some high energy scale. The full Lagrangian is invariant under G_f , which is subsequently broken down to different subgroups G_ν and G_l in the neutrino and charged lepton sectors respectively. The residual symmetry G_l can be any abelian subgroup of G_f , and the same holds for G_ν if neutrinos are Dirac particles. On the other hand G_ν can only be the Klein group K_4 (or a subgroup) for the case of Majorana neutrinos. Throughout this review, we shall focus on the scenario in which G_f is a non-abelian finite discrete group. In general, the three families of left-handed lepton doublets are assigned to an irreducible faithful three-dimensional representation $\rho_{\mathbf{3}}$ of G_f . We assume that the charged lepton and neutrino mass matrices are invariant under the action of the elements of G_l and G_ν , i.e.

$$\rho_{\mathbf{3}}^\dagger(g_l)m_l^\dagger m_l \rho_{\mathbf{3}}(g_l) = m_l^\dagger m_l, \quad g_l \in G_l, \quad (6.1)$$

and

$$\begin{aligned}\rho_{\mathbf{3}}^\dagger(g_\nu)m_\nu^\dagger m_\nu \rho_{\mathbf{3}}(g_\nu) &= m_\nu^\dagger m_\nu, & g_\nu \in G_\nu, & \text{ for Dirac neutrinos,} \\ \rho_{\mathbf{3}}^T(g_\nu)m_\nu \rho_{\mathbf{3}}(g_\nu) &= m_\nu, & g_\nu \in G_\nu, & \text{ for Majorana neutrinos.}\end{aligned}\quad (6.2)$$

Notice that it is sufficient to impose the conditions in Eqs. (6.1) and (6.2) on the generators of G_l and G_ν . Moreover, we see that these conditions imply

$$\left[\rho_{\mathbf{3}}(g_l), m_l^\dagger m_l\right] = 0, \quad \left[\rho_{\mathbf{3}}(g_\nu), m_\nu^\dagger m_\nu\right] = 0. \quad (6.3)$$

As $\rho_{\mathbf{3}}(g_l)$ and $m_l^\dagger m_l$ commute with each other, the unitary transformation U_l that diagonalizes $m_l^\dagger m_l$ also diagonalizes $\rho_{\mathbf{3}}(g_l)$ up to permutations and phases of columns

$$U_l^\dagger \rho_{\mathbf{3}}(g_l) U_l = \text{diag}(e^{i\alpha_e}, e^{i\alpha_\mu}, e^{i\alpha_\tau}). \quad (6.4)$$

Since g_l is an element of the discrete flavour symmetry group G_f , the $e^{i\alpha_{e,\mu,\tau}}$ are all roots of unity. Analogously $\rho_{\mathbf{3}}(g_\nu)$ and $m_\nu^\dagger m_\nu$ (or m_ν) are diagonalized by the same matrix U_ν ,

$$U_\nu^\dagger \rho_{\mathbf{3}}(g_\nu) U_\nu = \begin{cases} \text{diag}(e^{i\beta_e}, e^{i\beta_\mu}, e^{i\beta_\tau}), & \text{for Dirac neutrinos,} \\ \text{diag}(\pm 1, \pm 1, \pm 1), & \text{for Majorana neutrinos,} \end{cases} \quad (6.5)$$

where $\beta_{e,\mu,\tau}$ are rational multiples of π . Then the lepton mixing matrix U is determined as

$$U = U_l^\dagger U_\nu \quad (6.6)$$

up to independent row and column permutations. In short, given a family symmetry group G_f and the residual subgroups G_l and G_ν , the unitary transformations U_l and U_ν as well as the lepton matrix U can be obtained by diagonalizing the representation matrices of the generators of G_l and G_ν , as illustrated in the figure 17. In practice, we only need to find the eigenvectors of $\rho_{\mathbf{3}}(g_l)$ and $\rho_{\mathbf{3}}(g_\nu)$ that form the column vectors of U_l and U_ν . In this approach, it is not necessary to construct the explicit form of the mass matrices $m_l^\dagger m_l$ and $m_\nu^\dagger m_\nu$ (or m_ν) although this can be accomplished in a straightforward manner. Since the lepton masses cannot be predicted in this framework, in particular the neutrino mass spectrum can have either normal ordering or inverted ordering, the unitary matrices U_l and U_ν are uniquely fixed up to permutations and phases of their column vectors. As a consequence, the lepton mixing matrix U is determined up to independent row and column permutations and arbitrary phase matrices multiplied from the left and right sides. Therefore the Majorana CP phases are not constrained by the residual flavour symmetry.

Notice that if we switch the roles of the subgroups G_ν and G_l , the lepton matrix U would become its Hermitian conjugate. If two pairs of subgroups $\{G_l, G_\nu\}$ and $\{G'_l, G'_\nu\}$ are conjugate²⁰, both residual

²⁰The two pairs of groups are conjugate if their generators g_e, g_ν and g'_e, g'_ν are related by group conjugacy, i.e., $g'_l = h g_l h^{-1}$,

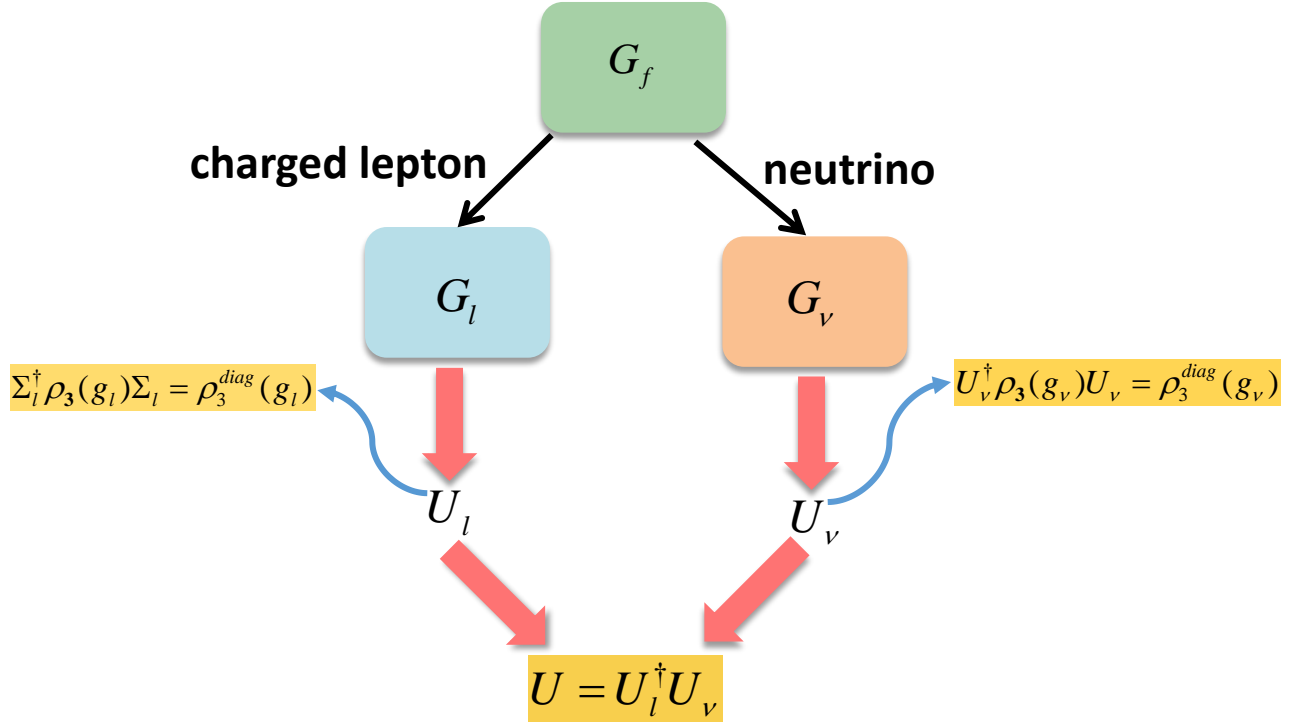


Figure 17: Model-independent predictions for the lepton mixing matrix from the flavour symmetry G_f broken to different residual subgroups G_l and G_ν in the neutrino and charged lepton sectors. Here g_l and g_ν are G_l and G_ν generators, respectively. See text for details.

symmetries would lead to the same result for the lepton mixing matrix. The reason is that if the generators of G_l and G_ν are diagonalized by U_l and U_ν respectively, $\rho_3(h)U_l$ and $\rho_3(h)U_\nu$ would diagonalize those of G'_l and G'_ν . On the other hand, if the left-handed lepton fields are assigned to the complex-conjugate of the triplet representation, the lepton mixing matrix would be complex conjugated, so that the predictions for the lepton mixing angles are unchanged and the signs of the CP violation phases are inverted.

6.1.1 Fully preserved residual symmetry $G_\nu = K_4$

As already mentioned, if the flavour group G_f is of finite order and the residual symmetries G_l and G_ν distinguish the three families of charged leptons and neutrinos then the lepton mixing matrix would be completely determined by the residual symmetries, regardless of the lepton masses or any other parameter of the underlying theory [259–263]. This is the so-called direct model building approach [88, 378]. This happens, for instance, if G_ν is the Klein group K_4 and G_l is a cyclic group Z_n with $n \geq 3$ or the product of several cyclic groups. A complete classification of all resulting mixing matrices has been performed by using theorems on roots of unity [261]. One finds that the lepton mixing matrix can take 17 sporadic patterns plus one infinite series, and only the latter could be compatible with the experimental data,

$g'_\nu = hg_\nu h^{-1}$, where h is an element of G_f .

given as [261, 263]

$$U = \frac{1}{\sqrt{3}} \begin{pmatrix} \sqrt{2} \cos \theta & 1 & -\sqrt{2} \sin \theta \\ -\sqrt{2} \cos(\theta - \frac{\pi}{3}) & 1 & \sqrt{2} \sin(\theta - \frac{\pi}{3}) \\ -\sqrt{2} \cos(\theta + \frac{\pi}{3}) & 1 & \sqrt{2} \sin(\theta + \frac{\pi}{3}) \end{pmatrix}, \quad (6.7)$$

where θ is a rational multiple of π , with its exact value completely determined by group-theoretical considerations. This result is consistent with comprehensive scanning over the finite groups and possible symmetry breaking patterns [262, 263, 379]. We obtain the following expressions for the lepton mixing angles

$$\sin^2 \theta_{13} = \frac{2}{3} \sin^2 \theta, \quad \sin^2 \theta_{12} = \frac{1}{1 + 2 \cos^2 \theta}, \quad \sin^2 \theta_{23} = \frac{2 \sin^2(\theta - \frac{\pi}{3})}{1 + 2 \cos^2 \theta}. \quad (6.8)$$

Combining the above equations one sees that the three mixing angles depend on a single parameter θ , consequently the following relations must be satisfied,

$$3 \sin^2 \theta_{12} \cos^2 \theta_{13} = 1, \quad \sin^2 \theta_{23} = \frac{1}{2} \pm \frac{1}{2} \tan \theta_{13} \sqrt{2 - \tan^2 \theta_{13}}. \quad (6.9)$$

Using the best fit value of the reactor mixing angle $\sin^2 \theta_{13} \simeq 0.022$ for NO [24, 25] we get

$$\sin^2 \theta_{12} \simeq 0.341, \quad \sin^2 \theta_{23} \simeq 0.605 \text{ or } 0.395. \quad (6.10)$$

The value of solar mixing angle is within the experimentally preferred 2σ region, the atmospheric angle $\sin^2 \theta_{23} \simeq 0.605$ lies in the 3σ region, while another possible value $\sin^2 \theta_{23} \simeq 0.395$ is disfavored by the present data [24, 25]. As regards the CP violation phases, the Majorana phases are unconstrained²¹ and the Dirac CP phase vanishes

$$\sin \delta_{CP} = 0. \quad (6.11)$$

Notice that current measurements still do not provide a fully robust global CP determination [24, 25].

In order to reproduce the experimentally favored mixing angles the minimal flavour symmetry group is $G_f = (Z_{18} \times Z_6) \times S_3$ [260, 263] for Majorana neutrinos, while for Dirac neutrinos the minimal flavour group is $G_f = (Z_9 \times Z_3) \times S_3$ [263]. Hence the order of the flavour symmetry group should be at least 648 and 162 for Majorana and Dirac neutrinos, respectively, leading to a realistic value of $\theta = \pi/18$. In concrete models, the residual symmetries G_l and G_ν are spoiled by higher order terms involving flavon fields. These induce corrections suppressed by the flavon VEVs with respect to the flavor scale.

6.1.2 Partially preserved residual symmetry $G_\nu = Z_2$

The idea of partially preserved residual symmetry was proposed [381–384] in order to accommodate a non-zero Dirac CP violation phase δ^ℓ and degrade the order of the flavour symmetry. In this approach, part of the residual symmetry of the neutrino mass matrix arises from the assumed flavour symmetry at

²¹One can predict the values of Majorana phases by including the generalized CP symmetry. For instance, for the flavor symmetry $\Delta(6n^2) = (Z_n \times Z_n) \times S_3$ in combination with CP, the Majorana phase ϕ_{12} can take several discrete values for each n , namely ϕ_{13} is a multiple of $\pi/2$ [380] if residual K_4 flavor symmetry and CP symmetry are preserved by neutrino mass matrix.

high the energy scale. A widely studied scenario is that a Z_2 (instead of K_4) subgroup is preserved in the neutrino sector, i.e. the residual group is $G_\nu = Z_2^{g_\nu}$, where g_ν refers to the generator of G_ν . Note that the presentation rule of the cyclic group Z_n^g is $Z_n^g \equiv \{1, g, g^2, \dots, g^{n-1}\}$.

The invariance of the neutrino mass matrix under $Z_2^{g_\nu}$ requires that Eq. (6.2) holds. Consequently the residual flavour symmetry imposes the following restriction on the unitary transformation

$$U_\nu^\dagger \rho_{\mathbf{3}}(g_\nu) U_\nu = \pm P_\nu^T \text{diag}(1, -1, -1) P_\nu, \quad (6.12)$$

where P_ν is a permutation matrix, and we have taken into account that the eigenvalues of $\rho_{\mathbf{3}}(g_\nu)$ is $+1$ or -1 , since g_ν is of order two. Let us denote U_0 as a diagonalization matrix of $\rho_{\mathbf{3}}(g_\nu)$ with

$$U_0^\dagger \rho_{\mathbf{3}}(g_\nu) U_0 = \pm \text{diag}(1, -1, -1), \quad (6.13)$$

Then the unitary transformation U_ν would be of the form

$$U_\nu = U_0 U_{23}(\theta, \delta) P_\nu, \quad (6.14)$$

where $U_{23}(\theta, \delta)$ is a block diagonal complex unitary rotation,

$$U_{23}(\theta, \delta) = \begin{pmatrix} 1 & 0 & 0 \\ 0 & \cos \theta & \sin \theta e^{-i\delta} \\ 0 & -\sin \theta e^{i\delta} & \cos \theta \end{pmatrix}. \quad (6.15)$$

Notice that, since the residual Z_2 flavour symmetry can not fully distinguish the three neutrino families in this case, only one column of U_ν is numerically fixed. In the charged lepton sector, a residual subgroup G_l is preserved, so that the unitary transformation U_l obeys the condition $U_l^\dagger \rho_{\mathbf{3}}(g_l) U_l = \text{diag}(e^{i\alpha_e}, e^{i\alpha_\mu}, e^{i\alpha_\tau})$ as shown in Eq. (6.4), where $\alpha_{e,\mu,\tau}$ are rational multiples of π . Thus the assumed residual symmetry allows us to determine the lepton mixing matrix in terms of two free parameters as

$$U = U_l^\dagger U_0 U_{23}(\theta, \delta) P_\nu. \quad (6.16)$$

Hence only one column is fixed by residual symmetry in this case, and this is dubbed semi-direct approach in [88]. For example, if the flavour group is S_4 and the residual symmetries are chosen as $G_\nu = Z_2^{SU}$ and $G_l = Z_3^T$, then $U_0 = U_{TBM}$ and the lepton mixing is

$$U = \frac{1}{\sqrt{6}} \begin{pmatrix} 2 & \sqrt{2} \cos \theta & \sqrt{2} e^{-i\delta} \sin \theta \\ -1 & \sqrt{2} \cos \theta - \sqrt{3} e^{i\delta} \sin \theta & \sqrt{3} \cos \theta + \sqrt{2} e^{-i\delta} \sin \theta \\ -1 & \sqrt{2} \cos \theta + \sqrt{3} e^{i\delta} \sin \theta & -\sqrt{3} \cos \theta + \sqrt{2} e^{-i\delta} \sin \theta \end{pmatrix}. \quad (6.17)$$

We see that the first column is $(2/\sqrt{6}, -1/\sqrt{6}, -1/\sqrt{6})^T$ which is in common with the TBM mixing pattern [296–298]. In fact, this is exactly the TM1 lepton mixing matrix in Eq. (3.7) [316–318]. In

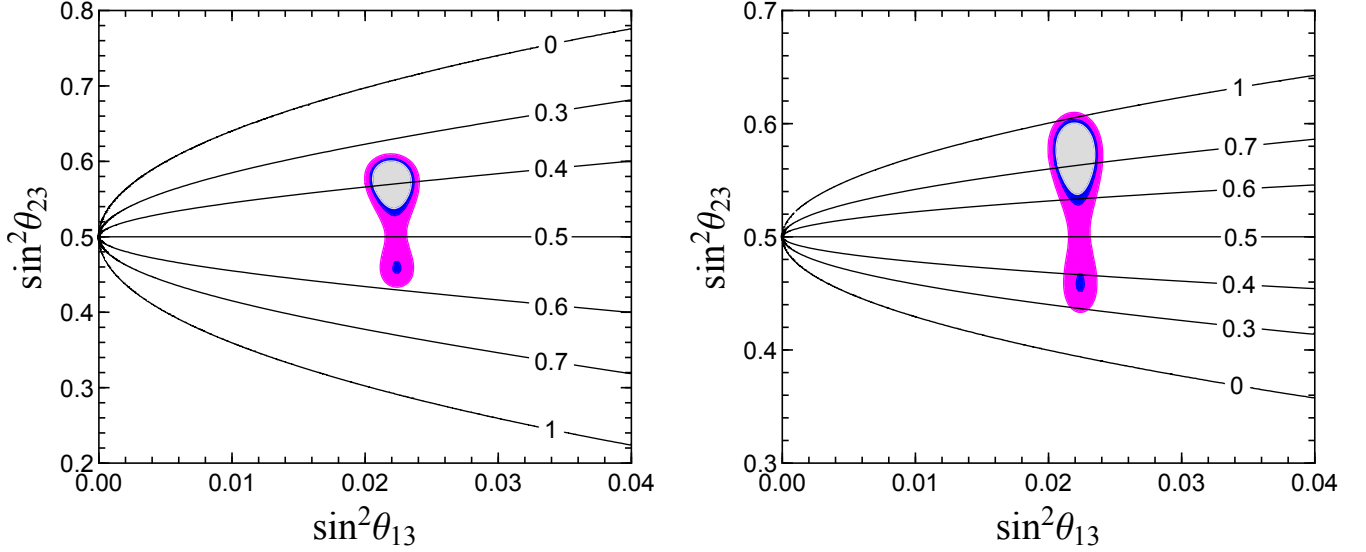


Figure 18: Contours of $|\delta_{CP}/\pi|$ in the $\sin^2 \theta_{23} - \sin^2 \theta_{13}$ plane. The left panel is for the case that the fixed column is $(2/\sqrt{6}, -1/\sqrt{6}, -1/\sqrt{6})^T$ (TM1), and the right panel is for $(1/\sqrt{3}, 1/\sqrt{3}, 1/\sqrt{3})^T$ (TM2). The global-fit allowed oscillation regions corresponding to 90%, 95% and 99% confidence level are shown [24, 25]

figure 18 we plot the contour of $|\delta_{CP}|$ in the plane $\sin^2 \theta_{23}$ versus $\sin^2 \theta_{13}$. The value of the Dirac CP phase δ_{CP} is not too constrained, as long as the atmospheric mixing angle θ_{23} remains poorly measured.

On the other hand, if the residual groups are $G_\nu = Z_2^S$ and $G_l = Z_3^T$ for either A_4 or S_4 flavour symmetry, one column of the lepton mixing matrix is enforced to be $(1/\sqrt{3}, 1/\sqrt{3}, 1/\sqrt{3})^T$ with,

$$U = \frac{1}{\sqrt{6}} \begin{pmatrix} 2 \cos \theta & \sqrt{2} & 2e^{-i\delta} \sin \theta \\ -\cos \theta - \sqrt{3} e^{i\delta} \sin \theta & \sqrt{2} & \sqrt{3} \cos \theta - e^{-i\delta} \sin \theta \\ -\cos \theta + \sqrt{3} e^{i\delta} \sin \theta & \sqrt{2} & -\sqrt{3} \cos \theta - e^{-i\delta} \sin \theta \end{pmatrix}, \quad (6.18)$$

which is exactly the tri-maximal mixing pattern TM2 in Eq. (3.10) [252, 321–323]. The predictions for the Dirac phase δ_{CP} are shown in figure 18. The figure refers to the case of normal mass ordering, with very similar results for the case of inverse-ordered masses.

6.2 Combining flavour and CP symmetry

We saw how a non-vanishing Dirac CP phase can be obtained if a Z_2 rather than the Klein group K_4 is the residual flavour symmetry preserved by the neutrino mass matrix. However, δ_{CP} can vary within a wide region. Moreover, the Majorana phases can not be predicted just from the flavour symmetry. In order to understand the CP violating phases, one can impose a generalized CP (gCP) symmetry [341–343], see [264, 344, 385] for discussions of gCP to the lepton flavor mixing problem. A simple example is the $\mu - \tau$ reflection symmetry [252–256], see Ref. [386] for review. The $\mu - \tau$ reflection symmetry is a combination of the canonical CP transformation with the $\mu - \tau$ exchange symmetry, which exchanges a muon (tau)

neutrino with a tau (muon) antineutrino,

$$\begin{pmatrix} \nu_e \\ \nu_\mu \\ \nu_\tau \end{pmatrix} \mapsto \begin{pmatrix} \nu_e^c \\ \nu_\tau^c \\ \nu_\mu^c \end{pmatrix} = \begin{pmatrix} 1 & 0 & 0 \\ 0 & 0 & 1 \\ 0 & 1 & 0 \end{pmatrix} \begin{pmatrix} \nu_e^c \\ \nu_\mu^c \\ \nu_\tau^c \end{pmatrix}. \quad (6.19)$$

Notice that the generalized CP transformation matrix is not diagonal in family space. In the charged lepton mass basis, the neutrino mass matrix invariant under $\mu - \tau$ reflection has the following form

$$m_\nu = \begin{pmatrix} a & b & b^* \\ b & c & d \\ b^* & d & c^* \end{pmatrix}, \quad (6.20)$$

where a and d are real, b and c are complex numbers. As a result, both atmospheric mixing angle θ_{23} and Dirac CP phase would be maximal, while Majorana phases take CP conserving values. These should be contrasted with present neutrino oscillation data [24, 25]. Deviations of θ_{23} and δ_{CP} from maximal values can easily arise from a more general $\mu - \tau$ reflection symmetry acting on the neutrino sector. Such CP transformation is of the following form [257],

$$\begin{pmatrix} \nu_e \\ \nu_\mu \\ \nu_\tau \end{pmatrix} \mapsto \begin{pmatrix} \nu_e^c \\ \cos \Theta \nu_\mu^c + i \sin \Theta \nu_\tau^c \\ \cos \Theta \nu_\tau^c + i \sin \Theta \nu_\mu^c \end{pmatrix} = \begin{pmatrix} 1 & 0 & 0 \\ 0 & \cos \Theta & i \sin \Theta \\ 0 & i \sin \Theta & \cos \Theta \end{pmatrix} \begin{pmatrix} \nu_e^c \\ \nu_\mu^c \\ \nu_\tau^c \end{pmatrix}, \quad (6.21)$$

where the angle Θ characterizes the CP transformation. It reduces to the $\mu - \tau$ reflection symmetry in the limit of $\Theta = \pi/2$. The atmospheric mixing angle θ_{23} and Dirac phase δ_{CP} are predicted to be strongly correlated as follows [257],

$$\sin^2 \delta_{CP} \sin^2 2\theta_{23} = \sin^2 \Theta, \quad (6.22)$$

while the Majorana phases take on trivial CP conserving values. The correlation in Eq. (6.22) allows us to predict the range of the Dirac CP violating phase $|\sin \delta_{CP}|$ as a function of the parameter Θ as shown in figure 19. Note that the sign of δ_{CP} can not be fixed.

6.2.1 Mathematical consistency

Family symmetries can be generated if one successively performs two generalized CP transformations. Hence generalized CP symmetries can be thought of as associated to some underlying flavour symmetry. A convenient strategy for defining such CP transformations is to start from a flavour symmetry group G_f and find all possible CP transformations H_{CP} which can generate the given flavour group transformations. The purpose of this section is to determine the restricted lepton mixing matrices that can be obtained from discrete flavour and CP symmetries.

It is highly non-trivial to define a CP transformation consistently in the presence of a family symmetry G_f [264, 344, 385, 387]. Let us consider a set of fields φ in a generic irreducible representation \mathbf{r} of G_f ,

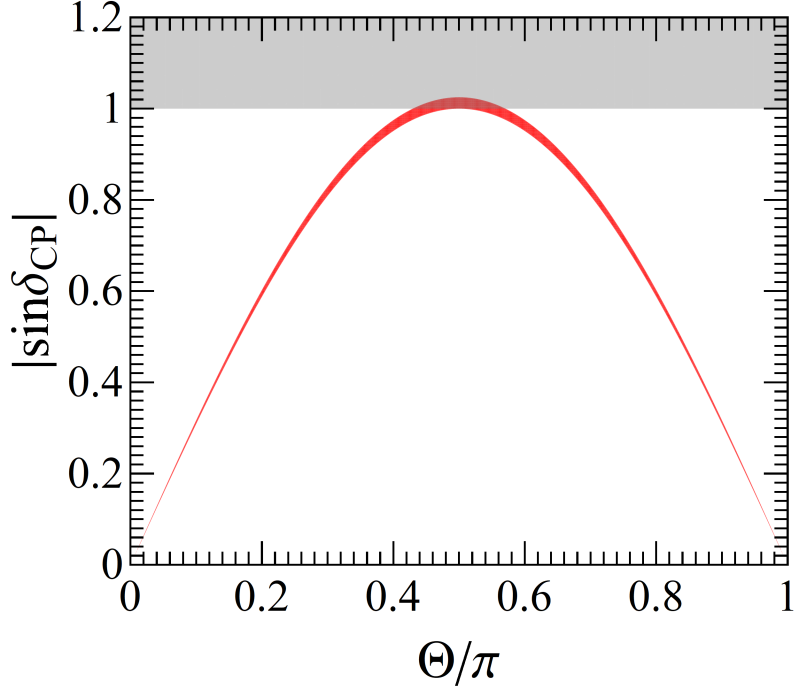


Figure 19: $|\sin \delta_{CP}|$ regions versus Θ characterizing the generalized $\mu - \tau$ reflection, where θ_{23} is required to lie in its 3σ allowed range [24, 25].

transforming under the action of G_f as

$$\varphi(x) \xrightarrow{G_f} \rho_{\mathbf{r}}(g)\varphi(x), \quad g \in G_f, \quad (6.23)$$

where $\rho_{\mathbf{r}}(g)$ denotes the representation matrix for any element g in the irreducible representation \mathbf{r} . The generalized CP acts on φ as

$$\varphi(x) \xrightarrow{\mathcal{CP}} X_{\mathbf{r}} \varphi^*(x_{\mathcal{P}}), \quad (6.24)$$

where $x_{\mathcal{P}} = (t, -\vec{x})$, and $X_{\mathbf{r}}$ is the CP transformation matrix in flavor space, assumed to be a unitary matrix, so as to leave the kinetic term invariant²². A physical CP transformation should map each field $\varphi(x)$ in any irreducible representation \mathbf{r} of G_f into its complex conjugate $\varphi^*(x_{\mathcal{P}})$ in the complex representation \mathbf{r}^* [387]. If we first perform a CP transformation, then apply a flavour symmetry transformation, and subsequently an inverse CP transformation we obtain

$$\varphi(x) \xrightarrow{\mathcal{CP}} X_{\mathbf{r}} \varphi^*(x_{\mathcal{P}}) \xrightarrow{G_f} X_{\mathbf{r}} \rho_{\mathbf{r}^*}(g) \varphi^*(x_{\mathcal{P}}) \xrightarrow{\mathcal{CP}^{-1}} X_{\mathbf{r}} \rho_{\mathbf{r}^*}(g) X_{\mathbf{r}}^{-1} \varphi(x). \quad (6.25)$$

As shown in figure 20, the theory should still be invariant since it is invariant under each transformation individually. To make the theory consistent the resulting net transformation should be equivalent to a flavour symmetry transformation $\rho_{\mathbf{r}}(g')$ of some flavour group element g' , i.e.

$$X_{\mathbf{r}} \rho_{\mathbf{r}^*}(g) X_{\mathbf{r}}^{-1} = \rho_{\mathbf{r}}(g'), \quad g, g' \in G_f \quad (6.26)$$

²²When φ denotes a spinor, the obvious action of CP on the spinor indices is understood.

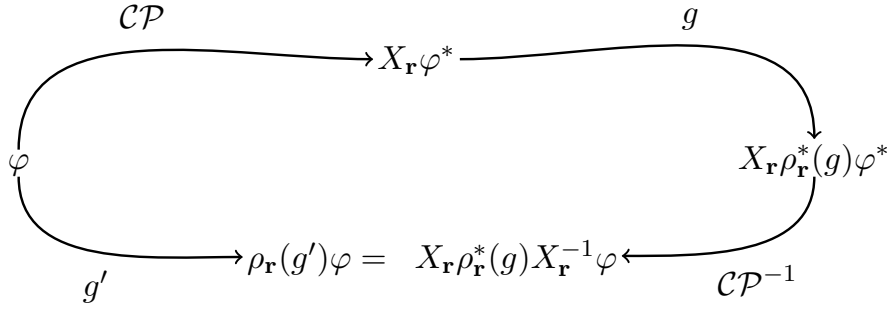


Figure 20: The consistency condition for flavour and generalized CP symmetries.

where the elements g and g' are independent of the representation \mathbf{r} . Eq. (6.26) is the important consistency condition which must be fulfilled for all irreducible representations of G_f in order to ensure generalized CP and flavour symmetry invariance simultaneously. If the condition Eq. (6.26) is not fulfilled, the group G_f is not the full symmetry group of the Lagrangian, and one would have to consider a larger group, which closes under CP transformations. The allowed form of the generalized CP transformations is strongly restricted by the consistency condition of Eq. (6.26).

In practice, it suffices to consider the consistency conditions for the generators of G_f . It is remarkable that both $e^{i\theta}X_{\mathbf{r}}$ and $\rho_{\mathbf{r}}(h)X_{\mathbf{r}}$ satisfy the consistency condition Eq. (6.26) for a generalized CP transformation $X_{\mathbf{r}}$, where θ is real and h is any element of G_f . For a well-defined CP transformation $X_{\mathbf{r}}$, $\rho_{\mathbf{r}}(h)X_{\mathbf{r}}$ is also a viable CP transformation for any $h \in G_f$. The two CP transformations $X_{\mathbf{r}}$ and $\rho_{\mathbf{r}}(h)X_{\mathbf{r}}$ differ by a flavour symmetry transformation $\rho_{\mathbf{r}}(h)$. Since the latter is certainly a symmetry of the Lagrangian, these two CP transformations are indistinguishable. Moreover, Eq. (6.26) implies that the generalized CP transformation $X_{\mathbf{r}}$ maps the group element g into g' and the flavour group multiplication is preserved under this mapping, i.e. $X_{\mathbf{r}}\rho_{\mathbf{r}}^*(g_1g_2)X_{\mathbf{r}}^{-1} = X_{\mathbf{r}}\rho_{\mathbf{r}}^*(g_1)X_{\mathbf{r}}^{-1}X_{\mathbf{r}}\rho_{\mathbf{r}}^*(g_2)X_{\mathbf{r}}^{-1}$. Therefore the CP transformation $X_{\mathbf{r}}$ defines a homomorphism $\mathbf{u} : g \rightarrow g'$, $g, g' \in G_f$ of the family symmetry group G_f . Note that the homomorphism \mathbf{u}' associated with the CP transformation $\rho_{\mathbf{r}}(h)X_{\mathbf{r}}$ for any $h \in G_f$ is related to \mathbf{u} by conjugation:

$$\mathbf{u}'(g) = h\mathbf{u}(g)h^{-1}, \quad \forall h, g \in G_f. \quad (6.27)$$

Notice that when $\rho_{\mathbf{r}}$ is a faithful representation, the elements g and g' have the same order, the mapping defined in Eq. (6.26) is bijective, and thus the associated CP transformation becomes an automorphism, see Ref. [344] for a more formal treatment. Furthermore, taking trace on both sides of the consistency condition in Eq. (6.26), we find that the group characters $\chi_{\mathbf{r}}$ fulfill

$$\chi_{\mathbf{r}}(g') = \text{tr}[\rho_{\mathbf{r}}(g')] = \text{tr}[X_{\mathbf{r}}\rho_{\mathbf{r}}^*(g)X_{\mathbf{r}}^{-1}] = \text{tr}[\rho_{\mathbf{r}}^*(g)] = \text{tr}[\rho_{\mathbf{r}}^\dagger(g)] = \chi_{\mathbf{r}}(g^{-1}). \quad (6.28)$$

Hence g' and g^{-1} should be in the same conjugacy class, that is to say the CP transformation corresponds to a class-inverting automorphism of G_f . As a consequence, when determining the generalized CP transformation compatible with a flavour symmetry group G_f it is sufficient to focus on the class-inverting automorphisms. Because g and g' in Eq. (6.26) are generally different group elements, flavour transfor-

mations and CP transformations in general do not commute. Hence the mathematical structure of the group comprising G_f and generalized CP is in general a semi-direct product, and the full symmetry is $G_f \rtimes H_{CP}$ [264], where H_{CP} is the group generated by generalized CP transformations. The semi-direct product would reduce to a direct product in the case $g = g'$.

6.2.2 Implications of residual flavour and CP symmetries

The presence of generalized CP allows for more symmetry breaking patterns than flavor symmetry alone. In this approach, the parent flavour and CP symmetries are broken down to different residual subgroups $G_l \rtimes H_{CP}^l$ and $G_\nu \rtimes H_{CP}^\nu$ in the charged lepton and neutrino sectors respectively. The mismatch between the residual symmetries $G_l \rtimes H_{CP}^l$ and $G_\nu \rtimes H_{CP}^\nu$ gives rise to a certain lepton mixing pattern. It is remarkable that the lepton flavour mixing is fixed by the group structure of $G_f \rtimes H_{CP}$ and the residual symmetries [265, 267]. The details of the breaking mechanisms realizing the assumed residual symmetries are irrelevant. In the following, we present the formalism to determine the residual symmetries on the charged lepton and neutrino mass matrices. We shall assume neutrinos to be Majorana particles, thus the residual flavour symmetry G_ν is a Z_2 or Klein subgroup K_4 (Dirac neutrinos can be discussed in a very similar way). As usual the three generations of left-handed leptons are assumed to transform as a faithful irreducible triplet $\mathbf{3}$ of the G_f symmetry.

For the residual symmetry $G_l \rtimes H_{CP}^l$ to hold, the Hermitian combination $m_l^\dagger m_l$ of the charged lepton mass matrix should be invariant under the action of $G_l \rtimes H_{CP}^l$, i.e.,

$$\rho_{\mathbf{3}}^\dagger(g_l) m_l^\dagger m_l \rho_{\mathbf{3}}(g_l) = m_l^\dagger m_l, \quad g_l \in G_l, \quad (6.29)$$

$$X_{l\mathbf{3}}^\dagger m_l^\dagger m_l X_{l\mathbf{3}} = (m_l^\dagger m_l)^*, \quad X_{l\mathbf{3}} \in H_{CP}^l, \quad (6.30)$$

where the charged lepton mass matrix m_l is given in the convention in which the left-handed (right-handed) fields are on the right-hand (left-hand) side of m_l . We denote the unitary diagonalization matrix of $m_l^\dagger m_l$ as U_l which satisfies $U_l^\dagger m_l^\dagger m_l U_l = \text{diag}(m_e^2, m_\mu^2, m_\tau^2)$. Once the residual symmetry $G_l \rtimes H_{CP}^l$ and the triplet representation $\mathbf{3}$ are specified, the explicit form of $m_l^\dagger m_l$ can be constructed from Eqs. (6.29, 6.30) in a straightforward way, and thus U_l can be determined. In fact, one can also directly extract the restrictions on U_l from Eqs. (6.29, 6.30) without working out the explicit form of $m_l^\dagger m_l$ as follows

$$U_l^\dagger \rho_{\mathbf{3}}(g_l) U_l = \rho_{\mathbf{3}}^{diag}(g_l), \quad U_l^\dagger X_{l\mathbf{3}} U_l^* = X_{l\mathbf{3}}^{diag}, \quad (6.31)$$

where both $\rho_{\mathbf{3}}^{diag}(g_l)$ and $X_{l\mathbf{3}}^{diag}$ are diagonal phase matrices.

The first identity in Eq. (6.31) comes from imposing the residual flavour symmetry G_l , and the latter arises from the residual CP symmetry H_{CP}^l . We see that both $\rho_{\mathbf{3}}(g_l)$ and $m_l^\dagger m_l$ can be diagonalized by the same unitary matrix U_l , and the residual CP transformation $X_{l\mathbf{3}} = U_l X_{l\mathbf{3}}^{diag} U_l^T$ should be a symmetric unitary matrix. Moreover, Eq. (6.31) implies that the residual flavour and CP symmetries should satisfy

the following restricted consistency conditions:

$$X_{l\mathbf{r}}\rho_{\mathbf{r}}^*(g_l)X_{l\mathbf{r}}^{-1} = \rho_{\mathbf{r}}(g_l^{-1}), \quad g_l \in G_l, \quad (6.32)$$

If the residual flavour symmetry G_l distinguishes the three families, the inclusion of generalized CP H_{CP}^l would not add any information as far as lepton mixing is concerned [335, 388]. Likewise, the requirement that $G_\nu \times H_{CP}^\nu$ is preserved in the neutrino sector implies that the neutrino mass matrix m_ν must be invariant under the action of $G_\nu \times H_{CP}^\nu$, i.e.,

$$\begin{aligned} \rho_{\mathbf{3}}^T(g_\nu)m_\nu\rho_{\mathbf{3}}(g_\nu) &= m_\nu, \quad g_\nu \in G_\nu, \\ X_{\nu\mathbf{3}}^T m_\nu X_{\nu\mathbf{3}} &= m_\nu^*, \quad X_{\nu\mathbf{3}} \in H_{CP}^\nu. \end{aligned} \quad (6.33)$$

Since G_ν is a Z_2 or K_4 subgroup for Majorana neutrinos, the eigenvalues of the representation matrix $\rho_{\mathbf{3}}(g_\nu)$ can only be $+1$ or -1 . The diagonalization matrix of m_ν is denoted as U_ν and satisfies $U_\nu^T m_\nu U_\nu = \text{diag}(m_1, m_2, m_3)$. From Eq. (6.33), we find that the residual symmetry $G_\nu \times H_{CP}^\nu$ leads to the following restrictions on the unitary transformation U_ν ,

$$U_{\nu\mathbf{3}}^\dagger \rho_{\mathbf{3}}(g_\nu) U_\nu = \text{diag}(\pm 1, \pm 1, \pm 1), \quad U_\nu^\dagger X_{\nu\mathbf{3}} U_\nu^* = \text{diag}(\pm 1, \pm 1, \pm 1). \quad (6.34)$$

Hence the residual CP transformation $X_{\nu\mathbf{3}}$ should be a symmetric matrix [264, 265, 267] and the restricted consistency condition in the neutrino sector is

$$X_{\nu\mathbf{r}}\rho_{\mathbf{r}}^*(g_\nu)X_{\nu\mathbf{r}}^{-1} = \rho_{\mathbf{r}}(g_\nu), \quad g_\nu \in G_\nu, \quad X_{\nu\mathbf{r}} \in H_{CP}^\nu, \quad (6.35)$$

which implies that the residual flavour symmetry G_ν and residual CP symmetry H_{CP}^ν in the neutrino sector commute with each other. Consequently, for Majorana neutrinos the mathematical structure of the residual symmetry is a direct product $G_\nu \times H_{CP}^\nu$. Solving the constraints Eqs. (6.31, 6.34) imposed by the residual symmetry, one can fix the unitary transformations U_l , U_ν and hence the lepton mixing matrix, as

$$U = U_l^\dagger U_\nu. \quad (6.36)$$

In the following, we present several different choices for the residual scheme and the corresponding predictions for the lepton mixing matrix.

6.3 Predictive scenarios with CP symmetry

Assuming a generalized CP symmetry, the Majorana CP violation phases can be predicted and we have more choices for the possible residual symmetries. In particular, some scenarios are quite predictive, with the lepton mixing matrix elements depending only on few free parameters, as shown in table 1. For notational simplicity, we denote $\mathcal{G}_l \equiv G_l \times H_{CP}^l$ and $\mathcal{G}_\nu \equiv G_\nu \times H_{CP}^\nu$ which are the residual symmetries

of the charged lepton and neutrino sectors respectively ²³. We have assumed that the residual flavour symmetry Z_n with $n \geq 3$ is sufficient to distinguish the three generations of charged leptons, otherwise it can be taken to be a product of cyclic groups. The unitary transformations Σ_l and Σ_ν are the Takagi factorizations of the residual CP transformations H_{CP}^l and H_{CP}^ν respectively, in the presence of residual CP. They should also diagonalize the residual flavour symmetry transformations G_l and G_ν respectively. Moreover, $R_{23}(\theta)$ is a rotation matrix in the (23)-plane, Eq. (4.45), while $O_3(\theta_1, \theta_2, \theta_3)$ is a general three-dimensional rotation matrix, Eq. (4.41). Both P_l and P_ν are permutation matrices since the neutrino and charged lepton masses are not constrained by the residual symmetry. Furthermore, Q_l and Q_ν are diagonal phase matrices, Q_l can be absorbed into the charged lepton fields, the non-zero elements of Q_ν encoding the CP parity of neutrinos are equal to ± 1 and $\pm i$ and they can shift the Majorana phases ϕ_{12} and ϕ_{13} by $\pm\pi/2$ or $\pm\pi$. In what follows, we present two predictive scenarios for illustration.

\mathcal{G}_l	\mathcal{G}_ν	U	number of parameters
Z_n	$K_4 \times CP$	$Q_l^\dagger P_l^T \Sigma_l^\dagger \Sigma_\nu P_\nu Q_\nu$	0
Z_n	$Z_2 \times CP$	$Q_l^\dagger P_l^T \Sigma_l^\dagger \Sigma_\nu R_{23}(\theta) P_\nu Q_\nu$	1
$Z_2 \times CP$	$K_4 \times CP'$	$Q_l^\dagger P_l^T R_{23}^T(\theta_l) \Sigma_l^\dagger \Sigma_\nu P_\nu Q_\nu$	
$Z_2 \times CP$	$Z_2 \times CP'$	$Q_l^\dagger P_l^T R_{23}^T(\theta_l) \Sigma_l^\dagger \Sigma_\nu R_{23}(\theta_\nu) P_\nu Q_\nu$	2
Z_2	$K_4 \times CP$	$Q_l^\dagger P_l^T U_{23}^\dagger(\theta_l, \delta_l) \Sigma_l^\dagger \Sigma_\nu P_\nu Q_\nu$	3
Z_n	CP	$Q_l^\dagger P_l^T \Sigma_l^\dagger \Sigma_\nu O_3(\theta_1, \theta_2, \theta_3) Q_\nu$	
CP	$K_4 \times CP'$	$Q_l^\dagger O_3^T(\theta_1, \theta_2, \theta_3) \Sigma_l^\dagger \Sigma_\nu Q_\nu$	
Z_2	$Z_2 \times CP$	$Q_l^\dagger P_l^T U_{23}^\dagger(\theta_l, \delta_l) \Sigma_l^\dagger \Sigma_\nu R_{23}(\theta_\nu) P_\nu Q_\nu$	

Table 1: Possible choices of residual symmetries and corresponding predictions for lepton mixing matrix, when the latter depends on up to three free parameters. If the residual CP is absent from \mathcal{G}_ν , the Majorana CP phases are not restricted.

6.3.1 $\mathcal{G}_l = Z_n$ ($n \geq 3$), $\mathcal{G}_\nu = Z_2 \times CP$

We consider the scenario where the three families of left-handed leptons transform inequivalently as one-dimensional representations under the residual flavour symmetry $G_l = Z_n$ with $n \geq 3$, so that they are distinguished by the abelian subgroup G_l . The representation matrix $\rho_3(g_l)$ can be diagonalized by a unitary matrix Σ_l fulfilling $\Sigma_l^\dagger \rho_3(g_l) \Sigma_l = \rho_3^{diag}(g_l)$, where the three columns of Σ_l are formed by the three eigenvectors of $\rho_3(g_l)$ and Σ_l is determined up to an arbitrary diagonal unitary matrix Q_l and a permutation matrix P_l . Eq. (6.31) implies that the charged lepton diagonalization matrix U_l coincides with Σ_l , i.e.,

$$U_l = \Sigma_l P_l Q_l. \quad (6.37)$$

Concerning the neutrino sector, since $X_{\nu\mathbf{3}}$ is a symmetric and unitary matrix, by performing the Takagi factorization $X_{\nu\mathbf{3}}$ can be written as

$$X_{\nu\mathbf{3}} = \Sigma_\nu \Sigma_\nu^T, \quad \text{with} \quad \Sigma_\nu^\dagger \rho_3(g_\nu) \Sigma_\nu = \pm \text{diag}(1, -1, -1). \quad (6.38)$$

²³In concrete model building, one could possibly have more branches of residual symmetry [389–392].

The procedure of obtaining the unitary matrix Σ_ν has been given in [345]. The neutrino diagonalization matrix U_ν satisfying the conditions in Eq. (6.34) is determined to be of the following form [264, 345]

$$U_\nu = \Sigma_\nu R_{23}(\theta) P_\nu Q_\nu, \quad (6.39)$$

where $R_{23}(\theta)$ stands for a rotation matrix through an angle θ in the (23)-plane and it takes the form of Eq. (4.45), and P_ν is a generic permutation matrix. Here Q_ν in Eq. (6.39) is a diagonal matrix with elements equal to ± 1 and $\pm i$. Hence, without loss of generality it can be given as,

$$Q_\nu = \begin{pmatrix} 1 & 0 & 0 \\ 1 & i^{k_1} & 0 \\ 0 & 0 & i^{k_2} \end{pmatrix} \quad (6.40)$$

with $k_{1,2} = 0, 1, 2, 3$. Hence the lepton mixing matrix U is of the form [264, 265, 345]

$$U = U_l^\dagger U_\nu = Q_l^\dagger P_l^T \Sigma_l^\dagger \Sigma_\nu R_{23}(\theta) P_\nu Q_\nu. \quad (6.41)$$

Notice that, as usual, the phase matrix Q_l can be absorbed into the charged lepton fields [30], while the effect of Q_ν is to shift the Majorana CP phases ϕ_{12} and ϕ_{13} by integral multiples of $\pi/2$. It is remarkable that the lepton mixing matrix is constrained to only depend on a single free parameter θ , whose value can be fixed by the precisely measured reactor mixing angle θ_{13} . We can therefore predict the values of the other two mixing angles θ_{12} , θ_{23} as well as the CP violation phases. The lepton mixing matrix is determined up to possible permutations of rows and columns, since both neutrino and charged lepton masses are not constrained in this approach. Moreover, the Z_2 residual flavour symmetry can only distinguish one neutrino family from the other two generations, so that only one column of the lepton mixing matrix is fixed through the choice of residual symmetry, as can be seen from Eq. (6.41). Comparing with the oscillation data in Eqs. (1.23, 1.24), one can determine the phenomenologically allowed permutation matrices P_l and P_ν .

It follows from the above that, for any postulated residual symmetry subgroups G_l and $Z_2 \times CP$, the lepton mixing matrix can be extracted by using Eq. (6.41) in a simple manner, the recipe is summarized in figure 21. The predicted lepton mixing matrix only depends on the structure of the symmetry group $G_f \times H_{CP}$ and the assumed residual symmetry, regardless of the underlying dynamics which breaks $G_f \times H_{CP}$ down to the residual subgroup.

As an illustration, we consider the S_4 flavor symmetry in combination with the generalized CP symmetry. The group theory and representation of S_4 are given in B. The outer automorphism group of S_4 is trivial [320, 344], all the automorphisms of S_4 are inner automorphisms which are group conjugations. Without loss of generality it is sufficient to consider the representative automorphism $\mathbf{u} : (s, t, u) \rightarrow (s, t^{-1}, u)$, where s , t and u are the generators of S_4 , the corresponding generalized CP transformation $X_{\mathbf{r}}^0$ is determined

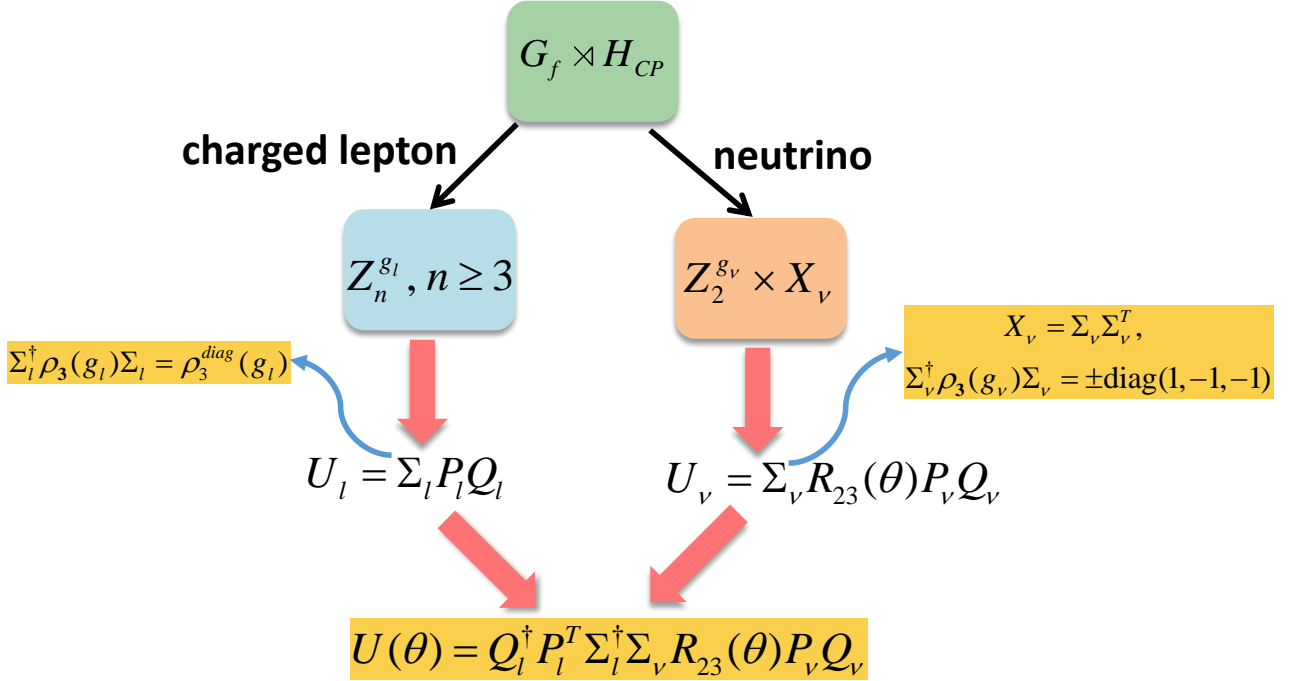


Figure 21: The model independent predictions for lepton mixing matrix for the preserved residual symmetry abelian subgroup G_l and $Z_2 \times CP$ in the charged lepton and neutrino sectors respectively.

by the following consistency equations

$$\begin{aligned}
X_{\mathbf{r}}^0 \rho_{\mathbf{r}}^*(s) (X_{\mathbf{r}}^0)^{-1} &= \rho_{\mathbf{r}}(\mathbf{u}(s)) = \rho_{\mathbf{r}}(s), \\
X_{\mathbf{r}}^0 \rho_{\mathbf{r}}^*(t) (X_{\mathbf{r}}^0)^{-1} &= \rho_{\mathbf{r}}(\mathbf{u}(t)) = \rho_{\mathbf{r}}(t^2), \\
X_{\mathbf{r}}^0 \rho_{\mathbf{r}}^*(u) (X_{\mathbf{r}}^0)^{-1} &= \rho_{\mathbf{r}}(\mathbf{u}(u)) = \rho_{\mathbf{r}}(u).
\end{aligned} \tag{6.42}$$

From the explicit form of the representation matrices in Eqs. (B.3, B.4, B.5), it follows that $X_{\mathbf{r}}^0$ is the unit matrix up to an arbitrary overall phase,

$$X_{\mathbf{r}}^0 = 1. \tag{6.43}$$

Including the family symmetry transformation, the generalized CP transformation consistent with the S_4 symmetry is given by [320, 325, 335]

$$X_{\mathbf{r}} = \rho_{\mathbf{r}}(g) X_{\mathbf{r}}^0 = \rho_{\mathbf{r}}(g), \quad g \in S_4. \tag{6.44}$$

It was found that three sets of residual symmetries are compatible with the experimental data [264]. Notice that a fourth residual symmetry with $G_l = Z_3^t$, $G_\nu = Z_2^{su}$, $X_\nu = 1$ is not phenomenologically viable, since the reactor and atmospheric angles can not be accommodated simultaneously.

- (i) $G_l = Z_3^t$, $G_\nu = Z_2^s$, $X_\nu = 1$

In this case, the unitary transformation Σ_l is the unit matrix since the representation matrix $\rho_{\mathbf{3}}(t)$ is diagonal, and the Takagi factorization matrix Σ_ν is found to be

$$\Sigma_\nu = \frac{1}{\sqrt{6}} \begin{pmatrix} \sqrt{2} & 2 & 0 \\ \sqrt{2} & -1 & \sqrt{3} \\ \sqrt{2} & -1 & -\sqrt{3} \end{pmatrix}. \quad (6.45)$$

Hence the lepton mixing matrix is determined to be

$$U = \frac{1}{\sqrt{6}} \begin{pmatrix} 2 \cos \theta & \sqrt{2} & 2 \sin \theta \\ -\cos \theta - \sqrt{3} \sin \theta & \sqrt{2} & \sqrt{3} \cos \theta - \sin \theta \\ -\cos \theta + \sqrt{3} \sin \theta & \sqrt{2} & -\sqrt{3} \cos \theta - \sin \theta \end{pmatrix} Q_\nu, \quad (6.46)$$

where we have taken $P_\nu = P_{12}$ such that $(1, 1, 1)^T/\sqrt{3}$ is in the second column, in order to be consistent with experimental data. We can extract the lepton mixing parameters as follows,

$$\begin{aligned} \sin^2 \theta_{13} &= \frac{2}{3} \sin^2 \theta, & \sin^2 \theta_{23} &= \frac{1}{2} - \frac{\sqrt{3} \sin 2\theta}{2(2 + \cos 2\theta)} = \frac{1}{2} \pm \frac{1}{2} \tan \theta_{13} \sqrt{2 - \tan^2 \theta_{13}}, \\ \sin^2 \theta_{12} &= \frac{1}{2 + \cos 2\theta} = \frac{1}{3 \cos^2 \theta_{13}}, & \sin 2\phi_{12} &= \sin 2\phi_{13} = \sin \delta_{CP} = 0. \end{aligned} \quad (6.47)$$

Using the experimental best fit value $(\sin^2 \theta_{13})^{\text{bf}} = 0.022$ [24, 25], we find the solar mixing angle $\sin^2 \theta_{12} \simeq 0.341$ and the atmospheric angle

$$\sin^2 \theta_{23} \simeq \begin{cases} 0.426 & \text{for } \theta < \pi/2 \\ 0.574 & \text{for } \theta > \pi/2 \end{cases}. \quad (6.48)$$

The Dirac and Majorana CP phases are determined to take on CP conserving values in this case.

(ii) $G_l = Z_3^t$, $G_\nu = Z_2^s$, $X_\nu = u$

This case differs from the previous one in the residual CP X_ν . The unitary matrix Σ_ν is

$$\Sigma_\nu = \frac{1}{\sqrt{6}} \begin{pmatrix} \sqrt{2}i & 2i & 0 \\ \sqrt{2}i & -i & \sqrt{3} \\ \sqrt{2}i & -i & -\sqrt{3} \end{pmatrix}. \quad (6.49)$$

Consequently, for $P_\nu = P_{12}$, the lepton mixing matrix is fixed to be

$$U = \frac{1}{\sqrt{6}} \begin{pmatrix} 2 \cos \theta & \sqrt{2} & 2 \sin \theta \\ -\cos \theta + i\sqrt{3} \sin \theta & \sqrt{2} & -\sin \theta - i\sqrt{3} \cos \theta \\ -\cos \theta - i\sqrt{3} \sin \theta & \sqrt{2} & -\sin \theta + i\sqrt{3} \cos \theta \end{pmatrix} Q_\nu. \quad (6.50)$$

We can extract the lepton mixing parameters as

$$\begin{aligned}\sin^2 \theta_{13} &= \frac{2}{3} \sin^2 \theta, & \sin^2 \theta_{12} &= \frac{1}{2 + \cos 2\theta} = \frac{1}{3 \cos^2 \theta_{13}}, \\ \sin^2 \theta_{23} &= \frac{1}{2}, & |\sin \delta_{CP}| &= 1, & \sin 2\phi_{12} &= \sin 2\phi_{13} = 0.\end{aligned}\quad (6.51)$$

Because the $\mu - \tau$ reflection symmetry $X_\nu = u$ is imposed on the neutrino mass matrix [252–255], both atmospheric angle θ_{23} and Dirac CP phase δ_{CP} are maximal, while the Majorana CP phases ϕ_{12} and ϕ_{13} are trivial.

(iii) $G_l = Z_3^t, G_\nu = Z_2^{su}, X_\nu = u$

The Takagi factorization matrix Σ_ν is determined to be

$$\Sigma_\nu = \frac{1}{\sqrt{6}} \begin{pmatrix} 2i & \sqrt{2}i & 0 \\ -i & \sqrt{2}i & -\sqrt{3} \\ -i & \sqrt{2}i & \sqrt{3} \end{pmatrix}. \quad (6.52)$$

Using the mater formula Eq. (6.41), we obtain the lepton mixing matrix as

$$U = \frac{1}{\sqrt{6}} \begin{pmatrix} 2 & \sqrt{2} \cos \theta & \sqrt{2} \sin \theta \\ -1 & \sqrt{2} \cos \theta - i\sqrt{3} \sin \theta & \sqrt{2} \sin \theta + i\sqrt{3} \cos \theta \\ -1 & \sqrt{2} \cos \theta + i\sqrt{3} \sin \theta & \sqrt{2} \sin \theta - i\sqrt{3} \cos \theta \end{pmatrix} Q_\nu. \quad (6.53)$$

The predictions for mixing angles and CP violation phases are

$$\begin{aligned}\sin^2 \theta_{13} &= \frac{1}{3} \sin^2 \theta, & \sin^2 \theta_{12} &= \frac{1 + \cos 2\theta}{5 + \cos 2\theta} = \frac{1 - 3 \sin^2 \theta_{13}}{3 \cos^2 \theta_{13}}, \\ \sin^2 \theta_{23} &= \frac{1}{2}, & |\sin \delta_{CP}| &= 1, & \sin 2\phi_{12} &= \sin 2\phi_{13} = 0.\end{aligned}\quad (6.54)$$

For $(\sin^2 \theta_{13})^{\text{bf}} = 0.022$ [24, 25] we find, from Eq. (6.54), the solar mixing angle as $\sin^2 \theta_{12} \simeq 0.318$. Similar to case ii, the $\mu - \tau$ reflection symmetry $X_\nu = u$ implies maximal values of θ_{23} and δ_{CP} , and CP conserving values of ϕ_{12}, ϕ_{13} .

The values of the effective $|m_{\beta\beta}|$ parameter characterizing the $0\nu\beta\beta$ decay amplitude can be determined for the viable cases associated to the lepton mixing matrices in Eqs. (6.46, 6.50, 6.53). This effective mass parameter depends on the CP parity encoded in Q_ν . Since the rotation angle θ is strongly constrained by the reactor angle θ_{13} and the Majorana phases can be predicted, the effective mass $|m_{\beta\beta}|$ is severely restricted, as shown in figure 22. The narrow width of each band comes from varying θ_{13} and the neutrino mass squared differences over their allowed 3σ ranges [24].

For inverted neutrino mass ordering, the term proportional to m_3 in $|m_{\beta\beta}|$ is suppressed by the small values of m_3 and $\sin^2 \theta_{13}$, consequently the value of k_2 is almost irrelevant. For $(k_1, k_2) = (0, 0), (0, 1)$, the effective mass $m_{\beta\beta}$ is close to the upper boundary of the IO region obtained by using the 3σ global

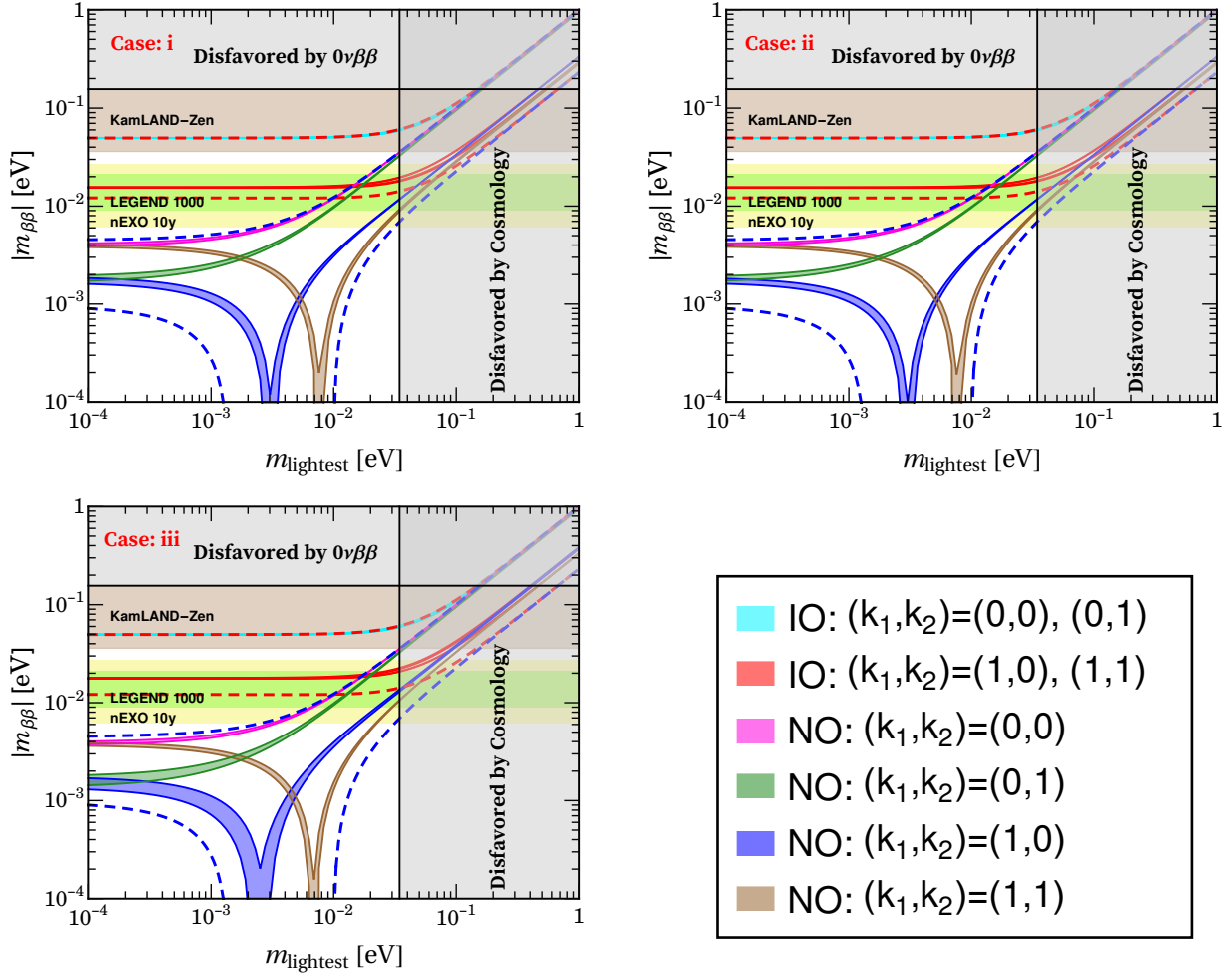


Figure 22: Predicted effective Majorana neutrino mass $|m_{\beta\beta}|$ for three viable mixing patterns when the S_4 flavour symmetry and CP symmetry are broken to an Abelian subgroup and $Z_2 \times CP$ in the charged lepton sector and neutrino sector respectively. The red (blue) dashed lines indicate the most general allowed regions for IO (NO) neutrino mass ordering obtained by varying the mixing parameters in their 3σ ranges [24, 25]. The current experimental bound $|m_{\beta\beta}| < (36 - 156)$ meV at 90% C.L. from KamLAND-Zen [125] and the future sensitivity ranges $|m_{\beta\beta}| < (9.0 - 21)$ meV from LEGEND-1000 [126] and $|m_{\beta\beta}| < (6.1 - 27)$ meV from nEXO [127] are indicated by light brown, light yellow and light green horizontal bands respectively. The vertical grey exclusion band represents the bound $\sum_i m_i < 0.120$ eV from Planck at 95% C.L. [128, 129].

data, while $|m_{\beta\beta}|$ is close to the lower boundary of IO for $(k_1, k_2) = (1, 0), (1, 1)$.

Symmetry breaking patterns of abelian subgroups in the charged lepton sector and $Z_2 \times CP$ in the neutrino sector have also been studied for many flavour symmetry groups combined with generalized CP, such as A_4 [264, 388, 393], S_4 [264, 320, 325, 335, 394–396], $\Delta(27)$ [397, 398], $\Delta(48)$ [399, 400], A_5 [401–405], $\Delta(96)$ [406] and the infinite group series $\Delta(3n^2) = (Z_n \times Z_n) \rtimes Z_3$ [407, 408], $\Delta(6n^2) = (Z_n \times Z_n) \rtimes S_3$ [407, 409] and $D_{9n, 3n}^{(1)} = (Z_{9n} \times Z_{3n}) \rtimes S_3$ [410]. For popular flavour symmetries A_4 , S_4 and A_5 , the Dirac CP phase is predicted to take simple values $\delta_{CP} = 0, \pi, \pm\pi/2$, and the Majorana phases take on CP conserving values for the experimentally viable mixing patterns. Moreover, the values of the Dirac

CP phase and atmospheric mixing angle are correlated in flavor groups A_4 , S_4 and A_5 , the atmospheric angle is maximal for $\delta_{CP} = \pm\pi/2$ and non-maximal for $\delta_{CP} = 0, \pi$. Both Dirac and Majorana CP phases can depend nontrivially on the parameter θ for larger flavour symmetry groups such as $\Delta(96)$ [406]. A systematical classification of the possible mixing patterns resulting from the pair of residual symmetry subgroups $\{G_l, Z_2 \times CP\}$ has been performed [345]. The neutrino mixing patterns compatible with oscillation data are given as follows [345]:

$$\begin{aligned}
U^{I(a)} &= \frac{1}{\sqrt{3}} \begin{pmatrix} \sqrt{2} \sin \varphi_1 & e^{i\varphi_2} & \sqrt{2} \cos \varphi_1 \\ \sqrt{2} \cos(\varphi_1 - \frac{\pi}{6}) & -e^{i\varphi_2} & -\sqrt{2} \sin(\varphi_1 - \frac{\pi}{6}) \\ \sqrt{2} \cos(\varphi_1 + \frac{\pi}{6}) & e^{i\varphi_2} & -\sqrt{2} \sin(\varphi_1 + \frac{\pi}{6}) \end{pmatrix} R_{23}(\theta) Q_\nu, \\
U^{I(b)} &= \frac{1}{\sqrt{3}} \begin{pmatrix} \sqrt{2} \cos \varphi_1 & e^{i\varphi_2} & \sqrt{2} \sin \varphi_1 \\ -\sqrt{2} \sin(\varphi_1 - \frac{\pi}{6}) & -e^{i\varphi_2} & \sqrt{2} \cos(\varphi_1 - \frac{\pi}{6}) \\ -\sqrt{2} \sin(\varphi_1 + \frac{\pi}{6}) & e^{i\varphi_2} & \sqrt{2} \cos(\varphi_1 + \frac{\pi}{6}) \end{pmatrix} R_{12}(\theta) Q_\nu, \\
U^{II} &= \frac{1}{\sqrt{3}} \begin{pmatrix} e^{i\varphi_1} & 1 & e^{i\varphi_2} \\ \omega e^{i\varphi_1} & 1 & \omega^2 e^{i\varphi_2} \\ \omega^2 e^{i\varphi_1} & 1 & \omega e^{i\varphi_2} \end{pmatrix} R_{13}(\theta) Q_\nu, \\
U^{III} &= \frac{1}{\sqrt{3}} \begin{pmatrix} \sqrt{2} e^{i\varphi_1} \sin \varphi_2 & 1 & \sqrt{2} e^{i\varphi_1} \cos \varphi_2 \\ \sqrt{2} e^{i\varphi_1} \cos(\varphi_2 + \frac{\pi}{6}) & 1 & -\sqrt{2} e^{i\varphi_1} \sin(\varphi_2 + \frac{\pi}{6}) \\ -\sqrt{2} e^{i\varphi_1} \cos(\varphi_2 - \frac{\pi}{6}) & 1 & \sqrt{2} e^{i\varphi_1} \sin(\varphi_2 - \frac{\pi}{6}) \end{pmatrix} R_{13}(\theta) Q_\nu, \\
U^{IV(a)} &= \frac{1}{\sqrt{2\sqrt{5}\phi_g}} \begin{pmatrix} -\sqrt{2}\phi_g & \sqrt{2} & 0 \\ 1 & \phi_g & -\sqrt{\sqrt{5}\phi_g} \\ 1 & \phi_g & \sqrt{\sqrt{5}\phi_g} \end{pmatrix} R_{13}(\theta) Q_\nu, \\
U^{IV(b)} &= \frac{1}{\sqrt{2\sqrt{5}\phi_g}} \begin{pmatrix} -\sqrt{2}\phi_g i & \sqrt{2} & 0 \\ i & \phi_g & -\sqrt{\sqrt{5}\phi_g} \\ i & \phi_g & \sqrt{\sqrt{5}\phi_g} \end{pmatrix} R_{13}(\theta) Q_\nu, \\
U^V &= \frac{1}{2} \begin{pmatrix} \phi_g & 1 & \phi_g - 1 \\ \phi_g - 1 & -\phi_g & 1 \\ 1 & 1 - \phi_g & -\phi_g \end{pmatrix} R_{23}(\theta) Q_\nu, \\
U^{VI} &= \frac{1}{2\sqrt{3}} \begin{pmatrix} (\sqrt{3}-1)e^{i\varphi} & 2 & -(\sqrt{3}+1)e^{i(\varphi+\frac{3\pi}{4})} \\ -(\sqrt{3}+1)e^{i\varphi} & 2 & (\sqrt{3}-1)e^{i(\varphi+\frac{3\pi}{4})} \\ 2e^{i\varphi} & 2 & 2e^{i(\varphi+\frac{3\pi}{4})} \end{pmatrix} R_{13}(\theta) Q_\nu, \\
U^{VII} &= \frac{1}{2\sqrt{6}} \begin{pmatrix} -\frac{\sqrt{3}}{s_3} & 2\sqrt{2} & \frac{s_2-s_1}{s_1s_2} \\ \frac{\sqrt{3}}{s_2} & 2\sqrt{2} & -\frac{s_1+s_3}{s_1s_3} \\ \frac{\sqrt{3}}{s_1} & 2\sqrt{2} & \frac{s_2+s_3}{s_2s_3} \end{pmatrix} R_{23}(\theta) Q_\nu, \tag{6.55}
\end{aligned}$$

up to row and column permutations, where $s_n \equiv \sin(2n\pi/7)$ with $n = 1, 2, 3$ and $R_{ij}(\theta)$ is the rotation

matrix through an angle θ in the (ij) -plane. The parameters φ_1 , φ_2 and φ are group theoretical indices characterizing the flavour group and the residual symmetry and they can only take some discrete values for a given flavour symmetry. The possible values of φ_1 , φ_2 and φ for different finite flavour group G_f up to order 2000 and the corresponding predictions for lepton mixing parameters are given in [345]. It is remarkable that the above mixing patterns can be obtained from the flavour groups $\Delta(6n^2)$, $D_{9n,3n}^{(1)}$, A_5 and $\Sigma(168)$ in combination with generalized CP symmetry.

As shown in table 1, if the residual symmetries $K_4 \times CP$ and $Z_2 \times CP'$ are preserved in the neutrino and charged lepton sectors respectively, the lepton mixing matrix would only depends on a single real parameter θ as well. In this case, one row of the mixing matrix is completely fixed by residual symmetry, regardless of the free parameter θ .

It turns out that only one type of mixing pattern can accommodate the oscillation data [345]:

$$U^{VIII} = \frac{1}{2} R_{13}^T(\theta) \begin{pmatrix} \sqrt{2}e^{i\varphi_1} & -\sqrt{2}e^{i\varphi_1} & 0 \\ 1 & 1 & -\sqrt{2}e^{i\varphi_2} \\ 1 & 1 & \sqrt{2}e^{i\varphi_2} \end{pmatrix} Q_\nu, \quad (6.56)$$

where φ_1 and φ_2 take discrete values determined by the choice of the residual symmetry and the flavour symmetry group.

6.3.2 $\mathcal{G}_l = Z_2 \times CP$, $\mathcal{G}_\nu = Z_2 \times CP'$

The residual subgroups in both the neutrino and charged lepton sectors are of the structure $Z_2 \times CP$ in this scheme [282, 284, 395]. Since the neutrino sector still preserves the residual symmetry $Z_2^{g_\nu} \times X_\nu$, the unitary transformation U_ν is given by Eq. (6.39). The residual symmetry of the charged lepton sector is denoted as $Z_2^{g_l} \times X_l$ in this scheme, and the constrained consistency condition in Eq. (6.32) should be fulfilled, i.e., $X_{l\mathbf{r}}\rho_{\mathbf{r}}^*(g_l)X_{l\mathbf{r}}^{-1} = \rho_{\mathbf{r}}(g_l)$. The three families of left-handed lepton doublets are assigned to transform as a faithful triplet ρ of the flavour group G_f , where the representation ρ can be either irreducible or reducible. The residual symmetry $Z_2^{g_l} \times X_l$ of the charged lepton sector requires that $m_l^\dagger m_l$ is invariant under $Z_2^{g_l} \times X_l$, where m_l is the charged lepton mass matrix. Thus the unitary transformation U_l of the charged leptons should fulfill

$$U_l^\dagger \rho(g_l) U_l = \text{diag}(\pm 1, \pm 1, \pm 1), \quad U_l^\dagger X_l U_l^* = \text{diag}(e^{-i\alpha_e}, e^{-i\alpha_\mu}, e^{-i\alpha_\tau}) \equiv Q_l^{\dagger 2}, \quad (6.57)$$

where $Q_l = \text{diag}(e^{i\alpha_e/2}, e^{i\alpha_\mu/2}, e^{i\alpha_\tau/2})$ is a diagonal phase matrix with $\alpha_{e,\mu,\tau}$ real. Notice that the eigenvalue of $\rho(g_l)$ is +1 or -1 because the generator g_l is of order 2. The residual CP transformation X_l should be a symmetric matrix, otherwise the charged lepton masses would be partially degenerate. Likewise, for the neutrino sector we can perform the Takagi factorization for X_l as follows

$$X_l = \Sigma_l \Sigma_l^T, \quad \Sigma_l^\dagger \rho(g_l) \Sigma_l = \pm \text{diag}(1, -1, -1). \quad (6.58)$$

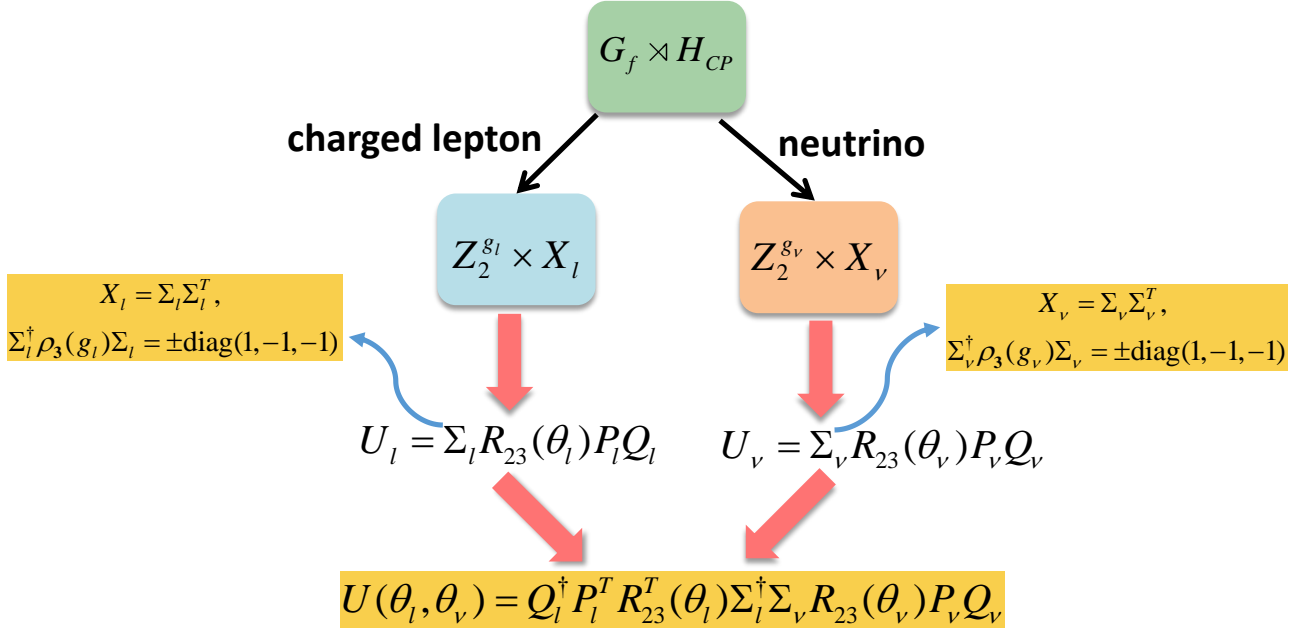


Figure 23: Model-independent predictions for the lepton mixing matrix when the residual symmetry has the structure $Z_2 \times CP$ in both neutrino and charged lepton sectors.

Then the residual symmetry constrains U_l to be

$$U_l = \Sigma_l R_{23}(\theta_l) P_l Q_l \quad (6.59)$$

where P_l is a generic three-dimensional permutation matrix, since the charged lepton masses are not predicted in this scheme. Hence the lepton mixing matrix is determined to be of the following form

$$U = U_l^\dagger U_nu = Q_l^\dagger P_l^T R_{23}^T(\theta_l) \Sigma_l^\dagger \Sigma_nu R_{23}(\theta_nu) P_nu Q_nu, \quad (6.60)$$

where the phase matrix Q_l can be absorbed into the charged lepton fields. In this scenario, the recipe for extracting the predicted lepton mixing matrix from the residual symmetry is summarized in figure 23. One sees that the resulting lepton mixing matrix only depends on two free rotation angles θ_l and θ_nu , lying in the range $0 \leq \theta_{l,\nu} < \pi$. The precisely measured reactor angle θ_{13} and the solar angle θ_{12} can be accommodated for certain values of θ_l and θ_nu , leading to relations for the other mixing parameters. Notice that in this scheme only one element of the mixing matrix is fixed to a constant value by the residual subgroups.

A comprehensive study of the lepton mixing patterns which can arise from the breaking of S_4 and CP symmetries into two distinct $Z_2 \times CP$ subgroups in the neutrino and charged lepton sectors leads to eighteen phenomenologically viable cases [395]. In the following, we give one typical example which predicts non-trivial CP violation phases. The three families of left-handed leptons are embedded in a triplet $\mathbf{3}$ of S_4 , and the residual symmetries of the neutrino and charged lepton mass matrices are $Z_2^{st^2su} \times X_l$ and $Z_2^s \times X_nu$ respectively, with $X_l = t^2$ and $X_nu = su$. The Takagi factorization Σ_l and Σ_nu are

found to be

$$\Sigma_l = \frac{1}{\sqrt{6}} \begin{pmatrix} 2 & 0 & -\sqrt{2} \\ e^{\frac{i\pi}{3}} & -\sqrt{3} e^{\frac{i\pi}{3}} & \sqrt{2} e^{\frac{i\pi}{3}} \\ e^{-\frac{i\pi}{3}} & \sqrt{3} e^{-\frac{i\pi}{3}} & \sqrt{2} e^{-\frac{i\pi}{3}} \end{pmatrix}, \quad \Sigma_\nu = \frac{1}{\sqrt{6}} \begin{pmatrix} \sqrt{2} i & 0 & -2 \\ \sqrt{2} i & -\sqrt{3} i & 1 \\ \sqrt{2} i & \sqrt{3} i & 1 \end{pmatrix} \quad (6.61)$$

The lepton mixing matrix can be easily obtained by using the master formula of Eq. (6.60), one of its elements is fixed to be $1/\sqrt{2}$. In order to be compatible with experimental data, the fixed element can be either the (23) or (33) entry, so that we can take the permutation matrices $(P_l, P_\nu) = (P_{12}, P_{13})$ or (P_{13}, P_{12}, P_{13}) . For the first case, $(P_l, P_\nu) = (P_{12}, P_{13})$, we find that the lepton mixing parameters are

$$\sin^2 \theta_{13} = \frac{1}{2} \cos^2 \theta_l, \quad \sin^2 \theta_{12} = \frac{1}{2} + \frac{(1 - 3 \cos 2\theta_l) \sin 2\theta_\nu}{6 - 2 \cos 2\theta_l}, \quad \sin^2 \theta_{23} = \frac{1}{2 - \cos^2 \theta_l}, \quad (6.62)$$

while the CP invariants are determined as

$$J_{CP} = \frac{\sin 2\theta_l \cos 2\theta_\nu}{8\sqrt{2}}, \quad I_1 = \frac{(2 \sin 2\theta_l - 3 \sin 4\theta_l) \cos 2\theta_\nu}{16\sqrt{2}}, \quad I_2 = \frac{\sin \theta_l \cos^3 \theta_l \cos 2\theta_\nu}{2\sqrt{2}}. \quad (6.63)$$

The Jarlskog invariant J_{CP} of neutrino oscillations is related to δ^ℓ in Eq. (1.22), while the other two invariants I_1 and I_2 are given in terms of the basic Majorana phases ϕ_{12}, ϕ_{13} involved in $0\nu\beta\beta$ decay, see section 1. One finds the following expressions [219, 411–413],

$$\begin{aligned} J_{CP} &= \text{Im}(U_{11}U_{33}U_{13}^*U_{31}^*) = \frac{1}{8} \sin 2\theta_{12} \sin 2\theta_{13} \sin 2\theta_{23} \cos \theta_{13} \sin \delta^\ell, \\ I_1 &= \text{Im}(U_{11}^{2*}U_{12}^2) = -\sin^2 \theta_{12} \cos^2 \theta_{12} \cos^4 \theta_{13} \sin 2\phi_{12}, \\ I_2 &= \text{Im}(U_{11}^{2*}U_{13}^2) = -\cos^2 \theta_{12} \cos^2 \theta_{13} \sin^2 \theta_{13} \sin 2\phi_{13}. \end{aligned} \quad (6.64)$$

The lepton mixing matrices corresponding to the two kinds of permutations $(P_l, P_\nu) = (P_{13}, P_{12}, P_{13})$ and $(P_l, P_\nu) = (P_{12}, P_{13})$ are related to each other by the exchange of the second and third rows. Thus the atmospheric angle θ_{23} and Dirac CP violation phase δ^ℓ become $\pi/2 - \theta_{23}$ and $\delta^\ell + \pi$ respectively, while the other mixing angles θ_{12}, θ_{13} and the Majorana CP phases ϕ_{12} and ϕ_{13} remain unchanged.

The results of the χ^2 analysis are presented in table 2. Moreover, a numerical analysis is performed, with both θ_l and θ_ν varying freely in the range of 0 to π , requiring all the three lepton mixing angles to lie in the experimental 3σ regions [24, 25]. In figure 24 we display the 3σ contour regions for $\sin^2 \theta_{12}$, $\sin^2 \theta_{13}$ and $\sin^2 \theta_{23}$, as well as their experimental best fit values in the $\theta_l - \theta_\nu$ plane. Dashed (solid) lines are the best fit mixing-angle values [24, 25]. Left (right) panels are for $(P_l, P_\nu) = (P_{12}, P_{13})$ and $(P_l, P_\nu) = (P_{13}, P_{12}, P_{13})$, respectively. One sees that the lepton mixing angles can be accommodated in the small regions around the best fit points.

In figure 25 we show the contour plots of the CP violation phases δ^ℓ, ϕ_{12} and ϕ_{13} in the plane θ_ν versus θ_l . The black areas denote the regions where the lepton mixing angles are compatible with oscillation data within 3σ . These will be testable at forthcoming long baseline neutrino oscillation experiments. Since all the lepton mixing angles and CP phases are predicted to lie in narrow regions, we also have tight predictions for the effective Majorana mass of neutrinoless double beta decay, as shown in figure 26.

	(P_l, P_ν)	χ^2_{\min}	$(\theta_l^{\text{bf}}, \theta_\nu^{\text{bf}})/\pi$	$\sin^2 \theta_{13}$	$\sin^2 \theta_{12}$	$\sin^2 \theta_{23}$	δ^ℓ/π	ϕ_{12}/π (mod 1/2)	ϕ_{13}/π (mod 1/2)
NO	(P_{12}, P_{13})	20.078	(0.433, 0.938)	0.022	0.318	0.511	0.539	0.397	0.468
			(0.567, 0.562)						
			(0.433, 0.562)				1.461	0.103	0.032
			(0.567, 0.938)						
	(P_{13}, P_{12}, P_{13})	37.057	(0.433, 0.938)	0.022	0.318	0.489	1.539	0.397	0.468
			(0.567, 0.562)						
			(0.433, 0.562)				0.461	0.103	0.032
			(0.567, 0.938)						
IO	(P_{12}, P_{13})	15.352	(0.432, 0.938)	0.022	0.318	0.511	0.539	0.396	0.468
			(0.568, 0.562)						
			(0.432, 0.562)				1.461	0.104	0.032
			(0.568, 0.938)						
	(P_{13}, P_{12}, P_{13})	27.629	(0.432, 0.938)	0.022	0.318	0.489	1.539	0.396	0.468
			(0.568, 0.562)						
			(0.432, 0.562)				0.461	0.104	0.032
			(0.568, 0.938)						

Table 2: χ^2 analysis for the residual symmetries $Z_2^{st^2su} \times X_l$ in the charged lepton sector and $Z_2^s \times X_\nu$ in the neutrino sector with $X_l = t^2$ and $X_\nu = su$. We give the best fit values θ_l^{bf} and θ_ν^{bf} for θ_l and θ_ν corresponding to χ^2_{\min} . We also list the mixing angles and CP violating phases at the best fit point.

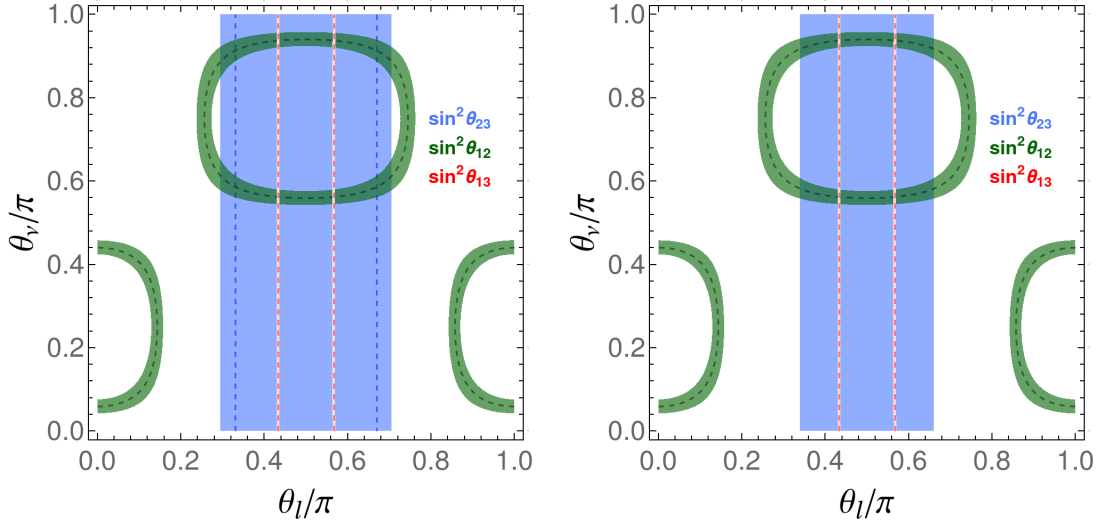


Figure 24: Contour plots of $\sin^2 \theta_{ij}$ in the plane θ_ν versus θ_l for the residual symmetries $Z_2^{st^2su} \times X_l$ in the charged lepton sector and $Z_2^s \times X_\nu$ in the neutrino sector with $X_l = t^2$ and $X_\nu = su$. The red, blue and green areas are the 3σ regions of $\sin^2 \theta_{13}$, $\sin^2 \theta_{23}$ and $\sin^2 \theta_{12}$ respectively. The dashed lines correspond to the best fit mixing angle values taken from [24, 25].

6.4 Quark and lepton mixing from a common flavour group

Discrete flavour symmetries are particularly suitable to account for the large lepton mixing angles. As discussed in [259, 263, 270, 278–281] they can also address the quark mixing pattern. Assuming that the flavour group of quarks is broken down to different residual subgroups in the up- and down-quark sectors, only the Cabibbo mixing between the first two quark families can be generated with only flavour symmetry [263, 270, 278, 280, 281]. It is remarkable that the hierarchical quark mixing angles and CP

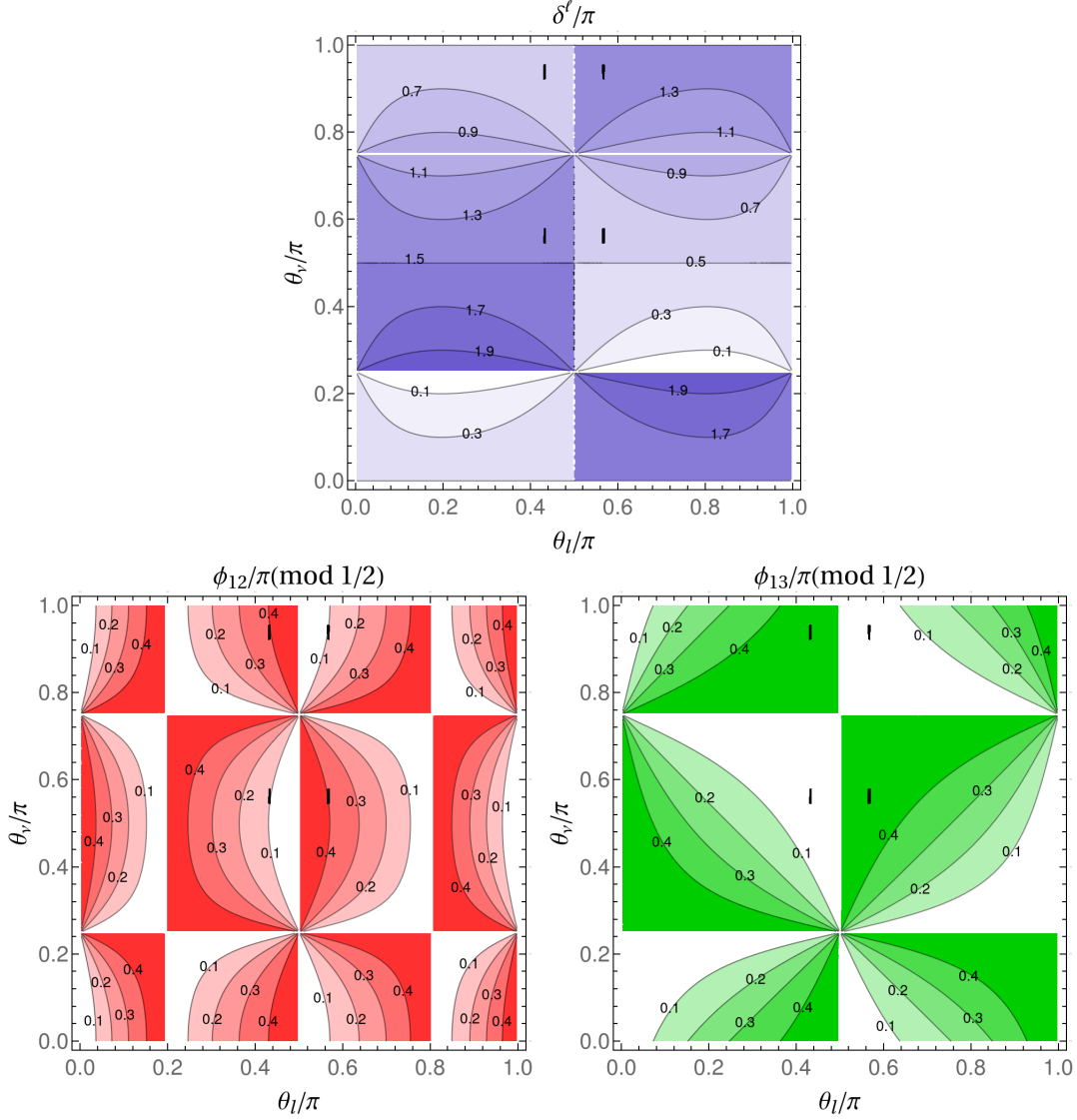


Figure 25: Contour plots of the CP violation phases δ^ℓ , ϕ_{12} and ϕ_{13} in the $\theta_l - \theta_\nu$ plane, where the residual symmetries are $Z_2^{st^2su} \times X_l$ in the charged lepton sector and $Z_2^s \times X_\nu$ in the neutrino sector with $X_l = t^2$ and $X_\nu = su$. In the black areas all three lepton mixing angles lie within their experimental 3σ ranges. Here we choose the row and column permutations $(P_l, P_\nu) = (P_{12}, P_{13})$, the Dirac CP phase δ^ℓ changes to $\delta^\ell + \pi$ while the Majorana phases ϕ_{12} and ϕ_{13} are invariant for $(P_l, P_\nu) = (P_{13}, P_{12}, P_{13})$.

violation can be explained if the flavour symmetry is extended with CP symmetry and the residual subgroups of the up- and down-quark sectors are $Z_2^{g_u} \times X_u$ and $Z_2^{g_d} \times X_d$ respectively [282, 284], where both CP transformations X_u and X_d are unitary and symmetric. The diagonalization matrices U_u and U_d would be restricted to be of the following form

$$U_u = \Sigma_u R_{23}(\theta_u) P_u Q_u, \quad U_d = \Sigma_d R_{23}(\theta_d) P_d Q_d \quad (6.65)$$

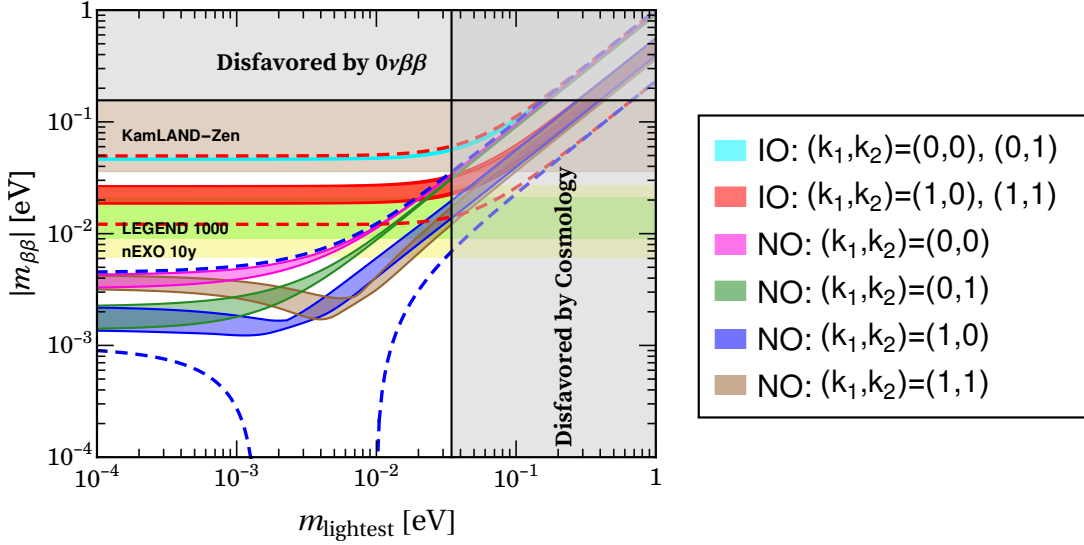


Figure 26: The effective Majorana neutrino mass $m_{\beta\beta}$ versus the lightest neutrino mass, for residual symmetries $Z_2^{st^2 su} \times X_l$ in the charged lepton and $Z_2^s \times X_\nu$ in the neutrino sector, with $X_l = t^2$ and $X_\nu = su$. Here we adopt the same convention for the different bands as used in figure 22.

where $P_{u,d}$ are three dimensional permutation matrices, $Q_{u,d}$ are generic phase matrices, and $\Sigma_{u,d}$ are the Takagi factorizations of $X_{u,d}$, fulfilling

$$\begin{aligned} X_u &= \Sigma_u \Sigma_u^T, & \Sigma_u^\dagger \rho(g_u) \Sigma_u &= \pm \text{diag}(1, -1, -1), \\ X_d &= \Sigma_d \Sigma_d^T, & \Sigma_d^\dagger \rho(g_d) \Sigma_d &= \pm \text{diag}(1, -1, -1). \end{aligned} \quad (6.66)$$

As a consequence, the CKM mixing matrix is predicted as

$$V_{CKM} = U_u^\dagger U_d = Q_u^\dagger P_u^T R_{23}^T(\theta_u) \Sigma_u^\dagger \Sigma_d R_{23}(\theta_d) P_d Q_d, \quad (6.67)$$

which only depends on two free rotation angles θ_u and θ_d , limited in the range $0 \leq \theta_{u,d} < \pi$. Notice that both Q_u and Q_d are unphysical, as they can be absorbed into quark fields. We take the flavour symmetry as the dihedral group D_n which has only one- and two-dimensional irreducible representations, as shown in C.

Since the top quark is much heavier than the others, the first two families of left-handed quarks are assigned to a doublet of D_n , while the third generation is a D_n singlet. Without loss of generality, we can take

$$\begin{pmatrix} Q_1 \\ Q_2 \end{pmatrix} \sim \mathbf{2}_1, \quad Q_3 \sim \mathbf{1}_1, \quad (6.68)$$

where $Q_1 \equiv (u_L, d_L)^T$, $Q_2 \equiv (c_L, s_L)^T$, and $Q_3 \equiv (t_L, b_L)^T$. The dihedral group and CP symmetry are broken down to $Z_2^{SR^{z_u}} \times X_u$ in up-quark sector and $Z_2^{SR^{z_d}} \times X_d$ in down-quark sector with $X_u = R^{-z_u + x_u}$ and $X_d = R^{-z_d + x_d}$, where $z_u, z_d = 0, 1, \dots, n-1$, $x_u = x_d = 0$ for odd n and $x_u, x_d = 0, n/2$ if the group

index n is even. The Takagi factorization of the residual symmetry $Z_2^{SR^z} \times R^{-z+x}$ is determined to be

$$\Sigma = \frac{i^{2x/n}}{\sqrt{2}} \begin{pmatrix} -e^{-\frac{i\pi z}{n}} & 0 & e^{-\frac{i\pi z}{n}} \\ e^{\frac{i\pi z}{n}} & 0 & e^{\frac{i\pi z}{n}} \\ 0 & \sqrt{2} i^{-2x/n} & 0 \end{pmatrix}. \quad (6.69)$$

From our master formula in Eq. (6.67), we find that the quark mixing matrix takes the following form,

$$V_{CKM} = \begin{pmatrix} \cos \varphi_1 & -c_d \sin \varphi_1 & s_d \sin \varphi_1 \\ c_u \sin \varphi_1 & s_d s_u e^{i\varphi_2} + c_d c_u \cos \varphi_1 & c_d s_u e^{i\varphi_2} - s_d c_u \cos \varphi_1 \\ -s_u \sin \varphi_1 & s_d c_u e^{i\varphi_2} - c_d s_u \cos \varphi_1 & c_d c_u e^{i\varphi_2} + s_d s_u \cos \varphi_1 \end{pmatrix}, \quad (6.70)$$

up to row and column permutations with

$$\varphi_1 = \frac{(z_u - z_d)\pi}{n}, \quad \varphi_2 = \frac{(x_u - x_d)\pi}{n} \quad (6.71)$$

and $c_d \equiv \cos \theta_d$, $s_d \equiv \sin \theta_d$, $c_u \equiv \cos \theta_u$, $s_u \equiv \sin \theta_u$. The parameters φ_1 and φ_2 depend on the choice of residual symmetry, and they can take the following discrete values

$$\begin{aligned} \varphi_1 \pmod{2\pi} &= 0, \frac{1}{n}\pi, \frac{2}{n}\pi, \dots, \frac{2n-1}{n}\pi, \\ \varphi_2 \pmod{2\pi} &= 0, \frac{1}{2}\pi, \frac{3}{2}\pi. \end{aligned} \quad (6.72)$$

One can straightforwardly extract the quark mixing parameters from Eq. (6.70). Eliminating the free parameters θ_u and θ_d , one obtains the following correlations among the quark mixing angles and CP phase [284],

$$\cos^2 \theta_{13}^q \cos^2 \theta_{12}^q = \cos^2 \varphi_1, \quad \sin \delta^q \simeq \frac{\sin 2\varphi_1 \sin \varphi_2}{\sin 2\theta_{12}^q \cos^2 \theta_{13}^q \cos \theta_{23}^q}. \quad (6.73)$$

The experimental data on the CKM matrix can be well accommodated for $\varphi_1 = \pi/14$, $\varphi_2 = \pi/2$, which can be achieved from the D_{14} flavour group with the residual symmetry indices $z_u = 1$, $z_d = 0$, $x_u = 7$, $x_d = 0$. The best-fit values of $\theta_{u,d}$ and mixing parameters are determined to be,

$$\begin{aligned} \theta_u &= 0.01237\pi, & \theta_d &= 0.99473\pi, & \sin \theta_{12}^q &= 0.22249, \\ \sin \theta_{13}^q &= 0.00369, & \sin \theta_{23}^q &= 0.04206, & J_{CP}^q &= 3.104 \times 10^{-5}. \end{aligned} \quad (6.74)$$

Notice that $\sin \theta_{13}^q$, $\sin \theta_{23}^q$ and J_{CP}^q are consistent with the global fit results of the UTfit collaboration [101]. The mixing angle $\sin \theta_{12}^q$ is about 1% smaller than its measured value, so that higher-order corrections in a concrete model are needed to reconcile it with the data.

The D_{14} flavour group can also explain the lepton flavour structure if it is broken down to $Z_2^{SR^{z_l}} \times X_l$ and $Z_2^{SR^{z_\nu}} \times X_\nu$ in the charged lepton and neutrino sector, respectively, where $X_l = R^{-z_l+x_l}$, $X_\nu = R^{-z_\nu+x_\nu}$ with $z_{l,\nu} = 0, 1, \dots, 13$ and $x_{l,\nu} = 0, 7$. The lepton mixing matrix has the same form as Eq. (6.70), the rotation angles θ_u and θ_d should be replaced with θ_l and θ_ν respectively. Choosing the residual

symmetry indices $z_l = 4$, $z_\nu = 0$, $x_l = 7$ and $x_\nu = 0$, we have $\varphi_1 = 2\pi/7$ and $\varphi_2 = \pi/2$. Choosing the permutations as $P_l = P_{12}P_{23}$ and $P_\nu = P_{13}$, the lepton mixing angles can be accommodated for certain values of the free parameters $\theta_{l,\nu}$:

$$\begin{aligned} \theta_e^{\text{bf}} &= 0.439\pi, \quad \theta_\nu^{\text{bf}} = 0.811\pi, \quad \chi_{\text{min}}^2 = 4.147, \quad \sin^2 \theta_{13} = 0.0220, \quad \sin^2 \theta_{12} = 0.318, \\ \sin^2 \theta_{23} &= 0.603, \quad \delta^\ell/\pi = 1.530, \quad \phi_{12}/\pi = -0.082 \pmod{1/2}, \quad \phi_{13}/\pi = 1.474 \pmod{1/2}. \end{aligned} \quad (6.75)$$

In summary, one sees how the dihedral group as well as the residual symmetry $Z_2 \times CP$ provide an interesting opportunity for model building. Indeed, we saw how the D_{14} flavour symmetry can provide a unified description of flavour mixing for both quarks and leptons.

If both left-handed quarks and leptons are assigned as irreducible triplets of the flavour symmetry and the residual symmetry is $Z_2 \times CP$, one finds that $\Delta(294)$ is the minimal flavour group that can generate realistic quark and lepton flavour mixing patterns [283]. In contrast, the singlet plus doublet assignment seems better than the triplet assignment. Once the CP symmetry is included, the order of the flavour symmetry group can be reduced considerably, i.e. 28 versus 294 in this scheme.

There are also other schemes to explain the mixing patterns of quarks and leptons using flavour and CP symmetries. For instance, quark and lepton mixing patterns can arise from the stepwise breaking of these symmetries to different residual subgroups in different sectors of the theory [285, 286], with charged fermion mass hierarchies generated by operators with different numbers of flavons. For a concrete model with $\Delta(384)$ flavour symmetry see [286].

6.5 Geometrical CP violation

It is well-known that CP symmetry is broken by complex Yukawa couplings in the SM, which leads to the CP violation in charged current interactions through the CKM matrix. However, the origin of CP violation is still a mystery. Analogous to the electroweak symmetry, the CP symmetry could be spontaneously broken by the VEVs of some scalar fields [414]. In models of spontaneous CP violation, the Lagrangian is invariant under the CP symmetry so that all parameters of the scalar potential are real in a certain basis. Spontaneous CP violation is achieved through complex VEVs for the Higgs multiplets which also break the gauge symmetry. Usually the phases of the fields depend on the coupling constants in the scalar potential.

The phases of the Higgs multiplets could have geometrical values, independently of the potential parameters if there is an additional (accidental) CP symmetry of the potential. The resulting CP breaking vacua lead to the so-called geometrical CP violation or calculable phases [415]. It has been shown that more than two Higgs doublets and non-abelian symmetry relating the Higgs multiplets are necessary conditions in order to realize the geometrical CP violation. It turns out that $\Delta(27)$ and $\Delta(54)$ are the smallest groups which lead to calculable phases [415, 416].

If one assigns three Higgs doublets $H \equiv (H_1, H_2, H_3)$ to a triplet of $\Delta(27)$ or $\Delta(54)$, the scalar potential

has only one relevant phase dependent term, i.e.

$$V = V_0 + \left[\lambda_4 \sum_{i \neq j \neq k} (H_i^\dagger H_j)(H_i^\dagger H_k) + \text{h.c.} \right]. \quad (6.76)$$

The traditional CP transformation $H_i \xrightarrow{CP} H_i^*$ forces the coupling λ_4 to be real. Then one can obtain the following two possible vacua with calculable phases [415]

$$\begin{aligned} \langle H \rangle &= \frac{v}{\sqrt{3}} \begin{pmatrix} 1 \\ \omega \\ \omega^2 \end{pmatrix}, & \lambda_4 < 0, \\ \langle H \rangle &= \frac{v}{\sqrt{3}} \begin{pmatrix} \omega^2 \\ 1 \\ 1 \end{pmatrix}, & \lambda_4 > 0. \end{aligned} \quad (6.77)$$

The same scalar potential as Eq. (6.76) and calculable phases in Eq. (6.77) can be obtained from other non-abelian symmetry groups such as $\Delta(3n^2)$ [417] and $\Delta(6n^2)$ [418], where n is a multiple of 3.

The observed fermion masses and flavor mixings could possibly be accommodated if one properly assigns the transformations of fermion fields under the symmetry group [416]. In short, the geometrical CP violation arises from the correct interplay among the scalar content, non-abelian symmetry group and CP symmetry.

7 Testing flavor and CP symmetries

As shown above, discrete flavor and generalized CP symmetries allow us to predict the lepton mixing matrix in terms of few parameters. Eliminating free parameters generally leads to correlations among the lepton mixing angles and CP violation phases. Such predictions are often called lepton mixing *sum rules* in the literature, though they are not always strictly so. For example, for the residual symmetry $\mathcal{G}_l = Z_n$ ($n \geq 3$), $\mathcal{G}_\nu = Z_2 \times CP$ discussed in section 6.3.1, the lepton mixing matrix depends on a unique real parameter θ , as shown in Eq. (6.41). The parameter θ becomes determined in terms of the precisely measured reactor mixing angle θ_{13} , leading to sharp predictions for the leptonic mixing angles and CP violation phases that can be tested at current and future neutrino oscillation experiments.

Ultimately they could be used to distinguish different symmetry-based flavor models. It is remarkable that, besides the mixing angles, flavor symmetry in combination with generalized CP symmetry allows us to predict both the Dirac and Majorana leptonic CP violation phases. Hence the effective neutrino mass $|m_{\beta\beta}|$ is constrained to lie within narrow regions, as can be seen from figures 22 and 26.

As a result one could also test flavor and CP symmetries by confronting with the data of the current and forthcoming $0\nu\beta\beta$ experiments. In fact, some flavor models relate the Majorana phases to the neutrino masses, which could also lead to restrictions on the effective mass $|m_{\beta\beta}|$, and a very powerful tool to test and discriminate flavour models.

7.1 Testing mixing predictions

Neutrino physics has entered the precision era, providing a good opportunity for probing different flavor models. The reactor angle θ_{13} is the best-measured leptonic mixing parameter. The precise measurement of nonzero θ_{13} by Daya Bay [21, 419], Double Chooz [420, 421], and RENO [22, 422] has excluded many flavor models predicting θ_{13} close to zero. The long baseline neutrino oscillation experiments NO ν A [423] and T2K [424] give measurements of the leptonic mixing angle θ_{23} and also the first hint of leptonic CP violation [425–427] associated to the leptonic Dirac CP violation phase δ_{CP} . However, the value of δ_{CP} has not been significantly constrained by neutrino oscillation experiments. The latest data of T2K favor near-maximal Dirac CP violation phase, the atmospheric mixing angle $\theta_{23} > 45^\circ$ and normal mass ordering [428]. The data of T2K constrain the CP phase δ_{CP} in the range $\delta_{CP} = -1.97^{+0.97}_{-0.70}$, and $\delta_{CP} = 0, \pi$ is excluded at more than 90% confidence level [428]. In comparison with T2K, the data of NO ν A exclude the CP phase in the vicinity of $\delta_{CP} = \pi/2$ at more than 3σ for the inverted mass ordering, and the values around $\delta_{CP} = 3\pi/2$ in the normal ordering are disfavored at 2σ confidence [429]. Improved CP measurements constitute the target of upcoming experiments such as DUNE. The future long baseline neutrino oscillation experiments DUNE [113, 430] and T2HK [431] should measure θ_{23} and δ_{CP} with very good precision. It is expected that DUNE can observe the signal of lepton CP violation with 5σ significance after about 7 years if $\delta_{CP} = -\pi/2$ and after about 10 years for 50% of δ_{CP} values, and CP violation can be observed with 3σ significance for 75% of δ_{CP} values after about 13 years of running [113, 430]. T2HK has shown that it can expect a discovery of CP violation over 76%(58%) of the parameter space at $3\sigma(5\sigma)$ [431]. The forthcoming medium baseline reactor neutrino experiment JUNO

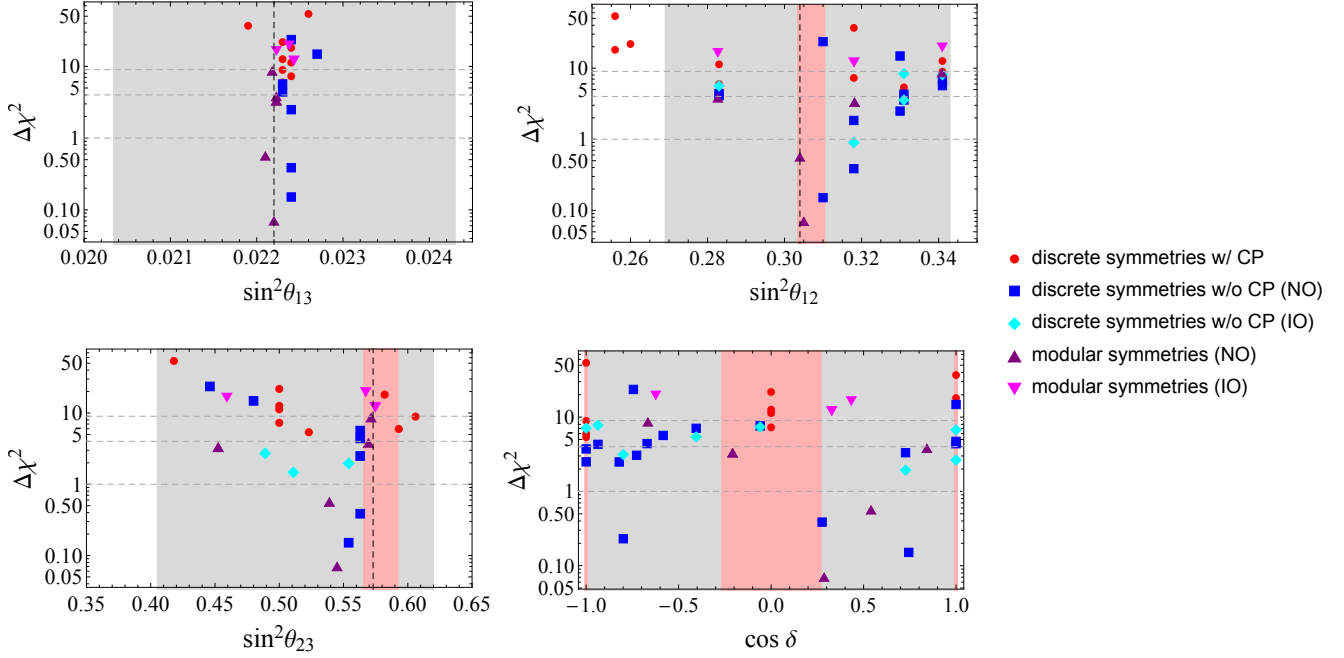


Figure 27: Best-fit predictions of the models based on discrete symmetries broken to certain residual symmetries of the lepton mass matrices [432, 433], and the models based on modular symmetries discussed in [434–436]. The gray regions are the 3σ ranges and the dashed line is the best fit value for normal-ordered neutrino masses. The red band in the panel of $\sin^2\theta_{12}$ is the prospective 3σ range after 6 years of JUNO running [115], and the red regions in the panels of $\sin^2\theta_{23}$ and $\cos\delta$ are the prospective 3σ ranges after 15 years of DUNE running [430]. This figure is taken from [437].

can make very precise measurement of the solar angle θ_{12} , and the error of $\sin^2\theta_{12}$ can be reduced to the level of 0.5% – 0.7% [115].

We show in figure 27 the best fit predictions for the mixing parameters in some typical models based on discrete flavor symmetry with or without generalized CP symmetry and modular symmetry. We see that the synergy between JUNO and long baseline neutrino experiments DUNE and T2HK will be extremely powerful for testing the huge number of flavor symmetry models.

As an illustration, we give an extensively discussed prediction for lepton mixing angles as follows [438, 439],

$$\cos\delta_{CP} = \frac{\tan\theta_{23}}{\sin 2\theta_{12} \sin\theta_{13}} [\cos 2\theta'_{12} + (\sin^2\theta_{12} - \cos^2\theta'_{12}) (1 - \cot^2\theta_{23} \sin^2\theta_{13})], \quad (7.1)$$

which generally arises when considering charged-lepton corrections to neutrino mixing matrices which are completely fixed by symmetry with the neutrino angle $\theta'_{13} = 0$ and charged lepton rotation angle $\theta^e_{13} = 0$. This prediction gives $\cos\delta_{CP}$ as a function of the measured lepton mixing angles and one fixed parameter θ'_{12} determined by the underlying discrete symmetry. It is noticeable that Eq. (7.1) is specified by fixing the value of just one parameter, the angle θ'_{12} . Thus one can enumerate the viable models of this type by deriving the values of θ'_{12} from symmetry considerations. This leads us the following well-motivated sum rules characterized by specific values of θ'_{12} , namely the one based on TBM mixing with

	Ranges of δ_{CP} obtained by varying			
	θ_{12} in 3σ	θ_{23} in 3σ	θ_{13} in 3σ	$\theta_{12}\&\theta_{23}\&\theta_{13}$ in 3σ
TBM	$\pm[240.54^\circ, 289.19^\circ]$	$\pm[264.58^\circ, 268.06^\circ]$	$\pm[264.86^\circ, 265.89^\circ]$	$\pm[235.27^\circ, 291.21^\circ]$
GRA	$\pm[271.01^\circ, 322.93^\circ]$	$\pm[289.72^\circ, 295.36^\circ]$	$\pm[292.95^\circ, 294.82^\circ]$	$\pm[270.22^\circ, 332.89^\circ]$
GRB	$\pm[233.08^\circ, 283.21^\circ]$	$\pm[258.11^\circ, 263.51^\circ]$	$\pm[258.57^\circ, 260.20^\circ]$	$\pm[226.19^\circ, 284.41^\circ]$
HG	$\pm[284.70^\circ, 360^\circ]$	$\pm[300.64^\circ, 312.11^\circ]$	$\pm[307.15^\circ, 310.98^\circ]$	$\pm[283.21^\circ, 360^\circ]$

Table 3: The prediction of the sum rule Eq. (7.1) for the allowed ranges of $|\delta_{CP}|$ due to the present 3σ uncertainties in the values of the neutrino mixing angles. Here we vary at least one lepton mixing angle in its corresponding 3σ intervals for the NO spectrum [24].

$\theta_{12}^\nu = \arcsin(1/\sqrt{3}) \approx 35.26^\circ$ [296–298], the one based on BM mixing with $\theta_{12}^\nu = 45^\circ$ [333], the one based on the type A golden ratio mixing (GRA) with $\theta_{12}^\nu = \arctan(1/\phi_g) \approx 31.72^\circ$ [328, 329], the one based on the type B golden ratio mixing (GRB) with $\theta_{12}^\nu = \arccos(\phi_g/2) = 36^\circ$ [326, 327], and the one based on hexagonal (HEX) mixing with $\theta_{12}^\nu = 30^\circ$ [317, 440].

Using the sum rule of Eq. (7.1) and plugging into the best fit values of the neutrino mixing angles for NO [24], one can straightforwardly determine the value of $\cos \delta_{CP}$ and the CP phase δ_{CP} for the above mentioned values of θ_{12}^ν ,

$$\begin{aligned}
\text{TBM : } & \cos \delta_{CP} \approx -0.08, \quad \delta_{CP} \approx \pm 94.65^\circ, \\
\text{GRA : } & \cos \delta_{CP} \approx 0.41, \quad \delta_{CP} \approx \pm 66.09^\circ, \\
\text{GRB : } & \cos \delta_{CP} \approx -0.18, \quad \delta_{CP} \approx \pm 100.65^\circ, \\
\text{HG : } & \cos \delta_{CP} \approx 0.63, \quad \delta_{CP} \approx \pm 50.90^\circ,
\end{aligned} \tag{7.2}$$

Notice that there are two values of δ_{CP} of opposite sign for each value of $\cos \delta_{CP}$. The sum rule of Eq. (7.1) for the BM case, $\theta_{12}^\nu = 45^\circ$, is not compatible with the current best fit values of the lepton mixing angles [24], and will be dropped hereafter. We also take into account the experimental uncertainties of the three lepton mixing angles by varying θ_{12} , θ_{23} , and θ_{13} in their 3σ experimentally allowed regions. The ranges of the CP violation δ_{CP} obtained from Eq. (7.1) are summarized in table 3. We see that out of all mixing angles, the 3σ allowed range of θ_{12} causes the largest uncertainty in δ_{CP} resulting from Eq. (7.1).

Future long baseline experiments DUNE and T2HK will be able to make precision measurement of δ_{CP} and θ_{23} . The combination of DUNE and T2HK provides better sensitivity to δ_{CP} than either of these two experiments in isolation. The prospective DUNE+T2HK data should allow one to test the predictions for $\cos \delta_{CP}$, as shown in figure 28. Given the 3σ range $\delta_{CP} \in [127.80^\circ, 358.20^\circ]$ of the Dirac phase δ_{CP} from the latest global analysis [24], only δ_{CP} values in the interval of 180° to 360° are considered in figure 28. We see that a significant part of the true value of δ_{CP} gets disfavoured at more than 3σ for each symmetry predicted value of the angle θ_{12}^ν . Furthermore, detailed analysis showed that future facilities DUNE and T2HK in combination with JUNO could distinguish the different cases of θ_{12}^ν [439, 441].

In summary, the existence of mixing predictions is a characteristic feature of flavor symmetry models, as explicitly shown in Eqs. (5.12, 5.18, 5.24, 6.9, 6.22, 6.47, 6.51, 6.54, 6.73). These relations highlight

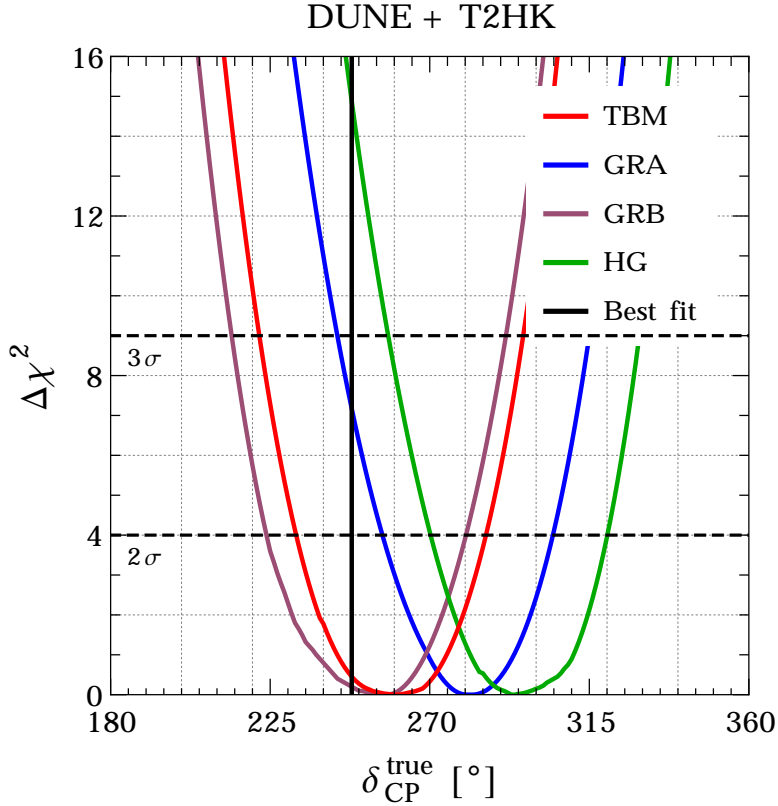


Figure 28: Compatibility of the prediction in Eq. (7.1) with any potentially true value of the Dirac CP phase δ_{CP} in the range $\delta_{CP} \in [180^\circ, 360^\circ]$. Four values of θ'_{12} are considered: $\theta'_{12} = \arcsin(1/\sqrt{3}) \approx 35.26^\circ$ for TBM, $\theta'_{12} = \arctan(1/\phi_g) \approx 31.72^\circ$ for GRA, $\theta'_{12} = 36^\circ$ for GRB, and $\theta'_{12} = 30^\circ$ for HG. From [441].

the testability of flavor symmetry, and there are many other possible relations among the lepton mixing parameters in the literature [355, 438, 439, 442–445]. The phenomenological implications of these sum rules and the prospects of testing them at precision neutrino facilities have been extensively discussed [433, 439, 441, 444, 446, 447].

7.2 Testing mass sum rules

The neutrino mass matrix leading to the three neutrino masses in discrete flavor symmetry models typically involves a reduced set of parameters. Indeed, several discrete flavor-symmetry-based models yield a constrained neutrino mass matrix, leading to specific neutrino mass sum-rules. This in turn is phenomenologically interesting, as it can lead to predictions for the effective neutrinoless double beta mass parameter [141]. For example, one can have a $0\nu\beta\beta$ lower bound on even for normal ordered neutrino spectrum [142].

If the light neutrino mass matrix depends on two complex parameters [448] one can extract a relation between the three complex neutrino mass eigenvalues, leading to a neutrino mass sum rule. Typically neutrino mass sum rules can arise from any neutrino mass generation mechanism in which the structure of the mass matrix is generated by two flavons. Prime examples neutrino mass sum rules are $2\tilde{m}_2 + \tilde{m}_3 = \tilde{m}_1$ and $2\tilde{m}_2^{-1} + \tilde{m}_3^{-1} = \tilde{m}_1^{-1}$ predicted by early A_4 models [70, 313, 449]. For systematic categorisation and

consequences of neutrino mass sum rules in beta decay, $0\nu\beta\beta$ decay and cosmology see Refs. [141,450–453]. A sample of the flavor models in the literature, includes the following twelve different neutrino mass sum rules [451]:

$$\begin{aligned}
\tilde{m}_1 + \tilde{m}_2 &= \tilde{m}_3, & \tilde{m}_1 + \tilde{m}_3 &= 2\tilde{m}_2, \\
2\tilde{m}_2 + \tilde{m}_3 &= \tilde{m}_1, & \tilde{m}_1 + \tilde{m}_2 &= 2\tilde{m}_3, \\
\tilde{m}_1 + \frac{\sqrt{3}+1}{2}\tilde{m}_3 &= \frac{\sqrt{3}-1}{2}\tilde{m}_2, & \tilde{m}_1^{-1} + \tilde{m}_2^{-1} &= \tilde{m}_3^{-1}, \\
2\tilde{m}_2^{-1} + \tilde{m}_3^{-1} &= \tilde{m}_1^{-1}, & \tilde{m}_1^{-1} + \tilde{m}_3^{-1} &= 2\tilde{m}_2^{-1}, \\
\tilde{m}_3^{-1} \pm 2i\tilde{m}_2^{-1} &= \tilde{m}_1^{-1}, & \tilde{m}_1^{1/2} - \tilde{m}_3^{1/2} &= 2\tilde{m}_2^{1/2}, \\
\tilde{m}_1^{1/2} + \tilde{m}_3^{1/2} &= 2\tilde{m}_2^{1/2}, & \tilde{m}_1^{-1/2} + \tilde{m}_2^{-1/2} &= 2\tilde{m}_3^{-1/2}, \tag{7.3}
\end{aligned}$$

where \tilde{m}_i stand for the complex neutrino mass eigenvalues, which can be expressed in terms of the Majorana phases $\phi_i \in [0, 2\pi)$ and the physical mass eigenvalues $m_i \geq 0$ as $\tilde{m}_i = m_i e^{-i\phi_i}$ with ϕ_3 chosen to be unphysical. These sum rules appeared in models based on A_4 , S_4 , A_5 , T' , T_7 , $\Delta(54)$ and $\Delta(96)$ flavor symmetry, when the three neutrino mass eigenvalues can be described by two model parameters only, see Ref. [451] for a very good discussion and references on models predicting these sum rules. In addition, five new mass sum rules have been identified in flavor models based on modular symmetries with residual symmetries [434]. From Eq. (7.3) one sees that all neutrino mass sum rules can be parametrized in the following manner [451, 452]:

$$c_1 \left(m_1 e^{-i\phi_1}\right)^d e^{i\Delta\chi_{13}} + c_2 \left(m_2 e^{-i\phi_2}\right)^d e^{i\Delta\chi_{23}} + m_3^d = 0, \tag{7.4}$$

with $c_1, c_2 > 0$, where ϕ_1 and ϕ_2 are the Majorana phases. The parameters c_1 , c_2 , d , $\Delta\chi_{13}$, and $\Delta\chi_{23}$ characterize the sum rule, and they can be straightforwardly read out for any of the above twelve known sum rules. Interpreting the complex numbers as vectors in the complex plane, the neutrino mass sum rule can be geometrically understood as a sum of three vectors which form a triangle in the complex plane [450]. Since the sum rule in Eq. (7.4) is a complex equation, it requires both real part and imaginary parts to be vanishing, i.e.,

$$\begin{aligned}
c_1 m_1^d \cos \beta + c_2 m_2^d \cos \alpha + m_3^d &= 0, \\
c_1 m_1^d \sin \beta + c_2 m_2^d \sin \alpha &= 0, \tag{7.5}
\end{aligned}$$

with the angles $\alpha \equiv -d\phi_2 + \Delta\chi_{23}$ and $\beta \equiv -d\phi_1 + \Delta\chi_{13}$. Eq. (7.5) allows to express α and β in terms of the parameters of the sum rule,

$$\cos \alpha = \frac{c_1^2 m_1^{2d} - c_2^2 m_2^{2d} - m_3^{2d}}{2c_2 m_2^d m_3^d}, \quad \cos \beta = \frac{c_2^2 m_2^{2d} - c_1^2 m_1^{2d} - m_3^{2d}}{2c_1 m_1^d m_3^d},$$

$$\begin{aligned}
\sin \alpha &= \pm \frac{\sqrt{4c_2^2 m_2^{2d} m_3^{2d} - (c_1^2 m_1^{2d} - c_2^2 m_2^{2d} - m_3^{2d})^2}}{2c_2 m_2^d m_3^d}, \\
\sin \beta &= \mp \frac{\sqrt{4c_2^2 m_2^{2d} m_3^{2d} - (c_1^2 m_1^{2d} - c_2^2 m_2^{2d} - m_3^{2d})^2}}{2c_1 m_1^d m_3^d},
\end{aligned} \tag{7.6}$$

which relate Majorana CP phases with light neutrino masses. Given that $|\cos \alpha| \leq 1$, $|\sin \alpha| \leq 1$, $|\cos \beta| \leq 1$ and $|\sin \beta| \leq 1$, it follows that the validity of the sum rule requires the three neutrino masses to satisfy the following triangle inequalities,

$$\begin{aligned}
|c_1 m_1^d e^{i\beta}| &\leq |c_2 m_2^d e^{i\alpha}| + |c_3 m_3^d|, \\
\text{and } |c_2 m_2^d e^{i\alpha}| &\leq |c_1 m_1^d e^{i\beta}| + |c_3 m_3^d|, \\
\text{and } |c_3 m_3^d| &\leq |c_1 m_1^d e^{i\beta}| + |c_2 m_2^d e^{i\alpha}|,
\end{aligned} \tag{7.7}$$

which implies a triangle formed out of the three vectors $c_1 m_1^d e^{i\beta}$, $c_2 m_2^d e^{i\alpha}$ and $c_3 m_3^d$ in the complex plane. Given the solar and atmospheric neutrino mass squared differences $\Delta m_{\text{sol}}^2 \equiv m_2^2 - m_1^2 = 7.50_{-0.20}^{+0.22} \times 10^{-5} \text{ eV}^2$ and $\Delta m_{\text{atm}}^2 \equiv |m_3^2 - m_1^2| = 2.55 (2.45)_{-0.03}^{+0.02} \times 10^{-3} \text{ eV}^2$ [24] for NO (IO), the light neutrino masses are related to the smallest mass m_1 (m_3) as follows,

$$\begin{aligned}
\text{NO : } m_2 &= \sqrt{\Delta m_{\text{sol}}^2 + m_1^2}, \quad m_3 = \sqrt{\Delta m_{\text{atm}}^2 + m_1^2}, \\
\text{IO : } m_1 &= \sqrt{\Delta m_{\text{atm}}^2 + m_3^2}, \quad m_2 = \sqrt{\Delta m_{\text{atm}}^2 + \Delta m_{\text{sol}}^2 + m_3^2}.
\end{aligned} \tag{7.8}$$

Thus mass rules usually lead to a lower limit on the lightest neutrino mass through the triangle inequalities in Eq. (7.7), and some sum rules may only allow for a certain mass ordering. For instance, neutrino masses can only be normal ordered for the sum rule $2\tilde{m}_2 + \tilde{m}_3 = \tilde{m}_1$ since the triangle inequality $m_3 + m_1 \geq 2m_2$ cannot be fulfilled for IO. Solving the inequality $m_3 \leq m_1 + 2m_2$ in the case of NO, one obtain the lower limit on m_1 ,

$$m_1 \geq \sqrt{\frac{\Delta m_{\text{atm}}^2}{8}} (1 - 3r) \simeq 0.016 \text{ eV}, \tag{7.9}$$

where the exact result has been expanded in terms of the small ratio $r \equiv \Delta m_{\text{sol}}^2 / \Delta m_{\text{atm}}^2$. Another benchmark sum rule $2\tilde{m}_2^{-1} + \tilde{m}_3^{-1} = \tilde{m}_1^{-1}$ works for both mass orderings, and the limits on the lightest neutrino mass from the triangle inequalities are found to be

$$\begin{aligned}
\text{NO : } 0.0043 \text{ eV} &\simeq \sqrt{\frac{\Delta m_{\text{sol}}^2}{3}} \left(1 - \frac{4\sqrt{3}r}{9}\right) \leq m_1 \leq \sqrt{\frac{\Delta m_{\text{sol}}^2}{3}} \left(1 + \frac{4\sqrt{3}r}{9}\right) \simeq 0.0057 \text{ eV}, \\
\text{IO : } m_3 &\geq \sqrt{\frac{\Delta m_{\text{atm}}^2}{8}} \left(1 + \frac{r}{3}\right) \simeq 0.018 \text{ eV}.
\end{aligned} \tag{7.10}$$

One sees that certain mass sum rules predict a value of the lightest neutrino mass close to the current upper limit from cosmology and therefore they could be probed in the near future. Moreover, the lower

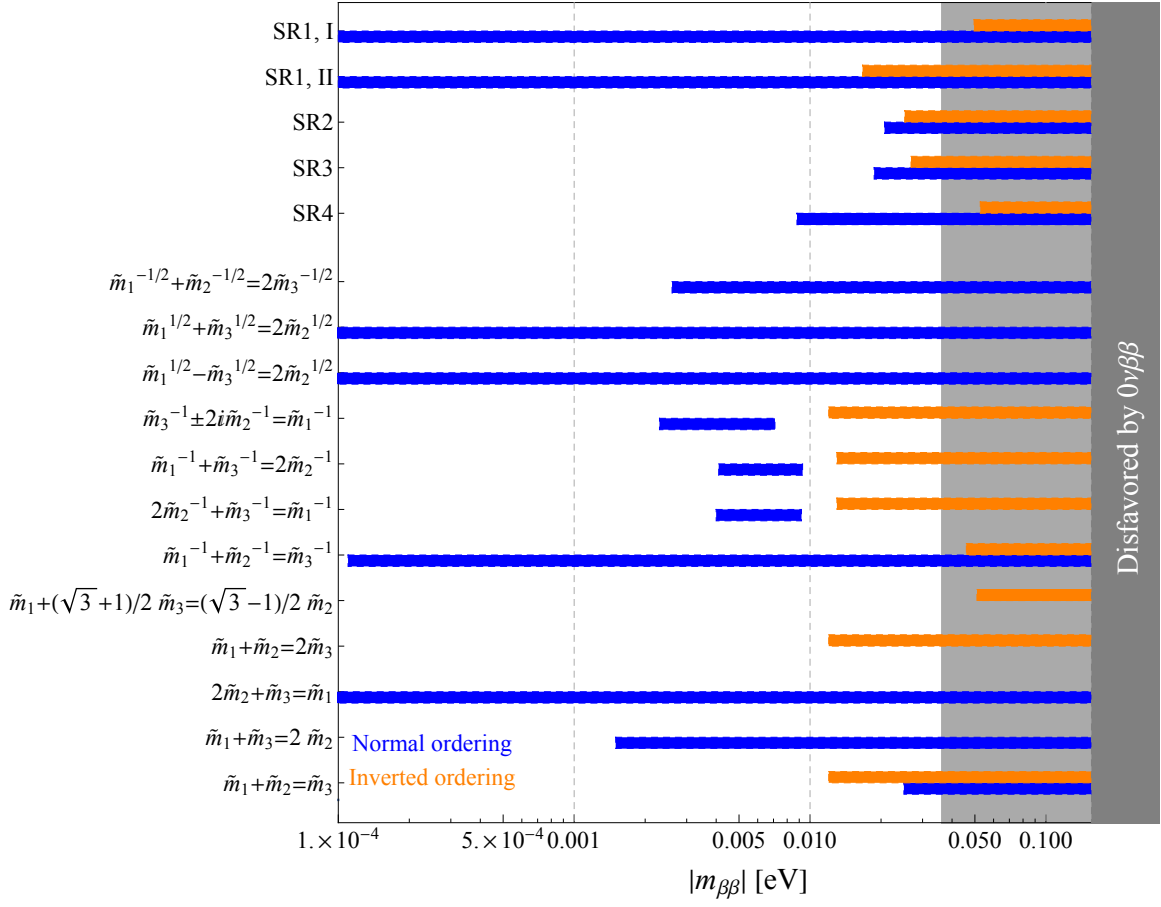


Figure 29: Predictions for $|m_{\beta\beta}|$ from different neutrino mass sum rules. The upper five mass sum rules have been derived in models based on modular symmetries [434], the lower twelve mass sum rules come from models based on discrete symmetries [451]. The grey regions show the constraints on $|m_{\beta\beta}|$ from Ref. [125] using commonly-adopted nuclear matrix-element calculations. Taken from [107].

bound on the lightest neutrino mass obtained in this way combined with the predictions for Majorana phases in Eq. (7.6) can be used to estimate the lower bound for the effective mass $|m_{\beta\beta}|$ from the general expression in Eq. (1.25). A detailed description of the analysis procedure can be found in Refs. [450, 451]. The predictions for the effective Majorana neutrino mass $|m_{\beta\beta}|$ for the different sum rules are displayed in figure 29.

One sees that certain sum rules can be fully or partially probed by the next generation of $0\nu\beta\beta$ decay experiments even taking into account the large uncertainties in the nuclear matrix element calculations. The exact mass sum rule could be violated by the higher-order terms resulting from flavour symmetry breaking or by the renormalization group evolution effects [452]. It was shown that the predictions of the sum rules are still valid at least qualitatively [452, 453]. To sum up one can say that, precision measurements of mixing angles, an observation of neutrinoless double beta decay can also provide insights into underlying flavor symmetries.

7.3 Flavor symmetry toolkit

One can check the validity of flavor symmetry models and constrain their predicted mixing parameters by comparing them those extracted from global oscillation fit results [24–27]. Nevertheless, numerical simulation of neutrino experiments and statistical analysis are often necessary to test and discriminate theoretical models in the current and future neutrino oscillation experiments such as NO ν A, T2K, JUNO, DUNE and T2HK. The public available software such as GLOBES [454, 455], Prob3++ [456], nuCRAFT [457] and nuSQuIDS [458] have been widely used to simulate the experimental characteristics of neutrino oscillation experiments. The compatibility between the experimental data and the expected outcome of a given neutrino experiment is frequently evaluated by the chi-square test. The involved simulation and analysis with GLOBES is quite involved and time-consuming. In order to facilitate the analysis of leptonic flavour symmetry models in neutrino oscillation experiments, a dedicated package FaSE-GLOBES has been recently developed [459] and is available via the link https://github.com/tcwphy/FASE_GLOBES. FaSE-GLOBES is a supplemental tool for GLOBES, written in c/c++ language, and allows users to assign any flavour symmetry model and analyze how it can be constrained and tested by the simulated neutrino oscillation experiments.

8 Benchmark UV-complete models in 4-D

In addition to the model-independent approaches described in previous chapters, the flavour problem may be tackled in a more complete, UV-complete manner, by guessing the structure of the underlying family symmetry and building explicit models on a case-by-case basis, for reviews see, e.g. Refs. [86–91]. In this chapter we present two simple extensions of the Standard Model implementing family symmetry within the renormalisable $SU(3)_c \otimes SU(2)_L \otimes U(1)_Y$ gauge field theoretic framework.

8.1 A_4 family symmetry in a scotogenic model

Here A_4 is used as flavour symmetry within the scotogenic picture [196] in which the neutrino masses are generated radiatively, and the lightest of the mediators is identified with the dark matter particle. We adopt the singlet-triplet extension [197–201] of the original model [196], making it substantially richer in the associated phenomenology [138]. We employ the Ma-Rajasekaran basis [53], the representation matrices of the generators and the Clebsch-Gordon coefficients are listed in table 12.

We now present a flavored extension of the theory proposed in [205]. The basic fields and their symmetry transformation properties are summarized in table 4. The left-handed leptons form an A_4 triplet, while right-handed ones come in as inequivalent singlets. Besides the SM fields, the original singlet-triplet scotogenic model [197] contains new weak iso-triplet and iso-singlet fermions Σ and F . Together with the Higgs scalars ϕ and Ω , these transform as triplets under the action of the family group A_4 , while the dark scalar η is a flavour singlet.

A characteristic prediction of this model is the lower bound for the $0\nu\beta\beta$ decay amplitude, discussed in section 1.4. This follows from its incomplete fermion multiplet nature, see figure 4. In contrast to its original form, both charged lepton and neutrino mass matrices will now have a non-trivial structure, predicting trimaximal neutrino mixing. As usual, the \mathbb{Z}_2 parity is imposed in order to ensure the stability of the dark matter candidate and the radiative nature of neutrino mass generation. With the fields and

	Standard Model		dark fermions		scalars		
	L	e_R, μ_R, τ_R	Σ	F	ϕ	η	Ω
multiplicity	3	3	3	3	3	1	3
$SU(3)_c$	1	1	1	1	1	1	1
$SU(2)_L$	2	1	3	1	2	2	3
$U(1)_Y$	-1	-2	0	0	1	1	0
\mathbb{Z}_2	1	1	-1	-1	1	-1	1
A_4	3	1, 1', 1''	3	3	3	1	3

Table 4: Transformation properties of the fields in the scotogenic model with A_4 family symmetry [205].

symmetry assignments in table 4, we can read out the Yukawa terms relevant to fermion masses as follows,

$$\begin{aligned}
 \mathcal{L}_Y \supset & -y_e(\bar{L}\phi)_1 e_R - y_\mu(\bar{L}\phi)_{1'} \mu_R - y_\tau(\bar{L}\phi)_{1''} \tau_R - Y_F (\bar{L}F)_1 \tilde{\eta} - Y_\Sigma (\bar{L}\tilde{\Sigma}^c)_1 \tilde{\eta} \\
 & - Y_{\Omega,1} \left(\text{Tr} \left[(\bar{\Sigma}\Omega)_{\mathbf{3}_S} \right] F \right)_1 - Y_{\Omega,2} \left(\text{Tr} \left[(\bar{\Sigma}\Omega)_{\mathbf{3}_A} \right] F \right)_1 + \text{h.c.} .
 \end{aligned}
 \tag{8.1}$$

In addition we have the bare mass terms

$$\mathcal{L}_{\mathcal{M}} \supset -\frac{1}{2}M_{\Sigma}\text{Tr}((\bar{\Sigma}\tilde{\Sigma}^c)_1) - \frac{1}{2}M_F(\bar{F}^c F)_1 + \text{h.c.}, \quad (8.2)$$

where $\tilde{\eta} = i\sigma_2\eta^*$. The $SU(2)_L$ triplets Σ and Ω are written in 2×2 matrix notation as

$$\Omega = \begin{pmatrix} \Omega^0/\sqrt{2} & \Omega^+ \\ \Omega^- & -\Omega^0/\sqrt{2} \end{pmatrix}, \quad \Sigma = \begin{pmatrix} \Sigma^0/\sqrt{2} & \Sigma^+ \\ \Sigma^- & -\Sigma^0/\sqrt{2} \end{pmatrix} \quad (8.3)$$

with $\tilde{\Sigma}^c \equiv i\sigma_2\Sigma^c i\sigma_2$. The scalar triplet Ω is assumed to be real.

The A_4 flavour symmetry is broken by the VEVs of the scalar fields ϕ and Ω , with the following VEV alignment in flavour space

$$\langle\phi\rangle = \begin{pmatrix} 1 \\ 1 \\ 1 \end{pmatrix} v_{\phi}, \quad \langle\Omega\rangle = \begin{pmatrix} 1 \\ 0 \\ 0 \end{pmatrix} v_{\Omega}, \quad \langle\eta\rangle = 0, \quad (8.4)$$

which can be a global minimum of the A_4 -invariant scalar potential in certain regions of parameter space [205]. Notice that the VEVs of ϕ and Ω break the A_4 flavour symmetry down to the subgroups Z_3^t and Z_2^s respectively, where the superscripts denote the generators of the subgroups. The ρ parameter constrains the VEV v_{Ω} to be small, and the current electroweak precision tests lead to [28]

$$v_{\Omega} \leq 4.5 \text{ GeV} \quad \text{at } 3\sigma \text{ CL} \quad (8.5)$$

8.1.1 Charged lepton masses

The first three terms in the Yukawa Lagrangian are responsible for the charged lepton masses. Inserting the VEV of ϕ and using the multiplication law for the contraction of two triplets in table 12, one can straightforwardly read out the charged lepton mass matrix as

$$M_{\ell} = \begin{pmatrix} y_e & y_{\mu} & y_{\tau} \\ y_e & \omega y_{\mu} & \omega^2 y_{\tau} \\ y_e & \omega^2 y_{\mu} & \omega y_{\tau} \end{pmatrix} v_{\phi}. \quad (8.6)$$

The matrix $M_{\ell}M_{\ell}^{\dagger}$ can be diagonalized to $\text{diag}(3|y_e v_{\phi}|^2, 3|y_{\mu} v_{\phi}|^2, 3|y_{\tau} v_{\phi}|^2)$ by means of the unitary transformation

$$U_{\ell} = \frac{1}{\sqrt{3}} \begin{pmatrix} 1 & 1 & 1 \\ 1 & \omega & \omega^2 \\ 1 & \omega^2 & \omega \end{pmatrix}, \quad (8.7)$$

which is a constant matrix.

8.1.2 Dark fermion masses

With the alignment of Ω in Eq. (8.4), we find the mass matrix of the dark fermions F and Σ^0 is of the following form

$$M_\chi = \begin{pmatrix} M_\Sigma & 0 & 0 & 0 & 0 & 0 \\ 0 & M_F & 0 & 0 & 0 & 0 \\ 0 & 0 & M_\Sigma & (Y_{\Omega,1} - Y_{\Omega,2})v_\Omega & 0 & 0 \\ 0 & 0 & (Y_{\Omega,1} - Y_{\Omega,2})v_\Omega & M_F & 0 & 0 \\ 0 & 0 & 0 & 0 & M_\Sigma & (Y_{\Omega,1} + Y_{\Omega,2})v_\Omega \\ 0 & 0 & 0 & 0 & (Y_{\Omega,1} + Y_{\Omega,2})v_\Omega & M_F \end{pmatrix} \quad (8.8)$$

in the convention of $-\frac{1}{2}(\overline{\Sigma}_1^0, \overline{F}_1^c, \overline{\Sigma}_2^0, \overline{F}_3^c, \overline{\Sigma}_3^0, \overline{F}_2^c)M_\chi(\Sigma_1^{0c}, F_1, \Sigma_2^{0c}, F_3, \Sigma_3^{0c}, F_2)^T$. The last block in Eq. (8.8) determines the masses of the dark Majorana fermions F and Σ . The symmetric complex 6×6 matrix M_χ can be diagonalized by a 6×6 block-diagonal matrix V :

$$V^T M_\chi V = \text{diag}(m_{\chi_1^0}, m_{\chi_2^0}, m_{\chi_3^0}, m_{\chi_4^0}, m_{\chi_5^0}, m_{\chi_6^0}), \quad (8.9)$$

with

$$V = \begin{pmatrix} 1 & 0 & 0 & 0 & 0 & 0 \\ 0 & 1 & 0 & 0 & 0 & 0 \\ 0 & 0 & \cos \theta_1 e^{i(\phi_1 + \varrho_1)/2} & \sin \theta_1 e^{i(\phi_1 + \sigma_1)/2} & 0 & 0 \\ 0 & 0 & -\sin \theta_1 e^{i(-\phi_1 + \varrho_1)/2} & \cos \theta_1 e^{i(-\phi_1 + \sigma_1)/2} & 0 & 0 \\ 0 & 0 & 0 & 0 & \cos \theta_2 e^{i(\phi_2 + \varrho_2)/2} & \sin \theta_2 e^{i(\phi_2 + \sigma_2)/2} \\ 0 & 0 & 0 & 0 & -\sin \theta_2 e^{i(-\phi_2 + \varrho_2)/2} & \cos \theta_2 e^{i(-\phi_2 + \sigma_2)/2} \end{pmatrix}. \quad (8.10)$$

Following the method described in D, one finds that the rotation angles θ_1 and θ_2 are given as

$$\tan 2\theta_1 = \frac{\Delta_{34}}{M_F^2 - M_\Sigma^2}, \quad \tan 2\theta_2 = \frac{\Delta_{56}}{M_F^2 - M_\Sigma^2}, \quad (8.11)$$

with

$$\begin{aligned} \Delta_{34} &= 2Y_- \sqrt{M_\Sigma^2 + M_F^2 + 2M_\Sigma M_F \cos 2\phi_{34}}, \\ \Delta_{56} &= 2Y_+ \sqrt{M_\Sigma^2 + M_F^2 + 2M_\Sigma M_F \cos 2\phi_{56}}, \\ Y_- &\equiv |(Y_{\Omega,1} - Y_{\Omega,2})v_\Omega|, \quad \phi_{34} \equiv \arg((Y_{\Omega,1} - Y_{\Omega,2})v_\Omega), \\ Y_+ &\equiv |(Y_{\Omega,1} + Y_{\Omega,2})v_\Omega|, \quad \phi_{56} \equiv \arg((Y_{\Omega,1} + Y_{\Omega,2})v_\Omega). \end{aligned} \quad (8.12)$$

The eigenvalues $M_{\chi_{1,2,3,4,5,6}^0}$ are given by

$$m_{\chi_1^0} = M_\Sigma, \quad m_{\chi_2^0} = M_F,$$

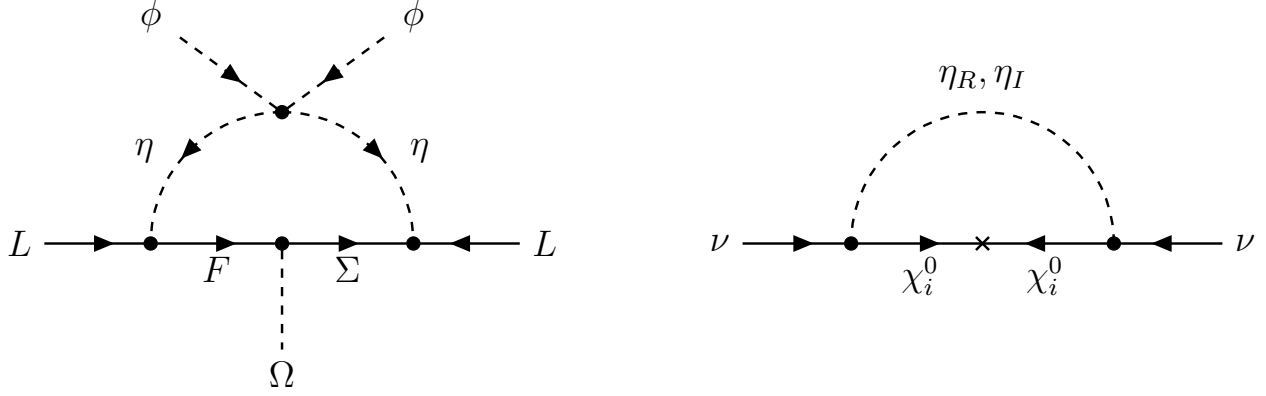


Figure 30: Feynman diagrams for scotogenic neutrino mass generation in the weak- (left panel) and mass-eigenstate basis (right panel).

$$\begin{aligned}
m_{\chi_3^0}^2 &= \frac{1}{2} \left(M_\Sigma^2 + M_F^2 + 2Y_-^2 - \sqrt{(M_F^2 - M_\Sigma^2)^2 + \Delta_{34}^2} \right), \\
m_{\chi_4^0}^2 &= \frac{1}{2} \left(M_\Sigma^2 + M_F^2 + 2Y_-^2 + \sqrt{(M_F^2 - M_\Sigma^2)^2 + \Delta_{34}^2} \right), \\
m_{\chi_5^0}^2 &= \frac{1}{2} \left(M_\Sigma^2 + M_F^2 + 2Y_+^2 - \sqrt{(M_F^2 - M_\Sigma^2)^2 + \Delta_{56}^2} \right), \\
m_{\chi_6^0}^2 &= \frac{1}{2} \left(M_\Sigma^2 + M_F^2 + 2Y_+^2 + \sqrt{(M_F^2 - M_\Sigma^2)^2 + \Delta_{56}^2} \right),
\end{aligned} \tag{8.13}$$

The Majorana fermion mass eigenstates $\chi_{1,2,3,4,5,6}^0$ are related with Σ_0^c and F by the unitary transformation V via

$$\begin{pmatrix} \Sigma_1^{0c} \\ F_1 \\ \Sigma_2^{0c} \\ F_3 \\ \Sigma_3^{0c} \\ F_2 \end{pmatrix} = V \begin{pmatrix} \chi_1^0 \\ \chi_2^0 \\ \chi_3^0 \\ \chi_4^0 \\ \chi_5^0 \\ \chi_6^0 \end{pmatrix}. \tag{8.14}$$

8.1.3 Scotogenic neutrino masses

We now turn to neutrino masses. These arise radiatively, at the one-loop level, as shown in figure 30, mediated by a “dark sector”, within a scotogenic setup. In contrast to the “flavour-blind” singlet-triplet scotogenic model, the dark fermions now transform as A_4 triplets and all of the six dark fermions mediate the one-loop diagrams. The interactions contributing to neutrino mass generation arise from the Yukawa terms involving Y_F and Y_Σ .

In the mass-eigenstate basis of dark Majorana fermions, the relevant Lagrangian is of the following

form

$$\mathcal{L}_\nu = -\frac{1}{\sqrt{2}}h_{\alpha i}\bar{\nu}_\alpha\eta_R\chi_i^0 + \frac{i}{\sqrt{2}}h_{\alpha i}\bar{\nu}_\alpha\eta_I\chi_i^0 - \frac{1}{\sqrt{2}}h_{\alpha i}^*\bar{\chi}_i^0\eta_R\nu_\alpha - \frac{i}{\sqrt{2}}h_{\alpha i}^*\bar{\chi}_i^0\eta_I\nu_\alpha, \quad (8.15)$$

where α is the family index and the rectangular matrix h is given by

$$h = \begin{pmatrix} \frac{Y_\Sigma}{\sqrt{2}} & Y_F & 0 & 0 & 0 & 0 \\ 0 & 0 & \frac{Y_\Sigma}{\sqrt{2}} & 0 & 0 & Y_F \\ 0 & 0 & 0 & Y_F & \frac{Y_\Sigma}{\sqrt{2}} & 0 \end{pmatrix} V. \quad (8.16)$$

Calculating the one-loop diagram in figure 30, we find that the radiatively generated neutrino mass matrix is given by

$$(m_\nu)_{\alpha\beta} = i \sum_i \frac{h_{\alpha i}h_{\beta i}}{32\pi^2} m_{\chi_i^0} \left(-\frac{m_{\eta_R}^2 \ln\left(\frac{m_{\eta_R}^2}{m_{\chi_i^0}^2}\right)}{m_{\eta_R}^2 - m_{\chi_i^0}^2} + \frac{m_{\eta_I}^2 \ln\left(\frac{m_{\eta_I}^2}{m_{\chi_i^0}^2}\right)}{m_{\eta_I}^2 - m_{\chi_i^0}^2} \right), \quad (8.17)$$

where m_{η_R} and m_{η_I} denote the masses of η_R and η_I respectively. Note that η_R and η_I are the real and imaginary parts of the neutral field $\eta^0 = (\eta_R + i\eta_I)/\sqrt{2}$. It is notable that the light neutrino mass matrix is predicted to be block-diagonal,

$$m_\nu = \begin{pmatrix} \times & 0 & 0 \\ 0 & \times & \times \\ 0 & \times & \times \end{pmatrix}, \quad (8.18)$$

where the symbol “ \times ” indicates a non-vanishing element. The reason is that only the flavon Ω is involved in the neutrino sector and its VEV preserves the Z_2^s subgroup, so that the light neutrino mass matrix is invariant under the action of the A_4 generator s , i.e., $\rho_{\mathbf{3}}^\dagger(s)m_\nu\rho_{\mathbf{3}}^*(s) = m_\nu$. This implies the form in Eq. (8.18). The corresponding neutrino diagonalization matrix is of the form

$$U_\nu = \begin{pmatrix} 1 & 0 & 0 \\ 0 & \cos\theta_\nu & \sin\theta_\nu e^{i\delta_\nu} \\ 0 & -\sin\theta_\nu e^{-i\delta_\nu} & \cos\theta_\nu \end{pmatrix}, \quad (8.19)$$

which satisfies $U_\nu^\dagger \mathcal{M}_\nu U_\nu^* = \text{diag}(m_1, m_2, m_3)$.

One sees that at this level there is no solar mixing. However, including the contribution from the charged lepton sector one obtains a realistic lepton mixing matrix given as

$$U = \frac{1}{\sqrt{3}} \begin{pmatrix} \cos\theta_\nu - \sin\theta_\nu e^{-i\delta_\nu} & 1 & \cos\theta_\nu + \sin\theta_\nu e^{i\delta_\nu} \\ \omega^2 \cos\theta_\nu - \omega \sin\theta_\nu e^{-i\delta_\nu} & 1 & \omega \cos\theta_\nu + \omega^2 \sin\theta_\nu e^{i\delta_\nu} \\ \omega \cos\theta_\nu - \omega^2 \sin\theta_\nu e^{-i\delta_\nu} & 1 & \omega^2 \cos\theta_\nu + \omega \sin\theta_\nu e^{i\delta_\nu} \end{pmatrix}. \quad (8.20)$$

with non-vanishing solar mixing angle. One sees the full lepton mixing matrix is predicted in terms of two free parameters θ_ν and δ_ν . Without loss of generality, these can be taken in the regions $0 \leq \theta_\nu \leq \pi$ and $0 \leq \delta_\nu \leq \pi$.

One also notes that the lepton mixing matrix U has the so-called trimaximal **TM2** form [205], since the second column is fixed to be $\frac{1}{\sqrt{3}}(1, 1, 1)^T$ [316–318]. From the mixing matrix (8.20) one can express the lepton mixing angles and the leptonic Jarlskog invariant in terms of just two free parameters

$$\begin{aligned}\sin^2 \theta_{13} &= \frac{1 + \sin 2\theta_\nu \cos \delta_\nu}{3}, & \sin^2 \theta_{12} &= \frac{1}{2 - \sin 2\theta_\nu \cos \delta_\nu}, \\ \sin^2 \theta_{23} &= \frac{1}{2} - \frac{\sqrt{3} \sin 2\theta_\nu \sin \delta_\nu}{4 - 2 \sin 2\theta_\nu \cos \delta_\nu}, & J_{CP} &= \frac{\cos 2\theta_\nu}{6\sqrt{3}}.\end{aligned}$$

One predicts the following relations amongst the mixing angles and the CP phase,

$$\cos^2 \theta_{13} \sin^2 \theta_{12} = \frac{1}{3}, \quad \cos \delta_{CP} = \frac{2(3 \cos^2 \theta_{12} \cos^2 \theta_{23} + 3 \sin^2 \theta_{12} \sin^2 \theta_{13} \sin^2 \theta_{23} - 1)}{3 \sin 2\theta_{23} \sin 2\theta_{12} \sin \theta_{13}}. \quad (8.21)$$

Using the 3σ range of the reactor angle $2.000 \times 10^{-2} \leq \sin^2 \theta_{13} \leq 2.405 \times 10^{-2}$ for NO and $2.018 \times 10^{-2} \leq \sin^2 \theta_{13} \leq 2.424 \times 10^{-2}$ for IO [24, 25], we predict narrow ranges for the solar mixing angle [205],

$$\text{NO: } 0.3401 \leq \sin^2 \theta_{12} \leq 0.3415, \quad \text{IO: } 0.3402 \leq \sin^2 \theta_{12} \leq 0.3416, \quad (8.22)$$

These predictions are very close to the 1σ upper limits from the general neutrino oscillation global fit [24, 25] and should be testable in forthcoming neutrino oscillation experiments.

To sum up we have obtained the three lepton mixing angles and the Dirac CP phase in terms of just two parameters θ_ν and δ_ν as given in figure 31. The resulting predictions for the two most poorly determined oscillation parameters $\sin^2 \theta_{23}$ and δ_{CP} are given in figure 32, where the star and dot stand

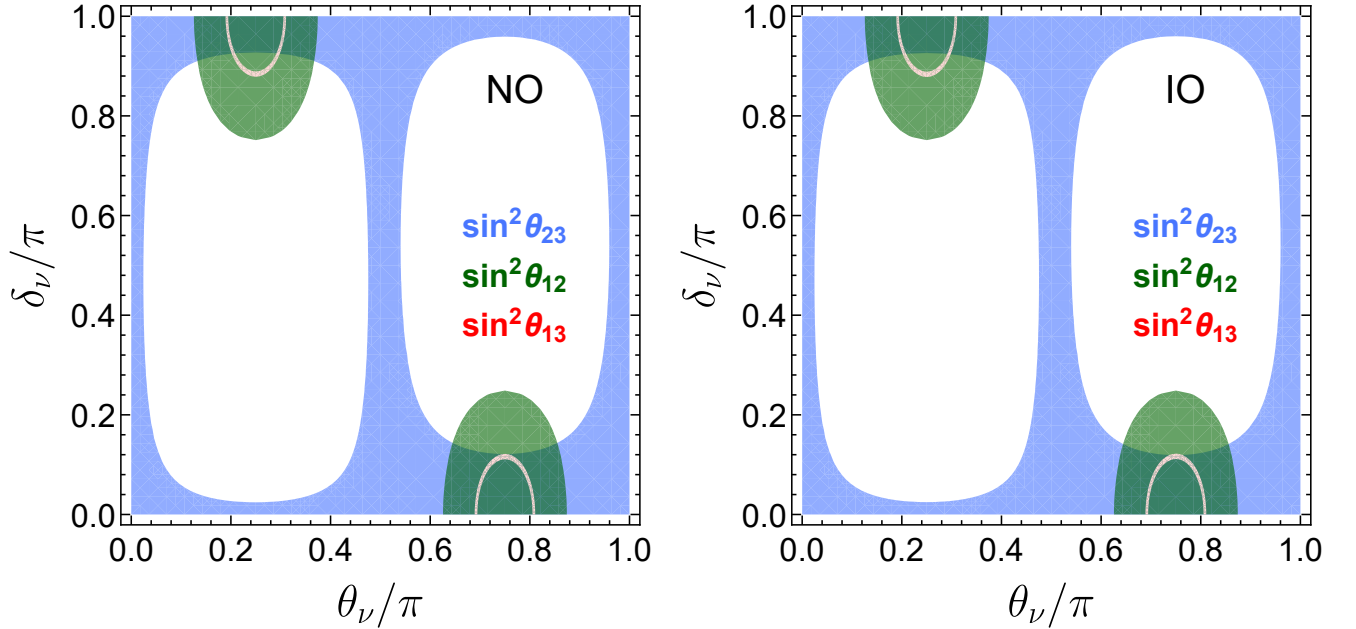


Figure 31: Contour plots of $\sin^2 \theta_{12}$, $\sin^2 \theta_{13}$, and $\sin^2 \theta_{23}$ in the $\theta_\nu - \delta_\nu$ plane. The red, green and blue areas denote the allowed 3σ regions of $\sin^2 \theta_{13}$, $\sin^2 \theta_{12}$ and $\sin^2 \theta_{23}$ respectively.

for the global best fit points for NO and IO respectively.

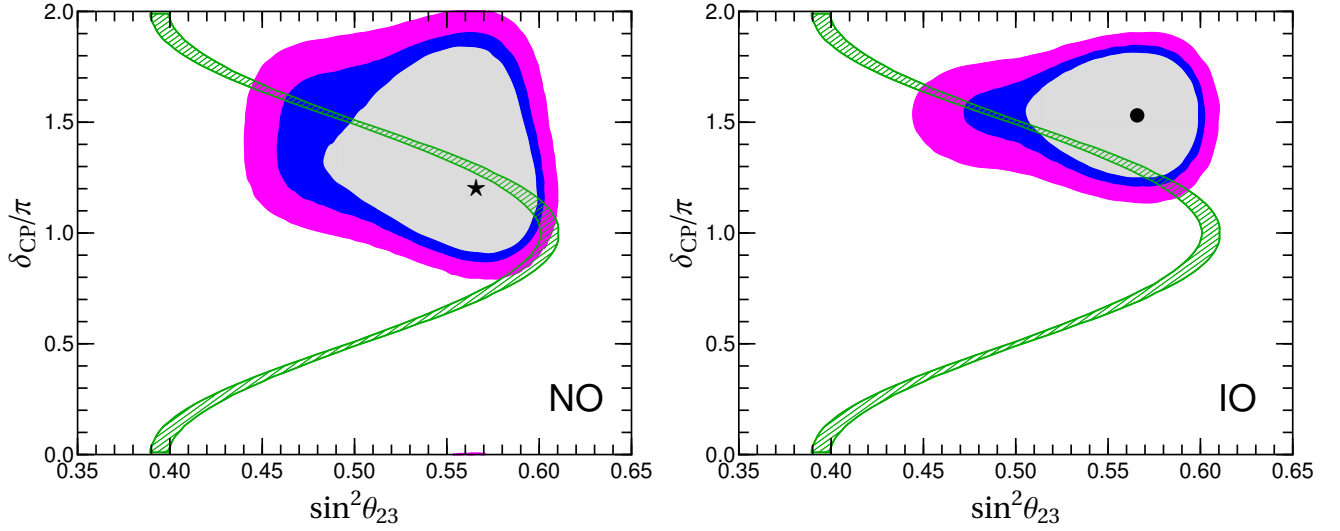


Figure 32: The hatched green bands indicate the predicted correlations between δ_{CP} and $\sin^2 \theta_{23}$ for both neutrino mass orderings. The undisplayed parameters $\sin^2 \theta_{13}$ and $\sin^2 \theta_{12}$ are required to lie within their 3σ regions from the current oscillation global fit [24, 25]. The generic 1σ , 2σ and 3σ regions from the current neutrino oscillation global fit are indicated by the shaded areas [24, 25].

One sees also that the CP phase δ_{CP} is predicted to lie in a range narrower than that obtained in the generic global fits of neutrino oscillations. We also mention that in this model the smallness of the reactor angle θ_{13} and CP violation parameter J_{CP} has a dynamical origin, given by the small ratio $v_\Omega/(M_F + M_\Sigma)$ involving the triple Higgs VEV, see [205] for details. Finally, as already mentioned, the incomplete fermion multiplet structure implies that one of the neutrinos is massless, leading to the $0\nu\beta\beta$ decay predictions in figure 4. All in all, this construction offers a serious benchmark theory for neutrino oscillations and dark matter.

8.2 A benchmark model with both flavour and CP symmetries

In this section, we describe a model implementing both the S_4 flavour symmetry and the generalized CP symmetry [325]. See Refs. [320, 394] for alternative models. It realizes the breaking patterns of flavour and CP symmetry analyzed in subsection 6.3.1. We adopt a supersymmetric (SUSY) formulation of the model in four dimensional space-time. The model is renormalizable at high energies, it gives rise to tri-bimaximal neutrino mixing at leading order, and the next-to-leading order contributions break the tri-bimaximal to a trimaximal mixing pattern. We introduce the auxiliary symmetry $Z_3 \times Z_4$ so as to generate charged lepton mass hierarchies and forbid unwanted operators.

In order to construct the superpotential responsible for the alignment of the flavon vacuum expectation values, we use the standard supersymmetric driving field mechanism [313]. We assume the existence of an R -symmetry $U(1)_R$ containing the usual R -parity, under which the Higgs and flavon fields are uncharged, while matter fields carry a $+1$ R -charge. In addition, the so-called driving fields are necessary and they

carry two units of R -charge. Therefore all terms in the superpotential should be bilinear in the matter superfields or linear in the driving field.

8.2.1 Flavon superpotential

The matter and flavon fields and their transformation properties under the flavour symmetry are summarized in table 5. On the other hand the driving fields in our model and their transformation rules under

Field	L	N^c	e^c	μ^c	τ^c	$H_{u,d}$	φ_T	η	φ_S	ϕ	ξ	Δ
S_4	3	3	1	1'	1	1	3	2	3'	2	1	1'
Z_3	ω	ω^2	ω^2	1	ω	1	ω	ω	ω^2	ω^2	ω^2	1
Z_4	1	1	i	-1	$-i$	1	i	i	1	1	1	1
$U(1)_R$	1	1	1	1	1	0	0	0	0	0	0	0

Table 5: Transformation properties of matter, Higgs and flavon fields.

the flavour symmetry group are listed in table 6. The most general driving superpotential \mathcal{W}_d invariant under $S_4 \times Z_3 \times Z_4$ with $R = 2$ is given by [325]

$$\begin{aligned}
\mathcal{W}_d = & g_1 (\varphi_T^0 (\varphi_T \varphi_T)_{\mathbf{3}'})_{\mathbf{1}} + g_2 (\varphi_T^0 (\eta \varphi_T)_{\mathbf{3}'})_{\mathbf{1}} + g_3 \zeta^0 (\varphi_T \varphi_T)_{\mathbf{1}} + g_4 \zeta^0 (\eta \eta)_{\mathbf{1}} \\
& + f_1 (\varphi_S^0 (\varphi_S \varphi_S)_{\mathbf{3}'})_{\mathbf{1}} + f_2 (\varphi_S^0 (\phi \varphi_S)_{\mathbf{3}'})_{\mathbf{1}} + f_3 (\varphi_S^0 \varphi_S)_{\mathbf{1}} \xi + f_4 (\tilde{\varphi}_S^0 (\phi \varphi_S)_{\mathbf{3}})_{\mathbf{1}} \\
& + f_5 \xi^0 (\varphi_S \varphi_S)_{\mathbf{1}} + f_6 \xi^0 (\phi \phi)_{\mathbf{1}} + f_7 \xi^0 \xi^2 + M^2 \Delta^0 + f_8 \Delta^0 \Delta^2.
\end{aligned} \tag{8.23}$$

Since we impose CP symmetry on the theory in the unbroken phase, all couplings in w_d are real. In the limit of unbroken supersymmetry, the minimum of the scalar potential is determined by vanishing F -terms for the driving fields. As a result, the VEVs of the flavons are aligned as follows [325]

$$\begin{aligned}
\langle \varphi_T \rangle &= \begin{pmatrix} 0 \\ 1 \\ 0 \end{pmatrix} v_T, & \langle \eta \rangle &= \begin{pmatrix} 0 \\ 1 \end{pmatrix} v_\eta, & \langle \Delta \rangle &= v_\Delta, \\
\langle \varphi_S \rangle &= \begin{pmatrix} 1 \\ 1 \\ 1 \end{pmatrix} v_S, & \langle \phi \rangle &= \begin{pmatrix} 1 \\ 1 \end{pmatrix} v_\phi, & \langle \xi \rangle &= v_\xi,
\end{aligned} \tag{8.24}$$

Field	φ_T^0	ζ^0	φ_S^0	$\tilde{\varphi}_S^0$	ξ^0	Δ^0	Ω_1	Ω_1^c	Ω_2	Ω_2^c	Ω_3	Ω_3^c	Σ	Σ^c
S_4	3'	1	3'	3	1	1	2	2	2	2	3	3	3'	3'
Z_3	ω	ω	ω^2	ω^2	ω^2	1	1	1	ω	ω^2	ω^2	ω	ω^2	ω
Z_4	-1	-1	1	1	1	1	-1	-1	$-i$	i	1	1	1	1
$U(1)_R$	2	2	2	2	2	2	1	1	1	1	1	1	1	1

Table 6: Transformation rules for driving and messenger fields under the $S_4 \times Z_4 \times Z_3$ and $U(1)_R$ symmetries.

with

$$v_T = \frac{g_2}{2g_1} v_\eta, \quad v_S^2 = -\frac{1}{6f_2^2 f_5} (f_3^2 f_6 + 2f_2^2 f_7) v_\xi^2, \quad v_\phi = -\frac{f_3}{2f_2} v_\xi, \quad v_\Delta^2 = -M^2/f_8, \quad (8.25)$$

where v_η and v_ξ are undetermined, as they are related to a flat direction. The phase of v_η can be absorbed into the lepton fields, thus we can take the VEVs v_η and v_T real without loss of generality. The common phase of v_S , v_ϕ and v_ξ does not affect neutrino masses and mixing, because it can be factored out in the light neutrino mass matrix. As a consequence, v_ϕ and v_ξ can be considered real while v_S is real or purely imaginary depending on the coefficient $-(f_3^2 f_6 + 2f_2^2 f_7)/(f_2^2 f_5)$ being positive or negative. Furthermore, the VEV v_Δ is real for $f_8 < 0$ and purely imaginary for $f_8 > 0$.

8.2.2 The charged lepton sector

The renormalizable Yukawa superpotential terms involving charged leptons is obtained by integrating out the three pairs of messengers Ω_i and Ω_i^c ($i = 1, 2, 3$). These are chiral superfields with non-vanishing hypercharge $+2(-2)$ for Ω_i (Ω_i^c). Given the field content and the symmetry assignments in tables 5 and 6, one can read off the superpotential for the charged leptons as follows,

$$\begin{aligned} \mathcal{W}_\ell = & z_1 (L\Omega_3)_1 H_d + z_2 (\Omega_3^c \varphi_T)_1 \tau^c + z_3 ((\Omega_3^c \varphi_T)_2 \Omega_2)_1 + z_4 (\Omega_2^c \eta)_1 \mu^c \\ & + z_5 ((\Omega_2^c \eta)_2 \Omega_1)_1 + z_6 (\Omega_1^c \eta)_1 e^c + M_{\Omega_1} (\Omega_1 \Omega_1^c)_1 + z_7 \Delta (\Omega_1 \Omega_1^c)_1 \\ & + M_{\Omega_2} (\Omega_2 \Omega_2^c)_1 + z_8 \Delta (\Omega_2 \Omega_2^c)_1 + M_{\Omega_3} (\Omega_3 \Omega_3^c)_1, \end{aligned} \quad (8.26)$$

where CP invariance requires all coupling constants z_i and messenger masses M_{Ω_1} , M_{Ω_2} and M_{Ω_3} to be real. The terms $\Delta (\Omega_1 \Omega_1^c)_1$ and $\Delta (\Omega_2 \Omega_2^c)_1$, lead to corrections to the Ω_1 and Ω_2 masses respectively. The mass scales of the messenger fields are much larger than the flavon VEVs, hence the contributions of these two operators can be safely neglected. Integrating out the messenger pairs Ω_i and Ω_i^c as shown in figure 33, we obtain the effective superpotential for the charged lepton masses as

$$\mathcal{W}_\ell^{eff} = -\frac{z_1 z_2}{M_{\Omega_3}} (L\varphi_T)_1 H_d \tau^c + \frac{z_1 z_3 z_4}{M_{\Omega_2} M_{\Omega_3}} ((L\varphi_T)_2 \eta)_1 \mu^c - \frac{z_1 z_3 z_5 z_6}{M_{\Omega_1} M_{\Omega_2} M_{\Omega_3}} ((L\varphi_T)_2 (\eta\eta)_2)_1 H_d e^c. \quad (8.27)$$

Using the flavon VEVs in Eq. (8.24), we find a diagonal charged lepton mass matrix with

$$m_\tau = -z_1 z_2 \frac{v_T}{M_{\Omega_3}} v_d, \quad m_\mu = z_1 z_3 z_4 \frac{v_T v_\eta}{M_{\Omega_2} M_{\Omega_3}} v_d, \quad m_e = -z_1 z_3 z_5 z_6 \frac{v_T v_\eta^2}{M_{\Omega_1} M_{\Omega_2} M_{\Omega_3}} v_d, \quad (8.28)$$

where $v_d = \langle H_d \rangle$ is the VEV of the Higgs field H_d . We see that the electron, muon and tau masses are suppressed by different powers of v_T and v_η , so that the mass hierarchies among the charged leptons are naturally reproduced.

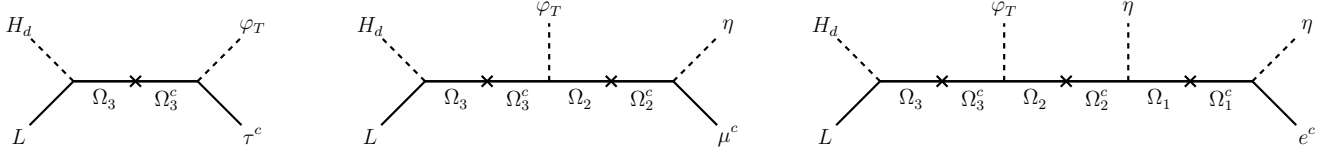


Figure 33: Diagrams for charged-lepton-mass effective operators, crosses indicating fermion mass insertions.

8.2.3 The neutrino sector

The renormalizable superpotential responsible for generating the light neutrino masses can be written as the sum of the leading-order terms and the relevant messenger terms:

$$\mathcal{W}_\nu = \mathcal{W}_\nu^{LO} + \mathcal{W}_\nu^\Sigma, \quad (8.29)$$

where

$$\begin{aligned} \mathcal{W}_\nu^{LO} &= y (LN^c)_1 H_u + y_1 ((N^c N^c)_{\mathbf{3}'})_1 \varphi_S + y_2 (N^c N^c)_1 \xi + y_3 ((N^c N^c)_2 \phi)_1, \\ \mathcal{W}_\nu^\Sigma &= x_1 ((N^c \Sigma)_{\mathbf{3}'})_1 \varphi_S + x_2 ((N^c \Sigma)_2 \phi)_1 + x_3 (N^c \Sigma^c)_1 \Delta + M_\Sigma (\Sigma \Sigma^c)_1. \end{aligned} \quad (8.30)$$

where the couplings x_i and y_i are real due to CP invariance and the messenger field Σ (Σ^c) is a chiral superfield with vanishing hypercharge. The first term of \mathcal{W}_ν^{LO} gives rise to a very simple form for the Dirac neutrino mass matrix,

$$m_D = y v_u \begin{pmatrix} 1 & 0 & 0 \\ 0 & 0 & 1 \\ 0 & 1 & 0 \end{pmatrix}, \quad (8.31)$$

with $v_u = \langle H_u \rangle$. On the other hand, the last three terms of \mathcal{W}_ν^{LO} lead to the mass matrix m_M^{LO} of the right-handed neutrinos. Given the alignment of φ_S , ϕ and ξ shown in Eq. (8.24), we have

$$m_M^{LO} = y_1 v_s \begin{pmatrix} 2 & -1 & -1 \\ -1 & 2 & -1 \\ -1 & -1 & 2 \end{pmatrix} + y_2 v_\xi \begin{pmatrix} 1 & 0 & 0 \\ 0 & 0 & 1 \\ 0 & 1 & 0 \end{pmatrix} + y_3 v_\phi \begin{pmatrix} 0 & 1 & 1 \\ 1 & 1 & 0 \\ 1 & 0 & 1 \end{pmatrix}. \quad (8.32)$$

The effective light neutrino mass matrix is given by the simplest type-I seesaw formula [32]

$$m_\nu^{LO} = -m_D (m_M^{LO})^{-1} m_D^T$$

which is exactly diagonalized by the tri-bimaximal mixing matrix U_{TBM} ,

$$U_{TBM}^T m_\nu^{LO} U_{TBM} = \text{diag}(m_1^{LO}, m_2^{LO}, m_3^{LO}), \quad (8.33)$$

so we obtain

$$m_1^{LO} = -\frac{y^2 v_u^2}{3y_1 v_S + y_2 v_\xi - y_3 v_\phi}, \quad m_2^{LO} = -\frac{y^2 v_u^2}{y_2 v_\xi + 2y_3 v_\phi}, \quad m_3^{LO} = -\frac{y^2 v_u^2}{3y_1 v_S - y_2 v_\xi + y_3 v_\phi}.$$

Note that the tri-bimaximal mixing pattern is produced at leading order. This follows from the fact that the VEVs of the flavons φ_S , ϕ and ξ involved in the neutrino mass term are invariant under the action of the Klein subgroup generated by the tri-bimaximal s and u generators.

The leading-order and next-to-leading order (NLO) contributions to the right-handed neutrino masses are depicted in figure 34.

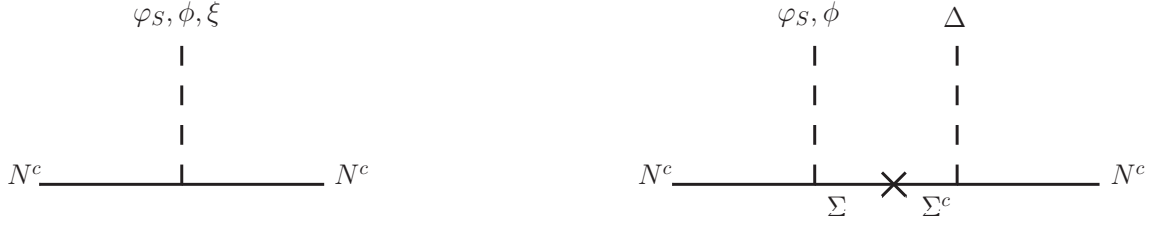


Figure 34: The diagrams for the RH neutrino masses, where the cross indicates a fermionic mass insertion.

Integrating out the messenger fields Σ and Σ^c , we obtain the following NLO effective operator

$$\mathcal{W}_\nu^{NLO} = -\frac{x_2 x_3}{M_\Sigma} \Delta ((N^c N^c)_2 \phi)_{1'}. \quad (8.34)$$

Notice that the VEV of the flavon Δ breaks the residual Klein symmetry down to a Z_2 subgroup generated by s at NLO. Consequently, the corrected right-handed neutrino mass matrix is given as

$$m_M = a \begin{pmatrix} 2 & -1 & -1 \\ -1 & 2 & -1 \\ -1 & -1 & 2 \end{pmatrix} + b \begin{pmatrix} 1 & 0 & 0 \\ 0 & 0 & 1 \\ 0 & 1 & 0 \end{pmatrix} + c \begin{pmatrix} 0 & 1 & 1 \\ 1 & 1 & 0 \\ 1 & 0 & 1 \end{pmatrix} + d \begin{pmatrix} 0 & 1 & -1 \\ 1 & -1 & 0 \\ -1 & 0 & 1 \end{pmatrix}, \quad (8.35)$$

with

$$a = y_1 v_S, \quad b = y_2 v_\xi, \quad c = y_3 v_\phi, \quad d = x_2 x_3 \frac{v_\Delta v_\phi}{M_\Sigma}. \quad (8.36)$$

Therefore, up to an overall factor $y^2 v_u^2$, the corrected light neutrino mass matrix obtained from the seesaw formula has the form

$$m_\nu = \alpha \begin{pmatrix} 2 & -1 & -1 \\ -1 & 2 & -1 \\ -1 & -1 & 2 \end{pmatrix} + \beta \begin{pmatrix} 1 & 0 & 0 \\ 0 & 0 & 1 \\ 0 & 1 & 0 \end{pmatrix} + \gamma \begin{pmatrix} 0 & 1 & 1 \\ 1 & 1 & 0 \\ 1 & 0 & 1 \end{pmatrix} + \epsilon \begin{pmatrix} 0 & 1 & -1 \\ 1 & -1 & 0 \\ -1 & 0 & 1 \end{pmatrix}, \quad (8.37)$$

where the parameters α , β , γ and ϵ are given by,

$$\alpha = \frac{a}{-9a^2 + (b-c)^2 + 3d^2}, \quad \beta = -\frac{1}{3(b+2c)} + \frac{2(b-c)}{3[9a^2 - (b-c)^2 - 3d^2]},$$

$$\gamma = -\frac{1}{3(b+2c)} - \frac{b-c}{3[9a^2 - (b-c)^2 - 3d^2]}, \quad \epsilon = \frac{d}{-9a^2 + (b-c)^2 + 3d^2}, \quad (8.38)$$

The first three terms in the light neutrino matrix of Eq. (8.37) preserve the tri-bimaximal mixing form. The last term, which is proportional to ϵ , violates it. The associated parameter ϵ is induced by the NLO contributions suppressed by v_Δ/M_Σ with respect to α , β and γ . This naturally accounts for the small reactor mixing angle θ_{13} and the small deviation from the maximal atmospheric mixing.

As shown in section 8.2.1, the VEVs v_ϕ and v_ξ can be assumed real, while v_S and v_Δ can be real or purely imaginary due to the generalized CP symmetry. If v_S and v_Δ are real, the vacuum alignment of the flavons φ_S , ϕ , ξ and Δ is invariant under the CP transformation $X_{\mathbf{r}} = 1$ and the residual flavour symmetry Z_2^s . The parameters α , β , γ and ϵ are all real, the lepton mixing matrix has the form of Eq. (6.46) with the rotation angle θ given by

$$\tan 2\theta = \frac{\sqrt{3}\epsilon}{\gamma - \beta}. \quad (8.39)$$

The lepton mixing angles and CP violation phases are given in Eq. (6.47). The light neutrino masses are

$$\begin{aligned} m_1 &= \left| 3\alpha - \text{sign}(\epsilon \sin 2\theta) \sqrt{(\gamma - \beta)^2 + 3\epsilon^2} \right|, \\ m_2 &= |\beta + 2\gamma|, \\ m_3 &= \left| 3\alpha + \text{sign}(\epsilon \sin 2\theta) \sqrt{(\gamma - \beta)^2 + 3\epsilon^2} \right|. \end{aligned} \quad (8.40)$$

This model allows for both neutrino mass orderings, either NO or IO.

Moreover, if the VEV v_S is real while v_Δ is pure imaginary, the neutrino sector would preserve the residual flavour symmetry Z_2^s and CP symmetry $X_{\mathbf{r}} = u$ which corresponds to the $\mu - \tau$ reflection symmetry. The parameters α , β , γ in Eq. (8.37) are real, and ϵ is pure imaginary. We find that the lepton mixing matrix is given by Eq. (6.50) with the rotation angle θ given as

$$\tan 2\theta = \frac{i\epsilon}{\sqrt{3}\alpha}. \quad (8.41)$$

Both the atmospheric angle θ_{23} and the CP violation phase δ_{CP} are maximal, as shown in Eq. (6.51). The light neutrino masses are given by

$$\begin{aligned} m_1 &= \left| \beta - \gamma + \text{sign}(\alpha \cos 2\theta) \sqrt{9\alpha^2 - 3\epsilon^2} \right|, \\ m_2 &= |\beta + 2\gamma|, \\ m_3 &= \left| \beta - \gamma - \text{sign}(\alpha \cos 2\theta) \sqrt{9\alpha^2 - 3\epsilon^2} \right|, \end{aligned} \quad (8.42)$$

Again, this is consistent with both neutrino mass orderings, either NO or IO.

All in all, this model implements the first two symmetry breaking patterns analyzed in detail in section 6.3.1. The reader is addressed to that section for a discussion of the corresponding neutrino

mixing, CP violation and $0\nu\beta\beta$ decay predictions. See Ref. [320] for an S_4 model realizing the third breaking pattern and the lepton mixing matrix of Eq. (6.53).

9 Family symmetry in 5-D models with a warped extra dimension

Extra dimensions [460] provide an interesting way to address the so-called hierarchy problem [461–463], by making the fundamental scale of gravity exponentially reduced from the Planck mass down to the TeV scale. This follows as a result of having the Standard Model fields localized near the boundary of the extra dimensions. Here we stress that the fermion mass hierarchies can also be addressed through the localization of fermion profiles which are fixed by the bulk mass parameters.

As we have shown in the previous section, the lepton and quark mixing angles can be well explained by using a discrete flavour symmetry within concrete 4-D models. One can also implement flavour symmetry in the context of extra dimensions, so that the structure of both mass hierarchies as well as mixing angles can be addressed in a clear manner. There has been intense activity using discrete family symmetries to build UV-complete 4-D gauge theories [85–93], describing the masses and mixing matrices of leptons and quarks. The pattern of fermion mixing could also arise from the imposition of family symmetries in extra dimensions, including holographic models [70–84].

In this section we consider warped flavourdynamics schemes, of which there have been two recent proposals in the literature [78, 79]. The first warped flavourdynamics model is based on the $\Delta(27)$ family symmetry, with neutrinos as Dirac fermions, and a predicted TM2 mixing pattern [78]. An alternative proposal for a warped flavourdynamics scheme is based on the T' family group [79]. Here neutrinos are Majorana fermions with a predicted TM1 mixing pattern. In what follows we develop the key features of this second example, and refer the interested reader to the original work in [78] for the other case.

9.1 Warped flavourdynamics with the T' family group

Here we present our benchmark extra-dimensional model with T' flavour symmetry [79]. The T' group is the double covering of A_4 . The relation between T' and A_4 is quite similar to the familiar relation between $SU(2)$ and $SO(3)$. Although $SU(2)$ and $SO(3)$ possess the same Lie algebra, $SO(3)$ has only odd-dimensional representations, while $SU(2)$ possesses both even and odd-dimensional representations. Likewise T' has three doublet representations $\mathbf{2}$, $\mathbf{2}'$ and $\mathbf{2}''$ besides the singlets $\mathbf{1}$, $\mathbf{1}'$, $\mathbf{1}''$ and triplet $\mathbf{3}$ of A_4 .

We formulate our model in the framework of the Randall-Sundrum model [462]. The bulk geometry is described by the following metric

$$ds^2 = e^{-2ky} \eta_{\mu\nu} dx^\mu dx^\nu - dy^2. \quad (9.1)$$

This extra dimension y is compactified, and the two 3-branes with opposite tension are located at $y = 0$, the UV brane, and the infra-red (IR) brane at $y = L$.

In order to comply with electroweak precision measurement constraints, the electroweak symmetry of the model is promoted to $G_{\text{bulk}} = SU(2)_L \otimes SU(2)_R \otimes U(1)_{B-L}$ [464, 465] and it is broken down to the standard model gauge group $G_{\text{SM}} = SU(2)_L \otimes U(1)_Y$ on the UV brane by the boundary conditions (BCs) of the gauge bosons. The Higgs field lives in the bulk, and it is in the $(\mathbf{2}, \mathbf{2})$ bi-doublet representation of

$SU(2)_L \otimes SU(2)_R$. The Kaluza-Klein (KK) Higgs field decomposition is [466]

$$H(x^\mu, y) = H(x^\mu) \frac{f_H(y)}{\sqrt{L}} + \text{heavy KK Modes}, \quad (9.2)$$

where $f_H(y)$ is the zero mode profile. For an adequate choice of BCs, we have

$$f_H(y) = \sqrt{\frac{2kL(1-\beta)}{1-e^{-2(1-\beta)kL}}} e^{kL} e^{(2-\beta)k(y-L)}, \quad (9.3)$$

with $\beta = \sqrt{4 + m_H^2/k^2}$ and m_H is the bulk mass of the Higgs field.

The three families of leptons and quarks transform under $SU(2)_L \otimes SU(2)_R$ in the following way,

$$\Psi_{\ell_i} = \begin{pmatrix} \nu_i^{[++]} \\ e_i^{[++]} \end{pmatrix} \sim (\mathbf{2}, \mathbf{1}), \quad \Psi_{e_i} = \begin{pmatrix} \tilde{\nu}_i^{[+-]} \\ e_i^{[--]} \end{pmatrix} \sim (\mathbf{1}, \mathbf{2}), \quad \Psi_{\nu_i} = \begin{pmatrix} N_i^{[--]} \\ \tilde{e}_i^{[+-]} \end{pmatrix} \sim (\mathbf{1}, \mathbf{2}), \quad (9.4)$$

$$\Psi_{Q_i} = \begin{pmatrix} u_i^{[++]} \\ d_i^{[++]} \end{pmatrix} \sim (\mathbf{2}, \mathbf{1}), \quad \Psi_{d_i} = \begin{pmatrix} \tilde{u}_i^{[+-]} \\ d_i^{[--]} \end{pmatrix} \sim (\mathbf{1}, \mathbf{2}), \quad \Psi_{u_i} = \begin{pmatrix} u_i^{[--]} \\ \tilde{d}_i^{[+-]} \end{pmatrix} \sim (\mathbf{1}, \mathbf{2}). \quad (9.5)$$

where the two signs in the bracket indicate Neumann (+) or Dirichlet (−) boundary conditions for the left-handed component of the corresponding field on UV and IR branes respectively. The Kaluza-Klein decomposition of a 5D fermion for the two different BCs are

$$\psi^{[++]}(x^\mu, y) = \frac{e^{2ky}}{\sqrt{L}} \left\{ \psi_L(x^\mu) f_L(y, c_L) + \text{heavy KK modes} \right\}, \quad (9.6)$$

$$\psi^{[--]}(x^\mu, y) = \frac{e^{2ky}}{\sqrt{L}} \left\{ \psi_R(x^\mu) f_R(y, c_R) + \text{heavy KK modes} \right\}. \quad (9.7)$$

The 5D fields with [++] BCs only have left-handed zero modes, while those with [--] BCs only have right-handed ones. The functions $f_L(y, c_L)$ and $f_R(y, c_R)$ are the zero mode profiles [467, 468]

$$f_L(y, c_L) = \sqrt{\frac{(1-2c_L)kL}{e^{(1-2c_L)kL}-1}} e^{-c_L ky}, \quad f_R(y, c_R) = \sqrt{\frac{(1+2c_R)kL}{e^{(1+2c_R)kL}-1}} e^{c_R ky}, \quad (9.8)$$

where c_L and c_R denote the bulk mass of the 5D fermions in units of the AdS_5 curvature k . As usual, we adopt the zero mode approximation which identifies the standard model fields with the zero modes of corresponding 5D fields.

9.1.1 Lepton masses and mixing

The field content and the symmetry assignment are given in table 7. The zero mode of Ψ_L is the left-handed lepton doublet, and the zero modes of $\Psi_{e,\mu,\tau}$ and Ψ_ν are the right-handed charged leptons and neutrinos respectively. The left-handed lepton fields are assumed to transform as a triplet under flavour symmetry group.

Field	Ψ_l	Ψ_e	Ψ_μ	Ψ_τ	Ψ_ν	H	$\varphi_l(IR)$	$\sigma_l(IR)$	$\varphi_\nu(UV)$	$\rho_\nu(UV)$
$SU(2)_L \times SU(2)_R \times U(1)_{B-L}$	(2, 1, -1)	(1, 2, -1)	(1, 2, -1)	(1, 2, -1)	(1, 2, -1)	(2, 2, 0)	(1, 1, 0)	(1, 1, 0)	(1, 1, 0)	(1, 1, 0)
T'	3	1'	1''	1	3	1	2	1''	3	3
Z_3	ω^2	1	1	1	ω^2	1	ω	ω	ω	ω
Z_4	i	i	i	i	i	1	-1	-1	i	$-i$

Table 7: Lepton and flavon fields under the $SU(2)_L \times SU(2)_R \times U(1)_{B-L}$ gauge group and the $T' \times Z_3 \times Z_4$ family symmetry, with $\omega = e^{2\pi i/3}$. Flavons φ_l , σ_l and φ_ν , ρ_ν lie on the IR and UV branes respectively.

Note that in order to forbid dangerous terms, besides the flavour group T' , we introduce the auxiliary symmetry $Z_3 \times Z_4$. Four flavons φ_l , σ_l , φ_ν and ρ_ν are introduced to break the T' family symmetry. The flavons φ_l and σ_l couple to the charged lepton sector, and are localized on the IR brane, while φ_ν and ρ_ν are localized on the UV brane. The vacuum expectation values of these flavons are aligned along the following directions

$$\langle \varphi_l \rangle = (1, 0)v_{\varphi_l}, \quad \langle \sigma_l \rangle = v_{\sigma_l}, \quad \langle \varphi_\nu \rangle = (1, -2\omega^2, -2\omega)v_{\varphi_\nu}, \quad \langle \rho_\nu \rangle = (1, -2\omega, -2\omega^2)v_{\rho_\nu}, \quad (9.9)$$

with $\omega = e^{2i\pi/3}$. The above vacuum alignment can be the global minimum of the scalar potential in certain regions of parameters [79]. At leading order, the lepton mass terms respecting both gauge symmetry as well as the flavour symmetry $T' \times Z_3 \times Z_4$ take the following form

$$\mathcal{L}_Y^l = \frac{\sqrt{G}}{\Lambda^3} \left[y_e (\varphi_l^2 \bar{\Psi}_l)_{\mathbf{1}''} H \Psi_e + y_\mu (\varphi_l^2 \bar{\Psi}_l)_{\mathbf{1}'} H \Psi_\mu + y_\tau (\varphi_l^2 \bar{\Psi}_l)_{\mathbf{1}} H \Psi_\tau \right] \delta(y-L) + \text{h.c.}, \quad (9.10)$$

$$\begin{aligned} \mathcal{L}_Y^\nu = & y_{\nu_1} \frac{\sqrt{G}}{\Lambda'} (\bar{\Psi}_l H \Psi_\nu)_{\mathbf{1}} \delta(y-L) + \frac{1}{2} \frac{\sqrt{G}}{\Lambda^2} \left[y_{\nu_2} (\bar{N}^C N)_{\mathbf{1}} (\varphi_\nu^2)_{\mathbf{1}} + y_{\nu_3} (\bar{N}^C N)_{\mathbf{1}} (\rho_\nu^2)_{\mathbf{1}} \right. \\ & \left. + y_{\nu_4} \left((\bar{N}^C N)_{\mathbf{3}_S} (\varphi_\nu^2)_{\mathbf{3}_S} \right)_{\mathbf{1}} + y_{\nu_5} \left((\bar{N}^C N)_{\mathbf{3}_S} (\rho_\nu^2)_{\mathbf{3}_S} \right)_{\mathbf{1}} \right] \delta(y) + \text{h.c.}, \end{aligned} \quad (9.11)$$

where $G = e^{-8ky}$ is the determinant of the 5D metric.

For the vacuum configuration in Eq. (9.9), the charged lepton mass matrix is diagonal and the three charged lepton masses are

$$m_e = \tilde{y}_e \frac{v_{\varphi_l}^2}{\Lambda'^2} v, \quad m_\mu = \tilde{y}_\mu \frac{v_{\varphi_l}^2}{\Lambda'^2} v, \quad m_\tau = \tilde{y}_\tau \frac{v_{\varphi_l}^2}{\Lambda'^2} v, \quad (9.12)$$

with

$$\tilde{y}_{e,\mu,\tau} = \frac{y_{e,\mu,\tau}}{L\Lambda'} f_L(L, c_\ell) f_R(L, c_{e,\mu,\tau}). \quad (9.13)$$

Neutrino masses are generated by the type-I seesaw mechanism, and the large seesaw scale arises naturally, since the Majorana mass terms of the right-handed neutrinos are UV-localized. The first term in Eq. (9.11) leads to a diagonal Dirac neutrino mass matrix $m_D = \tilde{y}_{\nu_1} v \mathbb{1}_3$ where $\tilde{y}_{\nu_1} = \frac{y_{\nu_1}}{L\Lambda'} f_L(L, c_\ell) f_R(L, c_\nu)$ and $\mathbb{1}_3$ is the 3×3 unit matrix. The last four are the Majorana mass terms for the right-handed neutrinos, leading

to the mass matrix

$$\begin{aligned}
m_N = & \left(\tilde{y}_{\nu_2} \frac{v_{\varphi\nu}^2}{\Lambda} + \tilde{y}_{\nu_3} \frac{v_{\rho\nu}^2}{\Lambda} \right) \begin{pmatrix} 1 & 0 & 0 \\ 0 & 0 & 1 \\ 0 & 1 & 0 \end{pmatrix} + \tilde{y}_{\nu_4} \frac{v_{\varphi\nu}^2}{\Lambda} \begin{pmatrix} 2 & 2\omega & 2\omega^2 \\ 2\omega & -4\omega^2 & -1 \\ 2\omega^2 & -1 & -4\omega \end{pmatrix} \\
& + \tilde{y}_{\nu_5} \frac{v_{\rho\nu}^2}{\Lambda} \begin{pmatrix} 2 & 2\omega^2 & 2\omega \\ 2\omega^2 & -4\omega & -1 \\ 2\omega & -1 & -4\omega^2 \end{pmatrix}, \tag{9.14}
\end{aligned}$$

where

$$\tilde{y}_{\nu_{2,3,4,5}} = \frac{y_{\nu_{2,3,4,5}}}{L\Lambda} f_R^2(0, c_\nu). \tag{9.15}$$

The light neutrino mass matrix is given by the simple type-I seesaw formula

$$m_\nu = -m_D m_N^{-1} m_D^T$$

After performing a tri-bimaximal transformation on the neutrino fields, m_ν acquires block diagonal form,

$$m'_\nu = U_{TBM}^\dagger m_\nu U_{TBM}^* = m_0 \begin{pmatrix} \frac{-1}{1+3(y_4+y_5)} & 0 & 0 \\ 0 & \frac{1-3(y_4+y_5)}{18(y_4-y_5)^2+3(y_4+y_5)-1} & \frac{3\sqrt{2}i(y_4-y_5)}{18(y_4-y_5)^2+3(y_4+y_5)-1} \\ 0 & \frac{3\sqrt{2}i(y_4-y_5)}{18(y_4-y_5)^2+3(y_4+y_5)-1} & \frac{-1}{18(y_4-y_5)^2+3(y_4+y_5)-1} \end{pmatrix}, \tag{9.16}$$

with $m_0 = \frac{\tilde{y}_{\nu_1}^2 \Lambda v^2}{\tilde{y}_{\nu_2} v_{\varphi\nu}^2 + \tilde{y}_{\nu_3} v_{\rho\nu}^2}$, $y_4 = \frac{\tilde{y}_{\nu_4} v_{\varphi\nu}^2}{\tilde{y}_{\nu_2} v_{\varphi\nu}^2 + \tilde{y}_{\nu_3} v_{\rho\nu}^2}$ and $y_5 = \frac{\tilde{y}_{\nu_5} v_{\rho\nu}^2}{\tilde{y}_{\nu_2} v_{\varphi\nu}^2 + \tilde{y}_{\nu_3} v_{\rho\nu}^2}$.

One sees from Eq. (9.16) that the light neutrino mass matrix only depends on two complex parameters y_4 and y_5 and on the overall scale m_0 . As a result one expects sharp predictions both for neutrino masses as well as mixing parameters. As shown in D, the above block-diagonal matrix is exactly diagonalized as

$$U'_\nu{}^\dagger m'_\nu U'_\nu{}^* = \text{diag}(m_1, m_2, m_3), \quad U'_\nu = \begin{pmatrix} 1 & 0 & 0 \\ 0 & \cos \theta_\nu & \sin \theta_\nu e^{i\delta_\nu} \\ 0 & -\sin \theta_\nu e^{-i\delta_\nu} & \cos \theta_\nu \end{pmatrix}, \tag{9.17}$$

The charged lepton mass matrix m_l is already in diagonal form, consequently the lepton mixing matrix is determined to be

$$U = U_{TBM} U'_\nu = \frac{1}{\sqrt{6}} \begin{pmatrix} 2 & \sqrt{2} \cos \theta_\nu & \sqrt{2} \sin \theta_\nu e^{i\delta_\nu} \\ -1 & \sqrt{2} \cos \theta_\nu - \sqrt{3} \sin \theta_\nu e^{-i\delta_\nu} & \sqrt{3} \cos \theta_\nu + \sqrt{2} \sin \theta_\nu e^{i\delta_\nu} \\ -1 & \sqrt{2} \cos \theta_\nu + \sqrt{3} \sin \theta_\nu e^{-i\delta_\nu} & -\sqrt{3} \cos \theta_\nu + \sqrt{2} \sin \theta_\nu e^{i\delta_\nu} \end{pmatrix}. \tag{9.18}$$

We notice that the first column of the lepton mixing matrix is fixed to be $(2, -1, -1)^T/\sqrt{6}$ which coincides with the first column of the TBM mixing pattern. In other words, the lepton mixing matrix has trimaximal TM1 form [316–318].

From Eq. (9.18) one can extract the mixing angles and the leptonic Jarlskog invariant in the usual way, to find

$$\begin{aligned} \sin^2 \theta_{13} &= \frac{1}{3} \sin^2 \theta_\nu, & \sin^2 \theta_{12} &= \frac{1 + \cos 2\theta_\nu}{5 + \cos 2\theta_\nu}, \\ \sin^2 \theta_{23} &= \frac{1}{2} + \frac{\sqrt{6} \sin 2\theta_\nu \cos \delta_\nu}{5 + \cos 2\theta_\nu}, & J_{CP} &= -\frac{\sin 2\theta_\nu \sin \delta_\nu}{6\sqrt{6}}. \end{aligned} \quad (9.19)$$

One sees from Eq. (9.19) that all the three mixing angles and the Dirac CP phase δ_{CP} are given in terms of just two free parameters δ_ν and θ_ν . The above relations imply two predicted correlations amongst the mixing angles and the Dirac CP violation phase,

$$\cos^2 \theta_{12} \cos^2 \theta_{13} = \frac{2}{3}, \quad \cos \delta_{CP} = \frac{(3 \cos 2\theta_{12} - 2) \cos 2\theta_{23}}{3 \sin 2\theta_{23} \sin 2\theta_{12} \sin \theta_{13}}. \quad (9.20)$$

that characterize the TM1 mixing pattern.

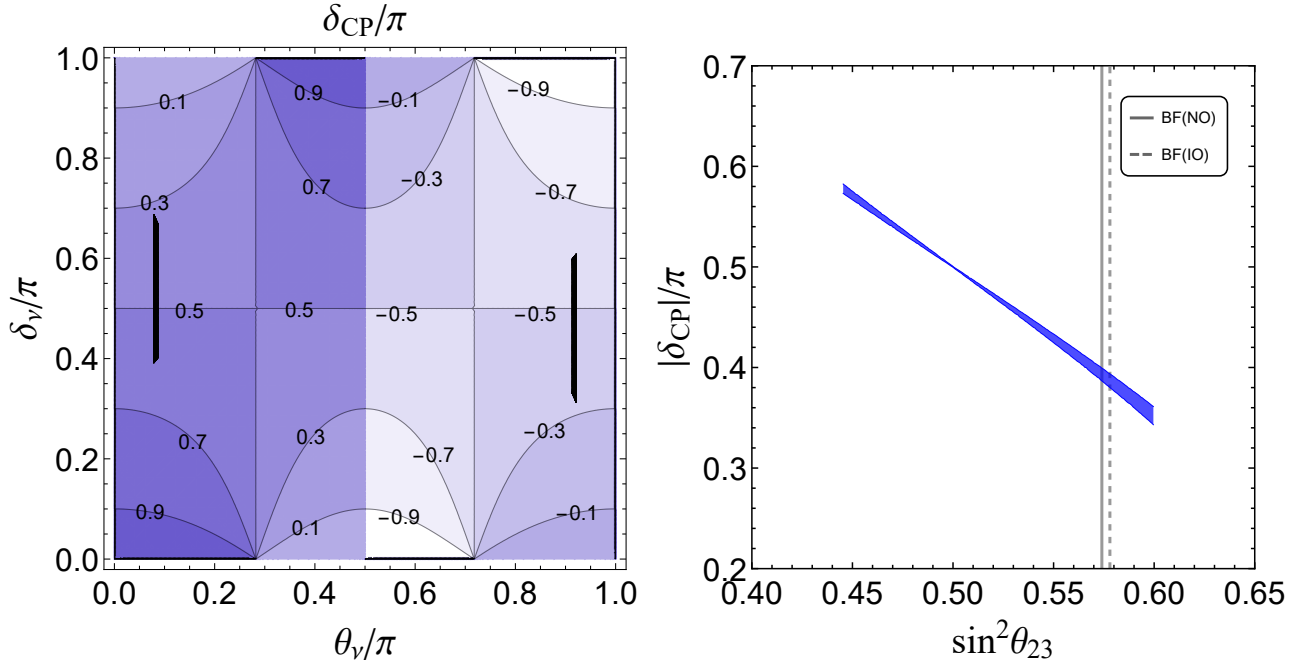


Figure 35: Contour plots of δ_{CP} in the $\theta_\nu - \delta_\nu$ plane (left) and predicted correlation between $|\delta_{CP}|$ and $\sin^2 \theta_{23}$ (right). The vertical solid/dashed lines in the right panel are the best-fit $\sin^2 \theta_{23}$ values for NO/IO spectra, respectively [24, 25].

In the left panel of figure 35 we display the contour plot of δ_{CP} in the plane δ_ν versus θ_ν . The small black areas in the left panel indicate the regions in which all three lepton mixing angles lie within their experimentally allowed 3σ ranges. The right panel of figure 35 shows a very tight correlation between $|\delta_{CP}|$ and the magnitude of the atmospheric angle θ_{23} . One sees that both octants are consistent, and that the CP phase parameter is predicted to lie in the restricted range $[0.325\pi, 0.592\pi]$. Upcoming long-baseline experiments will be able to test these predictions for θ_{23} and δ_{CP} [113, 114, 118].

We now turn to neutrinoless double beta decay. In figure 36 we display the expected values for the

effective Majorana neutrino mass $|m_{\beta\beta}|$ characterizing the $0\nu\beta\beta$ decay amplitude. If the neutrino mass spectrum is inverted-ordered (IO), the effective Majorana mass has a lower limit $|m_{\beta\beta}| \geq 0.0162$ eV, while the lightest neutrino mass satisfies $m_{\text{lightest}} \geq 0.0133$ eV. For the case of normal-ordering (NO), the effective mass $|m_{\beta\beta}|$ lies in the narrow interval $[5.2\text{meV}, 9.6\text{meV}]$, and the allowed range of m_{lightest} is $[4.8\text{meV}, 7.2\text{meV}]$. Clearly, as indicated in the figure, the predicted regions for the lightest neutrino mass and $|m_{\beta\beta}|$ are quite restricted. The existing experimental bounds as well as the estimated experimental sensitivities are also indicated by the horizontal bands [125–127] in figure 36. The predicted decay amplitudes do suggest a guaranteed $0\nu\beta\beta$ discovery at the forthcoming round of experiments [107].

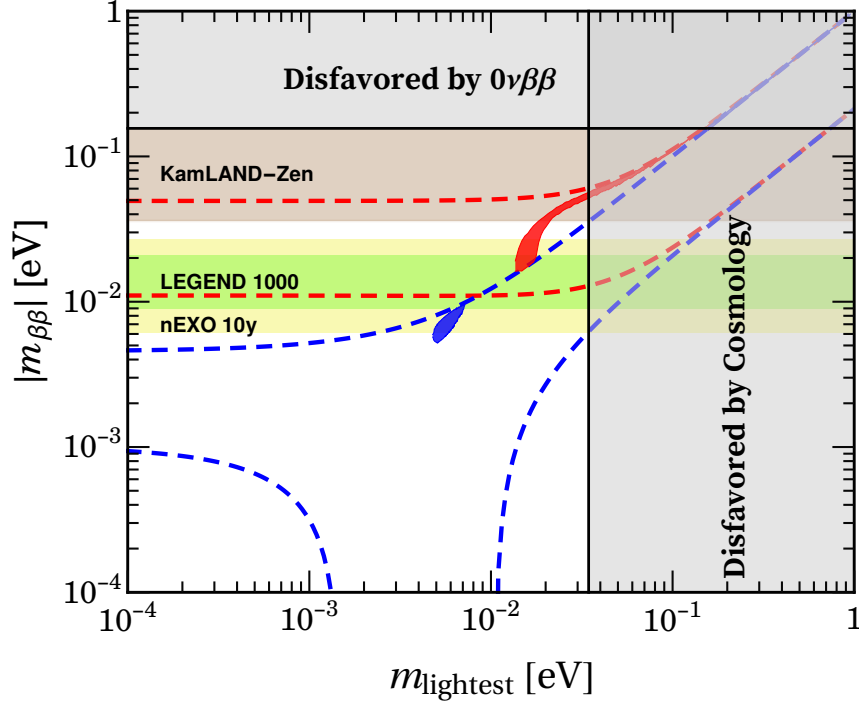


Figure 36: Predicted mass parameter characterizing the $0\nu\beta\beta$ decay amplitude; red and blue regions are for IO and NO neutrino mass spectra, respectively. Here we adopt the same convention as figure 22 for different bands and boundaries.

9.1.2 Quark masses and CKM matrix

This model can be extended to include quarks, the transformation properties of the quark fields under the family symmetry $T' \times Z_3 \times Z_4$ are listed in table 8. Note that no new scalars are needed, beyond the flavons φ_l and σ_l characterizing the lepton sector.

Field	Ψ_{UC}	Ψ_T	Ψ_u	Ψ_c	Ψ_t	Ψ_{ds}	Ψ_b	H	$\varphi_l(IR)$	$\sigma_l(IR)$
$SU(2)_L \times SU(2)_R \times U(1)_{B-L}$	$(2, 1, 1/3)$	$(2, 1, 1/3)$	$(1, 2, 1/3)$	$(1, 2, 1/3)$	$(1, 2, 1/3)$	$(1, 2, 1/3)$	$(1, 2, 1/3)$	$(2, 2, 0)$	$(1, 1, 0)$	$(1, 1, 0)$
T'	$\mathbf{2}$	$\mathbf{1}$	$\mathbf{1}'$	$\mathbf{1}''$	$\mathbf{1}'$	$\mathbf{2}'$	$\mathbf{1}''$	$\mathbf{1}$	$\mathbf{2}$	$\mathbf{1}''$
Z_3	ω^2	ω	1	ω^2	1	ω	ω^2	1	ω	ω
Z_4	1	-1	1	-1	-1	1	-1	1	-1	-1

Table 8: Classification of the quark fields under the bulk gauge group $SU(2)_L \times SU(2)_R \times U(1)_{B-L}$ and the flavour symmetry $T' \times Z_3 \times Z_4$.

The quark Yukawa interactions are localized on the IR brane and constrained by the T' flavour symmetry to be of the following form,

$$\begin{aligned}\mathcal{L}_Y^d &= \frac{\sqrt{G}}{\Lambda^3} \left[y_{ds_1} (\bar{\Psi}_{UC} H \Psi_{ds})_{\mathbf{3}} \varphi_l^{*2} + y_{ds_2} (\bar{\Psi}_{UC} H \Psi_{ds})_{\mathbf{1}'} \sigma_l^{*2} + y'_b (\bar{\Psi}_T H \Psi_b)_{\mathbf{1}''} \sigma_l^2 \right] \delta(y-L) + \text{h.c.} + \dots \\ \mathcal{L}_Y^u &= \frac{\sqrt{G}}{\Lambda^3} \left[y'_u \Lambda' (\bar{\Psi}_T H \Psi_u)_{\mathbf{1}'} \sigma_l + y_t \Lambda' (\bar{\Psi}_{UC} H \Psi_t)_{\mathbf{2}} \varphi_l^* + y_u (\bar{\Psi}_{UC} H \Psi_u)_{\mathbf{2}} \varphi_l \sigma_l \right. \\ &\quad \left. + y'_c (\bar{\Psi}_T H \Psi_c)_{\mathbf{1}''} \sigma_l^2 + y'_t (\bar{\Psi}_T H \Psi_t)_{\mathbf{1}'} \sigma_l^{*2} \right] \delta(y-L) + \text{h.c.} + \dots,\end{aligned}\quad (9.21)$$

for the down-type and up-type quark masses respectively. One can read out the mass matrices for the zero modes of the quark fields as

$$m^d = v \begin{pmatrix} \tilde{y}_{ds_2} v_{\sigma_1}^{*2} / \Lambda'^2 & 0 & 0 \\ \tilde{y}_{ds_1} v_{\varphi_1}^{*2} / \Lambda'^2 & \tilde{y}_{ds_2} v_{\sigma_1}^{*2} / \Lambda'^2 & 0 \\ 0 & 0 & \tilde{y}'_b v_{\sigma_1}^2 / \Lambda'^2 \end{pmatrix}, \quad (9.22)$$

$$m^u = v \begin{pmatrix} \tilde{y}_u v_{\varphi_1} v_{\sigma_1} / \Lambda'^2 & 0 & 0 \\ 0 & 0 & \tilde{y}_t v_{\varphi_1}^* / \Lambda' \\ \tilde{y}'_u v_{\sigma_1} / \Lambda' & \tilde{y}'_c v_{\sigma_1}^2 / \Lambda'^2 & \tilde{y}'_t v_{\sigma_1}^{*2} / \Lambda'^2 \end{pmatrix}. \quad (9.23)$$

where the parameters with tilde are given by

$$\tilde{y}_{u,t,ds_{1,2}} = \frac{y_{u,t,ds_{1,2}}}{L\Lambda'} f_L(L, c_{UC}) f_R(L, c_{u,t,ds}), \quad \tilde{y}'_{u,c,t,b} = \frac{y'_{u,c,t,b}}{L\Lambda'} f_L(L, c_T) f_R(L, c_{u,c,t,b}). \quad (9.24)$$

Notice that the down-quark mass matrix is block diagonal and the (11) and (22) entries are exactly equal. Note also that the up-quark sector gives a negligible contribution to the Cabibbo angle θ_c but is responsible for generating V_{ub} and V_{cb} . As a result this model gives rise to the well-known Gatto-Sartori relation $m_d/m_s \simeq \tan^2 \theta_c$ [469].

9.2 Global flavour fit

Let us now perform a global fit of the masses and flavour mixing parameters of both quarks and leptons within this model. The fundamental 5D scales on the UV and IR branes are taken to be $\Lambda \simeq k \simeq 2.44 \times 10^{18}$ GeV and $\Lambda' = k e^{-kL} \simeq 1.5$ TeV respectively. The vacuum expectation value of the Higgs field is fixed to its SM value $v \simeq 174$ GeV, and we choose the flavon VEVs as $v_{\varphi_1} / \Lambda' = v_{\sigma_1} / \Lambda' = v_{\varphi_\nu} / \Lambda = v_{\rho_\nu} / \Lambda = 0.2$. In what follows we give a typical set of values for the free parameters. The bulk mass parameters and the Yukawa coupling constants of the charged lepton and quarks are given by

$$\begin{aligned}c_l &= 0.460, \quad c_e = -0.725, \quad c_\mu = -0.553, \quad c_\tau = -0.117, \\ c_{UC} &= 0.587, \quad c_T = -0.980, \quad c_u = -0.516, \quad c_c = -0.555, \\ c_t &= 0.966, \quad c_{ds} = -0.503, \quad c_b = -0.532, \\ y_e &= y_\mu = y_\tau = 1.0, \quad y_u = 6.321, \quad y_t = 6.20, \quad y'_u = 4.00,\end{aligned}$$

$$y'_c = 1.00, \quad y'_t = 8.30, \quad y_{ds1} = 4.00, \quad y_{ds2} = 0.892, \quad y'_b = 4.00. \quad (9.25)$$

The values of the parameters in the neutrino sector depend on the neutrino mass ordering,

$$\begin{aligned} \text{NO} : c_\nu &= -0.404, \quad y_{\nu 1} = y_{\nu 2} = y_{\nu 3} = 1, \quad y_{\nu 4} = 0.235 + 0.0770i, \quad y_{\nu 5} = 0.340 + 0.0710i, \\ \text{IO} : c_\nu &= -0.383, \quad y_{\nu 1} = y_{\nu 2} = y_{\nu 3} = 1, \quad y_{\nu 4} = -0.354 + 0.275i, \quad y_{\nu 5} = -0.562 + 0.270i. \end{aligned} \quad (9.26)$$

The resulting predictions for flavour observables such as lepton and quark mass and mixing parameters are all listed in table 9. One sees that all Standard Model fermion masses and mixings can be very well reproduced.

parameters	best-fit $\pm 1\sigma$	predictions
$\sin \theta_{12}^q$	0.22500 ± 0.00100	0.22503
$\sin \theta_{13}^q$	0.003675 ± 0.000095	0.003668
$\sin \theta_{23}^q$	0.04200 ± 0.00059	0.04205
$\delta_{CP}^q / ^\circ$	66.9 ± 2	68.2
m_u [MeV]	$2.16^{+0.49}_{-0.26}$	2.16
m_c [GeV]	1.27 ± 0.02	1.27
m_t [GeV]	172.9 ± 0.4	172.90
m_d [MeV]	$4.67^{+0.48}_{-0.17}$	4.21
m_s [MeV]	93^{+11}_{-5}	93.00
m_b [GeV]	$4.18^{+0.03}_{-0.02}$	4.18
$\sin^2 \theta_{12}^l / 10^{-1}$ (NO)	$3.20^{+0.20}_{-0.16}$	3.19
$\sin^2 \theta_{12}^l / 10^{-1}$ (IO)		3.18
$\sin^2 \theta_{23}^l / 10^{-1}$ (NO)	$5.47^{+0.20}_{-0.30}$	5.47
$\sin^2 \theta_{23}^l / 10^{-1}$ (IO)		5.51
$\sin^2 \theta_{13}^l / 10^{-2}$ (NO)	$2.160^{+0.083}_{-0.069}$	2.160
$\sin^2 \theta_{13}^l / 10^{-2}$ (IO)		2.220
δ_{CP}^l / π (NO)	$1.32^{+0.21}_{-0.15}$	1.567
δ_{CP}^l / π (IO)		1.571
m_e [MeV]	$0.511 \pm 3.1 \times 10^{-9}$	0.511
m_μ [MeV]	$105.658 \pm 2.4 \times 10^{-6}$	105.658
m_τ [MeV]	1776.86 ± 0.12	1776.86
Δm_{21}^2 [10^{-5}eV^2] (NO)	$7.55^{+0.20}_{-0.16}$	7.55
Δm_{21}^2 [10^{-5}eV^2] (IO)		
$ \Delta m_{31}^2 $ [10^{-3}eV^2] (NO)	2.50 ± 0.03	2.50
$ \Delta m_{31}^2 $ [10^{-3}eV^2] (IO)		
χ^2 (NO)	—	7.65
χ^2 (IO)		7.66

Table 9: Global warped flavordynamics fit: neutrino oscillation parameters are taken from the global analysis in [24, 25], while the quark parameters are taken from the Review of Particle Physics [28].

All in all the model provides a consistent scenario for the flavour problem, in which fermion mass hierarchies are accounted for by adequate choices of the bulk mass parameters, while quark and lepton mixing angles are restricted by the assumed T' flavour symmetry. Note that in this model neutrinos are

Majorana particles, the tiny neutrino masses are generated by the type-I seesaw mechanism with “right-handed” neutrino masses in the range of $[10^{12}, 10^{13}]$ GeV and relatively sizeable rates for $0\nu\beta\beta$ decay, accessible within the next round of experiments. For an alternative warped flavourdynamics construction along the similar lines, see Ref. [78]. In that case the model uses the $\Delta(27)$ family symmetry, neutrinos are Dirac fermions, and the predicted neutrino mixing pattern is TM2.

10 Family symmetry from 6-D orbifolds

Underpinning the nature of the underlying family symmetry of particle physics amongst the huge plethora of possibilities constitutes a formidable task. As already seen in the previous section, a promising approach to the flavour problem is to imagine the existence of new dimensions in spacetime. In the present section we illustrate how the existence of extra dimensions may shed light on the nature of the family symmetry in four dimensions. The idea was suggested within six-dimensional setups compactified on a torus [292, 293].

The resulting theories share a realistic A_4 family symmetry, featuring the “golden” quark-lepton mass formula

$$\frac{m_\tau}{\sqrt{m_\mu m_e}} \approx \frac{m_b}{\sqrt{m_s m_d}}. \quad (10.1)$$

This formula was proposed in [288], and emerges also in other 4-D flavour schemes such as those in Refs. [289, 290] and [65, 66], as well as in implementations of the Peccei-Quinn symmetry [287]. It is remarkable that it also comes out neatly in scenarios where the family symmetry arises from the compactification of 6-dimensional orbifolds, as proposed in Refs. [143, 144, 294, 295] and considered next. Fermions are nicely arranged in terms of the A_4 family symmetry. Different setups can be identified, with very interesting phenomenology. Indeed, they bring in the possibility of predicting neutrino mixing angles and CP phases, as well as providing a good global description of flavour observables.

10.1 General preliminaries

Here we summarize the theory framework and survey its main features. First of all we have a 6-dimensional version of the standard $SU(3)_c \otimes SU(2)_L \otimes U(1)_Y$ gauge symmetry, supplemented with orbifold compactification, as outlined below. In the full six-dimensional theory, the spacetime manifold \mathcal{M} is identified as the direct product $\mathcal{M} = \mathbb{M}^4 \times (T^2/\mathbb{Z}_2)$, where \mathbb{M}^4 is the four-dimensional Minkowski spacetime, and T^2/\mathbb{Z}_2 is a one-parameter family (given by θ) of 2-D toroidal orbifolds defined by the following relations satisfied by the extra-dimensional coordinates

$$(x^5, x^6) = (x^5 + 2\pi R_1, x^6), \quad (10.2)$$

$$(x^5, x^6) = (x^5 + 2\pi R_2 \cos \theta, x^6 + 2\pi R_2 \sin \theta). \quad (10.3)$$

$$(x^5, x^6) = (-x^5, -x^6), \quad (10.4)$$

The first two equations define a torus, with θ describing its twist angle, and the third equation defines the \mathbb{Z}_2 orbifolding. For simplicity we assume that the characteristic radii of the compact extra dimensions are similar, i.e.

$$R_1 \sim R_2 \sim 1/M_c, \quad (10.5)$$

in terms of the compactification scale M_c . Moreover, the twist angle is assumed to be $\theta = 2\pi/3$. To simplify the analysis we define the scaled complex coordinate $z = M_c(x_5 + ix_6)/(2\pi)$ and rewrite Eqs. (10.2)-(10.4) as

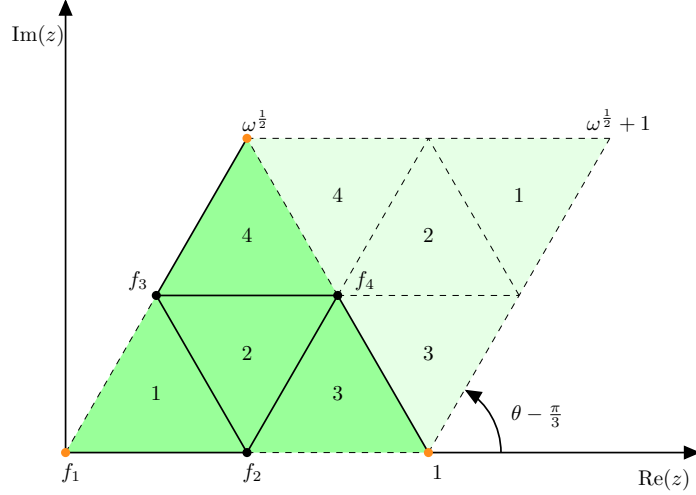


Figure 37: The fundamental domain of the T^2/\mathbb{Z}_2 orbifold is the darkest region, obtained after the compactification of the corresponding domain of the twisted torus, which includes the lightest region. The resulting space is reminiscent of a tetrahedron, and can be visualized by identifying the three orange dots into a single vertex. The fixed points of the orbifold are located at the vertices of the tetrahedron.

$$z = z + 1, \quad (10.6)$$

$$z = z + \omega, \quad (10.7)$$

$$z = -z, \quad (10.8)$$

where ω is the cubic root of unity

$$\omega \equiv e^{i\theta} = e^{i2\pi/3}. \quad (10.9)$$

A key feature of orbifolds is that they have singular points. In our case there are four of these, located at the points that remain fixed by the transformations in Eqs. (10.6)-(10.8), namely

$$f_1 = 0, \quad f_2 = \frac{1}{2}, \quad f_3 = \frac{\omega}{2}, \quad f_4 = \frac{1 + \omega}{2}. \quad (10.10)$$

These fixed points define the location of 4-dimensional branes embedded in the 6-dimensional space \mathcal{M} . In figure 37 we display both the fundamental domain of the twisted torus T^2 (light shaded green), as well as the fundamental domain of the T^2/\mathbb{Z}_2 orbifold (dark shaded green). After compactification, the continuous Poincaré symmetry of the two extra dimensions is broken, leaving a residual A_4 symmetry of the branes [314]. The appearance of the discrete A_4 symmetry can be understood as the invariance under permutations displayed by the four fixed points of the orbifold. Any of these can be written in terms of two independent transformations

$$S : z \longrightarrow z + 1/2, \quad T : z \longrightarrow \omega^2 z. \quad (10.11)$$

These can be also expressed as elements of the permutation group S_4 .

$$S = (12)(34), \quad T = (1)(243), \quad (10.12)$$

This way S and T are related to the generators of the A_4 group, satisfying

$$S^2 = T^3 = (ST)^3 = 1, \quad (10.13)$$

which are exactly the multiplication rules of the A_4 group in Eq. (A.1).

The model is based on this remnant A_4 as a family symmetry. Same-charge fields located on the four different branes would transform into each other by the remnant A_4 transformations. These four branes transform as the reducible representation $\mathbf{4}$, which decomposes as a sum of irreducible representations $\mathbf{4} \rightarrow \mathbf{3} + \mathbf{1}$. Thus, the brane-localized fields must transform under the flavour group as A_4 triplets or singlets, so the family symmetry is spontaneously broken. Below we show how this can provide a realistic pattern for the three families of leptons and quarks in a rather predictive and economical way.

Notice that the assumption of extra dimensions implies the existence of infinitely many 4-D fields associated with every bulk field, called a Kaluza-Klein (KK) tower. Their masses $(n^2 + m^2)M_c$ are determined by positive integers n, m . In our case, the fields in the bulk are the SM gauge fields g_μ, W_μ, B_μ , the right-handed quarks u_i^c and the gauge singlet scalar σ .

The tower of massive KK modes from the vector $SU(2)_L$ triplets can affect the Peskin-Takeuchi oblique parameters S, T and U in an important way. The current experimental bound for our setup (2 non-universal extra dimensions) is [470, 471]

$$M_c > 2.1 \text{ TeV}.$$

For a compactification scale sufficiently close to 2 TeV, the electroweak precision tests could in principle probe the extra dimensions at the High Luminosity LHC run.

10.2 Scotogenic orbifold

Our basic setup is a 6-dimensional extension of the Standard $SU(3)_c \otimes SU(2)_L \otimes U(1)_Y$ Model, featuring the orbifold compactification described in the previous section, and inheriting the A_4 discrete family symmetry in a natural manner. Its simplest model-realization includes three right-handed neutrinos, mediating neutrino mass generation through the type-I seesaw mechanism [143, 144]. Instead of pursuing such an approach, however, here we focus on a more complete, yet equally economical, scotogenic variant that also provides a WIMP dark matter candidate [294, 295].

The field content and transformation properties of our benchmark scotogenic variant under the various symmetry groups are shown in table 10. Note that all fermionic fields, except for the right-handed quarks, transform as flavour triplets and are localized in the orbifold branes.

Field	SU(3) _C	SU(2) _L	U(1) _Y	\mathbb{Z}_4	A_4	Location
L	1	2	-1	1	3	Brane
d^c	3	1	2/3	1	3	Brane
e^c	1	1	2	1	3	Brane
Q	3	2	1/3	1	3	Brane
$u_{1,2,3}^c$	3	1	-4/3	-1	1'', 1', 1	Bulk
F	1	1	0	i	3	Brane
H_u	1	2	1	-1	3	Brane
H_d	1	2	-1	1	3	Brane
η	1	2	1	$-i$	1	Brane
σ	1	1	0	-1	3	Bulk

Table 10: Field representation content and symmetries of the scotogenic orbifold model [295].

The model assumes an auxiliary lepton quarticity symmetry [165, 167]. This \mathbb{Z}_4 is spontaneously broken to a residual \mathbb{Z}_2 symmetry, defining the “dark sector” which comprises the dark fermion F and scalar η . Both transform non-trivially under the “dark symmetry” ensuring stability of the lightest \mathbb{Z}_2 -charged field. This makes it a potentially viable dark matter candidate, whose stability is directly related to the radiative origin of neutrino masses, Fig. 38.

The Higgs sector consists of two flavour-triplet weak iso-doublets, H_u and H_d and a SM singlet scalar σ driving the spontaneous breaking of both lepton number [32, 39], as well as family symmetry, a sort of “flavoured” Majoron scheme.

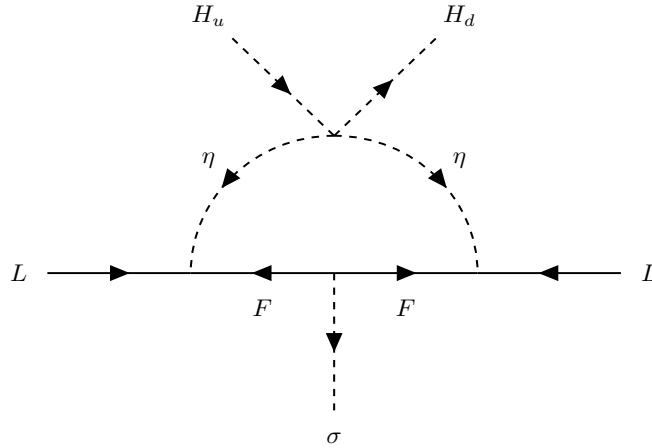


Figure 38: One-loop diagram for Majorana neutrino masses, mediated by the “dark sector” particles [295].

Given the defining symmetries of the model, one can write the most general effective Yukawa Lagrangian below the compactification scale. The Yukawa interaction terms of down-type quarks and charged leptons have the same structure, given by

$$\mathcal{L}_{H_d}^{\text{Yukawa}} = y_1^e (LH_d e^c)_{1_1} + y_2^e (LH_d e^c)_{1_2} + y_1^d (QH_d d^c)_{1_1} + y_2^d (QH_d d^c)_{1_2} + \text{H.c.}, \quad (10.14)$$

while the transformation properties of the up-type quark fields under A_4 yield

$$\mathcal{L}_{H_u}^{\text{Yukawa}} = y_1^u (QH_u)_{\mathbf{1}'} u_1^c + y_2^u (QH_u)_{\mathbf{1}''} u_2^c + y_3^u (QH_u)_{\mathbf{1}} u_3^c + \text{H.c.} \quad (10.15)$$

Notice that the bold subscripts in each term indicate its transformation properties under the remnant A_4 family symmetry. The explicit expressions for the invariant multiplet products are given in [A](#).

The dark fermion triplet F couples to the scalar field σ . The latter acquires a vacuum expectation value which drives the spontaneous breaking of lepton number symmetry, \mathbb{Z}_4 , and the A_4 family symmetry, giving rise to Majorana mass terms for the dark fermions,

$$\mathcal{L}_{\sigma}^{\text{Yukawa}} = y^{\sigma} (F^T F \sigma)_{\mathbf{1}_1} + \text{H.c.} \quad (10.16)$$

The dark scalar η plays a crucial role in the model, as it couples with both dark fermions and neutrinos

$$\mathcal{L}_{\eta}^{\text{Yukawa}} = y_1^{\eta} (L \eta F)_{\mathbf{1}} + \text{H.c.} \quad (10.17)$$

In the following, we will assume that all Yukawa couplings are real, and therefore that the model preserves a trivial CP symmetry.

10.3 Symmetry breaking and fermion masses

The scalar potential $V(H_d, H_u, \eta, \sigma)$ comprises all terms up to quartic interactions consistent with all the symmetries. Apart from the Higgs scalars H_d, H_u, σ it contains also the dark scalar η which does not develop a vacuum expectation value (VEV). The symmetry breakdown of the model proceeds in two steps. At high energies the electroweak singlet scalar field σ develops a VEV compatible with the extra-dimensional boundary conditions. Subsequently, at lower energies, the electroweak Higgs doublets H_u, H_d acquire VEVs according to the minimization of the scalar potential.

In order to describe the high-scale A_4 symmetry breaking produced by σ we introduce a boundary condition P , consistent with the orbifold construction. It defines a non-trivial gauge/Poincaré twist of the orbifold, and must be a symmetry of the Lagrangian. We assume that the transformation P acts trivially on the A_4 singlet bulk fields. Hence the only bulk field transforming non-trivially under P is the flavour triplet scalar σ , obeying the boundary condition

$$\sigma(x, z) = P\sigma(x, -z). \quad (10.18)$$

so as to be consistent with Eq. (10.8). The invariance of the kinetic term of the σ field in the 6-D Lagrangian implies that $P \in SU(3)$, while the condition in Eq. (10.18) ensures that the matrix P will leave invariant the interactions of fields in the brane. Thus the boundary condition matrix must satisfy

$$P \in SU(3), \quad P^2 = \mathbf{1}_{3 \times 3}, \quad P^\dagger = P. \quad (10.19)$$

The boundary condition on the σ field applies also to its VEV alignment. As a result, the masses of the dark fermions F are a direct outcome of the boundary condition of the bulk field σ in the two extra dimensions

$$\langle \sigma \rangle = P \langle \sigma \rangle. \quad (10.20)$$

The boundary condition matrix P is a property of the orbifold, its form is given explicitly in [295]. Here we adopt the most general VEV alignment consistent with the spontaneous breaking of lepton number and the A_4 family symmetry, expressed as

$$\langle \sigma \rangle = v_\sigma \begin{pmatrix} \epsilon_1^\sigma e^{i\varphi} \\ \epsilon_2^\sigma \\ 1 \end{pmatrix}, \quad \text{with} \quad v_\sigma, \epsilon_1^\sigma, \epsilon_2^\sigma \in \mathbb{R} \quad \text{and} \quad 0 \leq \varphi < \pi. \quad (10.21)$$

Here we will not present a dedicated analysis of the scalar potential, except to stress the importance of the λ_5 term for the neutrino mass generation mechanism, namely

$$V(H_u, H_d, \eta) \supset \frac{1}{2} \lambda_5 \left[(H_d^T (i\sigma_2) \eta)_{\mathbf{3}} (H_u^\dagger \eta)_{\mathbf{3}} \right]_1 + \text{H.c.} \quad (10.22)$$

Here λ_5 is a coupling constant and σ_2 is the second Pauli matrix. This term lifts the degeneracy of the mass eigenstates of the neutral components of η , denoted as $\sqrt{2} \text{Re}(\eta^0)$ and $\sqrt{2} \text{Im}(\eta^0)$, playing a key role in the scotogenic generation of neutrino masses at the one-loop level, as illustrated in Fig. 38. One can show that there is enough freedom in parameter space to drive the spontaneous breaking of the gauge symmetries down to $U(1)_{\text{EM}}$.

10.3.1 Quark and lepton masses

Since A_4 breaks spontaneously at the v_σ scale, in the second stage of spontaneous symmetry breaking, we assume that the weak iso-doublets H_u and H_d obtain the most general A_4 breaking VEVs consistent with trivial CP symmetry. For real $v_u, v_d, \epsilon_{1,2}^{u,d}$ it is given as

$$\langle H_u \rangle = v_u \begin{pmatrix} \epsilon_1^u \\ \epsilon_2^u \\ 1 \end{pmatrix}, \quad \langle H_d \rangle = v_d \begin{pmatrix} \epsilon_1^d \\ \epsilon_2^d \\ 1 \end{pmatrix}. \quad (10.23)$$

After spontaneous symmetry breaking, the up-quark mass matrix becomes

$$M_u = v_u \begin{pmatrix} y_1^u \epsilon_1^u & y_2^u \epsilon_1^u & y_3^u \epsilon_1^u \\ y_1^u \epsilon_2^u \omega^2 & y_2^u \epsilon_2^u \omega & y_3^u \epsilon_2^u \\ y_1^u \omega & y_2^u \omega^2 & y_3^u \end{pmatrix}, \quad (10.24)$$

while the down-quark and charged lepton mass matrices take the form

$$\begin{aligned}
M_d &= v_d \begin{pmatrix} 0 & y_1^d \epsilon_1^d & y_2^d \epsilon_2^d \\ y_2^d \epsilon_1^d & 0 & y_1^d \\ y_1^d \epsilon_2^d & y_2^d & 0 \end{pmatrix}, \\
M_e &= v_d \begin{pmatrix} 0 & y_1^e \epsilon_1^d & y_2^e \epsilon_2^d \\ y_2^e \epsilon_1^d & 0 & y_1^e \\ y_1^e \epsilon_2^d & y_2^e & 0 \end{pmatrix}.
\end{aligned} \tag{10.25}$$

All Yukawa couplings in the last two equations are assumed to be real due to our imposition of trivial CP symmetry.

10.3.2 Scotogenic neutrino masses

The A_4 flavour symmetry structure of the Yukawa term in Eq. (10.16) implies that the Majorana mass matrix of the dark fermions M_F must have the following structure

$$M_F = y_\sigma v_\sigma \begin{pmatrix} 0 & 1 & \epsilon_2^\sigma \\ 1 & 0 & \epsilon_1^\sigma e^{i\varphi} \\ \epsilon_2^\sigma & \epsilon_1^\sigma e^{i\varphi} & 0 \end{pmatrix}. \tag{10.26}$$

In order to describe our one-loop scotogenic mechanism for neutrino masses we write the dark fermion F fields in the mass eigenstate basis (\tilde{F}) by performing the singular value decomposition of the dark fermion mass matrix M_F . Since the latter is symmetric, only one unitary matrix V is needed in the Takagi decomposition [30],

$$y^\sigma (F^T F \sigma)_{\mathbf{1}_1} = F^T M_F F = F^T V^T D V F = (V F)^T D (V F) \equiv \tilde{F}^T D \tilde{F}, \tag{10.27}$$

where $D = \text{diag}(m_{F_1}, m_{F_2}, m_{F_3})$ and $\tilde{F} \equiv V F$ denotes the dark fermion triplet expressed in the mass eigenstate basis. We can then rewrite Eq. (10.17) as

$$\mathcal{L}_\eta^{\text{Yukawa}} = y_1^\eta \eta \left(L V^\dagger \tilde{F} \right) + \text{H.c.} \tag{10.28}$$

As already mentioned, neutrino masses are forbidden at tree-level due to the auxiliary \mathbb{Z}_4 symmetry. However, thanks to the mediation of the dark fields η and F , neutrino masses emerge at one-loop through the diagram depicted in Fig. 38, which has the basic scotogenic structure [196].

Defining $y_1^\eta V^\dagger \equiv h$ in Eq. (10.27) we can write the expression for the one-loop neutrino mass matrix M_ν as

$$(M_\nu)_{ij} = \sum_k^3 \frac{h_{ik} (h^T)_{kj}}{16\pi^2} S(m_{F_k}), \tag{10.29}$$

where $S(m_{F_k})$ is for the loop factor

$$S(m_{F_k}) = m_{F_k} \left(\frac{m_R^2}{m_R^2 - m_{F_k}^2} \ln \frac{m_R^2}{m_{F_k}^2} - \frac{m_I^2}{m_I^2 - m_{F_k}^2} \ln \frac{m_I^2}{m_{F_k}^2} \right), \quad (10.30)$$

with $m_R = m(\sqrt{2} \operatorname{Re} \eta^0)$, $m_I = m(\sqrt{2} \operatorname{Im} \eta^0)$ with

$$m_R^2 - m_I^2 \equiv 2\lambda_5 (\langle H_u \rangle_{\mathbf{3}} \langle H_d \rangle_{\mathbf{3}})_1. \quad (10.31)$$

Neutrino masses are not only loop-suppressed, but also symmetry-protected, as they vanish in the limit $\lambda_5 \rightarrow 0$, see Eq. (10.22).

After spontaneous symmetry breaking, the auxiliary \mathbb{Z}_4 breaks down to a residual \mathbb{Z}_2 that stabilizes the lightest dark particle. There are two possible dark matter candidates: the lightest state in the complex neutral scalar η , or the lightest Majorana fermion in the flavour triplet F . In either case, the phenomenology of dark matter is qualitatively similar to that of other scotogenic scenarios, which has been extensively discussed, see for example Ref. [138] and references therein.

10.4 Global fit of flavour observables

Before describing the global fit of flavour observables, some preliminaries are necessary. The bottom line is that, due to the reduced number of parameters, the model makes strong flavour predictions.

10.4.1 Preliminaries

Here we adopt the symmetrical parametrization of the quark and lepton mixing matrices [30], described in Sect. 1. For the case of quarks, choosing the PDG ordering prescription, the symmetrical form leads to the standard Cabibbo-Kobayashi-Maskawa (CKM) matrix in Eq. (1.8). On the other hand, for the mixing of leptons, it is described by Eq. (1.21)²⁴. In both cases the mixing matrix description is supplemented by the PDG factor ordering convention. However, in the leptonic case the symmetrical form provides a neater description of CP violation than the PDG form. In this case the Dirac CP phase that enters in neutrino oscillations is the leptonic analogue of the quark Jarlskog parameter, identified with the “rephasing-invariant” combination

$$\delta^\ell = \phi_{13} - \phi_{12} - \phi_{23}.$$

Notice that this phase must not be present in the effective mass parameter $\langle m_{\beta\beta} \rangle$ characterizing the amplitude for neutrinoless double beta decay, which involves only the two Majorana phases, Eq. (1.25). Hence the symmetrical presentation is more transparent for describing the $0\nu\beta\beta$ decay amplitude [99].

²⁴In both cases we assume unitarity, neglecting therefore possible mixing with exotic fermions that could be relevant, say, within a low-scale seesaw scheme [472].

10.4.2 Fit procedure

The above model is characterized by 16 independent parameters in the flavour sector, identified as follows: 8 real Yukawa couplings $y_{1,2}^{e,d}$, $y_{1,2,3}^u$, y_1^η , 6 real VEV ratios $\epsilon_{1,2}^{u,d}$, $\epsilon_{1,2}^\sigma$, one quartic coupling λ_5 and one CP violating phase φ contained in $\langle\sigma\rangle$. These parameters describe 22 observables, namely, 12 masses, 4 CKM matrix elements, plus 6 lepton mixing matrix parameters including the 2 Majorana phases.

In order to explore the predictivity of the model, we perform a global flavour fit to the available experimental data, by minimizing the chi-square function defined as

$$\chi^2 = \sum (\mu_{\text{exp}} - \mu_{\text{model}})^2 / \sigma_{\text{exp}}^2, \quad (10.32)$$

where the sum runs through the 19 measured physical parameters, i.e. 6 quark masses, 3 CKM mixing angles, 1 CKM CP phase, 3 charged lepton masses, 3 lepton mixing angles, 1 lepton CP violating phase and 2 neutrino squared mass splittings. Note that we have only limits on the lightest neutrino mass from experiment and no direct information on the Majorana $0\nu\beta\beta$ phases. The fit is performed by scanning the values of the 16 independent model parameters that provide a description of the above 22 flavour observables.

In our chi-square minimization with respect to the 16 independent model parameters, all quark and charged-lepton masses were evaluated at the same energy scale, chosen as M_Z [473]. This assumption was shown to be consistent with the golden mass relation [143]. Coming to the neutrino oscillation parameters, these were extracted from the global fit in [24, 25], neglecting the effect of running to M_Z [473, 474]. The remaining observables were taken from the PDG [28]. In order to extract the flavour observables from the mass matrices in Eqs. (10.24) and (10.25) we use the Mathematica Mixing Parameter Tools package [475].

The results of our flavour fit are summarized in table 11. The minimum at $\chi^2 \approx 2$ shows that the model reproduces the observed pattern of fermion masses and mixing rather well. From Table 11 one can read directly the predictions of the model concerning the mass of the lightest neutrino and the values of the CP phases characterizing the lepton sector.

10.5 Flavour predictions of the scotogenic orbifold model

We now discuss in more detail the flavour predictions of our scotogenic orbifold model, both in the quark and lepton sectors. These follow directly from the A_4 family symmetry that results from the orbifold compactification of the extra dimensions.

10.5.1 Golden quark-lepton mass relation

This is a key feature of the model that results from the down-type quarks and charged lepton assignments under the A_4 flavour symmetry. Indeed, after spontaneous symmetry breaking these obtain masses from the same common Higgs doublet H_d , leading to the mass matrices in Eq.(10.25). After diagonalization

to physical mass-eigenstates, one obtains the golden quark-lepton mass relation

$$\frac{m_\tau}{\sqrt{m_\mu m_e}} \approx \frac{m_b}{\sqrt{m_s m_d}}, \quad (10.33)$$

This relation emerges in models with SO(3) family symmetry implementing a Peccei-Quinn symmetry [287], and in the theories proposed in Refs. [65, 66] and [288–290].

In our case the golden relation is a common feature of the models with A_4 family symmetry arising from the compactification of 6-Dimensional orbifolds, proposed in Refs. [143, 144] and further discussed in [294, 295]. One can show that, given the current experimental measurements of the relevant masses, the golden relation holds with good precision, see for example, Fig.1 in [143]. Besides, it constitutes a very robust prediction under the renormalization group evolution, as it involves only fermion mass ratios.

Parameter	Value	Observable	Data		Model best fit
			Central value	1 σ range	
$y_1^e v_d / \text{GeV}$	-1.745	$\theta_{12}^\ell / ^\circ$	34.3	33.3 \rightarrow 35.3	33.0
$y_2^e v_d / (10^{-1} \text{GeV})$	1.021	$\theta_{13}^\ell / ^\circ$	8.45	8.31 \rightarrow 8.61	8.52
$y_1^d v_d / (10^{-2} \text{GeV})$	-5.039	$\theta_{23}^\ell / ^\circ$	49.26	48.47 \rightarrow 50.05	50.44
$y_2^d v_d / \text{GeV}$	2.852	$\delta^\ell / ^\circ$	194	172 \rightarrow 218	192
$y_1^u v_u / (10^{-1} \text{GeV})$	6.074	m_e / MeV	0.486	0.486 \rightarrow 0.486	0.486
$y_2^u v_u / (10^2 \text{GeV})$	1.712	m_μ / GeV	0.102	0.102 \rightarrow 0.102	0.102
$y_3^u v_u / \text{GeV}$	7.157	m_τ / GeV	1.745	1.743 \rightarrow 1.747	1.745
$\epsilon_1^u / 10^{-4}$	7.055	$\Delta m_{21}^2 / (10^{-5} \text{eV}^2)$	7.50	7.30 \rightarrow 7.72	7.50
$\epsilon_2^u / 10^{-2}$	-5.044	$\Delta m_{31}^2 / (10^{-3} \text{eV}^2)$	2.55	2.52 \rightarrow 2.57	2.54
$\epsilon_1^d / 10^{-3}$	-2.814	m_1 / meV			135.35
$\epsilon_2^d / 10^{-3}$	5.833	m_2 / meV			135.63
ϵ_1^σ	1.501	m_3 / meV			144.43
ϵ_2^σ	-0.654	$\phi_{12} / ^\circ$			87.01
φ	3.527	$\phi_{13} / ^\circ$			190.30
$(y_1^n)^2 y_\sigma v_\sigma / (\text{KeV})$	1.813	$\phi_{23} / ^\circ$			271.05
$2\lambda_5 \langle H_u \rangle \langle H_d \rangle / (\text{KeV})^2$	0.012	$\theta_{12}^q / ^\circ$	13.04	12.99 \rightarrow 13.09	13.04
		$\theta_{13}^q / ^\circ$	0.20	0.19 \rightarrow 0.22	0.20
		$\theta_{23}^q / ^\circ$	2.38	2.32 \rightarrow 2.44	2.38
		$\delta^q / ^\circ$	68.75	64.25 \rightarrow 73.25	60.23
		m_u / MeV	1.28	0.76 \rightarrow 1.55	1.28
		m_c / GeV	0.626	0.607 \rightarrow 0.645	0.626
		m_t / GeV	171.6	170 \rightarrow 173	171.6
		m_d / MeV	2.74	2.57 \rightarrow 3.15	2.49
		m_s / MeV	54	51 \rightarrow 57	54
		m_b / GeV	2.85	2.83 \rightarrow 2.88	2.85
		χ^2			1.96

Table 11: Flavour parameters and observables: measured versus predicted values for the best fit point.

10.5.2 Neutrino oscillation predictions

In order to identify the predictions of the model concerning the oscillation parameters we have randomly varied the parameters around the global best fit point in Table 11, while requiring compatibility with all measured flavour observables at 3σ . The results of the analysis are given in Fig 39, where the blue contours represent the 90, 95, and 99% C.L. profiles from the Valencia global oscillation fit in [24, 25], while the purple dots indicate regions compatible at 3σ with all experimental data. The best fit point of the global oscillation fit is marked with a black star, while that of the global flavour fit is indicated by a white cross. One sees from Fig. 39 how the predicted values of the leptonic Dirac CP phase are restricted

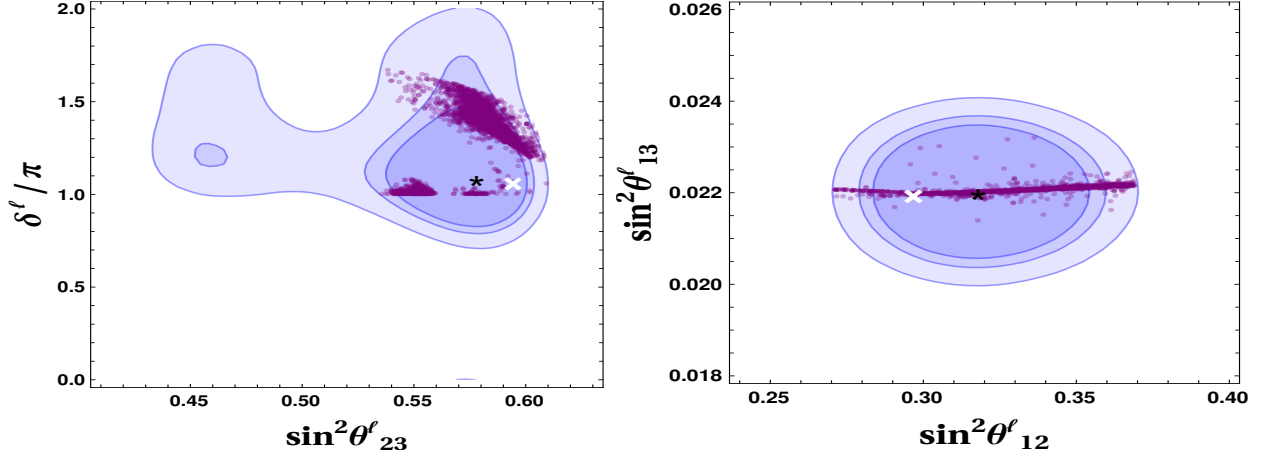


Figure 39: Allowed values for the mixing angles and the leptonic Dirac CP phase. The purple points are compatible at 3σ with all flavour observables, while the blue shades are the generic 90, 95 and 99% C.L. regions of the global oscillation fit in [24, 25]. The black star is the central point of the global oscillation fit, while the white cross stands for the best fit point in Table 11.

to the range $\delta^\ell \geq \pi$, while the atmospheric angle θ_{23}^ℓ is required to lie in the higher octant. Besides, one sees from the right panel in Fig. 39 a sharp prediction for the reactor angle θ_{13}^ℓ , see also table 11.

A scan of the parameter space of the model consistent at 3σ with all current experiments reveals that only the Normal Ordered (NO) neutrino mass spectrum is possible. Indeed, the best fit point in table 11 has positive Δm_{31}^2 , corresponding to NO, and a rather high absolute scale for the neutrino masses.

10.5.3 Neutrinoless double beta decay predictions

Concerning neutrinoless double beta decay, using the Majorana phase and neutrino mass predictions of table 11 in Eq. (1.25), one finds the preferred effective amplitude parameter:

$$|m_{\beta\beta}| = 58.08 \text{ meV}. \quad (10.34)$$

A detailed analysis is presented in figure 40, where we show in purple the region of predicted $|m_{\beta\beta}|$ values as a function of the lightest neutrino mass m_1 . To be conservative, we randomly varied the model parameters within the allowed 3σ range. The best fit point from table 11 is marked in red. One sees that the predicted central value of $|m_{\beta\beta}|$ lies inside the current exclusion band of Kamland-Zen (36 – 156 meV) [125].

shown in orange in Fig. 40. This will also be probed by cosmological observations and possibly by future beta decay endpoint studies. We also display the projected sensitivities of the next round of $0\nu\beta\beta$ experiments LEGEND [476] and nEXO [477] as the colored horizontal bands.

Notice that the central value of the lightest neutrino mass m_1 obtained from the global fit is disfavored by the latest results of the Planck collaboration on the sum of light neutrino masses [128]. This tension is further enhanced by the addition of Baryon Acoustic Oscillations (BAO) data [124], see vertical band in lighter gray in figure 40. Beyond the central prediction, however, there is a broad parameter region consistent both with measured flavour observables as well as with the cosmological bounds.

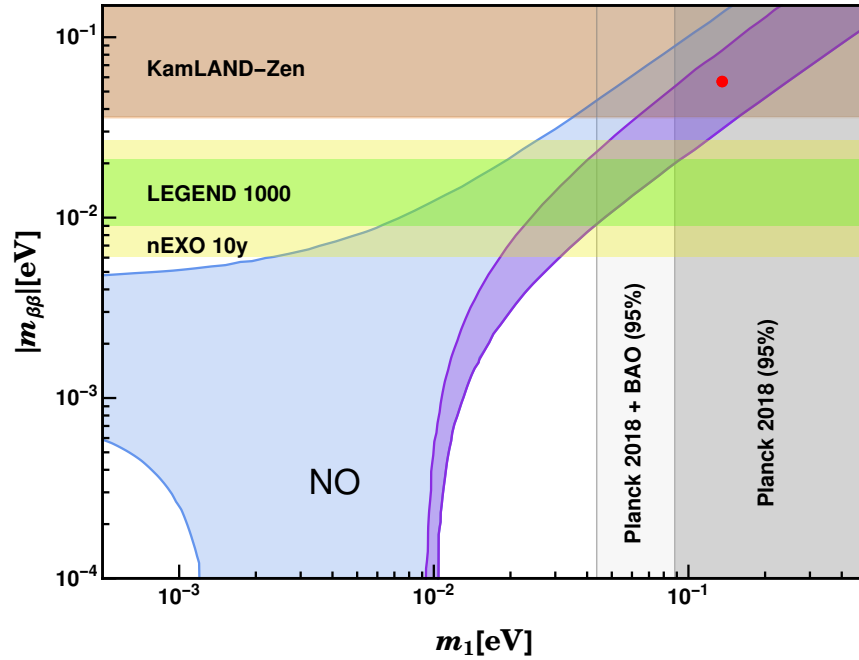


Figure 40: Effective $0\nu\beta\beta$ decay amplitude versus the lightest neutrino mass m_1 . From the global fit one finds that only normal ordering is allowed. The blue region is the generic one consistent with oscillations at 2σ . The purple region is the one allowed at 3σ around the global best fit point in table 11, marked in red. The current KamLAND-Zen limit is shown in brown, and the projected sensitivities of future experiments LEGEND-1000 and nEXO are indicated with light yellow and light green horizontal bands respectively. The vertical gray bands represent the current sensitivity of cosmological data from the Planck collaboration (dark gray), and in combination with BAO data (light gray) [128, 129]

11 Recent progress: modular symmetry

In flavour symmetry models, complicated vacuum alignment assumptions are often required to break the flavor symmetry. The vacuum expectation values of the associated flavons should be conveniently oriented in family space. Moreover, higher-dimensional operators with flavon insertions and unknown coefficients are often present, affecting the resulting model predictions. In order to alleviate these shortcomings modular invariance as flavor symmetry has been recently proposed [478]. In what follows we briefly sketch recent work, for dedicated reviews on modular symmetries see Refs. [91, 479, 480].

11.1 The modular group

The modular group $SL(2, \mathbb{Z})$ is the group of 2×2 integer matrices with determinant one,

$$SL(2, \mathbb{Z}) = \left\{ \begin{pmatrix} a & b \\ c & d \end{pmatrix} \middle| a, b, c, d \in \mathbb{Z}, ad - bc = 1 \right\}. \quad (11.1)$$

The modular group $SL(2, \mathbb{Z})$ acts on the complex variable τ in the upper-half plane as the linear fractional transformation [481]

$$\gamma\tau = \frac{a\tau + b}{c\tau + d} \quad \text{for } \gamma = \begin{pmatrix} a & b \\ c & d \end{pmatrix} \in SL(2, \mathbb{Z}) \quad \text{and } \text{Im}(\tau) > 0. \quad (11.2)$$

One sees that γ and $-\gamma$ induce the same linear fraction transformation.

The modular group can be generated by the two generators S and T ,

$$S = \begin{pmatrix} 0 & 1 \\ -1 & 0 \end{pmatrix}, \quad T = \begin{pmatrix} 1 & 1 \\ 0 & 1 \end{pmatrix}, \quad (11.3)$$

which lead to duality and shift symmetries of τ as follows,

$$\tau \xrightarrow{S} -\frac{1}{\tau}, \quad \tau \xrightarrow{T} \tau + 1. \quad (11.4)$$

Any value of τ in the upper half complex plane can be shifted in to the region of $-\frac{1}{2} \leq \text{Re}(\tau) < \frac{1}{2}$ by multiple T transformations. Moreover, it can be mapped to the region $|\tau| \leq 1$ by an S transformation. As a consequence, the complex modulus τ could be restricted to the fundamental domain \mathcal{F} of the modular group,

$$\mathcal{F} = \left\{ \tau \middle| -\frac{1}{2} \leq \text{Re}(\tau) < \frac{1}{2}, \text{Im}(\tau) > 0, |\tau| > 1 \right\} \cup \left\{ \tau \middle| -\frac{1}{2} \leq \text{Re}(\tau) \leq 0, \text{Im}(\tau) > 0, |\tau| = 1 \right\}, \quad (11.5)$$

which is displayed in figure 41. Every complex modulus τ can be mapped into the fundamental domain by a modular transformation of Eq. (11.2), and no two points in \mathcal{F} can be related by modular transformations. Notice the right half boundary of \mathcal{F} is not included into the fundamental domain, since it can related

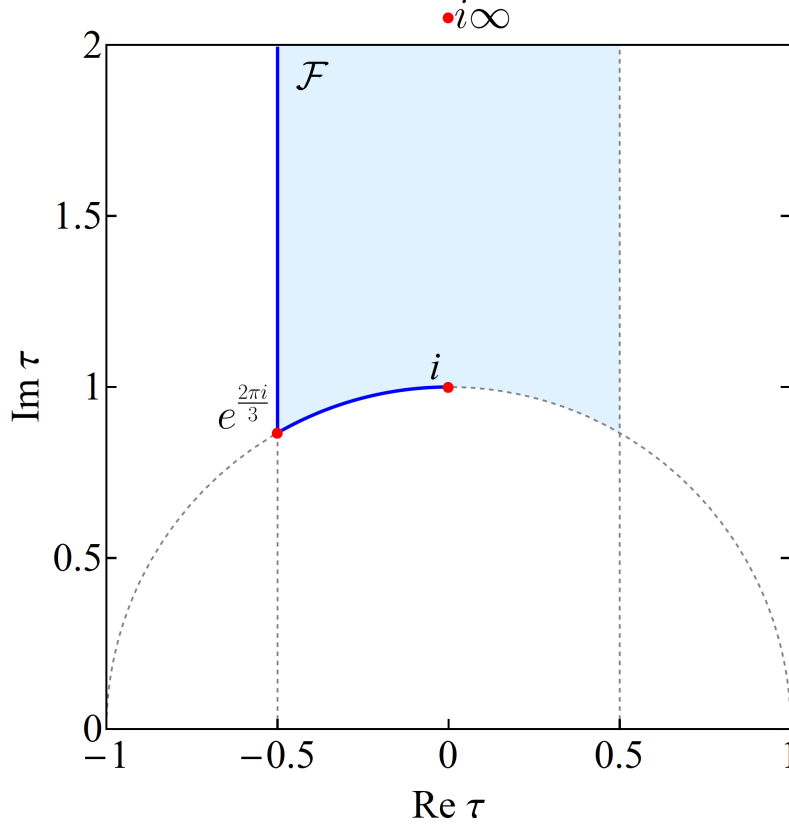


Figure 41: The fundamental domain \mathcal{F} of the modular group, where the red points denote the three fixed points $\tau_0 = i, e^{2\pi i/3}, i\infty$ which preserve a residual modular symmetry.

to the left half boundary by some modular transformation. Moreover, no value of τ is left invariant by the whole modular group action of Eq. (11.2). In the fundamental domain, there are only three fixed points $\tau_0 = i, e^{2\pi i/3}, i\infty$ which break the modular group $SL(2, \mathbb{Z})$ partially. These are invariant under the modular transformations S, ST and T respectively [481–483]. Notice that each τ is trivially invariant under S^2 which is a negative identity matrix.

Modular symmetry provides a novel origin of discrete flavor symmetry through the quotient of $SL(2, \mathbb{Z})$ by the principal congruence subgroup of level N which is defined as,

$$\Gamma(N) = \left\{ \begin{pmatrix} a & b \\ c & d \end{pmatrix} \in SL(2, \mathbb{Z}) \left| a, d = 1 \pmod{N}, b, c = 0 \pmod{N} \right. \right\}, \quad (11.6)$$

which is a normal subgroup of finite index in $SL(2, \mathbb{Z})$. The finite modular groups are the quotient groups $\Gamma_N = SL(2, \mathbb{Z}) / \pm\Gamma(N)$ which play the role of discrete flavor symmetry. Remarkably, for $N \leq 5$ the finite modular groups Γ_N are isomorphic to the permutation groups [259, 478]

$$\Gamma_2 \cong S_3, \quad \Gamma_3 \cong A_4, \quad \Gamma_4 \cong S_4, \quad \Gamma_5 \cong A_5, \quad (11.7)$$

which have been widely used as traditional flavor symmetries.

11.2 Modular invariance

A key concept of the theory of modular symmetries [478] is that of modular forms of level N and weight $2k$, denoted $Y(\tau)$. These are holomorphic functions of the modulus τ with the following transformation property

$$Y(\gamma\tau) = (c\tau + d)^{2k}Y(\tau), \quad \gamma = \begin{pmatrix} a & b \\ c & d \end{pmatrix} \in \Gamma(N), \quad (11.8)$$

where the integer $k \geq 0$ determines the weight $2k$.

There are only a finite number of linearly independent modular forms, denoted as $Y_i(\tau)$, and one can always choose a basis such that the transformation of the modular forms can be described by a unitary representation ρ of Γ_N :

$$Y_i(\gamma\tau) = (c\tau + d)^{2k} \rho_{ij}(\gamma) Y_j(\tau), \quad (11.9)$$

where $\gamma = \begin{pmatrix} a & b \\ c & d \end{pmatrix}$ refers to a representative element of Γ_N . Likewise, the modular transformation properties of matter fields $\varphi^{(I)}$ are completely specified by the weight k_I and the unitary representation $\rho^{(I)}$ of the finite modular group Γ_N ,

$$\varphi^I \rightarrow (c\tau + d)^{k_I} \rho^{(I)} \varphi^{(I)}. \quad (11.10)$$

Note that the modular flavor symmetry requires supersymmetry to preserve the holomorphicity of the modular form. Then the superpotential can be expanded in a power series of the matter fields $\varphi^{(I)}$ as follows,

$$\mathcal{W} = \sum_n Y_{I_1 I_2 \dots I_n}(\tau) \varphi^{(I_1)} \varphi^{(I_2)} \dots \varphi^{(I_n)}. \quad (11.11)$$

Modular invariance requires $Y_{I_1 I_2 \dots I_n}(\tau)$ to be a modular form of weight k_Y and level N transforming in the representation ρ of Γ_N ,

$$Y_{I_1 I_2 \dots I_n}(\gamma\tau) = (c\tau + d)^{k_Y} \rho(\gamma) Y_{I_1 I_2 \dots I_n}(\tau), \quad (11.12)$$

with the conditions

$$k_Y + k_{I_1} + k_{I_2} + \dots + k_{I_n} = 0, \quad \rho \otimes \rho^{(I_1)} \otimes \rho^{(I_2)} \otimes \dots \otimes \rho^{(I_n)} \supset \mathbf{1}, \quad (11.13)$$

where $\mathbf{1}$ denotes the invariant singlet representation of Γ_N . One sees that the modular flavor symmetry requires the Yukawa couplings to be modular forms $Y_{I_1 I_2 \dots I_n}(\tau)$. In the simplest implementation, flavons are not necessary and the complex modulus τ is the unique symmetry breaking parameter, greatly simplifying the alignment problem. Moreover, modular invariance requires the Yukawa couplings and fermion mass matrices to be combinations of modular forms, holomorphic functions of τ , all higher-dimensional operators are unambiguously determined in the limit of unbroken supersymmetry. As a result, flavour models with modular invariance depend on fewer parameters, enhancing their predictive power.

The above formalism of modular flavor symmetry has been extended to the double covers [435, 484–487] or the metaplectic covers [487, 488] of the finite group Γ_N , then the modular weights can take integer values or more general rational values.

11.3 Generalized CP in modular symmetry

The interplay of modular symmetry and generalized CP symmetry (gCP) has been studied [489–491]. The consistency between the modular symmetry and gCP fixes the CP transformation of the modulus τ to be [489, 492–495]

$$\tau \xrightarrow{CP} -\tau^* \quad (11.14)$$

up to modular transformations. For any modular transformation

$$\gamma = \begin{pmatrix} a & b \\ c & d \end{pmatrix} \in SL(2, \mathbb{Z}),$$

one can check that the action of the transformation chain $CP \rightarrow \gamma \rightarrow CP^{-1}$ on τ is,

$$\tau \xrightarrow{CP} -\tau^* \xrightarrow{\gamma} -\frac{a\tau^* + b}{c\tau^* + d} \xrightarrow{CP^{-1}} \frac{a\tau - b}{-c\tau + d}. \quad (11.15)$$

This implies that the CP transformation corresponds to an automorphism of the modular group, and it maps any modular transformation γ to another modular transformation $u(\gamma)$,

$$u(\gamma) \equiv CP \circ \gamma \circ CP^{-1} = \begin{pmatrix} a & -b \\ -c & d \end{pmatrix}. \quad (11.16)$$

In particular, one has

$$u(S) = CP \circ S \circ CP^{-1} = S^{-1}, \quad u(T) = CP \circ T \circ CP^{-1} = T^{-1}. \quad (11.17)$$

We proceed to consider the gCP transformation of an arbitrary chiral superfield multiplet $\varphi(x)$ in the representation \mathbf{r} of the finite modular group Γ_N ,

$$\varphi(x) \xrightarrow{CP} X_{\mathbf{r}} \bar{\varphi}(x_P), \quad (11.18)$$

where a bar denotes the Hermitian conjugate superfield, and where $x = (t, \mathbf{x})$, $x_P = (t, -\mathbf{x})$ and $X_{\mathbf{r}}$ is a unitary matrix acting on flavour space. Applying the consistency condition chain of Eq. (11.16) to the matter multiplet φ , one find that the CP transformation matrix $X_{\mathbf{r}}$ has to satisfy the following constraint [489],

$$X_{\mathbf{r}} \rho_{\mathbf{r}}^*(\gamma) X_{\mathbf{r}}^{-1} = \rho_{\mathbf{r}}(u(\gamma)). \quad (11.19)$$

It is sufficient to just consider the modular generators $\gamma = S, T$, namely

$$X_{\mathbf{r}} \rho_{\mathbf{r}}^*(S) X_{\mathbf{r}}^{-1} = \rho(S^{-1}), \quad X_{\mathbf{r}} \rho_{\mathbf{r}}^*(T) X_{\mathbf{r}}^{-1} = \rho(T^{-1}), \quad (11.20)$$

which fixes $X_{\mathbf{r}}$ up to an overall phase by Schur's lemma, for each irreducible representation \mathbf{r} . In the basis where both S and T are represented by symmetric and unitary matrices, $X_{\mathbf{r}} = \mathbb{1}_{\mathbf{r}}$ solves the consistency condition. As a consequence, CP symmetry imposition enforces all coupling constants to be real in such basis. The VEV of τ is the unique source breaking both modular and gCP symmetries. The combination of modular and CP symmetries allows one to construct quite predictive flavor models. Indeed, it is remarkable that all the lepton masses, mixing angles and CP violation phases could be described in terms of only four real couplings plus the complex modulus τ in the minimal modular model of Refs. [496, 497]. The gCP symmetry can also be consistently implemented in the context of multiple moduli [491].

11.4 Modular symmetry from top-down

The idea of modular flavor symmetry is inspired by top-down considerations from string theory. The modular symmetry can naturally appear in orbifold compactifications of the heterotic string [492, 498] and magnetized toroidal compactification [499–505]. The double covers and metaplectic covers of the finite modular groups could be reproduced from top-down constructions. Given the fact that string compactification generally yields several moduli, the modular invariance has been extended to involve multiple moduli based on the direct product of several $SL(2, \mathbb{Z})$ [506] or the Symplectic modular group $Sp(2g, \mathbb{Z})$ [507], where g is a generic positive integer called genus. Note that $Sp(2g, \mathbb{Z})$ can arise as the duality group in string Calabi-Yau compactifications [508–510], and the group $Sp(2, \mathbb{Z})$ is isomorphic to the modular group $SL(2, \mathbb{Z})$. Moreover, it has been found that the modular symmetry and traditional flavor symmetry appear together in top-down constructions. This leads to the concept of eclectic flavor group [511, 512], a maximal extension of the traditional flavor group by finite modular group. It is more predictive than the finite modular group and also the traditional flavor group by itself, combining the advantages of both approaches. In particular, the interplay of modular symmetry and traditional flavor symmetry can restrict the Kähler potential more severely than the modular symmetry by itself. The possibility of eclectic flavor group can also be consistently combined with the gCP symmetry [511].

11.5 Quark-lepton mass relations from modular symmetry

Quite generally, the problem of understanding the pattern of fermion masses and mixings presents a two-fold challenge. While predicting fermion mixings through the imposition of flavor symmetries is relatively straightforward, formulating a convincing theory of fermion masses seems tougher.

It has recently been shown that realistic fermion mass relations can arise naturally in modular invariant models [436, 513–515], without relying on *ad hoc* flavon alignments. As an example, Ref. [291] gave a set of viable fermion mass relations based on the $\Gamma_4 \cong S_4$ symmetry. The new versions exhibit calculable deviations from the usual Golden Mass Relation in Eq. (10.1). They were derived from modular flavor

symmetry in a rather general manner, relying only on the modular flavor group and its vector-valued modular forms, rather than *ad hoc* flavon alignments²⁵. The new relations were shown to be viable and experimentally testable, distinguishing modular models from the conventional flavon-based prediction in Eq. (10.1).

The method is largely model-independent, and can be adapted also to obtain predictions in the up-quark sector and neutrinos. It may also prove useful for more comprehensive modular invariant models and for top-down constructions.

11.6 Modular versus traditional flavor symmetry

We now comment on the predictive power of traditional flavor symmetry and modular symmetry. As we have shown in section 6, traditional flavor symmetry in combination with generalized CP symmetry allows one to predict lepton mixing angles and CP violation phases in terms of just one or two real free parameters when certain residual symmetry is preserved. In general, however, lepton masses are unconstrained by the residual symmetry.

In the case of modular symmetry, the fermion mass matrices exhibit certain symmetry-determined flavor structure through the modular forms which are functions of the modulus τ . One finds that both fermion masses as well as flavor mixing parameters can be determined within specific models. However, one must resort to numerical analysis to reveal the possible correlations amongst the flavor parameters, since a residual modular symmetry with a single modulus has not led to phenomenologically viable models. Concerning vacuum alignment, it is notoriously difficult to dynamically realize the alignment required by the residual symmetry within traditional flavor symmetry constructions. On the other hand, determining the VEV of the modulus τ from a dynamical principle is also an open question, some possible schemes have been proposed to stabilize the modular VEV [516–524]. In modular flavor models, the VEV of τ is usually treated as free parameter, and its value is determined by confronting the model predictions with experimental data.

In short, modular flavor symmetries may shed light on the ultimate symmetry underlying the flavor problem. They have been studied from both the bottom-up and top-down approaches. There are still some unsolved problems such as modulus stabilization and the Kähler potential problem. However, invoking modular symmetry seems a useful tool towards formulating theories of flavor. A comprehensive description of these recent developments lies outside the scope of the present work, see Refs. [91, 479, 480] dedicated modular symmetry reviews.

²⁵They are determined by the Clebsch-Gordan coefficients of the given finite modular group as well as the expansion coefficients of its modular forms.

12 Summary and outlook

The flavour problem constitutes perhaps one of the major open issues and deepest challenges of particle physics. Even more so after the revolutionary discovery and confirmation of neutrino oscillations. The main legacy of these experiments has been to show that leptons mix rather differently from quarks, providing a key input on the flavour issue. Indeed, it seems unlikely that the peculiar pattern of neutrino mixing angles extracted from experiment is just a random coincidence. Rather, it should have its roots in some, perhaps subtle, underlying symmetry of nature.

By itself, the Standard Model lacks an organizing principle in terms of which to understand the “flavours” of the fundamental building blocks of matter. First of all, the flavour challenge comprises an understanding of family replication, i.e. why nature repeats itself three times. Moreover, it also requires an explanation for the pattern of fermion masses and mixings. This review examined the possibility that the flavour puzzle has a symmetry explanation.

To set up the stage we started with an introductory section in which we gave basic preliminaries on the description of lepton and quark mixing, as well as a recap on the status of neutrino oscillations, Fig. 1 and Fig. 2, and neutrinoless double beta decay, e.g. Fig. 3. We discussed ways to have detectable $0\nu\beta\beta$ decay rates, in particular theories where the lightest neutrino is massless or nearly so, see Fig. 4, as occurs, for example, in the missing partner seesaw mechanism, where there are less “right” than “left”-handed neutrinos. We also commented on the detectability of $0\nu\beta\beta$ decay in schemes with family symmetries, e.g. Fig. 5, and also on the significance of a possible $0\nu\beta\beta$ discovery for particle physics, Fig. 6.

In Section 2 we briefly discussed the origin of neutrino masses, both from point of view of effective theories, e.g. the Weinberg operator in Fig. 7, as well as, for instance, the type-I realization of the seesaw paradigm, Fig. 8, or the “scotogenic” paradigm. In the latter dark matter mediates neutrino mass generation through radiative corrections. We also briefly discussed the idea that dark matter *seeds* neutrino mass generation that proceeds *a la seesaw*, as in the recent recently proposed low-scale seesaw variants dubbed “dark inverse” and “dark linear seesaw” Fig. 9. Finally, we mentioned the *flavour problem*, a major SM drawback and main thread of this review, and how it may be approached by symmetry, as illustrated in Fig. 10.

In Sect. 3 we described various phenomenological lepton mixing patterns, showing how most of them are at odds with current experimental data, especially from Daya Bay. In Sect. 4 we gave a bottom-up description of residual flavour and CP symmetries, both for the case of leptons as well as quarks. Indeed, the residual CP and flavor symmetries of quark and lepton mass terms are determined in terms of the experimentally measured mixing matrix, as given in Eqs. (4.11, 4.12, 4.13, 4.24, 4.25, 4.26) and Eqs. (4.55, 4.59). On the other hand, they may arise from the breaking of flavour and CP symmetries at high energies. It is remarkable that one can fix the quark and lepton mixing matrices from the structure of the flavour symmetry group and the residual symmetries, irrespective of the flavour symmetry breaking dynamics. Residual symmetries can restrict the mixing matrix as summarized in table 1. Moreover, remnant symmetries are quite useful as a guide to construct concrete flavour models. They can also

provide adequate revampings of various neutrino mixing patterns at odds with experiment so as to yield generalizations that are not only viable, but also predictive, as discussed in Sect. 5. For example, viable and predictive generalizations of the TBM mixing pattern are given in Figs. 11 and 12. On the other hand, similar generalizations of the Golden-ratio mixing pattern are given in Fig. 13. Soon after the first Daya-Bay results indicating a nonzero value of θ_{13} the bi-large mixing pattern was suggested, in which solar and atmospheric mixing angles as well as the Dirac CP phase are determined in terms of θ_{13} , as seen in Figs. 15 and 16.

Within the family symmetry paradigm, the symmetry group is usually broken down to different subgroups in the neutrino and charged lepton sectors, the lepton mixing matrix arises from the mismatch of the symmetry breaking patterns, as shown in Fig. 17 in Sect. 6. If a Klein subgroup is preserved by the (Majorana) neutrino mass term and the residual abelian subgroup of the charged lepton sector distinguishes the three generations, the lepton mixing matrix would be completely fixed from group theory up to row and column permutations. On the other hand, the Dirac CP phase δ_{CP} is predicted to take on CP conserving values, while the Majorana phases cannot be constrained. Instead, if a Z_2 subgroup is preserved in the neutrino sector, then only one column of the lepton mixing matrix is determined and δ_{CP} can lie in a relative large region, e.g. see Fig. 18. Generalized CP symmetries are very powerful to constrain the CP phase. For instance, the $\mu - \tau$ reflection symmetry on the neutrino fields enforces δ_{CP} to be maximal, while the predicted δ_{CP} values for the generalized $\mu - \tau$ reflection are displayed in Fig. 19.

A flavour symmetry transformation can be generated by performing two CP transformations, the interplay of flavour symmetry and generalized CP symmetry is highly nontrivial, requiring that the consistency condition in Fig. 20 must hold. The inclusion of generalized CP symmetry in flavour symmetry provides richer symmetry breaking patterns. For example, one usually assumes that the flavour and CP symmetry are broken to an abelian subgroup in the charged lepton sector and $Z_2 \times CP$ in the neutrino sector. In this case all the lepton mixing parameters depend only on a single real rotation angle θ in Fig. 21. The value of θ is fixed by the precisely measured reactor angle θ_{13} , leading to a determination of the other lepton mixing angles and CP violation phases, see, e.g. Eq. (6.47). This also implies definite predictions for the $0\nu\beta\beta$ decay amplitude, as shown in Fig. 22. Another possibility is that the remnant subgroup preserved by both neutrino and charged lepton mass terms has the structure $Z_2 \times CP$. In this case the lepton mixing matrix depends on two free rotation angles θ_l and θ_ν , see Fig. 23. All the mixing angles and CP violation phases as well as the effective $0\nu\beta\beta$ mass parameter are predicted to lie in very restricted regions, as shown in Figs. 24, 25, 26. It is remarkable that this scheme can be extended to the quark sector, both quark and lepton mixings can be accommodated using a single flavour group, in terms of total four free parameters. Generalized flavour and CP symmetries may also be employed for the case of Dirac neutrinos. Similar results hold true, except that the remnant flavour symmetry of neutrino sector can be an arbitrary abelian subgroup. In particular, the master formulas in Figs. 21 and 23 also hold for Dirac neutrinos.

In section 7 we gave a panoramic view illustrating possible tests of flavor symmetry models. The

existence of mixing predictions is a characteristic feature of flavor symmetry models. This follows from the fact that typically they have less free parameters than physical observables, therefore correlations between light neutrino observables are predicted. This is explicitly shown in Eqs. (5.12, 5.18, 5.24, 6.9, 6.22, 6.47, 6.51, 6.54, 6.73). For example the ranges of the CP violation δ_{CP} obtained from Eq. (7.1) are summarized in table 3. The predictions of some typical flavor models are displayed in figure 27. One can see that a precise measurement of the lepton mixing parameters at forthcoming neutrino facilities JUNO, DUNE and T2HK should provide a test of flavor models, see also figure 28. On the other hand, neutrino mass sum rules are generally parameterized as Eq. (7.4), providing another type of correlation. It relates the three complex light neutrino mass eigenvalues amongst each other and thus also relate the Majorana CP phases to the neutrino masses. The mass sum rules lead to strong restrictions on the lightest neutrino mass and to distinct predictions for the effective mass $|m_{\beta\beta}|$ probed in $0\nu\beta\beta$ decay, as shown in figure 29. Finally, we commented on a recently developed toolkit to contrast flavor models with upcoming oscillation experiments.

So far we have confined ourselves to model-independent approaches to the flavour puzzle, in which the underlying theory is unspecified and only the predictive power of symmetry is explored. As a next step we turned to various UV-complete approaches to the flavour puzzle. In Sect. 8 we gave two benchmarks for UV-complete constructions in 4 dimensions. The first incorporates dark matter in a “scotogenic” manner, Fig. 30 together with a successful family symmetry leading to the so-called trimaximal pattern TM2. The neutrino oscillation predictions are illustrated in Figs. 31 and 32. An alternative example given puts together family and CP symmetry within the same construction.

More ambitious approaches to the flavor problem have been proposed within extra spacetime dimensions. For example, in Sect. 9 we described a five-dimensional warped flavordynamics scenario in which mass hierarchies are accounted for by adequate choices of the bulk mass parameters, while quark and lepton mixing angles are restricted by the imposition of a family symmetry. We presented a T' model leading to Majorana neutrinos, with the TM1 mixing pattern and tight neutrino oscillation correlations, given in Fig. 35. The $0\nu\beta\beta$ decay rates lie within the sensitivities of the next round of experiments, as indicated in Fig. 36. Finally, one has a good global fit of all flavour observables, including quarks, see table 9.

Finally, in Sect. 10 we described orbifold compactification as a promising way to determine the structure of the family symmetry in four dimensions. The construction is illustrated in Fig. 37. We illustrated the idea with a benchmark 6-dimensional scotogenic (see Fig. 38) orbifold scenario, in which a 4-dimensional A_4 flavour group emerges from the symmetries between the branes in extra dimensions. Predictions include the “golden” quark-lepton mass relation, Eq. (10.33), and a very good global description of all flavour observables, including quarks, table 11. Concerning neutrino oscillations, the mass ordering and atmospheric octant are predicted, together with the reactor angle, see Fig. 39. The lightest neutrino mass can be probed in neutrinoless double beta decay searches as well as cosmology, Fig. 40.

We have also stressed that adequate vacuum alignment is required in flavour symmetry models. Generally one must introduce additional large shaping symmetries and many new fields so as to cleverly design the flavon potential needed to obtain the correct vacuum alignment. In Sec. 11 we discussed how

modular symmetry provides an interesting way to overcome this drawback [478]. In this case the role of flavor symmetry is played by the modular invariance, and the complex modulus τ could be the unique source of modular symmetry breaking. Modular invariance requires the Yukawa couplings to be modular forms, thus a small number of free parameters are involved in modular models. Such modular symmetry approach has been comprehensively reviewed elsewhere [91, 479, 480] within the bottom-up as well as top-down approaches.

Recent progress in the formulation of flavor models involving the use of modular symmetry is discussed in Sec. 11. This idea opens the door to a simpler description and deeper understanding of the flavor symmetry breaking required for obtaining viable flavor predictions without the need to invoke *flavons* in an *ad hoc* manner.

All in all, the legacy of the oscillation program over the past two decades has been a tremendous progress in the field, bringing neutrinos to the center of the particle physics stage. Indeed, addressing the dynamical origin of small neutrino masses touches the heart of the electroweak theory, such as the consistency of symmetry breaking. Moreover, the precise measurement of the neutrino mixing parameters could shed light into the flavor problem. One might have expected that this would bring a decisive boost towards the formulation of a comprehensive theory of fermion masses and mixings. It is somewhat frustrating, however, that so far no decisive flavor road map has emerged. One can reproduce the observations in many different ways, within a wide range of models that go all the way from anarchy to discrete family symmetries. While the latter seems intellectually more appealing, we have not yet been able to underpin a convincing final theory of flavor. Despite many interesting ideas and the formulation of a plethora elegant models, the structure of the three families of fermions remains mysterious.

From the experimental viewpoint in the coming decade we expect a vibrant period for oscillation studies, within and beyond the minimum paradigm. Current neutrino facilities as well as future ones, such as JUNO, DUNE and T2HK should be capable of measuring the solar angle θ_{12} , the atmospheric angle θ_{23} and the Dirac CP phase δ_{CP} with high sensitivity. The next generation of ton-scale $0\nu\beta\beta$ decay experiments will probe the Majorana nature of neutrinos, exploring the whole region associated with the inverted ordering spectrum. These experiments should provide important insights into the mysteries behind flavor mixing, fermion mass hierarchies and CP violation.

A The A_4 group

A_4 is the even permutation group of four objects, and it is isomorphic to the symmetry group of a regular tetrahedron. The A_4 group can be generated by two generators s and t which satisfy the following multiplication rules ²⁶,

$$s^2 = t^3 = (st)^3 = 1. \quad (\text{A.1})$$

The 12 elements of A_4 belong to four conjugacy classes:

$$\begin{aligned} 1C_1 &= \{1\}, & 3C_2 &= \{s, tst^2, t^2st\}, \\ 4C_3 &= \{t, st, ts, sts\}, & 4C'_3 &= \{t^2, st^2, t^2s, st^2s\}, \end{aligned} \quad (\text{A.2})$$

where the conjugacy class is denoted by kC_n , k is the number of elements belonging to it, and the subscript n is the order of the elements contained in it. A_4 has a unique Klein group $K_4^{(s, tst^2)}$ and three Z_3 subgroups generated by t , st , ts and sts respectively. The A_4 group has four inequivalent irreducible representations: three singlets $\mathbf{1}$, $\mathbf{1}'$, $\mathbf{1}''$ and a triplet $\mathbf{3}$. Two different bases are used in the literature, the Ma-Rajasekaran (MR) basis [53] and the Altarelli-Feruglio (AF) basis [313]. They differ in the three-dimensional irreducible representation $\mathbf{3}$, the representation matrix of the generator t is real in the MR basis [53] while it is complex and diagonal in AF basis [313]. The explicit form of the representation matrices are summarized in table 12. The two bases are related through a unitary transformation,

$$s_{AF} = V^\dagger s_{MR} V, \quad t_{AF} = V^\dagger t_{MR} V, \quad (\text{A.3})$$

where

$$V = \frac{1}{\sqrt{3}} \begin{pmatrix} 1 & 1 & 1 \\ 1 & \omega & \omega^2 \\ 1 & \omega^2 & \omega \end{pmatrix}. \quad (\text{A.4})$$

If we have two triplets $\alpha \sim (\alpha_1, \alpha_2, \alpha_3)$ and $\beta \sim (b_1, b_2, b_3)$, their product decomposes as the sum

$$\mathbf{3} \otimes \mathbf{3} = \mathbf{1} \oplus \mathbf{1}' \oplus \mathbf{1}'' \oplus \mathbf{3}_s \oplus \mathbf{3}_a, \quad (\text{A.5})$$

where $\mathbf{3}_s$ and $\mathbf{3}_a$ denote the symmetric and the antisymmetric triplet combinations respectively. The results for the contractions in the above two bases are summarized in table 12.

²⁶We use small s , t , u for the generators of A_4 and S_4 flavour groups in order to avoid confusion with oblique parameters S , T , U .

Representation matrices of A_4 generators				
	Ma-Rajasekaran basis		Altarelli-Feruglio basis	
	s	t	s	t
$\mathbf{1}$	1	1	1	1
$\mathbf{1}'$	1	ω	1	ω
$\mathbf{1}''$	1	ω^2	1	ω^2
$\mathbf{3}$	$\begin{pmatrix} 1 & 0 & 0 \\ 0 & -1 & 0 \\ 0 & 0 & -1 \end{pmatrix}$	$\begin{pmatrix} 0 & 1 & 0 \\ 0 & 0 & 1 \\ 1 & 0 & 0 \end{pmatrix}$	$\frac{1}{3} \begin{pmatrix} -1 & 2 & 2 \\ 2 & -1 & 2 \\ 2 & 2 & -1 \end{pmatrix}$	$\begin{pmatrix} 1 & 0 & 0 \\ 0 & \omega & 0 \\ 0 & 0 & \omega^2 \end{pmatrix}$
Tensor products of two A_4 triplets				
	Ma-Rajasekaran basis		Altarelli-Feruglio basis	
$(\alpha \otimes \beta)_{\mathbf{1}}$	$\alpha_1\beta_1 + \alpha_2\beta_2 + \alpha_3\beta_3$		$\alpha_1\beta_1 + \alpha_2\beta_3 + \alpha_3\beta_2$	
$(\alpha \otimes \beta)_{\mathbf{1}'}$	$\alpha_1\beta_1 + \omega^2\alpha_2\beta_2 + \omega\alpha_3\beta_3$		$\alpha_3\beta_3 + \alpha_1\beta_2 + \alpha_2\beta_1$	
$(\alpha \otimes \beta)_{\mathbf{1}''}$	$\alpha_1\beta_1 + \omega\alpha_2\beta_2 + \omega^2\alpha_3\beta_3$		$\alpha_2\beta_2 + \alpha_3\beta_1 + \alpha_1\beta_3$	
$(\alpha \otimes \beta)_{\mathbf{3}_s}$	$\begin{pmatrix} \alpha_2\beta_3 + \alpha_3\beta_2 \\ \alpha_3\beta_1 + \alpha_1\beta_3 \\ \alpha_1\beta_2 + \alpha_2\beta_1 \end{pmatrix}$		$\begin{pmatrix} 2\alpha_1\beta_1 - \alpha_2\beta_3 - \alpha_3\beta_2 \\ 2\alpha_3\beta_3 - \alpha_1\beta_2 - \alpha_2\beta_1 \\ 2\alpha_2\beta_2 - \alpha_3\beta_1 - \alpha_1\beta_3 \end{pmatrix}$	
$(\alpha \otimes \beta)_{\mathbf{3}_a}$	$\begin{pmatrix} \alpha_2\beta_3 - \alpha_3\beta_2 \\ \alpha_3\beta_1 - \alpha_1\beta_3 \\ \alpha_1\beta_2 - \alpha_2\beta_1 \end{pmatrix}$		$\begin{pmatrix} \alpha_2\beta_3 - \alpha_3\beta_2 \\ \alpha_1\beta_2 - \alpha_2\beta_1 \\ \alpha_3\beta_1 - \alpha_1\beta_3 \end{pmatrix}$	

Table 12: The representation matrices of the A_4 generators s and t in the different irreducible representations. We also give the tensor product rule of two A_4 triplets $\alpha = (\alpha_1, \alpha_2, \alpha_3) \sim \mathbf{3}$ and $\beta = (\beta_1, \beta_2, \beta_3) \sim \mathbf{3}$, where $\omega = e^{i2\pi/3} = -1/2 + i\sqrt{3}/2$ is a cubic root of unity.

B The S_4 group

S_4 is the permutation group of four distinct objects; geometrically it is the symmetry group of a regular octahedron. Its generators s , t and u obey the following multiplication rules [325, 395, 525],

$$s^2 = t^3 = u^2 = (st)^3 = (su)^2 = (tu)^2 = (stu)^4 = 1. \quad (\text{B.1})$$

Note that the generators s and t alone generate the group A_4 , while the generators t and u alone generate the group S_3 . The S_4 group elements can be divided into 5 conjugacy classes

$$\begin{aligned} 1C_1 &= \{1\}, \\ 3C_2 &= \{s, tst^2, t^2st\}, \\ 6C'_2 &= \{u, tu, su, ut, stsu, st^2su\}, \\ 8C_3 &= \{t, st, ts, sts, t^2, st^2, t^2s, st^2s\}, \\ 6C_4 &= \{stu, tsu, t^2su, st^2u, tst^2u, t^2stu\}, \end{aligned} \quad (\text{B.2})$$

The group structure of S_4 has been studied in detail in [526], it has thirty proper subgroups of orders 1, 2, 3, 4, 6, 8, 12 or 24. Since the number of inequivalent irreducible representations is equal to the number of conjugacy classes and the sum of the squares of the dimensions of the irreducible representations must be equal to the order of the group, it is easy to see that S_4 has two singlet irreducible representations $\mathbf{1}$ and $\mathbf{1}'$, one doublet representation $\mathbf{2}$ and two triplet representations $\mathbf{3}$ and $\mathbf{3}'$. In the singlet representations $\mathbf{1}$ and $\mathbf{1}'$, we have

$$\begin{aligned} \mathbf{1} &: s = t = u = 1, \\ \mathbf{1}' &: s = t = 1, \quad u = -1. \end{aligned} \quad (\text{B.3})$$

For the doublet representation $\mathbf{2}$, the generators are represented by

$$s = \begin{pmatrix} 1 & 0 \\ 0 & 1 \end{pmatrix}, \quad t = \begin{pmatrix} \omega & 0 \\ 0 & \omega^2 \end{pmatrix}, \quad u = \begin{pmatrix} 0 & 1 \\ 1 & 0 \end{pmatrix}, \quad (\text{B.4})$$

with $\omega = e^{2\pi i/3}$. In the triplet representations $\mathbf{3}$ and $\mathbf{3}'$, the generators are

$$\begin{aligned} \mathbf{3} : s &= \frac{1}{3} \begin{pmatrix} -1 & 2 & 2 \\ 2 & -1 & 2 \\ 2 & 2 & -1 \end{pmatrix}, \quad t = \begin{pmatrix} 1 & 0 & 0 \\ 0 & \omega^2 & 0 \\ 0 & 0 & \omega \end{pmatrix}, \quad u = - \begin{pmatrix} 1 & 0 & 0 \\ 0 & 0 & 1 \\ 0 & 1 & 0 \end{pmatrix}, \\ \mathbf{3}' : s &= \frac{1}{3} \begin{pmatrix} -1 & 2 & 2 \\ 2 & -1 & 2 \\ 2 & 2 & -1 \end{pmatrix}, \quad t = \begin{pmatrix} 1 & 0 & 0 \\ 0 & \omega^2 & 0 \\ 0 & 0 & \omega \end{pmatrix}, \quad u = \begin{pmatrix} 1 & 0 & 0 \\ 0 & 0 & 1 \\ 0 & 1 & 0 \end{pmatrix}. \end{aligned} \quad (\text{B.5})$$

Classes	$1C_1$	$3C_2$	$6C'_2$	$8C_3$	$6C_4$
1	1	1	1	1	1
1'	1	1	-1	1	-1
2	2	2	0	-1	0
3	3	-1	-1	0	1
3'	3	-1	1	0	-1

Table 13: Character table of the S_4 group.

Notice that the representations **3** and **3'** differ in the overall sign of the generator u . The character of an element is the trace of its representation matrix, then we can straightforwardly obtain the character table of S_4 , as shown in table 13. Moreover, the decompositions of the tensor product of the S_4 irreducible representations are as follows,

$$\begin{aligned}
\mathbf{1} \otimes \mathbf{r} &= \mathbf{r}, & \mathbf{1}' \otimes \mathbf{1}' &= \mathbf{1}, & \mathbf{1}' \otimes \mathbf{2} &= \mathbf{2}, & \mathbf{1}' \otimes \mathbf{3} &= \mathbf{3}', & \mathbf{1}' \otimes \mathbf{3}' &= \mathbf{3}, \\
\mathbf{2} \otimes \mathbf{2} &= \mathbf{1} \oplus \mathbf{1}' \oplus \mathbf{2}, & \mathbf{2} \otimes \mathbf{3} &= \mathbf{2} \otimes \mathbf{3}' = \mathbf{3} \otimes \mathbf{3}', \\
\mathbf{3} \otimes \mathbf{3} &= \mathbf{3}' \otimes \mathbf{3}' = \mathbf{1} \oplus \mathbf{2} \oplus \mathbf{3} \oplus \mathbf{3}', & \mathbf{3} \otimes \mathbf{3}' &= \mathbf{1}' \oplus \mathbf{2} \oplus \mathbf{3} \oplus \mathbf{3}',
\end{aligned} \tag{B.6}$$

where \mathbf{r} stands for any irreducible representation of S_4 . We proceed to present the Clebsch-Gordan (CG) coefficients in the above basis. The entries of the two multiplets in the tensor product are denoted by α_i and β_i respectively. For the product of the singlet $\mathbf{1}'$ with a doublet or a triplet, we have [325, 395, 525]

$$\mathbf{1}' \otimes \mathbf{2} = \mathbf{2} = \begin{pmatrix} \alpha\beta_1 \\ -\alpha\beta_2 \end{pmatrix}, \quad \mathbf{1}' \otimes \mathbf{3} = \mathbf{3}' = \begin{pmatrix} \alpha\beta_1 \\ \alpha\beta_2 \\ \alpha\beta_3 \end{pmatrix}, \quad \mathbf{1}' \otimes \mathbf{3}' = \mathbf{3} = \begin{pmatrix} \alpha\beta_1 \\ \alpha\beta_2 \\ \alpha\beta_3 \end{pmatrix}. \tag{B.7}$$

The CG coefficients for the products involving the doublet representation **2** are found to be

$$\mathbf{2} \otimes \mathbf{2} = \mathbf{1} \oplus \mathbf{1}' \oplus \mathbf{2}, \quad \text{with} \quad \begin{cases} \mathbf{1} = \alpha_1\beta_2 + \alpha_2\beta_1 \\ \mathbf{1}' = \alpha_1\beta_2 - \alpha_2\beta_1 \\ \mathbf{2} = \begin{pmatrix} \alpha_2\beta_2 \\ \alpha_1\beta_1 \end{pmatrix} \end{cases} \tag{B.8}$$

$$\mathbf{2} \otimes \mathbf{3} = \mathbf{3} \oplus \mathbf{3}', \quad \text{with} \quad \begin{cases} \mathbf{3} = \begin{pmatrix} \alpha_1\beta_2 + \alpha_2\beta_3 \\ \alpha_1\beta_3 + \alpha_2\beta_1 \\ \alpha_1\beta_1 + \alpha_2\beta_2 \end{pmatrix} \\ \mathbf{3}' = \begin{pmatrix} \alpha_1\beta_2 - \alpha_2\beta_3 \\ \alpha_1\beta_3 - \alpha_2\beta_1 \\ \alpha_1\beta_1 - \alpha_2\beta_2 \end{pmatrix} \end{cases} \tag{B.9}$$

$$\mathbf{2} \otimes \mathbf{3}' = \mathbf{3} \oplus \mathbf{3}', \quad \text{with} \quad \begin{cases} \mathbf{3} = \begin{pmatrix} \alpha_1\beta_2 - \alpha_2\beta_3 \\ \alpha_1\beta_3 - \alpha_2\beta_1 \\ \alpha_1\beta_1 - \alpha_2\beta_2 \end{pmatrix} \\ \mathbf{3}' = \begin{pmatrix} \alpha_1\beta_2 + \alpha_2\beta_3 \\ \alpha_1\beta_3 + \alpha_2\beta_1 \\ \alpha_1\beta_1 + \alpha_2\beta_2 \end{pmatrix} \end{cases} \quad (\text{B.10})$$

Similarly, for the tensor products among the triplet representations $\mathbf{3}$ and $\mathbf{3}'$, we have

$$\mathbf{3} \otimes \mathbf{3} = \mathbf{3}' \otimes \mathbf{3}' = \mathbf{1} \oplus \mathbf{2} \oplus \mathbf{3} \oplus \mathbf{3}', \quad \text{with} \quad \begin{cases} \mathbf{1} = \alpha_1\beta_1 + \alpha_2\beta_3 + \alpha_3\beta_2 \\ \mathbf{2} = \begin{pmatrix} \alpha_2\beta_2 + \alpha_1\beta_3 + \alpha_3\beta_1 \\ \alpha_3\beta_3 + \alpha_1\beta_2 + \alpha_2\beta_1 \end{pmatrix} \\ \mathbf{3} = \begin{pmatrix} \alpha_2\beta_3 - \alpha_3\beta_2 \\ \alpha_1\beta_2 - \alpha_2\beta_1 \\ \alpha_3\beta_1 - \alpha_1\beta_3 \end{pmatrix} \\ \mathbf{3}' = \begin{pmatrix} 2\alpha_1\beta_1 - \alpha_2\beta_3 - \alpha_3\beta_2 \\ 2\alpha_3\beta_3 - \alpha_1\beta_2 - \alpha_2\beta_1 \\ 2\alpha_2\beta_2 - \alpha_1\beta_3 - \alpha_3\beta_1 \end{pmatrix} \end{cases} \quad (\text{B.11})$$

$$\mathbf{3} \otimes \mathbf{3}' = \mathbf{1}' \oplus \mathbf{2} \oplus \mathbf{3} \oplus \mathbf{3}', \quad \text{with} \quad \begin{cases} \mathbf{1}' = \alpha_1\beta_1 + \alpha_2\beta_3 + \alpha_3\beta_2 \\ \mathbf{2} = \begin{pmatrix} \alpha_2\beta_2 + \alpha_1\beta_3 + \alpha_3\beta_1 \\ -(\alpha_3\beta_3 + \alpha_1\beta_2 + \alpha_2\beta_1) \end{pmatrix} \\ \mathbf{3} = \begin{pmatrix} 2\alpha_1\beta_1 - \alpha_2\beta_3 - \alpha_3\beta_2 \\ 2\alpha_3\beta_3 - \alpha_1\beta_2 - \alpha_2\beta_1 \\ 2\alpha_2\beta_2 - \alpha_1\beta_3 - \alpha_3\beta_1 \end{pmatrix} \\ \mathbf{3}' = \begin{pmatrix} \alpha_2\beta_3 - \alpha_3\beta_2 \\ \alpha_1\beta_2 - \alpha_2\beta_1 \\ \alpha_3\beta_1 - \alpha_1\beta_3 \end{pmatrix} \end{cases} \quad (\text{B.12})$$

C The dihedral group

The dihedral group D_n is the symmetry group of an n -sided regular polygon, which includes rotations and reflections. For instance, D_3 is the symmetry group of the regular triangle, and consequently it is isomorphic to S_3 . A regular polygon with n sides is invariant under a rotation of multiples of $2\pi/n$ about the origin. If n is odd, each reflection axis connects the midpoint of one side to the opposite vertex. If n is even, there are $n/2$ reflection axes connecting the midpoints of opposite sides and $n/2$ axes of symmetry connecting opposite vertices. Consequently the group D_n has $2n$ elements. The group D_n can be generated by a rotation R of order n and a reflection S of order 2, and they satisfy the following multiplication rules

$$R^n = S^2 = (RS)^2 = 1, \quad (\text{C.1})$$

where R denotes a rotation of $2\pi/n$ about the origin, and S is a reflection across n lines through the origin. Notice that D_1 is Z_2 group generated by S and D_2 is isomorphic to $Z_2 \times Z_2$. All the group elements of D_n can be expressed as

$$g = S^\alpha R^\beta \quad (\text{C.2})$$

where $\alpha = 0, 1$ and $\beta = 0, 1, \dots, n-1$. Then it is straightforward to determine the conjugacy classes of the dihedral group. Depending on whether the group index n is even or odd, the $2n$ group elements of D_n can be classified into three or five types of conjugacy classes.

- odd n

$$\begin{aligned} 1C_1 &= \{1\}, \\ 2C_m^{(\rho)} &= \{R^\rho, R^{-\rho}\}, \quad \text{with } \rho = 1, \dots, \frac{n-1}{2}, \\ nC_2 &= \{S, SR, SR^2, \dots, SR^{n-1}\}, \end{aligned} \quad (\text{C.3})$$

where m refers to the order of the element R^ρ .

- even n

$$\begin{aligned} 1C_1 &= \{1\}, \\ 1C_2 &= \{R^{n/2}\}, \\ 2C_m^{(\rho)} &= \{R^\rho, R^{-\rho}\}, \quad \text{with } \rho = 1, \dots, \frac{n-2}{2}, \\ \frac{n}{2}C_2 &= \{S, SR^2, SR^4, \dots, SR^{n-4}, SR^{n-2}\}, \\ \frac{n}{2}C_2 &= \{SR, SR^3, \dots, SR^{n-3}, SR^{n-1}\}. \end{aligned} \quad (\text{C.4})$$

The subgroups of D_n are either dihedral groups or cyclic groups, and they are given by

$$\begin{aligned} Z_j &= \langle R^{\frac{n}{j}} \rangle \quad \text{with } j|n, \\ Z_2^{(m)} &= \langle SR^m \rangle \quad \text{with } m = 0, 1, \dots, n-1, \\ D_j^{(m)} &= \langle R^{\frac{n}{j}}, SR^m \rangle \quad \text{with } j|n, m = 0, 1, \dots, \frac{n}{j} - 1, \end{aligned} \quad (\text{C.5})$$

where the elements inside the angle brackets denote the generators of the subgroups. We see that the total number of dihedral subgroups is the sum of positive divisors of n .

The group D_n is a subgroup of $SO(2)$, and it has only one-dimensional and two-dimensional irreducible representations. The representations of D_n crucially depend on the value of the group index n .

- odd n

If n is an odd integer, the group D_n has two singlet representations $\mathbf{1}_i$ and $\frac{n-1}{2}$ doublet representations $\mathbf{2}_j$, where the subscripts i and j take values $i = 1, 2$ and $j = 1, \dots, \frac{n-1}{2}$. The sum of the squares of the dimensions of the irreducible representations is

$$1^2 + 1^2 + 2^2 \times \frac{n-1}{2} = 2n, \quad (\text{C.6})$$

which is exactly the number of elements of the D_n group. In the singlet representations, the generators R and S are represented by

$$\mathbf{1}_1 : R = S = 1, \quad \mathbf{1}_2 : R = 1, S = -1. \quad (\text{C.7})$$

For the doublet representations, we have

$$\mathbf{2}_j : R = \begin{pmatrix} e^{2\pi i \frac{j}{n}} & 0 \\ 0 & e^{-2\pi i \frac{j}{n}} \end{pmatrix}, \quad S = \begin{pmatrix} 0 & 1 \\ 1 & 0 \end{pmatrix}, \quad (\text{C.8})$$

with $j = 1, \dots, \frac{n-1}{2}$.

- even n

For the case that the index n an even integer, the group D_n has four singlet representations $\mathbf{1}_i$ with $i = 1, 2, 3, 4$ and $\frac{n}{2} - 1$ doublet representations $\mathbf{2}_j$ with $j = 1, \dots, \frac{n}{2} - 1$. It is straightforward to obtain the generators R and S in the singlet representations

$$\begin{aligned} \mathbf{1}_1 : R = S = 1, & & \mathbf{1}_2 : R = 1, S = -1, \\ \mathbf{1}_3 : R = -1, S = 1, & & \mathbf{1}_4 : R = S = -1. \end{aligned} \quad (\text{C.9})$$

The explicit forms of these generators in the irreducible two-dimensional representations are

$$\mathbf{2}_j : R = \begin{pmatrix} e^{2\pi i \frac{j}{n}} & 0 \\ 0 & e^{-2\pi i \frac{j}{n}} \end{pmatrix}, \quad S = \begin{pmatrix} 0 & 1 \\ 1 & 0 \end{pmatrix}, \quad (\text{C.10})$$

with $j = 1, \dots, \frac{n}{2} - 1$. Notice that the doublet representation $\mathbf{2}_j$ and the complex conjugate $\bar{\mathbf{2}}_j$ are equivalent, and they are related through a similarity transformation, i.e., $R^* = VRV^{-1}$ and $S^* = VSV^{-1}$ with $V = \begin{pmatrix} 0 & 1 \\ 1 & 0 \end{pmatrix}$. Hence all the doublet representations of D_n are real, although the representation matrix of R is complex in our basis. Moreover, if $a = (a_1, a_2)^T$ is a doublet

transforming as $\mathbf{2}_j$, then $(a_2^*, a_1^*)^T$ transform as $\mathbf{2}_j$ under D_n as well.

The D_n group has a class-inverting outer automorphism \mathbf{u} , and its action on the generators R and S is

$$R \xrightarrow{\mathbf{u}} R^{-1}, \quad S \xrightarrow{\mathbf{u}} S. \quad (\text{C.11})$$

The CP transformation corresponding to \mathbf{u} is denoted by $X_{\mathbf{r}}^0$, its concrete form is determined by the following consistency conditions,

$$\begin{aligned} X_{\mathbf{r}}^0 \rho_{\mathbf{r}}^*(R) X_{\mathbf{r}}^{0\dagger} &= \rho_{\mathbf{r}}(\mathbf{u}(R)) = \rho_{\mathbf{r}}(R^{-1}), \\ X_{\mathbf{r}}^0 \rho_{\mathbf{r}}^*(S) X_{\mathbf{r}}^{0\dagger} &= \rho_{\mathbf{r}}(\mathbf{u}(S)) = \rho_{\mathbf{r}}(S). \end{aligned} \quad (\text{C.12})$$

Since both $\rho_{\mathbf{r}}(R)$ and $\rho_{\mathbf{r}}(S)$ are symmetric and unitary, $X_{\mathbf{r}}^0$ coincides the canonical CP transformation up to an overall irrelevant phase, i.e.,

$$X_{\mathbf{r}}^0 = \mathbb{1}. \quad (\text{C.13})$$

From $X_{\mathbf{r}}^0$ and the flavor symmetry transformations of D_n , we can obtain other generalized CP transformations $X_{\mathbf{r}} = \rho_{\mathbf{r}}(g) X_{\mathbf{r}}^0 = \rho_{\mathbf{r}}(g)$, $g \in D_n$, yet they don't impose any new restrictions.

D Diagonalization of a 2×2 complex symmetric matrix

A generic complex symmetric 2×2 matrix can be written as

$$M = \begin{pmatrix} a & c \\ c & b \end{pmatrix}, \quad (\text{D.1})$$

where a , b and c are complex. It can be diagonalized by a two dimensional unitary matrix U via

$$U^T M U = \text{diag}(\lambda_1, \lambda_2), \quad U = \begin{pmatrix} \cos\theta & e^{i\phi}\sin\theta \\ -e^{-i\phi}\sin\theta & \cos\theta \end{pmatrix} \begin{pmatrix} e^{-i\alpha} & 0 \\ 0 & e^{-i\beta} \end{pmatrix}. \quad (\text{D.2})$$

The eigenvalues $\lambda_{1,2}$ are non-negative with

$$\begin{aligned} \lambda_1^2 &= \frac{1}{2} \left[|a|^2 + |b|^2 + 2|c|^2 - \sqrt{(|b|^2 - |a|^2)^2 + 4|a^*c + bc^*|^2} \right] \\ \lambda_2^2 &= \frac{1}{2} \left[|a|^2 + |b|^2 + 2|c|^2 + \sqrt{(|b|^2 - |a|^2)^2 + 4|a^*c + bc^*|^2} \right] \end{aligned} \quad (\text{D.3})$$

Without loss of generality, the rotation angle θ can be limited in the region $0 \leq \theta \leq \pi/2$ and it satisfies

$$\tan 2\theta = \frac{2|a^*c + bc^*|}{|b|^2 - |a|^2}. \quad (\text{D.4})$$

The expressions of the phases ϕ , α and β are

$$\begin{aligned} \phi &= \arg(a^*c + bc^*), \\ \alpha &= \frac{1}{2} \arg [a(|b|^2 - |\lambda_1|^2) - b^*c^2], \\ \beta &= \frac{1}{2} \arg [b(|\lambda_2|^2 - |a|^2) + a^*c^2]. \end{aligned} \quad (\text{D.5})$$

The general case of an arbitrary dimension is given in Ref. [30].

Acknowledgements

This review is based on the fruitful collaboration with many friends and colleagues worldwide. We have also benefited from useful discussions with many others. We express our sincere gratitude to all of them. This work was supported by the Spanish grants PID2020-113775GB-I00 (AEI/10.13039/501100011033) and Prometeo CIPROM/2021/054 and by the National Natural Science Foundation of China under Nos. 12375104, 11975224, 11835013.

References

- [1] C.-N. Yang, R. L. Mills, Conservation of Isotopic Spin and Isotopic Gauge Invariance, *Phys. Rev.* 96 (1954) 191–195. [doi:10.1103/PhysRev.96.191](https://doi.org/10.1103/PhysRev.96.191).
- [2] S. L. Glashow, Partial Symmetries of Weak Interactions, *Nucl. Phys.* 22 (1961) 579–588. [doi:10.1016/0029-5582\(61\)90469-2](https://doi.org/10.1016/0029-5582(61)90469-2).
- [3] S. Weinberg, A Model of Leptons, *Phys. Rev. Lett.* 19 (1967) 1264–1266. [doi:10.1103/PhysRevLett.19.1264](https://doi.org/10.1103/PhysRevLett.19.1264).
- [4] A. Salam, Weak and Electromagnetic Interactions, *Conf. Proc. C 680519* (1968) 367–377. [doi:10.1142/9789812795915_0034](https://doi.org/10.1142/9789812795915_0034).
- [5] S. L. Glashow, J. Iliopoulos, L. Maiani, Weak Interactions with Lepton-Hadron Symmetry, *Phys. Rev. D* 2 (1970) 1285–1292. [doi:10.1103/PhysRevD.2.1285](https://doi.org/10.1103/PhysRevD.2.1285).
- [6] G. S. Guralnik, C. R. Hagen, T. W. B. Kibble, Global Conservation Laws and Massless Particles, *Phys. Rev. Lett.* 13 (1964) 585–587. [doi:10.1103/PhysRevLett.13.585](https://doi.org/10.1103/PhysRevLett.13.585).
- [7] F. Englert, R. Brout, Broken Symmetry and the Mass of Gauge Vector Mesons, *Phys. Rev. Lett.* 13 (1964) 321–323. [doi:10.1103/PhysRevLett.13.321](https://doi.org/10.1103/PhysRevLett.13.321).
- [8] P. W. Higgs, Spontaneous Symmetry Breakdown without Massless Bosons, *Phys. Rev.* 145 (1966) 1156–1163. [doi:10.1103/PhysRev.145.1156](https://doi.org/10.1103/PhysRev.145.1156).
- [9] G. Aad, et al., Observation of a new particle in the search for the Standard Model Higgs boson with the ATLAS detector at the LHC, *Phys. Lett. B* 716 (2012) 1–29. [arXiv:1207.7214](https://arxiv.org/abs/1207.7214), [doi:10.1016/j.physletb.2012.08.020](https://doi.org/10.1016/j.physletb.2012.08.020).
- [10] S. Chatrchyan, et al., Observation of a New Boson at a Mass of 125 GeV with the CMS Experiment at the LHC, *Phys. Lett. B* 716 (2012) 30–61. [arXiv:1207.7235](https://arxiv.org/abs/1207.7235), [doi:10.1016/j.physletb.2012.08.021](https://doi.org/10.1016/j.physletb.2012.08.021).
- [11] A. Abada, et al., HE-LHC: The High-Energy Large Hadron Collider: Future Circular Collider Conceptual Design Report Volume 4, *Eur. Phys. J. ST* 228 (5) (2019) 1109–1382. [doi:10.1140/epjst/e2019-900088-6](https://doi.org/10.1140/epjst/e2019-900088-6).
- [12] A. Abada, et al., FCC Physics Opportunities: Future Circular Collider Conceptual Design Report Volume 1, *Eur. Phys. J. C* 79 (6) (2019) 474. [doi:10.1140/epjc/s10052-019-6904-3](https://doi.org/10.1140/epjc/s10052-019-6904-3).
- [13] T. K. Charles, et al., The Compact Linear Collider (CLIC) - 2018 Summary Report 2/2018. [arXiv:1812.06018](https://arxiv.org/abs/1812.06018), [doi:10.23731/CYRM-2018-002](https://doi.org/10.23731/CYRM-2018-002).
- [14] P. Bambade, et al., The International Linear Collider: A Global Project [arXiv:1903.01629](https://arxiv.org/abs/1903.01629).

- [15] The International Linear Collider Technical Design Report - Volume 2: Physics [arXiv:1306.6352](#).
- [16] Physics and Detectors at CLIC: CLIC Conceptual Design Report [arXiv:1202.5940](#), [doi:10.5170/CERN-2012-003](#).
- [17] M. Dong, et al., CEPC Conceptual Design Report: Volume 2 - Physics & Detector [arXiv:1811.10545](#).
- [18] A. B. McDonald, Nobel Lecture: The Sudbury Neutrino Observatory: Observation of flavor change for solar neutrinos, *Rev. Mod. Phys.* 88 (3) (2016) 030502. [doi:10.1103/RevModPhys.88.030502](#).
- [19] T. Kajita, Nobel Lecture: Discovery of atmospheric neutrino oscillations, *Rev. Mod. Phys.* 88 (3) (2016) 030501. [doi:10.1103/RevModPhys.88.030501](#).
- [20] K. Eguchi, et al., First results from KamLAND: Evidence for reactor anti-neutrino disappearance, *Phys. Rev. Lett.* 90 (2003) 021802. [arXiv:hep-ex/0212021](#), [doi:10.1103/PhysRevLett.90.021802](#).
- [21] F. P. An, et al., Observation of electron-antineutrino disappearance at Daya Bay, *Phys. Rev. Lett.* 108 (2012) 171803. [arXiv:1203.1669](#), [doi:10.1103/PhysRevLett.108.171803](#).
- [22] J. K. Ahn, et al., Observation of Reactor Electron Antineutrino Disappearance in the RENO Experiment, *Phys. Rev. Lett.* 108 (2012) 191802. [arXiv:1204.0626](#), [doi:10.1103/PhysRevLett.108.191802](#).
- [23] K. Abe, et al., Indication of Electron Neutrino Appearance from an Accelerator-produced Off-axis Muon Neutrino Beam, *Phys. Rev. Lett.* 107 (2011) 041801. [arXiv:1106.2822](#), [doi:10.1103/PhysRevLett.107.041801](#).
- [24] P. F. de Salas, D. V. Forero, S. Gariazzo, P. Martínez-Miravé, O. Mena, C. A. Ternes, M. Tórtola, J. W. F. Valle, 2020 global reassessment of the neutrino oscillation picture, *JHEP* 02 (2021) 071. [arXiv:2006.11237](#), [doi:10.1007/JHEP02\(2021\)071](#).
- [25] P. F. De Salas, et al., *Chi2 profiles from Valencia neutrino global fit*, <http://globalfit.astroparticles.es/> (2021). [doi:10.5281/zenodo.4726908](#).
URL <https://doi.org/10.5281/zenodo.4726908>
- [26] F. Capozzi, E. Di Valentino, E. Lisi, A. Marrone, A. Melchiorri, A. Palazzo, Unfinished fabric of the three neutrino paradigm, *Phys. Rev. D* 104 (8) (2021) 083031. [arXiv:2107.00532](#), [doi:10.1103/PhysRevD.104.083031](#).
- [27] I. Esteban, M. C. Gonzalez-Garcia, M. Maltoni, T. Schwetz, A. Zhou, The fate of hints: updated global analysis of three-flavor neutrino oscillations, *JHEP* 09 (2020) 178. [arXiv:2007.14792](#), [doi:10.1007/JHEP09\(2020\)178](#).
- [28] R. L. Workman, Others, Review of Particle Physics, *PTEP* 2022 (2022) 083C01. [doi:10.1093/ptep/ptac097](#).
- [29] S. Weinberg, Baryon and Lepton Nonconserving Processes, *Phys. Rev. Lett.* 43 (1979) 1566–1570. [doi:10.1103/PhysRevLett.43.1566](#).
- [30] J. Schechter, J. W. F. Valle, Neutrino Masses in $SU(2) \times U(1)$ Theories, *Phys. Rev. D* 22 (1980) 2227. [doi:10.1103/PhysRevD.22.2227](#).
- [31] T. P. Cheng, L.-F. Li, Neutrino Masses, Mixings and Oscillations in $SU(2) \times U(1)$ Models of Electroweak Interactions, *Phys. Rev. D* 22 (1980) 2860. [doi:10.1103/PhysRevD.22.2860](#).
- [32] J. Schechter, J. W. F. Valle, Neutrino Decay and Spontaneous Violation of Lepton Number, *Phys. Rev. D* 25 (1982) 774. [doi:10.1103/PhysRevD.25.774](#).

- [33] P. Minkowski, $\mu \rightarrow e\gamma$ at a Rate of One Out of 10^9 Muon Decays?, Phys. Lett. B 67 (1977) 421–428. doi:[10.1016/0370-2693\(77\)90435-X](https://doi.org/10.1016/0370-2693(77)90435-X).
- [34] M. Gell-Mann, P. Ramond, R. Slansky, Complex Spinors and Unified Theories, Conf. Proc. C 790927 (1979) 315–321. arXiv:[1306.4669](https://arxiv.org/abs/1306.4669).
- [35] R. N. Mohapatra, G. Senjanovic, Neutrino Mass and Spontaneous Parity Nonconservation, Phys. Rev. Lett. 44 (1980) 912. doi:[10.1103/PhysRevLett.44.912](https://doi.org/10.1103/PhysRevLett.44.912).
- [36] M. Magg, C. Wetterich, Neutrino Mass Problem and Gauge Hierarchy, Phys. Lett. B 94 (1980) 61–64. doi:[10.1016/0370-2693\(80\)90825-4](https://doi.org/10.1016/0370-2693(80)90825-4).
- [37] G. Lazarides, Q. Shafi, C. Wetterich, Proton Lifetime and Fermion Masses in an SO(10) Model, Nucl. Phys. B 181 (1981) 287–300. doi:[10.1016/0550-3213\(81\)90354-0](https://doi.org/10.1016/0550-3213(81)90354-0).
- [38] R. N. Mohapatra, G. Senjanovic, Neutrino Masses and Mixings in Gauge Models with Spontaneous Parity Violation, Phys. Rev. D 23 (1981) 165. doi:[10.1103/PhysRevD.23.165](https://doi.org/10.1103/PhysRevD.23.165).
- [39] Y. Chikashige, R. N. Mohapatra, R. D. Peccei, Are There Real Goldstone Bosons Associated with Broken Lepton Number?, Phys. Lett. B 98 (1981) 265–268. doi:[10.1016/0370-2693\(81\)90011-3](https://doi.org/10.1016/0370-2693(81)90011-3).
- [40] M. C. Gonzalez-Garcia, J. W. F. Valle, Fast Decaying Neutrinos and Observable Flavor Violation in a New Class of Majoron Models, Phys. Lett. B 216 (1989) 360–366. doi:[10.1016/0370-2693\(89\)91131-3](https://doi.org/10.1016/0370-2693(89)91131-3).
- [41] S. M. Boucenna, S. Morisi, J. W. F. Valle, The low-scale approach to neutrino masses, Adv. High Energy Phys. 2014 (2014) 831598. arXiv:[1404.3751](https://arxiv.org/abs/1404.3751), doi:[10.1155/2014/831598](https://doi.org/10.1155/2014/831598).
- [42] Y. Cai, J. Herrero-García, M. A. Schmidt, A. Vicente, R. R. Volkas, From the trees to the forest: a review of radiative neutrino mass models, Front. in Phys. 5 (2017) 63. arXiv:[1706.08524](https://arxiv.org/abs/1706.08524), doi:[10.3389/fphy.2017.00063](https://doi.org/10.3389/fphy.2017.00063).
- [43] H. Georgi, S. L. Glashow, Unity of All Elementary Particle Forces, Phys. Rev. Lett. 32 (1974) 438–441. doi:[10.1103/PhysRevLett.32.438](https://doi.org/10.1103/PhysRevLett.32.438).
- [44] H. Georgi, H. R. Quinn, S. Weinberg, Hierarchy of Interactions in Unified Gauge Theories, Phys. Rev. Lett. 33 (1974) 451–454. doi:[10.1103/PhysRevLett.33.451](https://doi.org/10.1103/PhysRevLett.33.451).
- [45] H. Fritzsch, P. Minkowski, Unified Interactions of Leptons and Hadrons, Annals Phys. 93 (1975) 193–266. doi:[10.1016/0003-4916\(75\)90211-0](https://doi.org/10.1016/0003-4916(75)90211-0).
- [46] H. Georgi, C. Jarlskog, A New Lepton - Quark Mass Relation in a Unified Theory, Phys. Lett. B 86 (1979) 297–300. doi:[10.1016/0370-2693\(79\)90842-6](https://doi.org/10.1016/0370-2693(79)90842-6).
- [47] S. Dimopoulos, H. Georgi, Softly Broken Supersymmetry and SU(5), Nucl. Phys. B 193 (1981) 150–162. doi:[10.1016/0550-3213\(81\)90522-8](https://doi.org/10.1016/0550-3213(81)90522-8).
- [48] M. B. Green, J. H. Schwarz, E. Witten, SUPERSTRING THEORY. VOL. 1: INTRODUCTION, Cambridge Monographs on Mathematical Physics, 1988.
- [49] J. Polchinski, String theory. Vol. 2: Superstring theory and beyond, Cambridge Monographs on Mathematical Physics, Cambridge University Press, 2007. doi:[10.1017/CB09780511618123](https://doi.org/10.1017/CB09780511618123).
- [50] S. T. a. Dieter Lust, **Lectures on String Theory**, Lecture Notes in Physics 346, Springer Berlin Heidelberg, 1989.
URL <http://gen.lib.rus.ec/book/index.php?md5=a63659a291b19c9e6abc9856b960f536>

- [51] L. J. Hall, H. Murayama, N. Weiner, Neutrino mass anarchy, Phys. Rev. Lett. 84 (2000) 2572–2575. [arXiv:hep-ph/9911341](#), [doi:10.1103/PhysRevLett.84.2572](#).
- [52] A. de Gouvea, H. Murayama, Neutrino Mixing Anarchy: Alive and Kicking, Phys. Lett. B 747 (2015) 479–483. [arXiv:1204.1249](#), [doi:10.1016/j.physletb.2015.06.028](#).
- [53] E. Ma, G. Rajasekaran, Softly broken A_4 symmetry for nearly degenerate neutrino masses, Phys. Rev. D 64 (2001) 113012. [arXiv:hep-ph/0106291](#), [doi:10.1103/PhysRevD.64.113012](#).
- [54] K. S. Babu, E. Ma, J. W. F. Valle, Underlying A_4 symmetry for the neutrino mass matrix and the quark mixing matrix, Phys. Lett. B 552 (2003) 207–213. [arXiv:hep-ph/0206292](#), [doi:10.1016/S0370-2693\(02\)03153-2](#).
- [55] M. Hirsch, J. C. Romao, S. Skadhauge, J. W. F. Valle, A. Villanova del Moral, Phenomenological tests of supersymmetric $A(4)$ family symmetry model of neutrino mass, Phys. Rev. D 69 (2004) 093006. [arXiv:hep-ph/0312265](#), [doi:10.1103/PhysRevD.69.093006](#).
- [56] E. Ma, H. Sawanaka, M. Tanimoto, Quark Masses and Mixing with A_4 Family Symmetry, Phys. Lett. B 641 (2006) 301–304. [arXiv:hep-ph/0606103](#), [doi:10.1016/j.physletb.2006.08.062](#).
- [57] M. Hirsch, S. Morisi, J. W. F. Valle, Modelling tri-bimaximal neutrino mixing, Phys. Rev. D 79 (2009) 016001. [arXiv:0810.0121](#), [doi:10.1103/PhysRevD.79.016001](#).
- [58] M. Hirsch, S. Morisi, J. W. F. Valle, Tri-bimaximal neutrino mixing and neutrinoless double beta decay, Phys. Rev. D 78 (2008) 093007. [arXiv:0804.1521](#), [doi:10.1103/PhysRevD.78.093007](#).
- [59] M. Hirsch, S. Morisi, J. W. F. Valle, A_4 -based tri-bimaximal mixing within inverse and linear seesaw schemes, Phys. Lett. B 679 (2009) 454–459. [arXiv:0905.3056](#), [doi:10.1016/j.physletb.2009.08.003](#).
- [60] G.-J. Ding, D. Meloni, A Model for Tri-bimaximal Mixing from a Completely Broken A_4 , Nucl. Phys. B 855 (2012) 21–45. [arXiv:1108.2733](#), [doi:10.1016/j.nuclphysb.2011.10.001](#).
- [61] S. F. King, C. Luhn, Trimaximal neutrino mixing from vacuum alignment in A_4 and S_4 models, JHEP 09 (2011) 042. [arXiv:1107.5332](#), [doi:10.1007/JHEP09\(2011\)042](#).
- [62] Y. Shimizu, M. Tanimoto, A. Watanabe, Breaking Tri-bimaximal Mixing and Large θ_{13} , Prog. Theor. Phys. 126 (2011) 81–90. [arXiv:1105.2929](#), [doi:10.1143/PTP.126.81](#).
- [63] M. S. Boucenna, M. Hirsch, S. Morisi, E. Peinado, M. Taoso, J. W. F. Valle, Phenomenology of Dark Matter from A_4 Flavor Symmetry, JHEP 05 (2011) 037. [arXiv:1101.2874](#), [doi:10.1007/JHEP05\(2011\)037](#).
- [64] I. de Medeiros Varzielas, L. Lavoura, Flavour models for TM_1 lepton mixing, J. Phys. G 40 (2013) 085002. [arXiv:1212.3247](#), [doi:10.1088/0954-3899/40/8/085002](#).
- [65] S. Morisi, M. Nebot, K. M. Patel, E. Peinado, J. W. F. Valle, Quark-Lepton Mass Relation and CKM mixing in an A_4 Extension of the Minimal Supersymmetric Standard Model, Phys. Rev. D 88 (2013) 036001. [arXiv:1303.4394](#), [doi:10.1103/PhysRevD.88.036001](#).
- [66] S. F. King, S. Morisi, E. Peinado, J. W. F. Valle, Quark-Lepton Mass Relation in a Realistic A_4 Extension of the Standard Model, Phys. Lett. B 724 (2013) 68–72. [arXiv:1301.7065](#), [doi:10.1016/j.physletb.2013.05.067](#).
- [67] S. Morisi, D. V. Forero, J. C. Romão, J. W. F. Valle, Neutrino mixing with revamped A_4 flavor symmetry, Phys. Rev. D 88 (1) (2013) 016003. [arXiv:1305.6774](#), [doi:10.1103/PhysRevD.88.016003](#).

- [68] M. Hirsch, A. Villanova del Moral, J. W. F. Valle, E. Ma, Predicting neutrinoless double beta decay, *Phys. Rev. D* 72 (2005) 091301, [Erratum: *Phys.Rev.D* 72, 119904 (2005)]. [arXiv:hep-ph/0507148](#), [doi:10.1103/PhysRevD.72.091301](#).
- [69] M. Hirsch, A. S. Joshipura, S. Kaneko, J. W. F. Valle, Predictive flavour symmetries of the neutrino mass matrix, *Phys. Rev. Lett.* 99 (2007) 151802. [arXiv:hep-ph/0703046](#), [doi:10.1103/PhysRevLett.99.151802](#).
- [70] G. Altarelli, F. Feruglio, Tri-bimaximal neutrino mixing from discrete symmetry in extra dimensions, *Nucl. Phys. B* 720 (2005) 64–88. [arXiv:hep-ph/0504165](#), [doi:10.1016/j.nuclphysb.2005.05.005](#).
- [71] G. Altarelli, F. Feruglio, C. Hagedorn, A SUSY SU(5) Grand Unified Model of Tri-Bimaximal Mixing from A_4 , *JHEP* 03 (2008) 052. [arXiv:0802.0090](#), [doi:10.1088/1126-6708/2008/03/052](#).
- [72] C. Csaki, C. Delaunay, C. Grojean, Y. Grossman, A Model of Lepton Masses from a Warped Extra Dimension, *JHEP* 10 (2008) 055. [arXiv:0806.0356](#), [doi:10.1088/1126-6708/2008/10/055](#).
- [73] M.-C. Chen, K. T. Mahanthappa, F. Yu, A Viable Randall-Sundrum Model for Quarks and Leptons with T-prime Family Symmetry, *Phys. Rev. D* 81 (2010) 036004. [arXiv:0907.3963](#), [doi:10.1103/PhysRevD.81.036004](#).
- [74] T. J. Burrows, S. F. King, A(4) Family Symmetry from SU(5) SUSY GUTs in 6d, *Nucl. Phys. B* 835 (2010) 174–196. [arXiv:0909.1433](#), [doi:10.1016/j.nuclphysb.2010.04.002](#).
- [75] A. Kadosh, E. Pallante, An A(4) flavor model for quarks and leptons in warped geometry, *JHEP* 08 (2010) 115. [arXiv:1004.0321](#), [doi:10.1007/JHEP08\(2010\)115](#).
- [76] A. Kadosh, E. Pallante, CP violation and FCNC in a warped A_4 flavor model, *JHEP* 06 (2011) 121. [arXiv:1101.5420](#), [doi:10.1007/JHEP06\(2011\)121](#).
- [77] A. Kadosh, Θ_3 and charged Lepton Flavor Violation in "warped" A_4 models, *JHEP* 06 (2013) 114. [arXiv:1303.2645](#), [doi:10.1007/JHEP06\(2013\)114](#).
- [78] P. Chen, G.-J. Ding, A. D. Rojas, C. A. Vaquera-Araujo, J. W. F. Valle, Warped flavor symmetry predictions for neutrino physics, *JHEP* 01 (2016) 007. [arXiv:1509.06683](#), [doi:10.1007/JHEP01\(2016\)007](#).
- [79] P. Chen, et al., Predictions from warped flavor dynamics based on the T' family group, *Phys. Rev. D* 102 (9) (2020) 095014. [arXiv:2003.02734](#), [doi:10.1103/PhysRevD.102.095014](#).
- [80] F. del Aguila, A. Carmona, J. Santiago, Neutrino Masses from an A_4 Symmetry in Holographic Composite Higgs Models, *JHEP* 08 (2010) 127. [arXiv:1001.5151](#), [doi:10.1007/JHEP08\(2010\)127](#).
- [81] C. Hagedorn, M. Serone, Leptons in Holographic Composite Higgs Models with Non-Abelian Discrete Symmetries, *JHEP* 10 (2011) 083. [arXiv:1106.4021](#), [doi:10.1007/JHEP10\(2011\)083](#).
- [82] G.-J. Ding, Y.-L. Zhou, Dirac Neutrinos with S_4 Flavor Symmetry in Warped Extra Dimensions, *Nucl. Phys. B* 876 (2013) 418–452. [arXiv:1304.2645](#), [doi:10.1016/j.nuclphysb.2013.08.011](#).
- [83] C. Hagedorn, M. Serone, General Lepton Mixing in Holographic Composite Higgs Models, *JHEP* 02 (2012) 077. [arXiv:1110.4612](#), [doi:10.1007/JHEP02\(2012\)077](#).
- [84] A. E. Cárcamo Hernández, I. de Medeiros Varzielas, N. A. Neill, Novel Randall-Sundrum model with S_3 flavor symmetry, *Phys. Rev. D* 94 (3) (2016) 033011. [arXiv:1511.07420](#), [doi:10.1103/PhysRevD.94.033011](#).
- [85] H. Ishimori, T. Kobayashi, H. Ohki, Y. Shimizu, H. Okada, M. Tanimoto, Non-Abelian Discrete Symmetries in Particle Physics, *Prog. Theor. Phys. Suppl.* 183 (2010) 1–163. [arXiv:1003.3552](#), [doi:10.1143/PTPS.183.1](#).

- [86] G. Altarelli, F. Feruglio, Discrete Flavor Symmetries and Models of Neutrino Mixing, *Rev. Mod. Phys.* 82 (2010) 2701–2729. [arXiv:1002.0211](#), [doi:10.1103/RevModPhys.82.2701](#).
- [87] S. Morisi, J. W. F. Valle, Neutrino masses and mixing: a flavour symmetry roadmap, *Fortsch. Phys.* 61 (2013) 466–492. [arXiv:1206.6678](#), [doi:10.1002/prop.201200125](#).
- [88] S. F. King, C. Luhn, Neutrino Mass and Mixing with Discrete Symmetry, *Rept. Prog. Phys.* 76 (2013) 056201. [arXiv:1301.1340](#), [doi:10.1088/0034-4885/76/5/056201](#).
- [89] S. F. King, A. Merle, S. Morisi, Y. Shimizu, M. Tanimoto, Neutrino Mass and Mixing: from Theory to Experiment, *New J. Phys.* 16 (2014) 045018. [arXiv:1402.4271](#), [doi:10.1088/1367-2630/16/4/045018](#).
- [90] S. F. King, Unified Models of Neutrinos, Flavour and CP Violation, *Prog. Part. Nucl. Phys.* 94 (2017) 217–256. [arXiv:1701.04413](#), [doi:10.1016/j.pnpnp.2017.01.003](#).
- [91] F. Feruglio, A. Romanino, Lepton flavor symmetries, *Rev. Mod. Phys.* 93 (1) (2021) 015007. [arXiv:1912.06028](#), [doi:10.1103/RevModPhys.93.015007](#).
- [92] Z.-z. Xing, Flavor structures of charged fermions and massive neutrinos, *Phys. Rept.* 854 (2020) 1–147. [arXiv:1909.09610](#), [doi:10.1016/j.physrep.2020.02.001](#).
- [93] G. Chauhan, P. S. B. Dev, I. Dubovyk, B. Dziewit, W. Flieger, K. Grzanka, J. Gluza, B. Karmakar, S. Zieba, Phenomenology of Lepton Masses and Mixing with Discrete Flavor Symmetries, [arXiv:2310.20681](#).
- [94] M. E. Peskin, D. V. Schroeder, *An Introduction to quantum field theory*, Addison-Wesley, Reading, USA, 1995.
- [95] C. P. Burgess, G. D. Moore, *The standard model: A primer*, Cambridge University Press, 2006.
- [96] J. F. Donoghue, E. Golowich, B. R. Holstein, *Dynamics of the standard model*, Vol. 2, CUP, 2014. [doi:10.1017/CBO9780511524370](#).
- [97] N. Cabibbo, Unitary Symmetry and Leptonic Decays, *Phys. Rev. Lett.* 10 (1963) 531–533. [doi:10.1103/PhysRevLett.10.531](#).
- [98] M. Kobayashi, T. Maskawa, CP Violation in the Renormalizable Theory of Weak Interaction, *Prog. Theor. Phys.* 49 (1973) 652–657. [doi:10.1143/PTP.49.652](#).
- [99] W. Rodejohann, J. W. F. Valle, Symmetrical Parametrizations of the Lepton Mixing Matrix, *Phys. Rev. D* 84 (2011) 073011. [arXiv:1108.3484](#), [doi:10.1103/PhysRevD.84.073011](#).
- [100] M. Bona, et al., The Unitarity Triangle Fit in the Standard Model and Hadronic Parameters from Lattice QCD: A Reappraisal after the Measurements of $\Delta m(s)$ and $\text{BR}(B \rightarrow \tau \nu(\tau))$, *JHEP* 10 (2006) 081. [arXiv:hep-ph/0606167](#), [doi:10.1088/1126-6708/2006/10/081](#).
- [101] M. Bona, et al., [Ufit website](#).
URL <http://www.utfit.org/UTfit/>
- [102] J. W. F. Valle, J. C. Romao, *Neutrinos in high energy and astroparticle physics*, Physics textbook, Wiley-VCH, Weinheim, 2015.
URL <https://www.wiley.com/WileyCDA/WileyTitle/productCd-3527411976,descCd-buy.html>
- [103] M. Fukugita, T. Yanagida, *Physics of neutrinos and applications to astrophysics*, 2003.
- [104] C. Giunti, C. W. Kim, *Fundamentals of Neutrino Physics and Astrophysics*, 2007.

- [105] Z.-z. Xing, S. Zhou, Neutrinos in particle physics, astronomy and cosmology, 2011.
- [106] B. J. P. Jones, The Physics of Neutrinoless Double Beta Decay: A Primer, in: Theoretical Advanced Study Institute in Elementary Particle Physics: The Obscure Universe: Neutrinos and Other Dark Matters, 2021. [arXiv:2108.09364](#).
- [107] V. Cirigliano, et al., Neutrinoless Double-Beta Decay: A Roadmap for Matching Theory to Experiment [arXiv:2203.12169](#).
- [108] M. J. Dolinski, A. W. P. Poon, W. Rodejohann, Neutrinoless Double-Beta Decay: Status and Prospects, *Ann. Rev. Nucl. Part. Sci.* 69 (2019) 219–251. [arXiv:1902.04097](#), [doi:10.1146/annurev-nucl-101918-023407](#).
- [109] J. D. Vergados, H. Ejiri, F. Simkovic, Theory of Neutrinoless Double Beta Decay, *Rept. Prog. Phys.* 75 (2012) 106301. [arXiv:1205.0649](#), [doi:10.1088/0034-4885/75/10/106301](#).
- [110] J. Schechter, J. W. F. Valle, Neutrinoless Double beta Decay in $SU(2) \times U(1)$ Theories, *Phys. Rev. D* 25 (1982) 2951. [doi:10.1103/PhysRevD.25.2951](#).
- [111] J. Schechter, J. W. F. Valle, Neutrino Oscillation Thought Experiment, *Phys. Rev. D* 23 (1981) 1666. [doi:10.1103/PhysRevD.23.1666](#).
- [112] S. M. Bilenky, J. Hosek, S. T. Petcov, On Oscillations of Neutrinos with Dirac and Majorana Masses, *Phys. Lett. B* 94 (1980) 495–498. [doi:10.1016/0370-2693\(80\)90927-2](#).
- [113] R. Acciarri, et al., Long-Baseline Neutrino Facility (LBNF) and Deep Underground Neutrino Experiment (DUNE): Conceptual Design Report, Volume 2: The Physics Program for DUNE at LBNF [arXiv:1512.06148](#).
- [114] K. Abe, et al., Hyper-Kamiokande Design Report [arXiv:1805.04163](#).
- [115] F. An, et al., Neutrino Physics with JUNO, *J. Phys. G* 43 (3) (2016) 030401. [arXiv:1507.05613](#), [doi:10.1088/0954-3899/43/3/030401](#).
- [116] S. S. Chatterjee, P. Pasquini, J. W. F. Valle, Resolving the atmospheric octant by an improved measurement of the reactor angle, *Phys. Rev. D* 96 (1) (2017) 011303. [arXiv:1703.03435](#), [doi:10.1103/PhysRevD.96.011303](#).
- [117] R. Srivastava, C. A. Ternes, M. Tórtola, J. W. F. Valle, Zooming in on neutrino oscillations with DUNE, *Phys. Rev. D* 97 (9) (2018) 095025. [arXiv:1803.10247](#), [doi:10.1103/PhysRevD.97.095025](#).
- [118] M. S. Athar, et al., Status and perspectives of neutrino physics, *Prog. Part. Nucl. Phys.* 124 (2022) 103947. [arXiv:2111.07586](#), [doi:10.1016/j.ppnp.2022.103947](#).
- [119] M. Maltoni, T. Schwetz, M. A. Tortola, J. W. F. Valle, Status of global fits to neutrino oscillations, *New J. Phys.* 6 (2004) 122. [arXiv:hep-ph/0405172](#), [doi:10.1088/1367-2630/6/1/122](#).
- [120] M. Drewes, et al., A White Paper on keV Sterile Neutrino Dark Matter, *JCAP* 01 (2017) 025. [arXiv:1602.04816](#), [doi:10.1088/1475-7516/2017/01/025](#).
- [121] C. Giunti, T. Lasserre, eV-scale Sterile Neutrinos, *Ann. Rev. Nucl. Part. Sci.* 69 (2019) 163–190. [arXiv:1901.08330](#), [doi:10.1146/annurev-nucl-101918-023755](#).
- [122] S. Böser, C. Buck, C. Giunti, J. Lesgourgues, L. Ludhova, S. Mertens, A. Schukraft, M. Wurm, Status of Light Sterile Neutrino Searches, *Prog. Part. Nucl. Phys.* 111 (2020) 103736. [arXiv:1906.01739](#), [doi:10.1016/j.ppnp.2019.103736](#).

- [123] B. Dasgupta, J. Kopp, Sterile Neutrinos, *Phys. Rept.* 928 (2021) 1–63. [arXiv:2106.05913](#), [doi:10.1016/j.physrep.2021.06.002](#).
- [124] M. Lattanzi, M. Gerbino, K. Freese, G. Kane, J. W. F. Valle, Cornering (quasi) degenerate neutrinos with cosmology, *JHEP* 10 (2020) 213. [arXiv:2007.01650](#), [doi:10.1007/JHEP10\(2020\)213](#).
- [125] S. Abe, et al., Search for the Majorana Nature of Neutrinos in the Inverted Mass Ordering Region with KamLAND-Zen, *Phys. Rev. Lett.* 130 (5) (2023) 051801. [arXiv:2203.02139](#), [doi:10.1103/PhysRevLett.130.051801](#).
- [126] N. Abgrall, et al., The Large Enriched Germanium Experiment for Neutrinoless $\beta\beta$ Decay: LEGEND-1000 Preconceptual Design Report [arXiv:2107.11462](#).
- [127] G. Adhikari, et al., nEXO: neutrinoless double beta decay search beyond 10^{28} year half-life sensitivity, *J. Phys. G* 49 (1) (2022) 015104. [arXiv:2106.16243](#), [doi:10.1088/1361-6471/ac3631](#).
- [128] N. Aghanim, et al., Planck 2018 results. VI. Cosmological parameters, *Astron. Astrophys.* 641 (2020) A6, [Erratum: *Astron. Astrophys.* 652, C4 (2021)]. [arXiv:1807.06209](#), [doi:10.1051/0004-6361/201833910](#).
- [129] M. Gerbino, et al., Synergy between cosmological and laboratory searches in neutrino physics, *Phys. Dark Univ.* 42 (2023) 101333. [arXiv:2203.07377](#), [doi:10.1016/j.dark.2023.101333](#).
- [130] J. Leite, et al., A theory for scotogenic dark matter stabilised by residual gauge symmetry, *Phys. Lett. B* 802 (2020) 135254. [arXiv:1909.06386](#), [doi:10.1016/j.physletb.2020.135254](#).
- [131] S. F. King, Large mixing angle MSW and atmospheric neutrinos from single right-handed neutrino dominance and U(1) family symmetry, *Nucl. Phys. B* 576 (2000) 85–105. [arXiv:hep-ph/9912492](#), [doi:10.1016/S0550-3213\(00\)00109-7](#).
- [132] P. H. Frampton, S. L. Glashow, T. Yanagida, Cosmological sign of neutrino CP violation, *Phys. Lett. B* 548 (2002) 119–121. [arXiv:hep-ph/0208157](#), [doi:10.1016/S0370-2693\(02\)02853-8](#).
- [133] M. Raidal, A. Strumia, Predictions of the most minimal seesaw model, *Phys. Lett. B* 553 (2003) 72–78. [arXiv:hep-ph/0210021](#), [doi:10.1016/S0370-2693\(02\)03124-6](#).
- [134] M. Reig, D. Restrepo, J. W. F. Valle, O. Zapata, Bound-state dark matter with Majorana neutrinos, *Phys. Lett. B* 790 (2019) 303–307. [arXiv:1806.09977](#), [doi:10.1016/j.physletb.2019.01.023](#).
- [135] D. M. Barreiros, R. G. Felipe, F. R. Joaquim, Combining texture zeros with a remnant CP symmetry in the minimal type-I seesaw, *JHEP* 01 (2019) 223. [arXiv:1810.05454](#), [doi:10.1007/JHEP01\(2019\)223](#).
- [136] N. Rojas, R. Srivastava, J. W. F. Valle, Simplest Scoto-Seesaw Mechanism, *Phys. Lett. B* 789 (2019) 132–136. [arXiv:1807.11447](#), [doi:10.1016/j.physletb.2018.12.014](#).
- [137] S. Mandal, R. Srivastava, J. W. F. Valle, The simplest scoto-seesaw model: WIMP dark matter phenomenology and Higgs vacuum stability, *Phys. Lett. B* 819 (2021) 136458. [arXiv:2104.13401](#), [doi:10.1016/j.physletb.2021.136458](#).
- [138] I. M. Ávila, et al., Phenomenology of scotogenic scalar dark matter, *Eur. Phys. J. C* 80 (10) (2020) 908. [arXiv:1910.08422](#), [doi:10.1140/epjc/s10052-020-08480-z](#).
- [139] M. Agostini, et al., Probing Majorana neutrinos with double- β decay, *Science* 365 (2019) 1445. [arXiv:1909.02726](#), [doi:10.1126/science.aav8613](#).

- [140] M. Agostini, G. Benato, J. A. Detwiler, J. Menéndez, F. Vissani, Toward the discovery of matter creation with neutrinoless $\beta\beta$ decay, *Rev. Mod. Phys.* 95 (2) (2023) 025002. [arXiv:2202.01787](#), [doi:10.1103/RevModPhys.95.025002](#).
- [141] L. Dorame, D. Meloni, S. Morisi, E. Peinado, J. W. F. Valle, Constraining Neutrinoless Double Beta Decay, *Nucl. Phys. B* 861 (2012) 259–270. [arXiv:1111.5614](#), [doi:10.1016/j.nuclphysb.2012.04.003](#).
- [142] L. Dorame, S. Morisi, E. Peinado, J. W. F. Valle, A. D. Rojas, A new neutrino mass sum rule from inverse seesaw, *Phys. Rev. D* 86 (2012) 056001. [arXiv:1203.0155](#), [doi:10.1103/PhysRevD.86.056001](#).
- [143] F. J. de Anda, J. W. Valle, C. A. Vaquera-Araujo, Flavour and CP predictions from orbifold compactification, *Phys.Lett. B* 801 (2020) 135195. [arXiv:1910.05605](#), [doi:10.1016/j.physletb.2019.135195](#).
- [144] F. J. de Anda, et al., Probing the predictions of an orbifold theory of flavor, *Phys. Rev. D* 101 (11) (2020) 116012. [arXiv:2004.06735](#), [doi:10.1103/PhysRevD.101.116012](#).
- [145] J. A. Formaggio, A. L. C. de Gouvêa, R. G. H. Robertson, Direct Measurements of Neutrino Mass, *Phys. Rept.* 914 (2021) 1–54. [arXiv:2102.00594](#), [doi:10.1016/j.physrep.2021.02.002](#).
- [146] M. Aker, et al., Direct neutrino-mass measurement with sub-electronvolt sensitivity, *Nature Phys.* 18 (2) (2022) 160–166. [arXiv:2105.08533](#), [doi:10.1038/s41567-021-01463-1](#).
- [147] M. Aker, et al., Improved Upper Limit on the Neutrino Mass from a Direct Kinematic Method by KATRIN, *Phys. Rev. Lett.* 123 (22) (2019) 221802. [arXiv:1909.06048](#), [doi:10.1103/PhysRevLett.123.221802](#).
- [148] D. M. Barreiros, F. R. Joaquim, R. Srivastava, J. W. F. Valle, Minimal scoto-seesaw mechanism with spontaneous CP violation, *JHEP* 04 (2021) 249. [arXiv:2012.05189](#), [doi:10.1007/JHEP04\(2021\)249](#).
- [149] A. Gando, et al., Search for Majorana Neutrinos near the Inverted Mass Hierarchy Region with KamLAND-Zen, *Phys. Rev. Lett.* 117 (8) (2016) 082503, [Addendum: *Phys.Rev.Lett.* 117, 109903 (2016)]. [arXiv:1605.02889](#), [doi:10.1103/PhysRevLett.117.082503](#).
- [150] M. Agostini, et al., Final Results of GERDA on the Search for Neutrinoless Double- β Decay, *Phys. Rev. Lett.* 125 (25) (2020) 252502. [arXiv:2009.06079](#), [doi:10.1103/PhysRevLett.125.252502](#).
- [151] D. Q. Adams, et al., Improved Limit on Neutrinoless Double-Beta Decay in ^{130}Te with CUORE, *Phys. Rev. Lett.* 124 (12) (2020) 122501. [arXiv:1912.10966](#), [doi:10.1103/PhysRevLett.124.122501](#).
- [152] G. Anton, et al., Search for Neutrinoless Double- β Decay with the Complete EXO-200 Dataset, *Phys. Rev. Lett.* 123 (16) (2019) 161802. [arXiv:1906.02723](#), [doi:10.1103/PhysRevLett.123.161802](#).
- [153] M. Duerr, M. Lindner, A. Merle, On the Quantitative Impact of the Schechter-Valle Theorem, *JHEP* 06 (2011) 091. [arXiv:1105.0901](#), [doi:10.1007/JHEP06\(2011\)091](#).
- [154] L. Gráf, M. Lindner, O. Scholer, Unraveling the $0\nu\beta\beta$ decay mechanisms, *Phys. Rev. D* 106 (3) (2022) 035022. [arXiv:2204.10845](#), [doi:10.1103/PhysRevD.106.035022](#).
- [155] J. Heeck, W. Rodejohann, Neutrinoless Quadruple Beta Decay, *EPL* 103 (3) (2013) 32001. [arXiv:1306.0580](#), [doi:10.1209/0295-5075/103/32001](#).
- [156] R. Arnold, et al., Search for neutrinoless quadruple- β decay of ^{150}Nd with the NEMO-3 detector, *Phys. Rev. Lett.* 119 (4) (2017) 041801. [arXiv:1705.08847](#), [doi:10.1103/PhysRevLett.119.041801](#).
- [157] M. Hirsch, R. Srivastava, J. W. F. Valle, Can one ever prove that neutrinos are Dirac particles?, *Phys. Lett. B* 781 (2018) 302–305. [arXiv:1711.06181](#), [doi:10.1016/j.physletb.2018.03.073](#).

- [158] R. E. Marshak, R. N. Mohapatra, Quark - Lepton Symmetry and B-L as the U(1) Generator of the Electroweak Symmetry Group, *Phys. Lett. B* 91 (1980) 222–224. doi:[10.1016/0370-2693\(80\)90436-0](https://doi.org/10.1016/0370-2693(80)90436-0).
- [159] R. N. Mohapatra, R. E. Marshak, Local B-L Symmetry of Electroweak Interactions, Majorana Neutrinos and Neutron Oscillations, *Phys. Rev. Lett.* 44 (1980) 1316–1319, [Erratum: *Phys.Rev.Lett.* 44, 1643 (1980)]. doi:[10.1103/PhysRevLett.44.1316](https://doi.org/10.1103/PhysRevLett.44.1316).
- [160] C. Wetterich, Neutrino Masses and the Scale of B-L Violation, *Nucl. Phys. B* 187 (1981) 343–375. doi:[10.1016/0550-3213\(81\)90279-0](https://doi.org/10.1016/0550-3213(81)90279-0).
- [161] J. Leite, et al., Scotogenic dark matter and Dirac neutrinos from unbroken gauged B – L symmetry, *Phys. Lett. B* 807 (2020) 135537. arXiv:[2003.02950](https://arxiv.org/abs/2003.02950), doi:[10.1016/j.physletb.2020.135537](https://doi.org/10.1016/j.physletb.2020.135537).
- [162] E. Peinado, M. Reig, R. Srivastava, J. W. F. Valle, Dirac neutrinos from Peccei–Quinn symmetry: A fresh look at the axion, *Mod. Phys. Lett. A* 35 (21) (2020) 2050176. arXiv:[1910.02961](https://arxiv.org/abs/1910.02961), doi:[10.1142/S021773232050176X](https://doi.org/10.1142/S021773232050176X).
- [163] A. G. Dias, J. Leite, J. W. F. Valle, C. A. Vaquera-Araujo, Reloading the axion in a 3-3-1 setup, *Phys. Lett. B* 810 (2020) 135829. arXiv:[2008.10650](https://arxiv.org/abs/2008.10650), doi:[10.1016/j.physletb.2020.135829](https://doi.org/10.1016/j.physletb.2020.135829).
- [164] Y. Farzan, E. Ma, Dirac neutrino mass generation from dark matter, *Phys. Rev. D* 86 (2012) 033007. arXiv:[1204.4890](https://arxiv.org/abs/1204.4890), doi:[10.1103/PhysRevD.86.033007](https://doi.org/10.1103/PhysRevD.86.033007).
- [165] S. Centelles Chuliá, E. Ma, R. Srivastava, J. W. F. Valle, Dirac Neutrinos and Dark Matter Stability from Lepton Quarticity, *Phys.Lett. B* 767 (2017) 209–213. arXiv:[1606.04543](https://arxiv.org/abs/1606.04543), doi:[10.1016/j.physletb.2017.01.070](https://doi.org/10.1016/j.physletb.2017.01.070).
- [166] C. Bonilla, E. Ma, E. Peinado, J. W. F. Valle, Two-loop Dirac neutrino mass and WIMP dark matter, *Phys. Lett. B* 762 (2016) 214–218. arXiv:[1607.03931](https://arxiv.org/abs/1607.03931), doi:[10.1016/j.physletb.2016.09.027](https://doi.org/10.1016/j.physletb.2016.09.027).
- [167] R. Srivastava, C. A. Ternes, M. Tórtola, J. W. F. Valle, Testing a lepton quarticity flavor theory of neutrino oscillations with the DUNE experiment, *Phys. Lett. B* 778 (2018) 459–463. arXiv:[1711.10318](https://arxiv.org/abs/1711.10318), doi:[10.1016/j.physletb.2018.01.014](https://doi.org/10.1016/j.physletb.2018.01.014).
- [168] S. Centelles Chuliá, R. Srivastava, J. W. F. Valle, Generalized Bottom-Tau unification, neutrino oscillations and dark matter: predictions from a lepton quarticity flavor approach, *Phys. Lett. B* 773 (2017) 26–33. arXiv:[1706.00210](https://arxiv.org/abs/1706.00210), doi:[10.1016/j.physletb.2017.07.065](https://doi.org/10.1016/j.physletb.2017.07.065).
- [169] M. Reig, D. Restrepo, J. W. F. Valle, O. Zapata, Bound-state dark matter and Dirac neutrino masses, *Phys. Rev. D* 97 (11) (2018) 115032. arXiv:[1803.08528](https://arxiv.org/abs/1803.08528), doi:[10.1103/PhysRevD.97.115032](https://doi.org/10.1103/PhysRevD.97.115032).
- [170] C. Bonilla, S. Centelles-Chuliá, R. Cepedello, E. Peinado, R. Srivastava, Dark matter stability and Dirac neutrinos using only Standard Model symmetries, *Phys. Rev. D* 101 (3) (2020) 033011. arXiv:[1812.01599](https://arxiv.org/abs/1812.01599), doi:[10.1103/PhysRevD.101.033011](https://doi.org/10.1103/PhysRevD.101.033011).
- [171] C. Alvarado, C. Bonilla, J. Leite, J. W. F. Valle, Phenomenology of fermion dark matter as neutrino mass mediator with gauged B-L, *Phys. Lett. B* 817 (2021) 136292. arXiv:[2102.07216](https://arxiv.org/abs/2102.07216), doi:[10.1016/j.physletb.2021.136292](https://doi.org/10.1016/j.physletb.2021.136292).
- [172] M. Roncadelli, D. Wyler, Naturally Light Dirac Neutrinos in Gauge Theories, *Phys. Lett. B* 133 (1983) 325–329. doi:[10.1016/0370-2693\(83\)90156-9](https://doi.org/10.1016/0370-2693(83)90156-9).
- [173] P.-H. Gu, H.-J. He, Neutrino Mass and Baryon Asymmetry from Dirac Seesaw, *JCAP* 12 (2006) 010. arXiv:[hep-ph/0610275](https://arxiv.org/abs/hep-ph/0610275), doi:[10.1088/1475-7516/2006/12/010](https://doi.org/10.1088/1475-7516/2006/12/010).

- [174] C.-Y. Yao, G.-J. Ding, Systematic analysis of Dirac neutrino masses from a dimension five operator, *Phys. Rev. D* 97 (9) (2018) 095042. [arXiv:1802.05231](#), [doi:10.1103/PhysRevD.97.095042](#).
- [175] S. Centelles Chuliá, R. Srivastava, J. W. F. Valle, Seesaw roadmap to neutrino mass and dark matter, *Phys. Lett. B* 781 (2018) 122–128. [arXiv:1802.05722](#), [doi:10.1016/j.physletb.2018.03.046](#).
- [176] C.-Y. Yao, G.-J. Ding, Systematic Study of One-Loop Dirac Neutrino Masses and Viable Dark Matter Candidates, *Phys. Rev. D* 96 (9) (2017) 095004, [Erratum: *Phys.Rev.D* 98, 039901 (2018)]. [arXiv:1707.09786](#), [doi:10.1103/PhysRevD.96.095004](#).
- [177] S. Centelles Chuliá, R. Srivastava, J. W. F. Valle, Seesaw Dirac neutrino mass through dimension-six operators, *Phys. Rev. D* 98 (3) (2018) 035009. [arXiv:1804.03181](#), [doi:10.1103/PhysRevD.98.035009](#).
- [178] J. Elias-Miro, J. R. Espinosa, G. F. Giudice, G. Isidori, A. Riotto, A. Strumia, Higgs mass implications on the stability of the electroweak vacuum, *Phys. Lett. B* 709 (2012) 222–228. [arXiv:1112.3022](#), [doi:10.1016/j.physletb.2012.02.013](#).
- [179] C. Bonilla, R. M. Fonseca, J. W. F. Valle, Consistency of the triplet seesaw model revisited, *Phys. Rev. D* 92 (7) (2015) 075028. [arXiv:1508.02323](#), [doi:10.1103/PhysRevD.92.075028](#).
- [180] C. Bonilla, R. M. Fonseca, J. W. F. Valle, Vacuum stability with spontaneous violation of lepton number, *Phys. Lett. B* 756 (2016) 345–349. [arXiv:1506.04031](#), [doi:10.1016/j.physletb.2016.03.037](#).
- [181] S. Mandal, R. Srivastava, J. W. F. Valle, Consistency of the dynamical high-scale type-I seesaw mechanism, *Phys. Rev. D* 101 (11) (2020) 115030. [doi:10.1103/PhysRevD.101.115030](#).
- [182] S. Mandal, R. Srivastava, J. W. F. Valle, Electroweak symmetry breaking in the inverse seesaw mechanism, *JHEP* 03 (2021) 212. [arXiv:2009.10116](#), [doi:10.1007/JHEP03\(2021\)212](#).
- [183] S. Mandal, J. C. Romão, R. Srivastava, J. W. F. Valle, Dynamical inverse seesaw mechanism as a simple benchmark for electroweak breaking and Higgs boson studies, *JHEP* 07 (2021) 029. [arXiv:2103.02670](#), [doi:10.1007/JHEP07\(2021\)029](#).
- [184] R. Foot, H. Lew, X. G. He, G. C. Joshi, Seesaw Neutrino Masses Induced by a Triplet of Leptons, *Z. Phys. C* 44 (1989) 441. [doi:10.1007/BF01415558](#).
- [185] S. Mandal, O. G. Miranda, G. Sanchez Garcia, J. W. F. Valle, X.-J. Xu, Toward deconstructing the simplest seesaw mechanism, *Phys. Rev. D* 105 (9) (2022) 095020. [arXiv:2203.06362](#), [doi:10.1103/PhysRevD.105.095020](#).
- [186] P. Fileviez Perez, T. Han, G.-y. Huang, T. Li, K. Wang, Neutrino Masses and the CERN LHC: Testing Type II Seesaw, *Phys. Rev. D* 78 (2008) 015018. [arXiv:0805.3536](#), [doi:10.1103/PhysRevD.78.015018](#).
- [187] Y. Cai, T. Han, T. Li, R. Ruiz, Lepton Number Violation: Seesaw Models and Their Collider Tests, *Front. in Phys.* 6 (2018) 40. [arXiv:1711.02180](#), [doi:10.3389/fphy.2018.00040](#).
- [188] S. Mandal, O. G. Miranda, G. S. Garcia, J. W. F. Valle, X.-J. Xu, High-energy colliders as a probe of neutrino properties, *Phys. Lett. B* 829 (2022) 137110. [arXiv:2202.04502](#), [doi:10.1016/j.physletb.2022.137110](#).
- [189] J. W. F. Valle, Neutrino physics overview, *J. Phys. Conf. Ser.* 53 (2006) 473–505. [arXiv:hep-ph/0608101](#), [doi:10.1088/1742-6596/53/1/031](#).
- [190] J. W. F. Valle, C. A. Vaquera-Araujo, Dynamical seesaw mechanism for Dirac neutrinos, *Phys. Lett. B* 755 (2016) 363–366. [arXiv:1601.05237](#), [doi:10.1016/j.physletb.2016.02.031](#).

- [191] A. Aranda, C. Bonilla, S. Morisi, E. Peinado, J. W. F. Valle, Dirac neutrinos from flavor symmetry, *Phys. Rev. D* 89 (3) (2014) 033001. [arXiv:1307.3553](#), [doi:10.1103/PhysRevD.89.033001](#).
- [192] D. Borah, B. Karmakar, A_4 flavour model for Dirac neutrinos: Type I and inverse seesaw, *Phys. Lett. B* 780 (2018) 461–470. [arXiv:1712.06407](#), [doi:10.1016/j.physletb.2018.03.047](#).
- [193] G. Bertone, D. Hooper, J. Silk, Particle dark matter: Evidence, candidates and constraints, *Phys. Rept.* 405 (2005) 279–390. [arXiv:hep-ph/0404175](#), [doi:10.1016/j.physrep.2004.08.031](#).
- [194] G. Jungman, M. Kamionkowski, K. Griest, Supersymmetric dark matter, *Phys. Rept.* 267 (1996) 195–373. [arXiv:hep-ph/9506380](#), [doi:10.1016/0370-1573\(95\)00058-5](#).
- [195] Z.-j. Tao, Radiative seesaw mechanism at weak scale, *Phys. Rev. D* 54 (1996) 5693–5697. [arXiv:hep-ph/9603309](#), [doi:10.1103/PhysRevD.54.5693](#).
- [196] E. Ma, Verifiable radiative seesaw mechanism of neutrino mass and dark matter, *Phys. Rev. D* 73 (2006) 077301. [arXiv:hep-ph/0601225](#), [doi:10.1103/PhysRevD.73.077301](#).
- [197] M. Hirsch, R. A. Lineros, S. Morisi, J. Palacio, N. Rojas, J. W. F. Valle, WIMP dark matter as radiative neutrino mass messenger, *JHEP* 10 (2013) 149. [arXiv:1307.8134](#), [doi:10.1007/JHEP10\(2013\)149](#).
- [198] A. Merle, M. Platscher, N. Rojas, J. W. F. Valle, A. Vicente, Consistency of WIMP Dark Matter as radiative neutrino mass messenger, *JHEP* 07 (2016) 013. [arXiv:1603.05685](#), [doi:10.1007/JHEP07\(2016\)013](#).
- [199] M. A. Díaz, N. Rojas, S. Urrutia-Quiroga, J. W. F. Valle, Heavy Higgs Boson Production at Colliders in the Singlet-Triplet Scotogenic Dark Matter Model, *JHEP* 08 (2017) 017. [arXiv:1612.06569](#), [doi:10.1007/JHEP08\(2017\)017](#).
- [200] S. Choubey, S. Khan, M. Mitra, S. Mondal, Singlet-Triplet Fermionic Dark Matter and LHC Phenomenology, *Eur. Phys. J. C* 78 (4) (2018) 302. [arXiv:1711.08888](#), [doi:10.1140/epjc/s10052-018-5785-1](#).
- [201] D. Restrepo, A. Rivera, Phenomenological consistency of the singlet-triplet scotogenic model, *JHEP* 04 (2020) 134. [arXiv:1907.11938](#), [doi:10.1007/JHEP04\(2020\)134](#).
- [202] S. Mandal, N. Rojas, R. Srivastava, J. W. F. Valle, Dark matter as the origin of neutrino mass in the inverse seesaw mechanism, *Phys. Lett. B* 821 (2021) 136609. [arXiv:1907.07728](#), [doi:10.1016/j.physletb.2021.136609](#).
- [203] A. E. Cárcamo Hernández, V. K. N., J. W. F. Valle, Linear seesaw mechanism from dark sector, *JHEP* 09 (2023) 046. [arXiv:2305.02273](#), [doi:10.1007/JHEP09\(2023\)046](#).
- [204] A. Batra, H. B. Câmara, F. R. Joaquim, Dark linear seesaw mechanism, *Phys. Lett. B* 843 (2023) 138012. [arXiv:2305.01687](#), [doi:10.1016/j.physletb.2023.138012](#).
- [205] G.-J. Ding, J.-N. Lu, J. W. F. Valle, Trimaximal neutrino mixing from scotogenic A_4 family symmetry, *Phys. Lett. B* 815 (2021) 136122. [arXiv:2009.04750](#), [doi:10.1016/j.physletb.2021.136122](#).
- [206] V. Berezhinsky, J. W. F. Valle, The KeV majoron as a dark matter particle, *Phys. Lett. B* 318 (1993) 360–366. [arXiv:hep-ph/9309214](#), [doi:10.1016/0370-2693\(93\)90140-D](#).
- [207] M. Lattanzi, R. A. Lineros, M. Taoso, Connecting neutrino physics with dark matter, *New J. Phys.* 16 (12) (2014) 125012. [arXiv:1406.0004](#), [doi:10.1088/1367-2630/16/12/125012](#).
- [208] S. R. Coleman, Why There Is Nothing Rather Than Something: A Theory of the Cosmological Constant, *Nucl. Phys. B* 310 (1988) 643–668. [doi:10.1016/0550-3213\(88\)90097-1](#).

- [209] M. Lattanzi, J. W. F. Valle, Decaying warm dark matter and neutrino masses, *Phys. Rev. Lett.* 99 (2007) 121301. [arXiv:0705.2406](#), [doi:10.1103/PhysRevLett.99.121301](#).
- [210] M. Lattanzi, S. Riemer-Sorensen, M. Tortola, J. W. F. Valle, Updated CMB and x- and γ -ray constraints on Majoron dark matter, *Phys. Rev. D* 88 (6) (2013) 063528. [arXiv:1303.4685](#), [doi:10.1103/PhysRevD.88.063528](#).
- [211] J.-L. Kuo, M. Lattanzi, K. Cheung, J. W. F. Valle, Decaying warm dark matter and structure formation, *JCAP* 12 (2018) 026. [arXiv:1803.05650](#), [doi:10.1088/1475-7516/2018/12/026](#).
- [212] J. Schechter, J. W. F. Valle, Comment on the Lepton Mixing Matrix, *Phys. Rev. D* 21 (1980) 309. [doi:10.1103/PhysRevD.21.309](#).
- [213] R. N. Mohapatra, J. W. F. Valle, Neutrino Mass and Baryon Number Nonconservation in Superstring Models, *Phys. Rev. D* 34 (1986) 1642. [doi:10.1103/PhysRevD.34.1642](#).
- [214] J. Bernabeu, A. Santamaria, J. Vidal, A. Mendez, J. W. F. Valle, Lepton Flavor Nonconservation at High-Energies in a Superstring Inspired Standard Model, *Phys. Lett. B* 187 (1987) 303–308. [doi:10.1016/0370-2693\(87\)91100-2](#).
- [215] G. C. Branco, M. N. Rebelo, J. W. F. Valle, Leptonic CP Violation With Massless Neutrinos, *Phys. Lett. B* 225 (1989) 385–392. [doi:10.1016/0370-2693\(89\)90587-X](#).
- [216] N. Rius, J. W. F. Valle, Leptonic CP Violating Asymmetries in Z^0 Decays, *Phys. Lett. B* 246 (1990) 249–255. [doi:10.1016/0370-2693\(90\)91341-8](#).
- [217] H. Nunokawa, S. J. Parke, J. W. F. Valle, CP Violation and Neutrino Oscillations, *Prog. Part. Nucl. Phys.* 60 (2008) 338–402. [arXiv:0710.0554](#), [doi:10.1016/j.pnpnp.2007.10.001](#).
- [218] A. de Gouvea, B. Kayser, R. N. Mohapatra, Manifest CP Violation from Majorana Phases, *Phys. Rev. D* 67 (2003) 053004. [arXiv:hep-ph/0211394](#), [doi:10.1103/PhysRevD.67.053004](#).
- [219] G. C. Branco, R. G. Felipe, F. R. Joaquim, Leptonic CP Violation, *Rev. Mod. Phys.* 84 (2012) 515–565. [arXiv:1111.5332](#), [doi:10.1103/RevModPhys.84.515](#).
- [220] A. Vicente, Lepton flavor violation beyond the MSSM, *Adv. High Energy Phys.* 2015 (2015) 686572. [arXiv:1503.08622](#), [doi:10.1155/2015/686572](#).
- [221] A. Abada, J. Kriewald, A. M. Teixeira, On the role of leptonic CPV phases in cLFV observables, *Eur. Phys. J. C* 81 (11) (2021) 1016. [arXiv:2107.06313](#), [doi:10.1140/epjc/s10052-021-09754-w](#).
- [222] F. Deppisch, J. W. F. Valle, Enhanced lepton flavor violation in the supersymmetric inverse seesaw model, *Phys. Rev. D* 72 (2005) 036001. [arXiv:hep-ph/0406040](#), [doi:10.1103/PhysRevD.72.036001](#).
- [223] F. Deppisch, T. S. Kosmas, J. W. F. Valle, Enhanced μ - e conversion in nuclei in the inverse seesaw model, *Nucl. Phys. B* 752 (2006) 80–92. [arXiv:hep-ph/0512360](#), [doi:10.1016/j.nuclphysb.2006.06.032](#).
- [224] A. Ilakovac, A. Pilaftsis, Flavor violating charged lepton decays in seesaw-type models, *Nucl. Phys. B* 437 (1995) 491. [arXiv:hep-ph/9403398](#), [doi:10.1016/0550-3213\(94\)00567-X](#).
- [225] E. Arganda, M. J. Herrero, A. M. Teixeira, μ - e conversion in nuclei within the CMSSM seesaw: Universality versus non-universality, *JHEP* 10 (2007) 104. [arXiv:0707.2955](#), [doi:10.1088/1126-6708/2007/10/104](#).
- [226] A. Abada, V. De Romeri, S. Monteil, J. Orloff, A. M. Teixeira, Indirect searches for sterile neutrinos at a high-luminosity Z-factory, *JHEP* 04 (2015) 051. [arXiv:1412.6322](#), [doi:10.1007/JHEP04\(2015\)051](#).

- [227] A. Abada, M. Lucente, Looking for the minimal inverse seesaw realisation, Nucl. Phys. B 885 (2014) 651–678. [arXiv:1401.1507](#), [doi:10.1016/j.nuclphysb.2014.06.003](#).
- [228] A. Abada, V. De Romeri, A. M. Teixeira, Impact of sterile neutrinos on nuclear-assisted cLFV processes, JHEP 02 (2016) 083. [arXiv:1510.06657](#), [doi:10.1007/JHEP02\(2016\)083](#).
- [229] E. K. Akhmedov, M. Lindner, E. Schnapka, J. W. F. Valle, Dynamical left-right symmetry breaking, Phys. Rev. D 53 (1996) 2752–2780. [arXiv:hep-ph/9509255](#), [doi:10.1103/PhysRevD.53.2752](#).
- [230] E. K. Akhmedov, M. Lindner, E. Schnapka, J. W. F. Valle, Left-right symmetry breaking in NJL approach, Phys. Lett. B 368 (1996) 270–280. [arXiv:hep-ph/9507275](#), [doi:10.1016/0370-2693\(95\)01504-3](#).
- [231] M. Malinsky, J. C. Romao, J. W. F. Valle, Novel supersymmetric SO(10) seesaw mechanism, Phys. Rev. Lett. 95 (2005) 161801. [arXiv:hep-ph/0506296](#), [doi:10.1103/PhysRevLett.95.161801](#).
- [232] W.-Y. Keung, G. Senjanovic, Majorana Neutrinos and the Production of the Right-handed Charged Gauge Boson, Phys. Rev. Lett. 50 (1983) 1427. [doi:10.1103/PhysRevLett.50.1427](#).
- [233] M. Dittmar, A. Santamaria, M. C. Gonzalez-Garcia, J. W. F. Valle, Production Mechanisms and Signatures of Isosinglet Neutral Heavy Leptons in Z^0 Decays, Nucl. Phys. B 332 (1990) 1–19. [doi:10.1016/0550-3213\(90\)90028-C](#).
- [234] M. C. Gonzalez-Garcia, A. Santamaria, J. W. F. Valle, Isosinglet Neutral Heavy Lepton Production in Z Decays and Neutrino Mass, Nucl. Phys. B 342 (1990) 108–126. [doi:10.1016/0550-3213\(90\)90573-V](#).
- [235] J. A. Aguilar-Saavedra, F. Deppisch, O. Kittel, J. W. F. Valle, Flavour in heavy neutrino searches at the LHC, Phys. Rev. D 85 (2012) 091301. [arXiv:1203.5998](#), [doi:10.1103/PhysRevD.85.091301](#).
- [236] S. P. Das, F. F. Deppisch, O. Kittel, J. W. F. Valle, Heavy Neutrinos and Lepton Flavour Violation in Left-Right Symmetric Models at the LHC, Phys. Rev. D 86 (2012) 055006. [arXiv:1206.0256](#), [doi:10.1103/PhysRevD.86.055006](#).
- [237] F. F. Deppisch, N. Desai, J. W. F. Valle, Is charged lepton flavor violation a high energy phenomenon?, Phys. Rev. D 89 (5) (2014) 051302. [arXiv:1308.6789](#), [doi:10.1103/PhysRevD.89.051302](#).
- [238] G. Aad, et al., Search for heavy neutral leptons in decays of W bosons produced in 13 TeV pp collisions using prompt and displaced signatures with the ATLAS detector, JHEP 10 (2019) 265. [arXiv:1905.09787](#), [doi:10.1007/JHEP10\(2019\)265](#).
- [239] A. M. Sirunyan, et al., Search for heavy neutral leptons in events with three charged leptons in proton-proton collisions at $\sqrt{s} = 13$ TeV, Phys. Rev. Lett. 120 (22) (2018) 221801. [arXiv:1802.02965](#), [doi:10.1103/PhysRevLett.120.221801](#).
- [240] A. Tumasyan, et al., Inclusive nonresonant multilepton probes of new phenomena at $\sqrt{s}=13$ TeV, Phys. Rev. D 105 (11) (2022) 112007. [arXiv:2202.08676](#), [doi:10.1103/PhysRevD.105.112007](#).
- [241] A. Abada, et al., FCC-ee: The Lepton Collider: Future Circular Collider Conceptual Design Report Volume 2, Eur. Phys. J. ST 228 (2) (2019) 261–623. [doi:10.1140/epjst/e2019-900045-4](#).
- [242] J. L. Feng, et al., The Forward Physics Facility at the High-Luminosity LHC, J. Phys. G 50 (3) (2023) 030501. [arXiv:2203.05090](#), [doi:10.1088/1361-6471/ac865e](#).
- [243] A. M. Abdullahi, et al., The present and future status of heavy neutral leptons, J. Phys. G 50 (2) (2023) 020501. [arXiv:2203.08039](#), [doi:10.1088/1361-6471/ac98f9](#).

- [244] J. C. Helo, M. Hirsch, S. Kovalenko, Heavy neutrino searches at the LHC with displaced vertices, Phys. Rev. D 89 (2014) 073005, [Erratum: Phys.Rev.D 93, 099902 (2016)]. [arXiv:1312.2900](#), [doi:10.1103/PhysRevD.89.073005](#).
- [245] M. Drewes, J. Hajer, Heavy Neutrinos in displaced vertex searches at the LHC and HL-LHC, JHEP 02 (2020) 070. [arXiv:1903.06100](#), [doi:10.1007/JHEP02\(2020\)070](#).
- [246] R. Beltrán, G. Cottin, J. C. Helo, M. Hirsch, A. Titov, Z. S. Wang, Long-lived heavy neutral leptons at the LHC: four-fermion single- N_R operators, JHEP 01 (2022) 044. [arXiv:2110.15096](#), [doi:10.1007/JHEP01\(2022\)044](#).
- [247] A. Datta, B. Mukhopadhyaya, F. Vissani, Tevatron signatures of an R-parity violating supersymmetric theory, Phys. Lett. B 492 (2000) 324–330. [arXiv:hep-ph/9910296](#), [doi:10.1016/S0370-2693\(00\)01104-7](#).
- [248] W. Porod, M. Hirsch, J. Romao, J. W. F. Valle, Testing neutrino mixing at future collider experiments, Phys. Rev. D 63 (2001) 115004. [arXiv:hep-ph/0011248](#), [doi:10.1103/PhysRevD.63.115004](#).
- [249] F. de Campos, O. J. P. Eboli, M. B. Magro, W. Porod, D. Restrepo, J. W. F. Valle, Probing neutrino mass with displaced vertices at the Tevatron, Phys. Rev. D 71 (2005) 075001. [arXiv:hep-ph/0501153](#), [doi:10.1103/PhysRevD.71.075001](#).
- [250] A. D. Sakharov, Violation of CP Invariance, C asymmetry, and baryon asymmetry of the universe, Pisma Zh. Eksp. Teor. Fiz. 5 (1967) 32–35. [doi:10.1070/PU1991v034n05ABEH002497](#).
- [251] M. Fukugita, T. Yanagida, Baryogenesis Without Grand Unification, Phys. Lett. B 174 (1986) 45–47. [doi:10.1016/0370-2693\(86\)91126-3](#).
- [252] P. F. Harrison, W. G. Scott, Symmetries and generalizations of tri - bimaximal neutrino mixing, Phys. Lett. B 535 (2002) 163–169. [arXiv:hep-ph/0203209](#), [doi:10.1016/S0370-2693\(02\)01753-7](#).
- [253] P. F. Harrison, W. G. Scott, $\mu - \tau$ reflection symmetry in lepton mixing and neutrino oscillations, Phys. Lett. B 547 (2002) 219–228. [arXiv:hep-ph/0210197](#), [doi:10.1016/S0370-2693\(02\)02772-7](#).
- [254] W. Grimus, L. Lavoura, A Nonstandard CP transformation leading to maximal atmospheric neutrino mixing, Phys. Lett. B 579 (2004) 113–122. [arXiv:hep-ph/0305309](#), [doi:10.1016/j.physletb.2003.10.075](#).
- [255] P. F. Harrison, W. G. Scott, The Simplest neutrino mass matrix, Phys. Lett. B 594 (2004) 324–332. [arXiv:hep-ph/0403278](#), [doi:10.1016/j.physletb.2004.05.039](#).
- [256] Y. Farzan, A. Y. Smirnov, Leptonic CP violation: Zero, maximal or between the two extremes, JHEP 01 (2007) 059. [arXiv:hep-ph/0610337](#), [doi:10.1088/1126-6708/2007/01/059](#).
- [257] P. Chen, G.-J. Ding, F. Gonzalez-Canales, J. W. F. Valle, Generalized $\mu - \tau$ reflection symmetry and leptonic CP violation, Phys. Lett. B 753 (2016) 644–652. [arXiv:1512.01551](#), [doi:10.1016/j.physletb.2015.12.069](#).
- [258] P. Chen, S. Centelles Chuliá, G.-J. Ding, R. Srivastava, J. W. F. Valle, Neutrino Predictions from Generalized CP Symmetries of Charged Leptons, JHEP 07 (2018) 077. [arXiv:1802.04275](#), [doi:10.1007/JHEP07\(2018\)077](#).
- [259] R. de Adelhart Toorop, F. Feruglio, C. Hagedorn, Finite Modular Groups and Lepton Mixing, Nucl. Phys. B 858 (2012) 437–467. [arXiv:1112.1340](#), [doi:10.1016/j.nuclphysb.2012.01.017](#).

- [260] M. Holthausen, K. S. Lim, M. Lindner, Lepton Mixing Patterns from a Scan of Finite Discrete Groups, *Phys. Lett. B* 721 (2013) 61–67. [arXiv:1212.2411](#), [doi:10.1016/j.physletb.2013.02.047](#).
- [261] R. M. Fonseca, W. Grimus, Classification of lepton mixing matrices from finite residual symmetries, *JHEP* 09 (2014) 033. [arXiv:1405.3678](#), [doi:10.1007/JHEP09\(2014\)033](#).
- [262] J. Talbert, [Re]constructing Finite Flavour Groups: Horizontal Symmetry Scans from the Bottom-Up, *JHEP* 12 (2014) 058. [arXiv:1409.7310](#), [doi:10.1007/JHEP12\(2014\)058](#).
- [263] C.-Y. Yao, G.-J. Ding, Lepton and Quark Mixing Patterns from Finite Flavor Symmetries, *Phys. Rev. D* 92 (9) (2015) 096010. [arXiv:1505.03798](#), [doi:10.1103/PhysRevD.92.096010](#).
- [264] F. Feruglio, C. Hagedorn, R. Ziegler, Lepton Mixing Parameters from Discrete and CP Symmetries, *JHEP* 07 (2013) 027. [arXiv:1211.5560](#), [doi:10.1007/JHEP07\(2013\)027](#).
- [265] P. Chen, C.-C. Li, G.-J. Ding, Lepton Flavor Mixing and CP Symmetry, *Phys. Rev. D* 91 (2015) 033003. [arXiv:1412.8352](#), [doi:10.1103/PhysRevD.91.033003](#).
- [266] L. L. Everett, T. Garon, A. J. Stuart, A Bottom-Up Approach to Lepton Flavor and CP Symmetries, *JHEP* 04 (2015) 069. [arXiv:1501.04336](#), [doi:10.1007/JHEP04\(2015\)069](#).
- [267] P. Chen, C.-Y. Yao, G.-J. Ding, Neutrino Mixing from CP Symmetry, *Phys. Rev. D* 92 (7) (2015) 073002. [arXiv:1507.03419](#), [doi:10.1103/PhysRevD.92.073002](#).
- [268] L. L. Everett, A. J. Stuart, Lepton Sector Phases and Their Roles in Flavor and Generalized CP Symmetries, *Phys. Rev. D* 96 (3) (2017) 035030. [arXiv:1611.03020](#), [doi:10.1103/PhysRevD.96.035030](#).
- [269] C. S. Lam, Determining Horizontal Symmetry from Neutrino Mixing, *Phys. Rev. Lett.* 101 (2008) 121602. [arXiv:0804.2622](#), [doi:10.1103/PhysRevLett.101.121602](#).
- [270] C. S. Lam, Symmetry of Lepton Mixing, *Phys. Lett. B* 656 (2007) 193–198. [arXiv:0708.3665](#), [doi:10.1016/j.physletb.2007.09.032](#).
- [271] C. S. Lam, Group Theory and Dynamics of Neutrino Mixing, *Phys. Rev. D* 83 (2011) 113002. [arXiv:1104.0055](#), [doi:10.1103/PhysRevD.83.113002](#).
- [272] C. S. Lam, Horizontal Symmetry: Bottom Up and Top Down [arXiv:1105.5166](#).
- [273] S. Antusch, I. de Medeiros Varzielas, V. Maurer, C. Sluka, M. Spinrath, Towards predictive flavour models in SUSY SU(5) GUTs with doublet-triplet splitting, *JHEP* 09 (2014) 141. [arXiv:1405.6962](#), [doi:10.1007/JHEP09\(2014\)141](#).
- [274] F. Björkeröth, F. J. de Anda, I. de Medeiros Varzielas, S. F. King, Towards a complete $A_4 \times SU(5)$ SUSY GUT, *JHEP* 06 (2015) 141. [arXiv:1503.03306](#), [doi:10.1007/JHEP06\(2015\)141](#).
- [275] M. Reig, J. W. F. Valle, C. A. Vaquera-Araujo, F. Wilczek, A Model of Comprehensive Unification, *Phys. Lett. B* 774 (2017) 667–670. [arXiv:1706.03116](#), [doi:10.1016/j.physletb.2017.10.038](#).
- [276] C. D. Froggatt, H. B. Nielsen, Hierarchy of Quark Masses, Cabibbo Angles and CP Violation, *Nucl. Phys. B* 147 (1979) 277–298. [doi:10.1016/0550-3213\(79\)90316-X](#).
- [277] R. Barbieri, G. R. Dvali, L. J. Hall, Predictions from a U(2) flavor symmetry in supersymmetric theories, *Phys. Lett. B* 377 (1996) 76–82. [arXiv:hep-ph/9512388](#), [doi:10.1016/0370-2693\(96\)00318-8](#).

- [278] A. Blum, C. Hagedorn, M. Lindner, Fermion Masses and Mixings from Dihedral Flavor Symmetries with Preserved Subgroups, *Phys. Rev. D* 77 (2008) 076004. [arXiv:0709.3450](#), [doi:10.1103/PhysRevD.77.076004](#).
- [279] M. Holthausen, K. S. Lim, Quark and Leptonic Mixing Patterns from the Breakdown of a Common Discrete Flavor Symmetry, *Phys. Rev. D* 88 (2013) 033018. [arXiv:1306.4356](#), [doi:10.1103/PhysRevD.88.033018](#).
- [280] T. Araki, H. Ishida, H. Ishimori, T. Kobayashi, A. Ogasahara, CKM matrix and flavor symmetries, *Phys. Rev. D* 88 (2013) 096002. [arXiv:1309.4217](#), [doi:10.1103/PhysRevD.88.096002](#).
- [281] I. de Medeiros Varzielas, R. W. Rasmussen, J. Talbert, Bottom-Up Discrete Symmetries for Cabibbo Mixing, *Int. J. Mod. Phys. A* 32 (06n07) (2017) 1750047. [arXiv:1605.03581](#), [doi:10.1142/S0217751X17500476](#).
- [282] C.-C. Li, J.-N. Lu, G.-J. Ding, Toward a unified interpretation of quark and lepton mixing from flavor and CP symmetries, *JHEP* 02 (2018) 038. [arXiv:1706.04576](#), [doi:10.1007/JHEP02\(2018\)038](#).
- [283] J.-N. Lu, G.-J. Ding, Quark and lepton mixing patterns from a common discrete flavor symmetry with a generalized CP symmetry, *Phys. Rev. D* 98 (5) (2018) 055011. [arXiv:1806.02301](#), [doi:10.1103/PhysRevD.98.055011](#).
- [284] J.-N. Lu, G.-J. Ding, Dihedral flavor group as the key to understand quark and lepton flavor mixing, *JHEP* 03 (2019) 056. [arXiv:1901.07414](#), [doi:10.1007/JHEP03\(2019\)056](#).
- [285] C. Hagedorn, J. König, Lepton and quark mixing from a stepwise breaking of flavor and CP , *Phys. Rev. D* 100 (7) (2019) 075036. [arXiv:1811.07750](#), [doi:10.1103/PhysRevD.100.075036](#).
- [286] C. Hagedorn, J. König, Lepton and quark masses and mixing in a SUSY model with $\Delta(384)$ and CP, *Nucl. Phys. B* 953 (2020) 114953. [arXiv:1811.09262](#), [doi:10.1016/j.nuclphysb.2020.114953](#).
- [287] M. Reig, J. W. F. Valle, F. Wilczek, $SO(3)$ family symmetry and axions, *Phys. Rev. D* 98 (9) (2018) 095008. [arXiv:1805.08048](#), [doi:10.1103/PhysRevD.98.095008](#).
- [288] S. Morisi, E. Peinado, Y. Shimizu, J. W. F. Valle, Relating quarks and leptons without grand-unification, *Phys. Rev. D* 84 (2011) 036003. [arXiv:1104.1633](#), [doi:10.1103/PhysRevD.84.036003](#).
- [289] C. Bonilla, S. Morisi, E. Peinado, J. W. F. Valle, Relating quarks and leptons with the T_7 flavour group, *Phys. Lett. B* 742 (2015) 99–106. [arXiv:1411.4883](#), [doi:10.1016/j.physletb.2015.01.017](#).
- [290] C. Bonilla, J. M. Lamprea, E. Peinado, J. W. F. Valle, Flavour-symmetric type-II Dirac neutrino seesaw mechanism, *Phys. Lett. B* 779 (2018) 257–261. [arXiv:1710.06498](#), [doi:10.1016/j.physletb.2018.02.022](#).
- [291] M.-C. Chen, S. F. King, O. Medina, J. W. F. Valle, Quark-lepton mass relations from modular flavor symmetry [arXiv:2312.09255](#).
- [292] F. J. de Anda, S. F. King, An $S_4 \times SU(5)$ SUSY GUT of flavour in 6d, *JHEP* 07 (2018) 057. [arXiv:1803.04978](#), [doi:10.1007/JHEP07\(2018\)057](#).
- [293] F. J. de Anda, S. F. King, $SU(3) \times SO(10)$ in 6d, *JHEP* 10 (2018) 128. [arXiv:1807.07078](#), [doi:10.1007/JHEP10\(2018\)128](#).
- [294] F. J. de Anda, I. Antoniadis, J. W. F. Valle, C. A. Vaquera-Araujo, Scotogenic dark matter in an orbifold theory of flavor, *JHEP* 10 (2020) 190. [arXiv:2007.10402](#), [doi:10.1007/JHEP10\(2020\)190](#).
- [295] F. J. de Anda, O. Medina, J. W. F. Valle, C. A. Vaquera-Araujo, Scotogenic Majorana neutrino masses in a predictive orbifold theory of flavor, *Phys. Rev. D* 105 (5) (2022) 055030. [arXiv:2110.06810](#), [doi:10.1103/PhysRevD.105.055030](#).

- [296] P. F. Harrison, D. H. Perkins, W. G. Scott, Tri-bimaximal mixing and the neutrino oscillation data, Phys. Lett. B 530 (2002) 167. [arXiv:hep-ph/0202074](#), [doi:10.1016/S0370-2693\(02\)01336-9](#).
- [297] Z.-z. Xing, Nearly tri bimaximal neutrino mixing and CP violation, Phys. Lett. B 533 (2002) 85–93. [arXiv:hep-ph/0204049](#), [doi:10.1016/S0370-2693\(02\)01649-0](#).
- [298] X. G. He, A. Zee, Some simple mixing and mass matrices for neutrinos, Phys. Lett. B 560 (2003) 87–90. [arXiv:hep-ph/0301092](#), [doi:10.1016/S0370-2693\(03\)00390-3](#).
- [299] S. Luo, Z.-z. Xing, Generalized tri-bimaximal neutrino mixing and its sensitivity to radiative corrections, Phys. Lett. B 632 (2006) 341–348. [arXiv:hep-ph/0509065](#), [doi:10.1016/j.physletb.2005.10.068](#).
- [300] F. Plentinger, W. Rodejohann, Deviations from tribimaximal neutrino mixing, Phys. Lett. B 625 (2005) 264–276. [arXiv:hep-ph/0507143](#), [doi:10.1016/j.physletb.2005.08.092](#).
- [301] M. Hirsch, E. Ma, J. C. Romao, J. W. F. Valle, A. Villanova del Moral, Minimal supergravity radiative effects on the tri-bimaximal neutrino mixing pattern, Phys. Rev. D 75 (2007) 053006. [arXiv:hep-ph/0606082](#), [doi:10.1103/PhysRevD.75.053006](#).
- [302] P. Wilina, M. S. Singh, N. N. Singh, Deviations from tribimaximal and golden ratio mixings under radiative corrections of neutrino masses and mixings, Int. J. Mod. Phys. A 37 (25) (2022) 2250156. [arXiv:2205.01936](#), [doi:10.1142/S0217751X22501561](#).
- [303] F. P. An, et al., Improved Measurement of Electron Antineutrino Disappearance at Daya Bay, Chin. Phys. C 37 (2013) 011001. [arXiv:1210.6327](#), [doi:10.1088/1674-1137/37/1/011001](#).
- [304] F. P. An, et al., Spectral measurement of electron antineutrino oscillation amplitude and frequency at Daya Bay, Phys. Rev. Lett. 112 (2014) 061801. [arXiv:1310.6732](#), [doi:10.1103/PhysRevLett.112.061801](#).
- [305] K. Luk, [Daya-bay talk on final 3158-day data](#) (International Conference on Neutrino Physics and Astrophysics, 2022).
URL <https://neutrino2022.org/>
- [306] F. P. An, et al., Precision Measurement of Reactor Antineutrino Oscillation at Kilometer-Scale Baselines by Daya Bay, Phys. Rev. Lett. 130 (16) (2023) 161802. [arXiv:2211.14988](#), [doi:10.1103/PhysRevLett.130.161802](#).
- [307] T. Fukuyama, H. Nishiura, Mass matrix of Majorana neutrinos [arXiv:hep-ph/9702253](#).
- [308] E. Ma, M. Raidal, Neutrino mass, muon anomalous magnetic moment, and lepton flavor nonconservation, Phys. Rev. Lett. 87 (2001) 011802, [Erratum: Phys.Rev.Lett. 87, 159901 (2001)]. [arXiv:hep-ph/0102255](#), [doi:10.1103/PhysRevLett.87.011802](#).
- [309] K. R. S. Balaji, W. Grimus, T. Schwetz, The Solar LMA neutrino oscillation solution in the Zee model, Phys. Lett. B 508 (2001) 301–310. [arXiv:hep-ph/0104035](#), [doi:10.1016/S0370-2693\(01\)00532-9](#).
- [310] C. S. Lam, A 2-3 symmetry in neutrino oscillations, Phys. Lett. B 507 (2001) 214–218. [arXiv:hep-ph/0104116](#), [doi:10.1016/S0370-2693\(01\)00465-8](#).
- [311] W. Grimus, L. Lavoura, Softly broken lepton numbers and maximal neutrino mixing, JHEP 07 (2001) 045. [arXiv:hep-ph/0105212](#), [doi:10.1088/1126-6708/2001/07/045](#).
- [312] C. S. Lam, Magic neutrino mass matrix and the Bjorken-Harrison-Scott parameterization, Phys. Lett. B 640 (2006) 260–262. [arXiv:hep-ph/0606220](#), [doi:10.1016/j.physletb.2006.08.007](#).

- [313] G. Altarelli, F. Feruglio, Tri-bimaximal neutrino mixing, A_4 and the modular symmetry, Nucl. Phys. B 741 (2006) 215–235. [arXiv:hep-ph/0512103](#), [doi:10.1016/j.nuclphysb.2006.02.015](#).
- [314] G. Altarelli, F. Feruglio, Y. Lin, Tri-bimaximal neutrino mixing from orbifolding, Nucl. Phys. B 775 (2007) 31–44. [arXiv:hep-ph/0610165](#), [doi:10.1016/j.nuclphysb.2007.03.042](#).
- [315] G. Altarelli, F. Feruglio, L. Merlo, Tri-Bimaximal Neutrino Mixing and Discrete Flavour Symmetries, Fortsch. Phys. 61 (2013) 507–534. [arXiv:1205.5133](#), [doi:10.1002/prop.201200117](#).
- [316] C. H. Albright, W. Rodejohann, Comparing Trimaximal Mixing and Its Variants with Deviations from Tri-bimaximal Mixing, Eur. Phys. J. C 62 (2009) 599–608. [arXiv:0812.0436](#), [doi:10.1140/epjc/s10052-009-1074-3](#).
- [317] C. H. Albright, A. Dueck, W. Rodejohann, Possible Alternatives to Tri-bimaximal Mixing, Eur. Phys. J. C 70 (2010) 1099–1110. [arXiv:1004.2798](#), [doi:10.1140/epjc/s10052-010-1492-2](#).
- [318] X.-G. He, A. Zee, Minimal Modification to Tri-bimaximal Mixing, Phys. Rev. D 84 (2011) 053004. [arXiv:1106.4359](#), [doi:10.1103/PhysRevD.84.053004](#).
- [319] C. Luhn, Trimaximal TM_1 neutrino mixing in S_4 with spontaneous CP violation, Nucl. Phys. B 875 (2013) 80–100. [arXiv:1306.2358](#), [doi:10.1016/j.nuclphysb.2013.07.003](#).
- [320] C.-C. Li, G.-J. Ding, Generalised CP and trimaximal TM_1 lepton mixing in S_4 family symmetry, Nucl. Phys. B 881 (2014) 206–232. [arXiv:1312.4401](#), [doi:10.1016/j.nuclphysb.2014.02.002](#).
- [321] J. D. Bjorken, P. F. Harrison, W. G. Scott, Simplified unitarity triangles for the lepton sector, Phys. Rev. D 74 (2006) 073012. [arXiv:hep-ph/0511201](#), [doi:10.1103/PhysRevD.74.073012](#).
- [322] X.-G. He, A. Zee, Minimal modification to the tri-bimaximal neutrino mixing, Phys. Lett. B 645 (2007) 427–431. [arXiv:hep-ph/0607163](#), [doi:10.1016/j.physletb.2006.11.055](#).
- [323] W. Grimus, L. Lavoura, A Model for trimaximal lepton mixing, JHEP 09 (2008) 106. [arXiv:0809.0226](#), [doi:10.1088/1126-6708/2008/09/106](#).
- [324] W. Grimus, L. Lavoura, A. Singraber, Trimaximal lepton mixing with a trivial Dirac phase, Phys. Lett. B 686 (2010) 141–145. [arXiv:0911.5120](#), [doi:10.1016/j.physletb.2010.02.032](#).
- [325] G.-J. Ding, S. F. King, C. Luhn, A. J. Stuart, Spontaneous CP violation from vacuum alignment in S_4 models of leptons, JHEP 05 (2013) 084. [arXiv:1303.6180](#), [doi:10.1007/JHEP05\(2013\)084](#).
- [326] W. Rodejohann, Unified Parametrization for Quark and Lepton Mixing Angles, Phys. Lett. B 671 (2009) 267–271. [arXiv:0810.5239](#), [doi:10.1016/j.physletb.2008.12.010](#).
- [327] A. Adulpravitchai, A. Blum, W. Rodejohann, Golden Ratio Prediction for Solar Neutrino Mixing, New J. Phys. 11 (2009) 063026. [arXiv:0903.0531](#), [doi:10.1088/1367-2630/11/6/063026](#).
- [328] A. Datta, F.-S. Ling, P. Ramond, Correlated hierarchy, Dirac masses and large mixing angles, Nucl. Phys. B 671 (2003) 383–400. [arXiv:hep-ph/0306002](#), [doi:10.1016/j.nuclphysb.2003.08.026](#).
- [329] Y. Kajiyama, M. Raidal, A. Strumia, The Golden ratio prediction for the solar neutrino mixing, Phys. Rev. D 76 (2007) 117301. [arXiv:0705.4559](#), [doi:10.1103/PhysRevD.76.117301](#).
- [330] L. L. Everett, A. J. Stuart, Icosahedral ($A(5)$) Family Symmetry and the Golden Ratio Prediction for Solar Neutrino Mixing, Phys. Rev. D 79 (2009) 085005. [arXiv:0812.1057](#), [doi:10.1103/PhysRevD.79.085005](#).

- [331] F. Feruglio, A. Paris, The Golden Ratio Prediction for the Solar Angle from a Natural Model with A_5 Flavour Symmetry, *JHEP* 03 (2011) 101. [arXiv:1101.0393](#), [doi:10.1007/JHEP03\(2011\)101](#).
- [332] G.-J. Ding, L. L. Everett, A. J. Stuart, Golden Ratio Neutrino Mixing and A_5 Flavor Symmetry, *Nucl. Phys. B* 857 (2012) 219–253. [arXiv:1110.1688](#), [doi:10.1016/j.nuclphysb.2011.12.004](#).
- [333] V. D. Barger, S. Pakvasa, T. J. Weiler, K. Whisnant, Bimaximal mixing of three neutrinos, *Phys. Lett. B* 437 (1998) 107–116. [arXiv:hep-ph/9806387](#), [doi:10.1016/S0370-2693\(98\)00880-6](#).
- [334] G. Altarelli, F. Feruglio, L. Merlo, Revisiting Bimaximal Neutrino Mixing in a Model with $S(4)$ Discrete Symmetry, *JHEP* 05 (2009) 020. [arXiv:0903.1940](#), [doi:10.1088/1126-6708/2009/05/020](#).
- [335] C.-C. Li, G.-J. Ding, Deviation from bimaximal mixing and leptonic CP phases in S_4 family symmetry and generalized CP, *JHEP* 08 (2015) 017. [arXiv:1408.0785](#), [doi:10.1007/JHEP08\(2015\)017](#).
- [336] R. de Adelhart Toorop, F. Feruglio, C. Hagedorn, Discrete Flavour Symmetries in Light of T2K, *Phys. Lett. B* 703 (2011) 447–451. [arXiv:1107.3486](#), [doi:10.1016/j.physletb.2011.08.013](#).
- [337] G.-J. Ding, TFH Mixing Patterns, Large θ_{13} and $\Delta(96)$ Flavor Symmetry, *Nucl. Phys. B* 862 (2012) 1–42. [arXiv:1201.3279](#), [doi:10.1016/j.nuclphysb.2012.04.002](#).
- [338] C. Hagedorn, A. Meroni, L. Vitale, Mixing patterns from the groups $\Sigma(n\phi)$, *J. Phys. A* 47 (2014) 055201. [arXiv:1307.5308](#), [doi:10.1088/1751-8113/47/5/055201](#).
- [339] G. Ecker, W. Grimus, W. Konetschny, Quark Mass Matrices in Left-right Symmetric Gauge Theories, *Nucl. Phys. B* 191 (1981) 465–492. [doi:10.1016/0550-3213\(81\)90309-6](#).
- [340] G. Ecker, W. Grimus, H. Neufeld, Spontaneous CP Violation in Left-right Symmetric Gauge Theories, *Nucl. Phys. B* 247 (1984) 70–82. [doi:10.1016/0550-3213\(84\)90373-0](#).
- [341] J. Bernabeu, G. C. Branco, M. Gronau, CP Restrictions on Quark Mass Matrices, *Phys. Lett. B* 169 (1986) 243–247. [doi:10.1016/0370-2693\(86\)90659-3](#).
- [342] G. Ecker, W. Grimus, H. Neufeld, A Standard Form for Generalized CP Transformations, *J. Phys. A* 20 (1987) L807. [doi:10.1088/0305-4470/20/12/010](#).
- [343] H. Neufeld, W. Grimus, G. Ecker, Generalized CP Invariance, Neutral Flavor Conservation and the Structure of the Mixing Matrix, *Int. J. Mod. Phys. A* 3 (1988) 603–616. [doi:10.1142/S0217751X88000254](#).
- [344] M. Holthausen, M. Lindner, M. A. Schmidt, CP and Discrete Flavour Symmetries, *JHEP* 04 (2013) 122. [arXiv:1211.6953](#), [doi:10.1007/JHEP04\(2013\)122](#).
- [345] C.-Y. Yao, G.-J. Ding, CP Symmetry and Lepton Mixing from a Scan of Finite Discrete Groups, *Phys. Rev. D* 94 (7) (2016) 073006. [arXiv:1606.05610](#), [doi:10.1103/PhysRevD.94.073006](#).
- [346] A. Abada, G. Arcadi, V. Domcke, M. Drewes, J. Klarić, M. Lucente, Low-scale leptogenesis with three heavy neutrinos, *JHEP* 01 (2019) 164. [arXiv:1810.12463](#), [doi:10.1007/JHEP01\(2019\)164](#).
- [347] M. Drewes, Y. Georis, J. Klarić, Mapping the Viable Parameter Space for Testable Leptogenesis, *Phys. Rev. Lett.* 128 (5) (2022) 051801. [arXiv:2106.16226](#), [doi:10.1103/PhysRevLett.128.051801](#).
- [348] C.-C. Li, G.-J. Ding, Implications of residual CP symmetry for leptogenesis in a model with two right-handed neutrinos, *Phys. Rev. D* 96 (7) (2017) 075005. [arXiv:1701.08508](#), [doi:10.1103/PhysRevD.96.075005](#).

- [349] A. S. Joshipura, K. M. Patel, Horizontal symmetries of leptons with a massless neutrino, *Phys. Lett. B* 727 (2013) 480–487. [arXiv:1306.1890](#), [doi:10.1016/j.physletb.2013.11.003](#).
- [350] A. S. Joshipura, K. M. Patel, A massless neutrino and lepton mixing patterns from finite discrete subgroups of $U(3)$, *JHEP* 04 (2014) 009. [arXiv:1401.6397](#), [doi:10.1007/JHEP04\(2014\)009](#).
- [351] S. F. King, P. O. Ludl, Direct and Semi-Direct Approaches to Lepton Mixing with a Massless Neutrino, *JHEP* 06 (2016) 147. [arXiv:1605.01683](#), [doi:10.1007/JHEP06\(2016\)147](#).
- [352] R. Barbieri, L. J. Hall, S. Raby, A. Romanino, Unified theories with $U(2)$ flavor symmetry, *Nucl. Phys. B* 493 (1997) 3–26. [arXiv:hep-ph/9610449](#), [doi:10.1016/S0550-3213\(97\)00134-X](#).
- [353] R. Barbieri, L. J. Hall, A. Romanino, Consequences of a $U(2)$ flavor symmetry, *Phys. Lett. B* 401 (1997) 47–53. [arXiv:hep-ph/9702315](#), [doi:10.1016/S0370-2693\(97\)00372-9](#).
- [354] M. Linster, R. Ziegler, A Realistic $U(2)$ Model of Flavor, *JHEP* 08 (2018) 058. [arXiv:1805.07341](#), [doi:10.1007/JHEP08\(2018\)058](#).
- [355] S. F. King, Predicting neutrino parameters from $SO(3)$ family symmetry and quark-lepton unification, *JHEP* 08 (2005) 105. [arXiv:hep-ph/0506297](#), [doi:10.1088/1126-6708/2005/08/105](#).
- [356] S. F. King, M. Malinsky, Towards a Complete Theory of Fermion Masses and Mixings with $SO(3)$ Family Symmetry and 5-D $SO(10)$ Unification, *JHEP* 11 (2006) 071. [arXiv:hep-ph/0608021](#), [doi:10.1088/1126-6708/2006/11/071](#).
- [357] I. de Medeiros Varzielas, G. G. Ross, $SU(3)$ family symmetry and neutrino bi-tri-maximal mixing, *Nucl. Phys. B* 733 (2006) 31–47. [arXiv:hep-ph/0507176](#), [doi:10.1016/j.nuclphysb.2005.10.039](#).
- [358] S. Antusch, S. F. King, M. Malinsky, Solving the SUSY Flavour and CP Problems with $SU(3)$ Family Symmetry, *JHEP* 06 (2008) 068. [arXiv:0708.1282](#), [doi:10.1088/1126-6708/2008/06/068](#).
- [359] F. Bazzocchi, S. Morisi, M. Picariello, E. Torrente-Lujan, Embedding $A(4)$ into $SU(3) \times U(1)$ flavor symmetry: Large neutrino mixing and fermion mass hierarchy in $SO(10)$ GUT, *J. Phys. G* 36 (2009) 015002. [arXiv:0802.1693](#), [doi:10.1088/0954-3899/36/1/015002](#).
- [360] S. Weinberg, The Problem of Mass, *Trans. New York Acad. Sci.* 38 (1977) 185–201. [doi:10.1111/j.2164-0947.1977.tb02958.x](#).
- [361] H. Fritzsch, Calculating the Cabibbo Angle, *Phys. Lett. B* 70 (1977) 436–440. [doi:10.1016/0370-2693\(77\)90408-7](#).
- [362] H. Fritzsch, Weak Interaction Mixing in the Six - Quark Theory, *Phys. Lett. B* 73 (1978) 317–322. [doi:10.1016/0370-2693\(78\)90524-5](#).
- [363] P. H. Frampton, S. L. Glashow, D. Marfatia, Zeroes of the neutrino mass matrix, *Phys. Lett. B* 536 (2002) 79–82. [arXiv:hep-ph/0201008](#), [doi:10.1016/S0370-2693\(02\)01817-8](#).
- [364] P. Chen, G.-J. Ding, F. Gonzalez-Canales, J. W. F. Valle, Classifying CP transformations according to their texture zeros: theory and implications, *Phys. Rev. D* 94 (3) (2016) 033002. [arXiv:1604.03510](#), [doi:10.1103/PhysRevD.94.033002](#).
- [365] P. Chen, S. Centelles Chuliá, G.-J. Ding, R. Srivastava, J. W. F. Valle, CP symmetries as guiding posts: revamping tri-bi-maximal mixing. Part I, *JHEP* 03 (2019) 036. [arXiv:1812.04663](#), [doi:10.1007/JHEP03\(2019\)036](#).

- [366] S. Centelles Chuliá, A. Trautner, Asymmetric tri-bi-maximal mixing and residual symmetries, *Mod.Phys.Lett.A* 35 (35) (2020) 2050292. [arXiv:1911.12043](#), [doi:10.1142/S0217732320502922](#).
- [367] P. Chen, S. Centelles Chuliá, G.-J. Ding, R. Srivastava, J. W. F. Valle, Realistic tribimaximal neutrino mixing, *Phys. Rev. D* 98 (5) (2018) 055019. [arXiv:1806.03367](#), [doi:10.1103/PhysRevD.98.055019](#).
- [368] J. Schechter, J. W. F. Valle, Majorana Neutrinos and Magnetic Fields, *Phys. Rev. D* 24 (1981) 1883–1889, [Erratum: *Phys.Rev.D* 25, 283 (1982)]. [doi:10.1103/PhysRevD.25.283](#).
- [369] L. Wolfenstein, CP Properties of Majorana Neutrinos and Double beta Decay, *Phys. Lett. B* 107 (1981) 77–79. [doi:10.1016/0370-2693\(81\)91151-5](#).
- [370] P. Chen, S. Centelles Chuliá, G.-J. Ding, R. Srivastava, J. W. F. Valle, CP symmetries as guiding posts: Revamping tribimaximal mixing. II., *Phys. Rev. D* 100 (5) (2019) 053001. [arXiv:1905.11997](#), [doi:10.1103/PhysRevD.100.053001](#).
- [371] S. M. Boucenna, S. Morisi, M. Tortola, J. W. F. Valle, Bi-large neutrino mixing and the Cabibbo angle, *Phys. Rev. D* 86 (2012) 051301. [arXiv:1206.2555](#), [doi:10.1103/PhysRevD.86.051301](#).
- [372] G.-J. Ding, S. Morisi, J. W. F. Valle, Bilarge neutrino mixing and Abelian flavor symmetry, *Phys. Rev. D* 87 (5) (2013) 053013. [arXiv:1211.6506](#), [doi:10.1103/PhysRevD.87.053013](#).
- [373] S. Roy, S. Morisi, N. N. Singh, J. W. F. Valle, The Cabibbo angle as a universal seed for quark and lepton mixings, *Phys. Lett. B* 748 (2015) 1–4. [arXiv:1410.3658](#), [doi:10.1016/j.physletb.2015.06.052](#).
- [374] P. Chen, G.-J. Ding, R. Srivastava, J. W. F. Valle, Predicting neutrino oscillations with “bi-large” lepton mixing matrices, *Phys. Lett. B* 792 (2019) 461–464. [arXiv:1902.08962](#), [doi:10.1016/j.physletb.2019.04.022](#).
- [375] S. Roy, K. Sashikanta Singh, J. Borah, Revamped Bi-Large neutrino mixing with Gatto-Sartori-Tonin like relation, *Nucl. Phys. B* 960 (2020) 115204. [arXiv:2001.07401](#), [doi:10.1016/j.nuclphysb.2020.115204](#).
- [376] H. Ishimori, T. Kobayashi, H. Ohki, H. Okada, Y. Shimizu, M. Tanimoto, An introduction to non-Abelian discrete symmetries for particle physicists, Vol. 858, 2012. [doi:10.1007/978-3-642-30805-5](#).
- [377] Y. Abe, et al., Reactor electron antineutrino disappearance in the Double Chooz experiment, *Phys. Rev. D* 86 (2012) 052008. [arXiv:1207.6632](#), [doi:10.1103/PhysRevD.86.052008](#).
- [378] S. F. King, C. Luhn, On the origin of neutrino flavour symmetry, *JHEP* 10 (2009) 093. [arXiv:0908.1897](#), [doi:10.1088/1126-6708/2009/10/093](#).
- [379] S. F. King, T. Neder, A. J. Stuart, Lepton mixing predictions from $\Delta(6n^2)$ family Symmetry, *Phys. Lett. B* 726 (2013) 312–315. [arXiv:1305.3200](#), [doi:10.1016/j.physletb.2013.08.052](#).
- [380] S. F. King, T. Neder, Lepton mixing predictions including Majorana phases from $\Delta(6n^2)$ flavour symmetry and generalised CP, *Phys. Lett. B* 736 (2014) 308–316. [arXiv:1403.1758](#), [doi:10.1016/j.physletb.2014.07.043](#).
- [381] S.-F. Ge, D. A. Dicus, W. W. Repko, \mathbb{Z}_2 Symmetry Prediction for the Leptonic Dirac CP Phase, *Phys. Lett. B* 702 (2011) 220–223. [arXiv:1104.0602](#), [doi:10.1016/j.physletb.2011.06.096](#).
- [382] S.-F. Ge, D. A. Dicus, W. W. Repko, Residual Symmetries for Neutrino Mixing with a Large θ_{13} and Nearly Maximal δ_D , *Phys. Rev. Lett.* 108 (2012) 041801. [arXiv:1108.0964](#), [doi:10.1103/PhysRevLett.108.041801](#).

- [383] D. Hernandez, A. Y. Smirnov, Lepton mixing and discrete symmetries, Phys. Rev. D 86 (2012) 053014. [arXiv:1204.0445](#), [doi:10.1103/PhysRevD.86.053014](#).
- [384] D. Hernandez, A. Y. Smirnov, Discrete symmetries and model-independent patterns of lepton mixing, Phys. Rev. D 87 (5) (2013) 053005. [arXiv:1212.2149](#), [doi:10.1103/PhysRevD.87.053005](#).
- [385] W. Grimus, M. N. Rebelo, Automorphisms in gauge theories and the definition of CP and P, Phys. Rept. 281 (1997) 239–308. [arXiv:hep-ph/9506272](#), [doi:10.1016/S0370-1573\(96\)00030-0](#).
- [386] Z.-z. Xing, Z.-h. Zhao, A review of μ - τ flavor symmetry in neutrino physics, Rept. Prog. Phys. 79 (7) (2016) 076201. [arXiv:1512.04207](#), [doi:10.1088/0034-4885/79/7/076201](#).
- [387] M.-C. Chen, M. Fallbacher, K. T. Mahanthappa, M. Ratz, A. Trautner, CP Violation from Finite Groups, Nucl. Phys. B 883 (2014) 267–305. [arXiv:1402.0507](#), [doi:10.1016/j.nuclphysb.2014.03.023](#).
- [388] G.-J. Ding, S. F. King, A. J. Stuart, Generalised CP and A_4 Family Symmetry, JHEP 12 (2013) 006. [arXiv:1307.4212](#), [doi:10.1007/JHEP12\(2013\)006](#).
- [389] S. F. King, Littlest Seesaw, JHEP 02 (2016) 085. [arXiv:1512.07531](#), [doi:10.1007/JHEP02\(2016\)085](#).
- [390] G.-J. Ding, S. F. King, C.-C. Li, Tri-Direct CP in the Littlest Seesaw Playground, JHEP 12 (2018) 003. [arXiv:1807.07538](#), [doi:10.1007/JHEP12\(2018\)003](#).
- [391] G.-J. Ding, S. F. King, C.-C. Li, Lepton mixing predictions from S_4 in the tridirect CP approach to two right-handed neutrino models, Phys. Rev. D 99 (7) (2019) 075035. [arXiv:1811.12340](#), [doi:10.1103/PhysRevD.99.075035](#).
- [392] P.-T. Chen, G.-J. Ding, S. F. King, C.-C. Li, A New Littlest Seesaw Model, J. Phys. G 47 (6) (2020) 065001. [arXiv:1906.11414](#), [doi:10.1088/1361-6471/ab7e8d](#).
- [393] C.-C. Li, J.-N. Lu, G.-J. Ding, A_4 and CP symmetry and a model with maximal CP violation, Nucl. Phys. B 913 (2016) 110–131. [arXiv:1608.01860](#), [doi:10.1016/j.nuclphysb.2016.09.005](#).
- [394] F. Feruglio, C. Hagedorn, R. Ziegler, A realistic pattern of lepton mixing and masses from S_4 and CP, Eur. Phys. J. C 74 (2014) 2753. [arXiv:1303.7178](#), [doi:10.1140/epjc/s10052-014-2753-2](#).
- [395] J.-N. Lu, G.-J. Ding, Alternative Schemes of Predicting Lepton Mixing Parameters from Discrete Flavor and CP Symmetry, Phys. Rev. D 95 (1) (2017) 015012. [arXiv:1610.05682](#), [doi:10.1103/PhysRevD.95.015012](#).
- [396] J. T. Penedo, S. T. Petcov, A. V. Titov, Neutrino mixing and leptonic CP violation from S_4 flavour and generalised CP symmetries, JHEP 12 (2017) 022. [arXiv:1705.00309](#), [doi:10.1007/JHEP12\(2017\)022](#).
- [397] G. C. Branco, I. de Medeiros Varzielas, S. F. King, Invariant approach to CP in family symmetry models, Phys. Rev. D 92 (3) (2015) 036007. [arXiv:1502.03105](#), [doi:10.1103/PhysRevD.92.036007](#).
- [398] G. C. Branco, I. de Medeiros Varzielas, S. F. King, Invariant approach to \mathcal{CP} in unbroken $\Delta(27)$, Nucl. Phys. B 899 (2015) 14–36. [arXiv:1505.06165](#), [doi:10.1016/j.nuclphysb.2015.07.024](#).
- [399] G.-J. Ding, Y.-L. Zhou, Predicting lepton flavor mixing from $\Delta(48)$ and generalized \mathcal{CP} symmetries, Chin. Phys. C 39 (2) (2015) 021001. [arXiv:1312.5222](#), [doi:10.1088/1674-1137/39/2/021001](#).
- [400] G.-J. Ding, Y.-L. Zhou, Lepton mixing parameters from $\Delta(48)$ family symmetry and generalised CP, JHEP 06 (2014) 023. [arXiv:1404.0592](#), [doi:10.1007/JHEP06\(2014\)023](#).

- [401] C.-C. Li, G.-J. Ding, Lepton Mixing in A_5 Family Symmetry and Generalized CP, JHEP 05 (2015) 100. [arXiv:1503.03711](#), [doi:10.1007/JHEP05\(2015\)100](#).
- [402] A. Di Iura, C. Hagedorn, D. Meloni, Lepton mixing from the interplay of the alternating group A_5 and CP, JHEP 08 (2015) 037. [arXiv:1503.04140](#), [doi:10.1007/JHEP08\(2015\)037](#).
- [403] P. Ballett, S. Pascoli, J. Turner, Mixing angle and phase correlations from A_5 with generalized CP and their prospects for discovery, Phys. Rev. D 92 (9) (2015) 093008. [arXiv:1503.07543](#), [doi:10.1103/PhysRevD.92.093008](#).
- [404] J. Turner, Predictions for leptonic mixing angle correlations and nontrivial Dirac CP violation from A_5 with generalized CP symmetry, Phys. Rev. D 92 (11) (2015) 116007. [arXiv:1507.06224](#), [doi:10.1103/PhysRevD.92.116007](#).
- [405] A. Di Iura, M. L. López-Ibáñez, D. Meloni, Neutrino masses and lepton mixing from $A_5 \times CP$, Nucl. Phys. B 949 (2019) 114794. [arXiv:1811.09662](#), [doi:10.1016/j.nuclphysb.2019.114794](#).
- [406] G.-J. Ding, S. F. King, Generalized CP and $\Delta(96)$ family symmetry, Phys. Rev. D 89 (9) (2014) 093020. [arXiv:1403.5846](#), [doi:10.1103/PhysRevD.89.093020](#).
- [407] C. Hagedorn, A. Meroni, E. Molinaro, Lepton mixing from $\Delta(3n^2)$ and $\Delta(6n^2)$ and CP, Nucl. Phys. B 891 (2015) 499–557. [arXiv:1408.7118](#), [doi:10.1016/j.nuclphysb.2014.12.013](#).
- [408] G.-J. Ding, S. F. King, Generalized CP and $\Delta(3n^2)$ Family Symmetry for Semi-Direct Predictions of the PMNS Matrix, Phys. Rev. D 93 (2016) 025013. [arXiv:1510.03188](#), [doi:10.1103/PhysRevD.93.025013](#).
- [409] G.-J. Ding, S. F. King, T. Neder, Generalised CP and $\Delta(6n^2)$ family symmetry in semi-direct models of leptons, JHEP 12 (2014) 007. [arXiv:1409.8005](#), [doi:10.1007/JHEP12\(2014\)007](#).
- [410] C.-C. Li, C.-Y. Yao, G.-J. Ding, Lepton Mixing Predictions from Infinite Group Series $D_{9n,3n}^{(1)}$ with Generalized CP, JHEP 05 (2016) 007. [arXiv:1601.06393](#), [doi:10.1007/JHEP05\(2016\)007](#).
- [411] C. Jarlskog, Commutator of the Quark Mass Matrices in the Standard Electroweak Model and a Measure of Maximal CP Nonconservation, Phys. Rev. Lett. 55 (1985) 1039. [doi:10.1103/PhysRevLett.55.1039](#).
- [412] G. C. Branco, L. Lavoura, M. N. Rebelo, Majorana Neutrinos and CP Violation in the Leptonic Sector, Phys. Lett. B 180 (1986) 264–268. [doi:10.1016/0370-2693\(86\)90307-2](#).
- [413] J. F. Nieves, P. B. Pal, Minimal Rephasing Invariant CP Violating Parameters With Dirac and Majorana Fermions, Phys. Rev. D 36 (1987) 315. [doi:10.1103/PhysRevD.36.315](#).
- [414] T. D. Lee, A Theory of Spontaneous T Violation, Phys. Rev. D 8 (1973) 1226–1239. [doi:10.1103/PhysRevD.8.1226](#).
- [415] G. C. Branco, J. M. Gerard, W. Grimus, Geometrical T Violation, Phys. Lett. B 136 (1984) 383–386. [doi:10.1016/0370-2693\(84\)92024-0](#).
- [416] I. de Medeiros Varzielas, D. Emmanuel-Costa, Geometrical CP Violation, Phys. Rev. D 84 (2011) 117901. [arXiv:1106.5477](#), [doi:10.1103/PhysRevD.84.117901](#).
- [417] C. Luhn, S. Nasri, P. Ramond, The Flavor group $\Delta(3n^2)$, J. Math. Phys. 48 (2007) 073501. [arXiv:hep-th/0701188](#), [doi:10.1063/1.2734865](#).
- [418] J. A. Escobar, C. Luhn, The Flavor Group $\Delta(6n^2)$, J. Math. Phys. 50 (2009) 013524. [arXiv:0809.0639](#), [doi:10.1063/1.3046563](#).

- [419] D. Adey, et al., Measurement of the Electron Antineutrino Oscillation with 1958 Days of Operation at Daya Bay, *Phys. Rev. Lett.* 121 (24) (2018) 241805. [arXiv:1809.02261](#), [doi:10.1103/PhysRevLett.121.241805](#).
- [420] Y. Abe, et al., Indication of Reactor $\bar{\nu}_e$ Disappearance in the Double Chooz Experiment, *Phys. Rev. Lett.* 108 (2012) 131801. [arXiv:1112.6353](#), [doi:10.1103/PhysRevLett.108.131801](#).
- [421] Y. Abe, et al., Improved measurements of the neutrino mixing angle θ_{13} with the Double Chooz detector, *JHEP* 10 (2014) 086, [Erratum: *JHEP* 02, 074 (2015)]. [arXiv:1406.7763](#), [doi:10.1007/JHEP02\(2015\)074](#).
- [422] G. Bak, et al., Measurement of Reactor Antineutrino Oscillation Amplitude and Frequency at RENO, *Phys. Rev. Lett.* 121 (20) (2018) 201801. [arXiv:1806.00248](#), [doi:10.1103/PhysRevLett.121.201801](#).
- [423] D. S. Ayres, et al., NOvA: Proposal to Build a 30 Kiloton Off-Axis Detector to Study $\nu_\mu \rightarrow \nu_e$ Oscillations in the NuMI Beamline [arXiv:hep-ex/0503053](#).
- [424] K. Abe, et al., The T2K Experiment, *Nucl. Instrum. Meth. A* 659 (2011) 106–135. [arXiv:1106.1238](#), [doi:10.1016/j.nima.2011.06.067](#).
- [425] K. Abe, et al., Search for CP Violation in Neutrino and Antineutrino Oscillations by the T2K Experiment with 2.2×10^{21} Protons on Target, *Phys. Rev. Lett.* 121 (17) (2018) 171802. [arXiv:1807.07891](#), [doi:10.1103/PhysRevLett.121.171802](#).
- [426] M. A. Acero, et al., First Measurement of Neutrino Oscillation Parameters using Neutrinos and Antineutrinos by NOvA, *Phys. Rev. Lett.* 123 (15) (2019) 151803. [arXiv:1906.04907](#), [doi:10.1103/PhysRevLett.123.151803](#).
- [427] K. Abe, et al., Constraint on the matter–antimatter symmetry-violating phase in neutrino oscillations, *Nature* 580 (7803) (2020) 339–344, [Erratum: *Nature* 583, E16 (2020)]. [arXiv:1910.03887](#), [doi:10.1038/s41586-020-2177-0](#).
- [428] K. Abe, et al., Measurements of neutrino oscillation parameters from the T2K experiment using 3.6×10^{21} protons on target, *Eur. Phys. J. C* 83 (9) (2023) 782. [arXiv:2303.03222](#), [doi:10.1140/epjc/s10052-023-11819-x](#).
- [429] M. A. Acero, et al., Improved measurement of neutrino oscillation parameters by the NOvA experiment, *Phys. Rev. D* 106 (3) (2022) 032004. [arXiv:2108.08219](#), [doi:10.1103/PhysRevD.106.032004](#).
- [430] B. Abi, et al., Deep Underground Neutrino Experiment (DUNE), Far Detector Technical Design Report, Volume II: DUNE Physics [arXiv:2002.03005](#).
- [431] K. Abe, et al., Physics potential of a long-baseline neutrino oscillation experiment using a J-PARC neutrino beam and Hyper-Kamiokande, *PTEP* 2015 (2015) 053C02. [arXiv:1502.05199](#), [doi:10.1093/ptep/ptv061](#).
- [432] S. T. Petcov, A. V. Titov, Assessing the Viability of A_4 , S_4 and A_5 Flavour Symmetries for Description of Neutrino Mixing, *Phys. Rev. D* 97 (11) (2018) 115045. [arXiv:1804.00182](#), [doi:10.1103/PhysRevD.97.115045](#).
- [433] M. Blennow, M. Ghosh, T. Ohlsson, A. Titov, Testing Lepton Flavor Models at ESSnuSB, *JHEP* 07 (2020) 014. [arXiv:2004.00017](#), [doi:10.1007/JHEP07\(2020\)014](#).
- [434] J. Gehrlein, M. Spinrath, Leptonic Sum Rules from Flavour Models with Modular Symmetries, *JHEP* 03 (2021) 177. [arXiv:2012.04131](#), [doi:10.1007/JHEP03\(2021\)177](#).

- [435] P. P. Novichkov, J. T. Penedo, S. T. Petcov, Double cover of modular S_4 for flavour model building, Nucl. Phys. B 963 (2021) 115301. [arXiv:2006.03058](#), [doi:10.1016/j.nuclphysb.2020.115301](#).
- [436] P. P. Novichkov, J. T. Penedo, S. T. Petcov, Fermion mass hierarchies, large lepton mixing and residual modular symmetries, JHEP 04 (2021) 206. [arXiv:2102.07488](#), [doi:10.1007/JHEP04\(2021\)206](#).
- [437] J. Gehrlein, S. Petcov, M. Spinrath, A. Titov, Testing neutrino flavor models, in: Snowmass 2021, 2022. [arXiv:2203.06219](#).
- [438] D. Marzocca, S. T. Petcov, A. Romanino, M. C. Sevilla, Nonzero $|U_{e3}|$ from Charged Lepton Corrections and the Atmospheric Neutrino Mixing Angle, JHEP 05 (2013) 073. [arXiv:1302.0423](#), [doi:10.1007/JHEP05\(2013\)073](#).
- [439] P. Ballett, S. F. King, C. Luhn, S. Pascoli, M. A. Schmidt, Testing solar lepton mixing sum rules in neutrino oscillation experiments, JHEP 12 (2014) 122. [arXiv:1410.7573](#), [doi:10.1007/JHEP12\(2014\)122](#).
- [440] J. E. Kim, M.-S. Seo, Quark and lepton mixing angles with a dodeca-symmetry, JHEP 02 (2011) 097. [arXiv:1005.4684](#), [doi:10.1007/JHEP02\(2011\)097](#).
- [441] S. K. Agarwalla, S. S. Chatterjee, S. T. Petcov, A. V. Titov, Addressing Neutrino Mixing Models with DUNE and T2HK, Eur. Phys. J. C 78 (4) (2018) 286. [arXiv:1711.02107](#), [doi:10.1140/epjc/s10052-018-5772-6](#).
- [442] I. Masina, A Maximal atmospheric mixing from a maximal CP violating phase, Phys. Lett. B 633 (2006) 134–140. [arXiv:hep-ph/0508031](#), [doi:10.1016/j.physletb.2005.10.097](#).
- [443] S. Antusch, S. F. King, Charged lepton corrections to neutrino mixing angles and CP phases revisited, Phys. Lett. B 631 (2005) 42–47. [arXiv:hep-ph/0508044](#), [doi:10.1016/j.physletb.2005.09.075](#).
- [444] P. Ballett, S. F. King, C. Luhn, S. Pascoli, M. A. Schmidt, Testing atmospheric mixing sum rules at precision neutrino facilities, Phys. Rev. D 89 (1) (2014) 016016. [arXiv:1308.4314](#), [doi:10.1103/PhysRevD.89.016016](#).
- [445] I. Girardi, S. T. Petcov, A. V. Titov, Predictions for the Leptonic Dirac CP Violation Phase: a Systematic Phenomenological Analysis, Eur. Phys. J. C 75 (2015) 345. [arXiv:1504.00658](#), [doi:10.1140/epjc/s10052-015-3559-6](#).
- [446] M. Blennow, M. Ghosh, T. Ohlsson, A. Titov, Probing Lepton Flavor Models at Future Neutrino Experiments, Phys. Rev. D 102 (11) (2020) 115004. [arXiv:2005.12277](#), [doi:10.1103/PhysRevD.102.115004](#).
- [447] G.-J. Ding, Y.-F. Li, J. Tang, T.-C. Wang, Confronting tridirect CP -symmetry models with neutrino oscillation experiments, Phys. Rev. D 100 (5) (2019) 055022. [arXiv:1905.12939](#), [doi:10.1103/PhysRevD.100.055022](#).
- [448] J. Gehrlein, M. Spinrath, Neutrino Mass Sum Rules and Symmetries of the Mass Matrix, Eur. Phys. J. C 77 (5) (2017) 281. [arXiv:1704.02371](#), [doi:10.1140/epjc/s10052-017-4817-6](#).
- [449] E. Ma, Aspects of the tetrahedral neutrino mass matrix, Phys. Rev. D 72 (2005) 037301. [arXiv:hep-ph/0505209](#), [doi:10.1103/PhysRevD.72.037301](#).
- [450] J. Barry, W. Rodejohann, Neutrino Mass Sum-rules in Flavor Symmetry Models, Nucl. Phys. B 842 (2011) 33–50. [arXiv:1007.5217](#), [doi:10.1016/j.nuclphysb.2010.08.015](#).
- [451] S. F. King, A. Merle, A. J. Stuart, The Power of Neutrino Mass Sum Rules for Neutrinoless Double Beta Decay Experiments, JHEP 12 (2013) 005. [arXiv:1307.2901](#), [doi:10.1007/JHEP12\(2013\)005](#).

- [452] J. Gehrlein, A. Merle, M. Spinrath, Renormalisation Group Corrections to Neutrino Mass Sum Rules, JHEP 09 (2015) 066. [arXiv:1506.06139](#), [doi:10.1007/JHEP09\(2015\)066](#).
- [453] J. Gehrlein, A. Merle, M. Spinrath, Predictivity of Neutrino Mass Sum Rules, Phys. Rev. D 94 (9) (2016) 093003. [arXiv:1606.04965](#), [doi:10.1103/PhysRevD.94.093003](#).
- [454] P. Huber, M. Lindner, W. Winter, Simulation of long-baseline neutrino oscillation experiments with GLoBES (General Long Baseline Experiment Simulator), Comput. Phys. Commun. 167 (2005) 195. [arXiv:hep-ph/0407333](#), [doi:10.1016/j.cpc.2005.01.003](#).
- [455] P. Huber, J. Kopp, M. Lindner, M. Rolinec, W. Winter, New features in the simulation of neutrino oscillation experiments with GLoBES 3.0: General Long Baseline Experiment Simulator, Comput. Phys. Commun. 177 (2007) 432–438. [arXiv:hep-ph/0701187](#), [doi:10.1016/j.cpc.2007.05.004](#).
- [456] R. G. Calland, A. C. Kaboth, D. Payne, Accelerated Event-by-Event Neutrino Oscillation Reweighting with Matter Effects on a GPU, JINST 9 (2014) P04016. [arXiv:1311.7579](#), [doi:10.1088/1748-0221/9/04/P04016](#).
- [457] M. Wallraff, C. Wiebusch, Calculation of oscillation probabilities of atmospheric neutrinos using nuCraft, Comput. Phys. Commun. 197 (2015) 185–189. [arXiv:1409.1387](#), [doi:10.1016/j.cpc.2015.07.010](#).
- [458] C. A. Argüelles, J. Salvado, C. N. Weaver, nuSQuIDS: A toolbox for neutrino propagation, Comput. Phys. Commun. 277 (2022) 108346. [arXiv:2112.13804](#), [doi:10.1016/j.cpc.2022.108346](#).
- [459] J. Tang, T.-C. Wang, Flavour Symmetry Embedded - GLoBES (FaSE-GLoBES), Comput. Phys. Commun. 263 (2021) 107899. [arXiv:2006.14886](#), [doi:10.1016/j.cpc.2021.107899](#).
- [460] I. Antoniadis, N. Arkani-Hamed, S. Dimopoulos, G. R. Dvali, New dimensions at a millimeter to a Fermi and superstrings at a TeV, Phys. Lett. B 436 (1998) 257–263. [arXiv:hep-ph/9804398](#), [doi:10.1016/S0370-2693\(98\)00860-0](#).
- [461] N. Arkani-Hamed, S. Dimopoulos, G. R. Dvali, The Hierarchy problem and new dimensions at a millimeter, Phys. Lett. B 429 (1998) 263–272. [arXiv:hep-ph/9803315](#), [doi:10.1016/S0370-2693\(98\)00466-3](#).
- [462] L. Randall, R. Sundrum, A Large mass hierarchy from a small extra dimension, Phys. Rev. Lett. 83 (1999) 3370–3373. [arXiv:hep-ph/9905221](#), [doi:10.1103/PhysRevLett.83.3370](#).
- [463] N. Arkani-Hamed, S. Dimopoulos, G. R. Dvali, Phenomenology, astrophysics and cosmology of theories with submillimeter dimensions and TeV scale quantum gravity, Phys. Rev. D 59 (1999) 086004. [arXiv:hep-ph/9807344](#), [doi:10.1103/PhysRevD.59.086004](#).
- [464] K. Agashe, A. Delgado, M. J. May, R. Sundrum, RS1, custodial isospin and precision tests, JHEP 08 (2003) 050. [arXiv:hep-ph/0308036](#), [doi:10.1088/1126-6708/2003/08/050](#).
- [465] K. Agashe, R. Contino, L. Da Rold, A. Pomarol, A Custodial symmetry for $Zb\bar{b}$, Phys. Lett. B 641 (2006) 62–66. [arXiv:hep-ph/0605341](#), [doi:10.1016/j.physletb.2006.08.005](#).
- [466] G. Cacciapaglia, C. Csaki, G. Marandella, J. Terning, The Gaugephobic Higgs, JHEP 02 (2007) 036. [arXiv:hep-ph/0611358](#), [doi:10.1088/1126-6708/2007/02/036](#).
- [467] Y. Grossman, M. Neubert, Neutrino masses and mixings in nonfactorizable geometry, Phys. Lett. B 474 (2000) 361–371. [arXiv:hep-ph/9912408](#), [doi:10.1016/S0370-2693\(00\)00054-X](#).

- [468] T. Gherghetta, A. Pomarol, Bulk fields and supersymmetry in a slice of AdS, Nucl. Phys. B 586 (2000) 141–162. [arXiv:hep-ph/0003129](#), [doi:10.1016/S0550-3213\(00\)00392-8](#).
- [469] R. Gatto, G. Sartori, M. Tonin, Weak Selfmasses, Cabibbo Angle, and Broken $SU(2) \times SU(2)$, Phys. Lett. B 28 (1968) 128–130. [doi:10.1016/0370-2693\(68\)90150-0](#).
- [470] N. Deutschmann, T. Flacke, J. S. Kim, Current LHC Constraints on Minimal Universal Extra Dimensions, Phys. Lett. B 771 (2017) 515–520. [arXiv:1702.00410](#), [doi:10.1016/j.physletb.2017.06.004](#).
- [471] N. Ganguly, A. Datta, Exploring non minimal Universal Extra Dimensional Model at the LHC, JHEP 10 (2018) 072. [arXiv:1808.08801](#), [doi:10.1007/JHEP10\(2018\)072](#).
- [472] F. J. Escrihuela, D. V. Forero, O. G. Miranda, M. Tortola, J. W. F. Valle, On the description of nonunitary neutrino mixing, Phys. Rev. D 92 (5) (2015) 053009, [Erratum: Phys.Rev.D 93, 119905 (2016)]. [arXiv:1503.08879](#), [doi:10.1103/PhysRevD.92.053009](#).
- [473] S. Antusch, V. Maurer, Running quark and lepton parameters at various scales, JHEP 11 (2013) 115. [arXiv:1306.6879](#), [doi:10.1007/JHEP11\(2013\)115](#).
- [474] Z.-z. Xing, H. Zhang, S. Zhou, Updated Values of Running Quark and Lepton Masses, Phys. Rev. D 77 (2008) 113016. [arXiv:0712.1419](#), [doi:10.1103/PhysRevD.77.113016](#).
- [475] S. Antusch, J. Kersten, M. Lindner, M. Ratz, M. A. Schmidt, Running neutrino mass parameters in see-saw scenarios, JHEP 03 (2005) 024. [arXiv:hep-ph/0501272](#), [doi:10.1088/1126-6708/2005/03/024](#).
- [476] N. Abgrall, et al., The Large Enriched Germanium Experiment for Neutrinoless Double Beta Decay (LEGEND), AIP Conf. Proc. 1894 (1) (2017) 020027. [arXiv:1709.01980](#), [doi:10.1063/1.5007652](#).
- [477] J. B. Albert, et al., Sensitivity and Discovery Potential of nEXO to Neutrinoless Double Beta Decay, Phys. Rev. C 97 (6) (2018) 065503. [arXiv:1710.05075](#), [doi:10.1103/PhysRevC.97.065503](#).
- [478] F. Feruglio, Are neutrino masses modular forms?, 2019, pp. 227–266. [arXiv:1706.08749](#), [doi:10.1142/9789813238053_0012](#).
- [479] T. Kobayashi, M. Tanimoto, Modular flavor symmetric models, 2023. [arXiv:2307.03384](#).
- [480] G.-J. Ding, S. F. King, Neutrino Mass and Mixing with Modular Symmetry [arXiv:2311.09282](#).
- [481] H. Cohen, F. Strömberg, **Modular Forms: A Classical Approach**, Graduate studies in mathematics, American Mathematical Society, 2017.
URL <https://books.google.com.hk/books?id=1MmctQEACAAJ>
- [482] P. P. Novichkov, S. T. Petcov, M. Tanimoto, Trimaximal Neutrino Mixing from Modular A_4 Invariance with Residual Symmetries, Phys. Lett. B 793 (2019) 247–258. [arXiv:1812.11289](#), [doi:10.1016/j.physletb.2019.04.043](#).
- [483] G.-J. Ding, S. F. King, X.-G. Liu, J.-N. Lu, Modular S_4 and A_4 symmetries and their fixed points: new predictive examples of lepton mixing, JHEP 12 (2019) 030. [arXiv:1910.03460](#), [doi:10.1007/JHEP12\(2019\)030](#).
- [484] X.-G. Liu, G.-J. Ding, Neutrino Masses and Mixing from Double Covering of Finite Modular Groups, JHEP 08 (2019) 134. [arXiv:1907.01488](#), [doi:10.1007/JHEP08\(2019\)134](#).
- [485] X.-G. Liu, C.-Y. Yao, G.-J. Ding, Modular invariant quark and lepton models in double covering of S_4 modular group, Phys. Rev. D 103 (5) (2021) 056013. [arXiv:2006.10722](#), [doi:10.1103/PhysRevD.103.056013](#).

- [486] X. Wang, B. Yu, S. Zhou, Double covering of the modular A_5 group and lepton flavor mixing in the minimal seesaw model, Phys. Rev. D 103 (7) (2021) 076005. [arXiv:2010.10159](#), [doi:10.1103/PhysRevD.103.076005](#).
- [487] C.-Y. Yao, X.-G. Liu, G.-J. Ding, Fermion masses and mixing from the double cover and metaplectic cover of the A_5 modular group, Phys. Rev. D 103 (9) (2021) 095013. [arXiv:2011.03501](#), [doi:10.1103/PhysRevD.103.095013](#).
- [488] X.-G. Liu, C.-Y. Yao, B.-Y. Qu, G.-J. Ding, Half-integral weight modular forms and application to neutrino mass models, Phys. Rev. D 102 (11) (2020) 115035. [arXiv:2007.13706](#), [doi:10.1103/PhysRevD.102.115035](#).
- [489] P. P. Novichkov, J. T. Penedo, S. T. Petcov, A. V. Titov, Generalised CP Symmetry in Modular-Invariant Models of Flavour, JHEP 07 (2019) 165. [arXiv:1905.11970](#), [doi:10.1007/JHEP07\(2019\)165](#).
- [490] T. Kobayashi, Y. Shimizu, K. Takagi, M. Tanimoto, T. H. Tatsuishi, H. Uchida, CP violation in modular invariant flavor models, Phys. Rev. D 101 (5) (2020) 055046. [arXiv:1910.11553](#), [doi:10.1103/PhysRevD.101.055046](#).
- [491] G.-J. Ding, F. Feruglio, X.-G. Liu, CP symmetry and symplectic modular invariance, SciPost Phys. 10 (6) (2021) 133. [arXiv:2102.06716](#), [doi:10.21468/SciPostPhys.10.6.133](#).
- [492] A. Baur, H. P. Nilles, A. Trautner, P. K. S. Vaudrevange, Unification of Flavor, CP, and Modular Symmetries, Phys. Lett. B 795 (2019) 7–14. [arXiv:1901.03251](#), [doi:10.1016/j.physletb.2019.03.066](#).
- [493] B. S. Acharya, D. Bailin, A. Love, W. A. Sabra, S. Thomas, Spontaneous breaking of CP symmetry by orbifold moduli, Phys. Lett. B 357 (1995) 387–396, [Erratum: Phys.Lett.B 407, 451–451 (1997)]. [arXiv:hep-th/9506143](#), [doi:10.1016/0370-2693\(95\)00945-H](#).
- [494] T. Dent, CP violation and modular symmetries, Phys. Rev. D 64 (2001) 056005. [arXiv:hep-ph/0105285](#), [doi:10.1103/PhysRevD.64.056005](#).
- [495] J. Giedt, CP violation and moduli stabilization in heterotic models, Mod. Phys. Lett. A 17 (2002) 1465–1473. [arXiv:hep-ph/0204017](#), [doi:10.1142/S0217732302007879](#).
- [496] G.-J. Ding, X.-G. Liu, C.-Y. Yao, A minimal modular invariant neutrino model, JHEP 01 (2023) 125. [arXiv:2211.04546](#), [doi:10.1007/JHEP01\(2023\)125](#).
- [497] G.-J. Ding, X.-G. Liu, J.-N. Lu, M.-H. Weng, Modular binary octahedral symmetry for flavor structure of Standard Model, JHEP 11 (2023) 083. [arXiv:2307.14926](#), [doi:10.1007/JHEP11\(2023\)083](#).
- [498] A. Baur, H. P. Nilles, A. Trautner, P. K. S. Vaudrevange, A String Theory of Flavor and CP , Nucl. Phys. B 947 (2019) 114737. [arXiv:1908.00805](#), [doi:10.1016/j.nuclphysb.2019.114737](#).
- [499] T. Kobayashi, S. Nagamoto, S. Uemura, Modular symmetry in magnetized/intersecting D-brane models, PTEP 2017 (2) (2017) 023B02. [arXiv:1608.06129](#), [doi:10.1093/ptep/ptw184](#).
- [500] T. Kobayashi, S. Nagamoto, S. Takada, S. Tamba, T. H. Tatsuishi, Modular symmetry and non-Abelian discrete flavor symmetries in string compactification, Phys. Rev. D 97 (11) (2018) 116002. [arXiv:1804.06644](#), [doi:10.1103/PhysRevD.97.116002](#).
- [501] T. Kobayashi, S. Tamba, Modular forms of finite modular subgroups from magnetized D-brane models, Phys. Rev. D 99 (4) (2019) 046001. [arXiv:1811.11384](#), [doi:10.1103/PhysRevD.99.046001](#).

- [502] Y. Kariyazono, T. Kobayashi, S. Takada, S. Tamba, H. Uchida, Modular symmetry anomaly in magnetic flux compactification, *Phys. Rev. D* 100 (4) (2019) 045014. [arXiv:1904.07546](#), [doi:10.1103/PhysRevD.100.045014](#).
- [503] H. Ohki, S. Uemura, R. Watanabe, Modular flavor symmetry on a magnetized torus, *Phys. Rev. D* 102 (8) (2020) 085008. [arXiv:2003.04174](#), [doi:10.1103/PhysRevD.102.085008](#).
- [504] S. Kikuchi, T. Kobayashi, S. Takada, T. H. Tatsuishi, H. Uchida, Revisiting modular symmetry in magnetized torus and orbifold compactifications, *Phys. Rev. D* 102 (10) (2020) 105010. [arXiv:2005.12642](#), [doi:10.1103/PhysRevD.102.105010](#).
- [505] Y. Almumin, M.-C. Chen, V. Knapp-Pérez, S. Ramos-Sánchez, M. Ratz, S. Shukla, Metaplectic Flavor Symmetries from Magnetized Tori, *JHEP* 05 (2021) 078. [arXiv:2102.11286](#), [doi:10.1007/JHEP05\(2021\)078](#).
- [506] I. de Medeiros Varzielas, S. F. King, Y.-L. Zhou, Multiple modular symmetries as the origin of flavor, *Phys. Rev. D* 101 (5) (2020) 055033. [arXiv:1906.02208](#), [doi:10.1103/PhysRevD.101.055033](#).
- [507] G.-J. Ding, F. Feruglio, X.-G. Liu, Automorphic Forms and Fermion Masses, *JHEP* 01 (2021) 037. [arXiv:2010.07952](#), [doi:10.1007/JHEP01\(2021\)037](#).
- [508] K. Ishiguro, T. Kobayashi, H. Otsuka, Spontaneous CP violation and symplectic modular symmetry in Calabi-Yau compactifications, *Nucl. Phys. B* 973 (2021) 115598. [arXiv:2010.10782](#), [doi:10.1016/j.nuclphysb.2021.115598](#).
- [509] A. Baur, M. Kade, H. P. Nilles, S. Ramos-Sanchez, P. K. S. Vaudrevange, Siegel modular flavor group and CP from string theory, *Phys. Lett. B* 816 (2021) 136176. [arXiv:2012.09586](#), [doi:10.1016/j.physletb.2021.136176](#).
- [510] H. P. Nilles, S. Ramos-Sanchez, A. Trautner, P. K. S. Vaudrevange, Orbifolds from $Sp(4, \mathbb{Z})$ and their modular symmetries, *Nucl. Phys. B* 971 (2021) 115534. [arXiv:2105.08078](#), [doi:10.1016/j.nuclphysb.2021.115534](#).
- [511] H. P. Nilles, S. Ramos-Sánchez, P. K. S. Vaudrevange, Eclectic Flavor Groups, *JHEP* 02 (2020) 045. [arXiv:2001.01736](#), [doi:10.1007/JHEP02\(2020\)045](#).
- [512] H. P. Nilles, S. Ramos-Sanchez, P. K. S. Vaudrevange, Lessons from eclectic flavor symmetries, *Nucl. Phys. B* 957 (2020) 115098. [arXiv:2004.05200](#), [doi:10.1016/j.nuclphysb.2020.115098](#).
- [513] F. Feruglio, V. Gherardi, A. Romanino, A. Titov, Modular invariant dynamics and fermion mass hierarchies around $\tau = i$, *JHEP* 05 (2021) 242. [arXiv:2101.08718](#), [doi:10.1007/JHEP05\(2021\)242](#).
- [514] F. Feruglio, Universal Predictions of Modular Invariant Flavor Models near the Self-Dual Point, *Phys. Rev. Lett.* 130 (10) (2023) 101801. [arXiv:2211.00659](#), [doi:10.1103/PhysRevLett.130.101801](#).
- [515] F. Feruglio, Fermion masses, critical behavior and universality, *JHEP* 03 (2023) 236. [arXiv:2302.11580](#), [doi:10.1007/JHEP03\(2023\)236](#).
- [516] M. Cvetič, A. Font, L. E. Ibanez, D. Lust, F. Quevedo, Target space duality, supersymmetry breaking and the stability of classical string vacua, *Nucl. Phys. B* 361 (1991) 194–232. [doi:10.1016/0550-3213\(91\)90622-5](#).
- [517] E. Gonzalo, L. E. Ibáñez, A. M. Uranga, Modular symmetries and the swampland conjectures, *JHEP* 05 (2019) 105. [arXiv:1812.06520](#), [doi:10.1007/JHEP05\(2019\)105](#).

- [518] T. Kobayashi, Y. Shimizu, K. Takagi, M. Tanimoto, T. H. Tatsuishi, A_4 lepton flavor model and modulus stabilization from S_4 modular symmetry, Phys. Rev. D 100 (11) (2019) 115045, [Erratum: Phys.Rev.D 101, 039904 (2020)]. [arXiv:1909.05139](#), [doi:10.1103/PhysRevD.100.115045](#).
- [519] K. Ishiguro, T. Kobayashi, H. Otsuka, Landscape of Modular Symmetric Flavor Models, JHEP 03 (2021) 161. [arXiv:2011.09154](#), [doi:10.1007/JHEP03\(2021\)161](#).
- [520] P. P. Novichkov, J. T. Penedo, S. T. Petcov, Modular flavour symmetries and modulus stabilisation, JHEP 03 (2022) 149. [arXiv:2201.02020](#), [doi:10.1007/JHEP03\(2022\)149](#).
- [521] J. M. Leedom, N. Righi, A. Westphal, Heterotic de Sitter beyond modular symmetry, JHEP 02 (2023) 209. [arXiv:2212.03876](#), [doi:10.1007/JHEP02\(2023\)209](#).
- [522] V. Knapp-Perez, X.-G. Liu, H. P. Nilles, S. Ramos-Sanchez, M. Ratz, Matter matters in moduli fixing and modular flavor symmetries, Phys. Lett. B 844 (2023) 138106. [arXiv:2304.14437](#), [doi:10.1016/j.physletb.2023.138106](#).
- [523] S. Kikuchi, T. Kobayashi, K. Nasu, Y. Yamada, Moduli trapping mechanism in modular flavor symmetric models, JHEP 08 (2023) 081. [arXiv:2307.13230](#), [doi:10.1007/JHEP08\(2023\)081](#).
- [524] S. F. King, X. Wang, Modulus stabilisation in the multiple-modulus framework [arXiv:2310.10369](#).
- [525] C. Hagedorn, S. F. King, C. Luhn, A SUSY GUT of Flavour with $S_4 \times SU(5)$ to NLO, JHEP 06 (2010) 048. [arXiv:1003.4249](#), [doi:10.1007/JHEP06\(2010\)048](#).
- [526] G.-J. Ding, Fermion Masses and Flavor Mixings in a Model with $S(4)$ Flavor Symmetry, Nucl. Phys. B 827 (2010) 82–111. [arXiv:0909.2210](#), [doi:10.1016/j.nuclphysb.2009.10.021](#).